

Spinal Interneurons in Sensorimotor Integration

Ting Ting Liu

**Thesis submitted for the degree of Doctor of Philosophy
Neuroscience and Molecular Pharmacology
Faculty of Biomedical and Life Sciences**



September 2009

Summary

Even though spinal cord research has expanded enormously during the past decades, we still lack a precise understanding of how spinal interneuron networks perfectly integrate sensory feedback with motor control, and how these neuron circuits give rise to specific functions. The present study thus has three basic aims: (1) to investigate propriospinal interneurons connecting rostral and caudal lumbar spinal cord in the rat; (2) to investigate input properties of identified spinal interneurons interposed in different pathways; (3) to investigate cholinergic terminals in the ventral horn of adult rat and cat.

To realize the first aim, the B-subunit of cholera toxin (CTb) was injected into the motor nuclei at the L1 or L3 segmental level to retrogradely label propriospinal interneurons in the L5 segment of rat spinal cord. These cells had a clear distribution pattern which showed that they were located mainly in ipsilateral dorsal horn and contralateral lamina VIII. A series triple-labelling experiments revealed that about 1/4 of the CTb-positive cells were immunoreactive for calbindin and/or calretinin. It was also found that a small population of CTb labelled cells were cholinergic and were observed mainly in three locations: lamina X, the medial part of intermediate zone and lamina VIII. In addition, injection of CTb also anterogradely labelled axon terminals, which arose from the commissural interneurons (CINs) within the site of injection, crossed the midline and arborized in the contralateral lateral motor nuclei of the L5 segment. The neurotransmitter systems in labelled axon terminals of CINs were investigated by using antibodies raised against specific transmitter-related proteins. The results showed that approximately 3/4 terminals were excitatory and among those excitatory terminals about 3/4 forming contacts with motoneurons.

To achieve the second aim, 21 interneurons located in the intermediate zone and lamina VIII from 7 adult cats were characterised electrophysiologically and labelled intracellularly with Neurobiotin. Seventeen of these cells were activated monosynaptically from primary muscle afferents but the remaining four cells received monosynaptic inputs from the medial longitudinal fasciculus (MLF). Quantitative analysis revealed that cells in the first group received many contacts from excitatory terminals that were immunoreactive for the vesicular glutamate transporter 1 (VGLUT1) but those cells from the second group received few contacts of this type and were predominantly contacted by terminals immunoreactive for

vesicular glutamate transporter 2 (VGLUT2). This result was as predicted because VGLUT1 is found principally in the terminals of myelinated primary afferent axons whereas VGLUT2 is located in the terminals of interneurons in the spinal cord. Interneurons in the first group were then characterised as excitatory and inhibitory on the basis of the transmitter content contained within their axon terminals. Although there was a greater density of VGLUT1 contacts on excitatory rather than inhibitory cells, the difference was not statistically significant. GABAergic terminals formed close appositions with VGLUT1 contacts on both excitatory and inhibitory cells. These appositions were likely to be axoaxonic synapses which mediate presynaptic inhibition. In addition, the densities of VGLUT1 and VGLUT2 contacts on 30 dorsal horn CINs and 60 lamina VIII CINs that were retrogradely labelled with CTb from 3 adult rats were compared. The results showed that VGLUT2 terminals formed the majority of excitatory inputs to both dorsal horn and lamina VIII CINs but dorsal horn CINs received a significantly greater density of VGLUT1/2 inputs than lamina VIII CINs.

In order to achieve the third aim, i.e. whether glutamate is a cotransmitter at motoneuron axon collateral terminals in the ventral horn, a series of anatomical experiments were performed on axon collaterals obtained from motoneurons from an adult cat and retrogradely labelled by CTb in adult rats. There was no evidence to support the presence of vesicular glutamate transporters in motoneuron axon terminals of either species. In addition, there was no obvious relationship between motoneuron terminals and R2 subunit of the AMPA receptor (GluR2). However, a population of cholinergic terminals in lamina VII, which did not originate from motoneurons, was found to be immunoreactive for VGLUT2 and formed appositions with GluR2 subunits. These terminals were smaller than motoneuron terminals and, unlike them, formed no relationship with Renshaw cells. The evidence suggests that glutamate does not act as a cotransmitter with acetylcholine at central synapses of motoneurons in the adult cat and rat. However, glutamate is present in a population of cholinergic terminals which probably originate from interneurons where its action is via an AMPA receptor.

In conclusion, the present studies add to the understanding of the organization of neuronal networks involved in sensorimotor integration. Propriospinal interneurons located within the lumbar segments have extensive intra-segmental projections to motor nuclei. First order interneurons interposed in reflex pathways and descending pathways receive a significantly different pattern of inputs. A similar proportion of monosynaptic excitatory input from

primary afferents has been found in both excitatory and inhibitory interneurons and these two types of cells are subject to presynaptic inhibitory control of this input.

CONTENTS

Summary	i
Acknowledgement	x
Declaration	xi
List of abbreviations	xii
<i>Chapter 1</i> General Introduction	1
1.1. General properties of four identified populations of interneurons that play essential roles in sensorimotor integration.....	2
1.1.1 Group Ia inhibitory interneurons.....	3
1.1.2 Group Ib interneurons.....	4
1.1.3 Group II interneurons.....	6
1.1.4 Commissural interneurons.....	8
1.2. Elementary organizations of spinal interneuronal networks for sensorimotor integration.....	10
1.2.1 Spinal reflex pathways: from sensorimotor connectivity to function.....	11
1.2.2 Basic models of functionally reconstructed interneuronal networks.....	13
1.2.3 CINs incorporated neuronal networks.....	16
1.3. Modulatory actions on interneuronal networks: presynaptic inhibition and effects of monoamines.....	18
1.3.1 Presynaptic inhibition.....	18
1.3.2 Modulatory actions of monoamines.....	20
1.4. Ascending and descending pathways in the rat spinal cord.....	22
1.4.1 Ascending pathways.....	22
1.4.2 Descending pathways.....	24
<i>Chapter 2</i> General Experimental Procedures	30
2.1. Multiple immunolabelling for confocal microscopy.....	31
2.2. Confocal microscopy.....	32
<i>Chapter 3</i> <u>Investigation 1: Propriospinal interneurons connecting rostral and caudal lumbar spinal cord in the rat</u>	38
3.1. Introduction.....	39
3.2. Experimental Procedures.....	40
3.3. Results.....	47
3.4. Discussion.....	53

<i>Chapter 4</i>	<u>Investigation 2: Input properties of identified spinal interneurons</u>	
	interposed in different pathways.....	108
4.1.	Introduction.....	109
4.2.	Experimental Procedures.....	110
4.3.	Results.....	116
4.4.	Discussion.....	121
<i>Chapter 5</i>	<u>Investigation 3: Cholinergic terminals in the ventral horn of adult rat and</u>	
	cat.....	180
5.1.	Introduction.....	181
5.2.	Experimental Procedures.....	182
5.3.	Results.....	188
5.4.	Discussion.....	191
<i>Chapter 6</i>	General Discussion.....	220
	References.....	226
	Publications.....	246

LIST OF FIGURES AND TABLES

Chapter 1 **General Introduction**

Figure 1.1. Five basic models illustrating the reconfigurations of spinal interneuronal networks.....	14
Figure 1.2. Schematic diagrams illustrating CINs incorporated neuronal networks.....	27
Figure 1.3. The main courses of the ascending and descending axons in the white matter of rat spinal cord.....	29

Chapter 2 **General Experimental Procedures**

Table 2.1. Excitation-emission wavelengths corresponding to the fluorophores used.....	33
Figure 2.1. Diagram and confocal images to illustrate triple-labelling immunofluorescence.....	35
Figure 2.2. Flow diagram and confocal images to illustrate triple-labelling and sequential immunofluorescence.....	37

Chapter 3 **Investigation 1: Propriospinal interneurons connecting rostral and caudal lumbar spinal cord in the rat**

Table 3.1. Summary of primary and secondary antibody combinations and connections used in the current study.....	43
Table 3.2. The average number of CTb retrogradely labeled cells per 100 μ m of length in different laminae of the L5 segment.....	104
Table 3.3. The average numbers and proportions of CTb labeled cells with calbindin and/or calretinin immunostaining per 100 μ m within laminae at L5 segmental level.....	105
Table 3.4. The percentage of VGLUT- or VGAT-immunopositive CTb terminals in contralateral-lateral motor nuclei of the L5 segment.....	106
Table 3.5. The percentage of CTb labeled terminals with different immunoproperties in contralateral-lateral motor nuclei of the L5 segment.....	107
Figure 3.1. Photomicrograph of representative sections illustrating the injection site of CTb in the motor nuclei of the L1/L3 segment.....	65
Figure 3.2. Reconstruction of the injection sites for all 7 experiments.....	67
Figure 3.3. Retrograde labeling of neurons in the L5 segment following CTb injections in the L3 segment.....	69
Figure 3.4. Distribution of cells retrogradely labeled by CTb in the L5 segment.....	71

Figure 3.5. Laminar distribution of CTb retrogradely labeled cells in the L5 segment.....	73
Figure 3.6. Three colour confocal microscope images illustrating the distribution of CTb labeled cells and their immunoreactivities for calbindin and/or calretinin.....	75
Figure 3.7. Distribution of CTb labeled cells with calbindin immunoreactivity in the L5 segment.....	79
Figure 3.8. Distribution of CTb labeled cells with calretinin immunoreactivity in the L5 segment.....	81
Figure 3.9. Distribution of CTb labeled cells with calbindin and calretinin immunoreactivity in the L5 segment.....	83
Figure 3.10. Laminar distribution of CTb labeled cells with calbindin and/or calretinin immunoreactivity.....	85
Figure 3.11. Distribution of cells within laminae at the L5 segmental level for the 7 experiments.....	87
Figure 3.12. Single optical sections illustrate CTb labeled neurons that were immunopositive for ChAT.....	89
Figure 3.13. Sequential immunocytochemistry for CTb labeled terminals with VGLUT1/2 or VGAT immunoreactivity.....	93
Figure 3.14. The proportions of excitatory and inhibitory CIN axon terminals in the lateral motor nuclei at L5 segmental level for all 7 experiments.....	97
Figure 3.15. Single optical sections illustrating neurotransmitter content of CTb labeled terminals.....	99
Figure 3.16. Single optical sections illustrating neurotransmitter content of CTb labeled terminals.....	101
Figure 3.17. The neurotransmitter content in CIN axon terminals in the lateral motor nuclei at L5 segmental level for all 7 experiments.....	103
<i>Chapter 4</i> <u>Investigation 2: Input properties of identified spinal interneurons interposed in different pathways</u>	
Table 4.1. Summary of primary and secondary antibody combinations and connections used in the current study.....	114
Table 4.2. Summary of morphological, neurochemical and electrophysiological data.....	177
Table 4.3. The density of VGLUT1 and VGLUT2 contacts per 100 μm^2 of each cell...	178
Table 4.4. Comparison of density of VGLUT1 terminals for each individual cell.....	179

Figure 4.1. Examples of PSPs used to identify the 21 interneurons analysed morphologically.....	133
Figure 4.2. Location of identified spinal interneurons.....	139
Figure 4.3. Cell body size distribution for the 21 cells examined.....	141
Figure 4.4. Axonal projections of glutamatergic and glycinergic interneurons.....	143
Figure 4.5. Morphology and immunocytochemical characteristics of VGLUT1 and VGLUT2 terminals in contact with postsynaptic interneurons.....	146
Figure 4.6. Reconstructions of cells with and without monosynaptic primary afferent input showing the distribution of VGLUT1 and VGLUT2 contacts.....	148
Figure 4.7. Reconstructions of cells with monosynaptic primary afferent input showing the distribution of VGLUT1 and VGLUT2 contacts.....	150
Figure 4.8. Reconstructions of cells without monosynaptic primary afferent input showing the distribution of VGLUT1 and VGLUT2 contacts.....	159
Figure 4.9. Comparison of the mean numbers of VGLUT1 and VGLUT2 terminals contacting neurons with or without monosynaptic primary afferent inputs...	162
Figure 4.10. Immunocytochemical characteristics of a glutamatergic interneuron and a glycinergic interneuron.....	164
Figure 4.11. A series of confocal microscope images illustrating neurotransmitter content of terminals contacting the labeled interneuron and their relationship with GABA-containing terminals.....	166
Figure 4.12. A series of confocal microscope images illustrating CTb retrogradely labeled CINs located in contralateral lamia VIII and neurotransmitter content of terminals contacting the labeled CINs.....	168
Figure 4.13. A series of confocal microscope images illustrating CTb retrogradely labeled CINs located in contralateral lamiae V-VII and neurotransmitter content of terminals contacting the labeled CINs.....	170
Figure 4.14. The synapses formed with the intermediate zone interneurons and by their axon collaterals.....	172
Figure 4.15. Schematic diagrams illustrating postsynaptic excitation and presynaptic inhibition in flexor reflex pathways.....	174
Figure 4.16. Summarized diagram illustrating the excitatory contacts to dorsal horn and lamia VIII CINs from interneurons with monosynaptic group I/II inputs.....	176

<i>Chapter 5</i>	<u>Investigation 3: Cholinergic terminals in the ventral horn of adult rat and cat</u>	
Table 5.1.	Summary of primary and secondary antibody combinations and connections used in the current study.....	199
Figure 5.1.	A reconstruction of a cat motoneuron and a series of confocal microscope images illustrating the absence of VGLUT1 and -2 immunoreactivity within the motoneuron axon terminals.....	201
Figure 5.2.	Three color confocal images showing CTb-labelled motoneuron terminals that are positive for VAcHT-immunoreactivity but are negatively labeled for all three VGLUTs.....	203
Figure 5.3.	Single optical sections illustrating CTb-labelled motoneuron terminals in contact with Renshaw cells.....	207
Figure 5.4.	Sequential immunocytochemistry for CTb-labelled terminals in contact with Renshaw cell.....	209
Figure 5.5.	Reconstruction of a motoneuron and its axon collaterals that was intracellularly labeled with neurobiotin.....	211
Figure 5.6.	Relationship between intracellularly labeled cat motoneuron axon terminals and immunoreactivity for the GluR2 subunit of the AMPA receptor following antigen unmasking with pepsin.....	213
Figure 5.7.	Relationship between intracellularly labeled cat interneuron axon terminals and immunoreactivity for the GluR2 subunit of the AMPA receptor following antigen unmasking with pepsin.....	215
Figure 5.8.	Relationship between VAcHT-labelled terminals and VGLUT-labelled terminals and immunoreactivity for the GluR2 subunit of the AMPA receptor following antigen unmasking with pepsin.....	217
Figure 5.9.	Comparison of the mean equivalent diameters of five groups of terminals....	219
<i>Chapter 6</i>	General Discussion	
Figure 6.1.	Schematic diagram illustrating putative organizations of interneurons in sensory-motor circuit assembly.....	225

ACKNOWLEDGEMENTS

Firstly and the most importantly, I would like to express my sincere gratitude to my supervisor, Professor David Maxwell. Professor Maxwell is the best professor I have ever had because he not only “gives me fish” but also “teach me how to fish”. Thank you very much, David. It was you who kindly offered me such a fantastic opportunity, who gave me endless help and who always encouraged me throughout my studies.

I would also like to extend a big thank you to Dr. Anne Bannatyne for being such a fantastic friend as well as great person to work with. You not only shared your scientific knowledge with me but also made the scientific life so colourful with many tips, jokes, and gossips.....

There have been a number of other people who have helped in this project; thank you to Professor Elzbieta Jankowska for performing the very technical surgical procedures and electrophysiological recordings that were required for this project. Thank you also to Professor Andrew Todd and Dr. David Hughes for their communication and comments on the thesis. A huge thank you is due to all my friends in the spinal cord group! It was all of you who made the bad times seem good and the good times seem fantastic.

Last but certainly not least I would like to thank my family. Thank you so much for always being there and giving me constant love, encouragement and support.

DECLARATION

I hereby declare that this thesis has been composed by myself, and that the work presented in this thesis is my own. Professor David Maxwell contributed to this work by performing surgical procedures and CTb injections in rats. Professor Elzbieta Jankowska contributed to this work by performing surgical procedures and electrophysiological recordings in cats. I also confirm that it has not been submitted in any previous application for a higher degree.

Ting Ting Liu
September 2009

LIST OF ABBREVIATIONS

(Terms in *italic* are not defined in the text)

5-HT, serotonin

ABSM, Anterior biceps and semimembranosus

ACh, acetylcholine

AMPA, alpha-amino-3-hydroxy-5-methyl-4-isoxazole propionic acid (receptor)

ANOVA, analysis of variance

BDA, Biotinylated Dextran Amine

ChAT, choline acetyltransferase

CINS, commissural interneurons

CNQX, 6-cyano-7-nitroquinoxaline-2, 3-dione

CPG, central pattern generator

CTb, B-subunit of cholera toxin

DAB, 3,3'-diaminobenzidine

DP, deep peroneus

DH β E, di-hydro- β -erythroidine

EPSP, excitatory postsynaptic potential

FRA, flexor reflex afferents

GABA, gamma-aminobutyric acid

GAD, glutamic acid decarboxylase

GlyT2, glycine transporter 2

GS, gastrocnemius and soleus

HRP, horseradish peroxidase

Ig, immunoglobulin

IPSP, inhibitory postsynaptic potential

i.p., intraperitoneal

LSN, lateral spinal nucleus

MLR, mesencephalic locomotor region

MLF, medial longitudinal fasciculus

NA, noradrenaline

NBQX, 2, 3-dihydroxy-6-nitro-7-sulfamoyl-benzo[f]quinoxaline-2, 3-dione

NMDA, N-methyl-D-aspartate (receptor)

NOS, nitric oxide synthase

PAD, primary afferent depolarization
PB, phosphate buffer
PBS, phosphate-buffered saline
PBST, phosphate-buffered saline containing 0.3% triton X-100
PBST, posterior biceps and semitendinosus
PI, plantaris
PSDC, postsynaptic dorsal column
PSP, postsynaptic potential
PT, pyramidal tract fibres
Q, quadriceps
RS, reticulospinal (tract)
Sart, sartorius
SD, standard deviation
T, threshold
TSA, tyramide signal amplification
VACHT, vesicular cholinergic transporter
VN, vestibular nuclei
VGLUT, vesicular glutamate transporter
VGAT, vesicular GABA transporter
VS, vestibulospinal (tract)

Chapter 2

General Experimental Procedures

The purpose of this chapter is to give a brief account of the three principal aims pursued, and experimental approaches that were used throughout all the three investigations. The specific experimental procedures, which were applied in each of the three studies, are explained in detail in the corresponding chapters. The aim of the first study (chapter 3) was to examine several features of propriospinal interneurons connecting rostral and caudal lumbar spinal cord. The second investigation (chapter 4) focused on the input properties of identified spinal interneurons (including CINs) interposed in different pathways. Finally, in chapter 5, cholinergic terminals in the ventral horn of spinal cord were investigated to determine whether glutamate is colocalized within them.

In order to facilitate the understanding of the specific experimental protocols applied in chapters 3, 4, and 5, aspects of them including immunocytochemistry and confocal microscopy is provided here.

2.1 Multiple immunolabelling for confocal microscopy

This technique allows the identification of more than one antigen in the same section of spinal cord. The antigens used in the present work include transporters, neurotransmitters, enzymes, and receptors. The rationale of the protocol can be summarised in two essential general steps ([Figure 2.1, diagram](#)):

1. Incubation of spinal cord sections with primary antibodies that have been raised in different species. Normally a primary antisera cocktail contains two or three primary antibodies and each one is derived from a different species.
2. Incubation of sections in a cocktail containing species specific-secondary antibodies, which are coupled to different fluorophores. Generally a secondary antibody is an immunoglobulin (Ig) raised in donkey, which is detected against an Ig of a particular (X) species. The resulting secondary antibody will bind to any antigen of the X species and will be readily identified by means of the fluorophore coupled to it.

Following the incubations and rinses, sections are mounted and are ready to be scanned with the confocal microscope. Immunoreactivity for each of the antigens can be independently

visualised as revealed by the corresponding fluorophore-coupled secondary antibody. Images from the same optical section can be merged in order to study the relative spatial distribution of the antigens. For instance it can be assessed if two or three antigens colocalise ([Figure 2.1, images](#)).

It is possible to use a fourth antibody with different species by sequential incubation. This procedure requires additional steps: 1) incubation in the primary and secondary antisera cocktails; 2) scanning of the regions of interest in the section; 3) re-incubation with the additional primary antibody (this will be a different species from any of the antibodies used originally); 4) re-incubation with species specific-secondary antibody. But this secondary antibody has one of the fluorophores, which has already been used, so it will then be displayed by any additional colour. For example, if it is in the blue channel, then any additional blue structures will represent the immunoreactivity for this antibody; 5) re-location and re-scanning of the area of interest selected previously; and 6) comparison of the scans obtained before and after re-incubation allows detection of extra labelling in the corresponding channel which represents immunoreactivity for the sequentially added antibody ([Figure 2.2](#)).

In addition, it is also possible to use two primary antibodies of the same species to identify different structures if the incubation is performed sequentially and the two secondary antibodies, which reveal the two primary antibodies with the same species, are associated with different fluorophores. As a result, the first primary antibody will combine with both of the two secondaries; thus its immunoreactivity will display both colours corresponding to the two secondaries. In contrast, the immunoreactivity of the sequentially incubated primary antibody displays a single colour corresponding to the sequentially applied secondary antibody ([Figure 4.5](#) in Chapter 4).

2.2 Confocal microscopy

The confocal laser scanning microscope used in the present investigations is a Radiance 2100 microscope (Bio-Rad, Hemel Hempstead UK), and three lasers were used which are Argon, Green Helium Neon, and Far red. These three lasers allowed the scanning of sections that had been labelled with the secondary antibodies, each of which is coupled to a different

fluorophore. [Table 2.1](#) (below) shows the excitation-emission wavelengths corresponding to the fluorophores coupled with three secondary antibodies used in the present studies.

Table 2.1. Excitation-emission wavelengths corresponding to the fluorophores used

Fluorophore	excitation (λ)	emission (λ)
Alexa-fluor 488 (Alexa488)	488	517
Rhodamine-red (RR)	543	591
Cyanine 5.18 (Cy-5)	635	665

Figure 2.1. Diagram and confocal images to illustrate triple-labelling immunofluorescence. Above, a flow diagram simplifies the two basic steps of a protocol for triple-labelling immunocytochemistry of the vesicular acetylcholine transporter (VACHT), B-subunit of cholera toxin (CTb), and vesicular glutamate transporter 1 (VGLUT1). Below, confocal images exemplify how the distribution of each antigen can be studied independently in the same optical plane: VACHT (green), CTb (red) and VGLUT1 (blue). The relative spatial distribution of the antigens can be assessed by merging the images. In this case the merged images show an overlap of the immunoreactivities in yellow and purple, indicating the colocalization of VACHT/CTb and of CTb/VGLUT1, respectively.

Triple-labelling
immunocytochemistry for:

Axon terminals containing **VACHT**
Axon terminals retrogradely labelled by **CTb**
Axon terminals containing **VGLUT1**

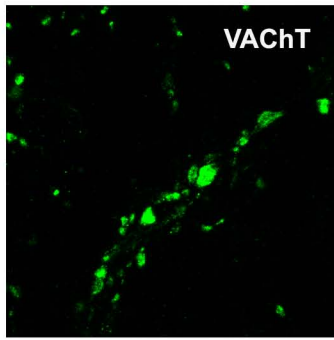
Primary Antibodies

goat anti-VACHT
mouse anti-CTb
guinea pig anti-VGLUT1

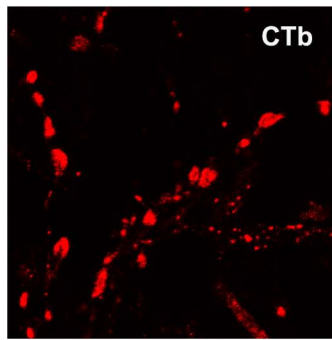
Secondary Antibodies + Fluorescent Particles

donkey anti-goat + **Alexa488**
donkey anti-mouse + **Rhodamine-Red**
donkey anti-guinea pig + **Cy-5**

Alexa488



Rhodamine-Red



Cy-5

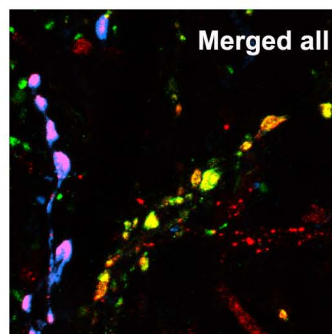
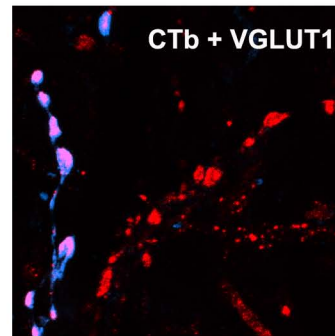
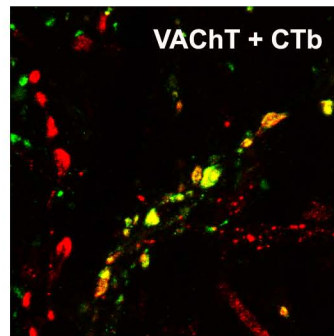
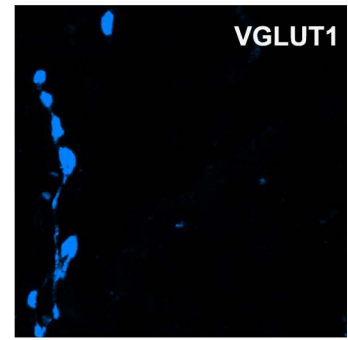


Figure 2.2. Flow diagram and confocal images to illustrate triple-labelling and sequential immunofluorescence. Above, a flow diagram indicates the essential steps to perform triple-labelling immunocytochemistry for CTb, vesicular glutamate transporter 2 (VGLUT2) and calbindin. (A), A series of four confocal images show how the three types of labelling can be visualised independently (CTb, red; VGLUT2, green; calbindin; blue) and how the images can be merged to study the relative spatial distribution of the antigens. In order to perform sequential immunocytochemistry with an additional primary antibody, the section is removed from the slide and re-incubated in the primary and then secondary antisera cocktail. In this example, the sequentially added primary antibody is a goat-anti-VACHT, which is revealed with a donkey anti-goat Ig coupled to the Cy-5; i.e. the same secondary antibody used originally to label calbindin. Once the section is mounted, the same area is re-located and re-scanned. (B), a series of four confocal images shows the resulting labelling. The additional VGLUT2 labelling can be differentiated from the calbindin labelling by comparing (A) and (B). The extra-blue labelling in (B; calbindin+VACHT) represents VACHT immunoreactivity, while the labelling of CTb in (B; CTb) and VGLUT2 (in B; VGLUT2) are not altered. Merging of the images reveals the localisation of VACHT in relation to the rest of the antigens. Scale bar = 10µm.

Triple-labelling immunocytochemistry for:

Axon terminals retrogradely labelled by **CTb**
Axon terminals containing **VGLUT2**
Neurons expressing **calbindin**

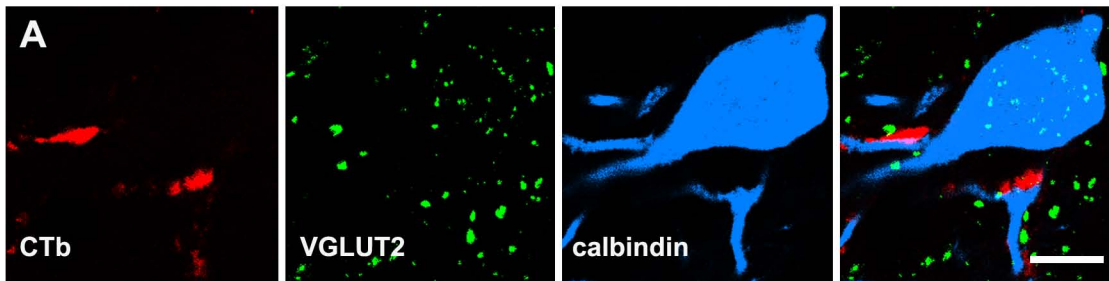
Primary Antibodies

mouse anti-CTb
guinea pig anti-VGLUT2
rabbit anti-calbindin

Secondary Antibodies + Fluorescent Particle

donkey anti-*mouse* + **Rhodamine-Red**
donkey anti-*guinea pig* + **Alexa488**
donkey anti-*rabbit* + **Cy-5**

Scan Cell



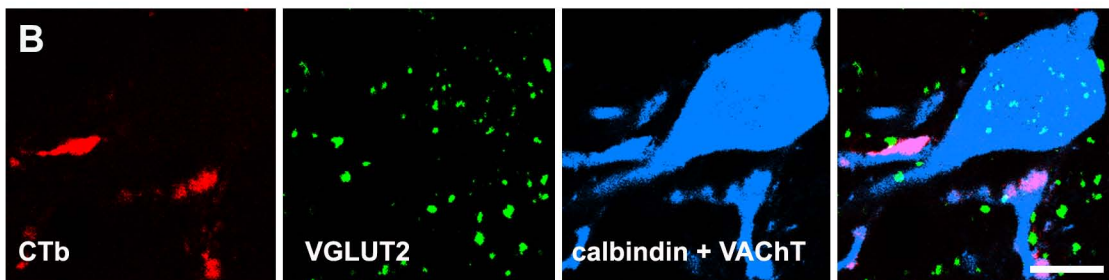
Removal of spinal cord section from slide

Sequential incubation with a fourth antibody against VACHT

goat anti-VACHT

donkey anti-*goat* + **Cy-5**

Re-scan cell



Chapter 3

Investigation 1:

**Propriospinal interneurons connecting rostral and caudal
lumbar spinal cord in the rat**

3.1. Introduction

It is generally accepted that the CPG is a crucial component of the spinal cord in generating rhythmic limb movements in vertebrates, such as locomotion and scratching. The CPG is able to mediate these patterned movements even in the absence of input from the brain and peripheral movement-related sensory feedback (Berkowitz, 2004; Grillner, 2006). However, the capacity to generate rhythmic motor patterns varies in different segments. For example, Ballion et al (2001) reported that caudal segments are more rhythmogenic than rostral segments in cervical enlargements of neonatal rat spinal cord. In contrast, a number of studies, using in vitro preparations of lumbar segments of spinal cord, have demonstrated a rostro-caudal gradient for rhythmogenesis in both neonatal and adult rats (Cazalets et al., 1995, 1996; Kjaerulff and Kiehn, 1996; Magnuson et al, 2005). The underlying mechanisms for segmental variations in rhythmogenic capacity are not clear; however, there are two potential explanations.

The first possibility is that CPGs, located in different rostral-caudal levels, receive inputs from distinct sets of propriospinal interneurons. Propriospinal interneurons are groups of neurons with cell bodies and axonal terminations at different rostral and caudal segments within the spinal cord. This group of interneurons is known to convey signals between CPGs and has a crucial importance in coordinating complex multi-limb movements such as locomotion (Berkowitz, 2004; Dutton et al., 2006; Reed et al., 2006). A number of studies have investigated long range propriospinal neurons that form inter-enlargement pathways (e.g. Alstermark et al., 1987; Berkowitz, 2004; Leah and Menetry, 1989; Masson et al., 1991; Matsushita et al., 1979; Miller et al., 1998; Reed et al., 2006; Skinner et al., 1979;). For example, Dutton et al. (2006) reported that propriospinal interneurons located in the ventromedial cord and the intermediate zone of lumbosacral segments have direct projections to the contralateral upper cervical ventromedial cord, while those located in superficial dorsal horn of lumbosacral segments mainly project to the contralateral upper cervical dorsal horn. Short range propriospinal interneurons form intra-segmental connections, and those located in the cervical enlargement have been studied in some experiments. However, relatively little is known about those located in lumbar enlargements which are involved in hindlimb movements.

A second possible explanation for variations in rhythmogenic capacity is that the component cells of rostral and caudal CPGs are heterogeneous, and have different electrical properties leading to different excitability or rhythmogenicity. Commissural interneurons (CINs) are groups of neurons connecting the CPGs located in the left and right sides of spinal cord. These are essential for coordinating alternation of activities of motoneurons located on the two sides of the same spinal segment and synchronous activity of flexor and extensor motoneurons located in different spinal segments (Cazalets et al., 1995; Kjaerulff and Kiehn, 1996; Kremer and Lev-Tov, 1997). Numerous physiological and anatomical studies have demonstrated that many CINs establish monosynaptic contacts with motoneurons (e.g. see Bannatyne et al., 2003; 2006; 2009; Brink et al., 1983; Cavallari et al., 1987; Edgley and Jankowska, 1987b; Harrison et al., 1984; 1986; Jankowska and Noga, 1990; Maxwell et al., 2000; Puskar and Antal, 1997). Thus, different proportions of excitatory and inhibitory premotor CINs involved in rhythmic movements will produce different or completely opposite motor output. For example, studies of fictive swimming in *Xenopus* tadpole and lamprey reported that the contralateral motoneuron discharge is terminated by glycinergic CINs in swimming CPGs during the period of ipsilateral motoneuron activation (Grillner et al., 1995; Roberts et al., 2008). Although it has been known that CINs form heterogeneous populations which have both excitatory and inhibitory actions in contralateral motor nuclei, both the proportions of excitatory/inhibitory terminals and the neurotransmitter content of these terminals remain to be established.

As these two possibilities are not mutually exclusive, both were investigated and the three principal aims of the present study were: (1) to establish the distribution of propriospinal interneurons in both sides of the L5 segment with projections to L1 or L3 segments (afterwards referred as short ascending propriospinal interneurons); (2) to investigate the neurochemical properties of these interneurons; and (3) to determine the proportions of excitatory and inhibitory CIN axons that terminate in contralateral-lateral motor nuclei of L5 segments. Two further questions arose from the third aim: (a) do the majority of the excitatory or inhibitory CIN terminals make contact on motoneuron cell bodies or dendrites; (b) which neurotransmitters are contained within these terminals?

3.2. Experimental procedures

3.2.1 Surgical procedure and labelling of commissural interneurons

Experiments were performed on 10 adult male Sprague-Dawley rats (250-350g; Harlan, Bicester, UK). All procedures were conducted according to British Home Office legislation and were approved by the University of Glasgow Ethics Committee. Using aseptic techniques, rats were deeply anesthetized with halothane. According to the location of the last rib, Th13 vertebra was identified and a small dorsal midline incision was made at this level. Then a small hole with a diameter of 1mm was made near midline in the caudal part of the Th13 vertebrae to expose the dorsal surface of the spinal cord. The tip of the injection needle was inserted into the spinal cord to a depth of up to 1.5 mm from the surface at an angle of 15°. A 0.2µl volume of 1% B-subunit of cholera toxin (CTb; Sigma-Aldrich, Co., Poole, UK) in distilled water was microinjected at the target site. The needle was left in place for 5 min following the injection and then removed to prevent backflow of tracer. The wound was sutured closed and all animals recovered uneventfully. Following a 5 day survival period, the rats were reanaesthetized with pentobarbitone (1 ml i.p.) and perfused through the left ventricle with saline followed by a fixative containing 4% formaldehyde in 0.1 M phosphate buffer (PB; pH 7.4) at room temperature. The entire spinal cord was removed and post-fixed for 8 hours at 4 °C. The spinal cord was then dissected into C1 to L6 segments according to the dorsal roots.

3.2.2 Immunocytochemical processing of tissue

The segments were cut into 50µm thick transverse sections with a Vibratome (Oxford Instruments, Technical Products International, Inc., USA). In order to perform different experiments and avoid biases of the experiment results from selecting sections, sections were collected sequentially into six bottles, named group A to F, to ensure that each bottle contained a representative series of sections for each of the segments. All sections were treated with an aqueous solution of 50% ethanol for 30 min to enhance antibody penetration.

Sections were incubated in the combinations of primary antibodies listed in [Table 3.1](#). All antibodies were diluted in phosphate-buffered saline containing 0.3% Triton X-100 (PBST) and incubated for 48 hours at 4 °C with agitation. After rinsing three times with phosphate-buffer saline (PBS), sections were then incubated for 3 hours in solutions of secondary antibodies coupled to fluorophores (see [Table 3.1](#) for details).

All secondary antibodies were raised in donkey and conjugated to biotin (1:500), or Rhodamine Red (Rh. Red; 1:100), or Cyanine 5.18 (Cy-5; 1:100; all three supplied by Jackson ImmunoResearch, West Grove, USA), or Alexa-fluor 488 (Alexa488; 1:500; Molecular Probes, Eugene, USA). CB, calbindin; ChAT, choline acetyltransferase; CR, calretinin; CTb, B-subunit of cholera toxin; GAD, glutamic acid decarboxylase; GlyT2, glycine transporter 2; VGAT, vesicular GABA transporter; VGLUT vesicular glutamate transporter; mo., mouse; rbt, rabbit; gt, goat; gp, guinea pig. * DAB was used as a substrate to visualise staining. Both Avidin-HRP and DAB were supplied by Sigma, dorset, UK.

Table 3.1. Summary of primary and secondary antibody combinations and concentrations used in the current study

Group	Aim	Primary antibody combination	Primary antibody concentration	Supplier	Secondary antibodies	Sequential immunoreaction	Secondary antibodies
Injection site		gt. CTb	1:50,000	List Biological Laboratories, Campell, CA	Biotinylated IgG	Avidin-HRP (1:1000)	DAB*
A	1	gt. CTb	1:50,000	List Biological Laboratories, Campell, CA	Biotinylated IgG	Avidin-HRP (1:1000)	DAB*
B	2	mo. CTb rbt CB gt. CR	1:250 1:1000 1:1000	A. Wikström, University of Gothenburg Swant, Bellizona, Switzerland Swant, Bellizona, Switzerland	Rh.Red Alexa488 Cy-5		
C	2	mo. CTb gt. ChAT	1:250 1:100	Chemicon, Harrow, UK	Rh.Red Cy-5		
D	3	mo. CTb rbt VGAT gp VGLUT1 gp VGLUT2	1:250 1:1000 1:5000 1:5000	Synaptic System, Göttingen, Germany Chemicon, Harrow, UK Chemicon, Harrow, UK	Rh.Red Alexa488 Cy-5 Cy-5	gt. ChAT	Alexa488
E	3	mo. CTb rbt GAD gp VGLUT1	1:250 1:2000 1:5000	Sigma, Poole, UK	Rh.Red Alexa488 Cy-5		
F	3	mo. CTb rbt GlyT2 gp VGLUT2	1:250 1:1000 1:5000	Chemicon, Harrow, UK	Rh.Red Alexa488 Cy-5		

Identification of injection sites and Aim 1: how are short ascending propriospinal interneurons with projection to L1 or L3 segments distributed on both sides of the L5 segment?

The injection sites were visualised by using 3,3'-diaminobenzidine (DAB) as a chromogen. Sections were incubated in goat anti- CTb for 48 hours followed by a reaction with secondary antibody of biotinylated anti-goat IgG for 8 hours. Sections were then incubated overnight in avidin-horseradish peroxidase (HRP). Finally, hydrogen peroxide plus DAB was applied for a period of approximately 10 minutes to show golden-brown immunoreactivity at injection sites and in retrogradely labelled cells. During this time, the sections were monitored constantly. Sections in group A of the L5 segment were processed in the same way as injection sites. Following dehydration in a series of ethanol solutions, all the sections were mounted on gelatinised slides, observed under a microscope and photographed with a digital camera. The segmental locations of injection sites were finally assessed and confirmed using the stereotaxic atlas of Paxinos and Watson (1997) according to the shape of the grey matter.

Aim 2: what are the neurochemical properties of short ascending propriospinal interneurons with projections to L1 or L3 segments located in both sides of the L5 segment?

The short ascending propriospinal interneurons in L5 segments were identified by the presence of retrogradely transported CTb from the injection sites (L1 or L3 segments). Immunoreactivities to calbindin and calretinin can be used to identify neuron populations in the central nervous system (Celio, 1990; Garcia-Segura et al., 1984; Resibois and Rogers, 1992; Rogers and Resibois, 1992), and the immunohistochemical demonstration of choline acetyltransferase (ChAT) has served to identify cholinergic neurons (Huang et al., 2000; Barber et al., 1984; Borges and Inversen 1986). Therefore, the L5 sections were reacted with CTb antiserum along with the following antibodies: calbindin and calretinin (group B in [Table 3.1](#)) or ChAT (group C in [Table 3.1](#)).

Aim 3: what is the proportion of excitatory and inhibitory CIN axons that terminate in contralateral lateral motor nuclei of L5 segments? Do they make synapses on motoneurons and which neurotransmitters are contained within their terminals?

The CIN axon terminals in contralateral lateral motor nuclei of L5 segments were identified by the presence of CTb anterogradely transported from the injection sites. Triple labelling immunofluorescence was performed with CTb antisera along with one of the following three antibody combinations: VGAT and VGLUT1 and -2 (group D in [Table 3.1](#)); GAD and VGLUT1 (group E in [Table 3.1](#)); or GlyT2 and VGLUT2 (group F in [Table 3.1](#)).

As motoneurons are cholinergic and ChAT is a reliable marker for identifying cholinergic neurons (Barber et al., 1984; Borges and Inversen 1986), sequential immunocytochemistry was performed on sections from group D. When analysis of sections with the initial combination of antibodies was complete, sections were re-incubated with a fourth antibody: goat anti-ChAT. The sections were remounted and the same field that had been scanned previously was identified and scanned again. By comparing labelling before and after the re-incubation in the ChAT antiserum, the additional staining could be detected, which represents immunoreactivity for ChAT. All sections were finally mounted in a glycerol-based antifade medium (Vectashield, Vector Laboratories, Peterborough, UK)

3.2.3 Data analysis

Sections with DAB reactions (i.e. sections in injection site group and group A) were examined under a light microscope (Nikon Eclipse E600, Technical Instrument, Burlingame CA) and photomicrographed using an AxioCam digital camera (Carl ZEISS, Inc, Germany) and AxioVision 3.1 software (ZEISS, Germany). Every fifth section was processed immunohistochemically (i.e. 250µm intervals) to avoid the possibility of double cell counts, and all CTb-labelled cells in each L5 section were counted. Only retrogradely labelled cell bodies with visible proximal dendrites were counted as neurons. A photomicrograph of each section was superimposed on a template of the L5 segment (taken from the stereotaxic atlas of Paxinos and Watson, 1997) using the graphics software Xara Xtreme 2.0e (Xara Group Ltd, Hemel Hempstead, UK), and the location of each CTb-labelled cell was transferred onto the corresponding site on the template as a dot. Separate cell counts were made for the following locations: laminae I-II, laminae III-IV, laminae V-VI, lamina VII, lamina VIII, lamina X, and the lateral spinal nucleus (LSN). Between-group comparisons of cell counts for each laminae and within-group comparisons of ipsi- and contralateral cell counts were made by using a

Student's *t*-test. Multi-comparisons of cell counts in different laminae within the same side for each experiment were made by analysis of variance (ANOVA) followed by a *post hoc* Tukey's analysis. A $p < 0.05$ was considered to be statistically significant.

Sections with immunocytochemical reactions (i.e. sections in group B-F) were examined with a Bio-Rad MRC 2100 confocal laser scanning microscope (Bio-Rad, Hemel Hempstead, UK) using Red, Green, and Far-red spectra. Four sections were selected randomly from group B (i.e. sections reacted with CTb, calbindin and calretinin) and the entire sections were systematically scanned to obtain a complete series of images in order to make a montage (see [Figure 3.6A](#)). Images were gathered with a x20 lens at 1 μ m steps in the z-axis, using a zoom factor of 1. Image stacks were analyzed with Xara Xtreme software, teamed with Neurolucida for Confocal software (MBF Bioscience, Colchester, VT, USA) and Confocal Assistant. To avoid bias, the total numbers of CTb-labelled cells, calbindin-positive CTb cells, calretinin-positive CTb cells, and double-labelled (for calbindin and calretinin) CTb cells were counted in their own individual channels for every single optical section initially and then examined in merged image stacks showing all three channels by switching between different channels. The montage of each section was superimposed on a template of the L5 segment using Xara Xtreme software and all the CTb labelled cells were transferred onto the corresponding site on the template as dots with different colours according to their different immunostaining properties. The four types of cells were counted separately for the following locations: laminae I-II, laminae III-IV, laminae V-VI, lamina VII, lamina VIII, lamina X, and the LSN. Between-group comparisons of cell counts for each laminae and within-group comparisons of ipsi- and contralateral cell counts were made by using Student's *t*-test. Multi-comparisons of cell counts in different laminae within the same side for each experiment were made by ANOVA followed by a *post hoc* Tukey's analysis. A $p < 0.05$ was considered to be statistically significant.

Sections reacted with CTb and ChAT (group C) were examined with a confocal microscope at low magnification (x20 lens; zoom factor 1; 602x602 micron area). These images were used to search for CTb cells with ChAT immunoreactivity. After identifying these CTb/ChAT cells, scanning was repeated at higher magnification in the area containing the cells by using a x60 oil-immersion lens with a zoom factor of 2 at 0.5 μ m steps in the z-axis. Image stacks were analyzed with Neurolucida software. To avoid bias, the immunoreactivities for CTb and

ChAT were examined separately in single channel for each optical section initially and then examined in merged image stacks showing both channels and switching between different channels.

In order to determine the proportion of terminals examined that displayed immunoreactivity for transmitter specific proteins, the lateral motoneuron pools of the ventral horn in sections reacted for CTb, VGLUTs and VGAT (i.e. group D), GAD (i.e. group E) or GlyT2 (i.e. group F) were examined on the side contralateral to the injection site. Fields containing CTb-labelled CIN axon terminals were scanned by using a x60 oil-immersion lens with a zoom factor of 2 at 0.5 μ m intervals. For each section, four fields were obtained from lateral motor nuclei with a 100 x100 μ m scanning area. By using Neurolucida software, image stacks were initially viewed so that only CTb immunoreactivity was visible. All CTb labelled CIN terminals within the scanning box from each animal were selected for analysis. Then the terminals were examined in the blue channel (representing the VGLUT) to determine whether they were positive for VGLUT immunoreactivity; afterwards they were viewed in the green channel which corresponds to VGAT- (for group D), GAD- (for group E), or GlyT2-immunostaining (for group F).

The brightness and contrast of the images for illustration were adjusted by using Adobe Photoshop (Adobe Systems, Mountain View, CA, USA).

3.3. Results

3.3.1 Injection sites

The injection of CTb into the lumbar spinal cord at the level of L1 or L3 segments yielded unilateral, well defined injection sites that were surrounded by a shell of diffuse CTb staining. The experiments were performed on 11 animals, but because of inappropriate localization of the injection sites of the tracer, 4 animals had to be excluded from the final evaluation. Representative photomicrographs of injection sites for the 7 animals examined are shown in [figure 3.1](#).

On the basis of the location of CTb injections, the animals were divided into two experimental groups in two ways: 1) according to motor nuclei targeted: sections were divided into either the medial or the lateral motor nuclei injection groups; 2) according to injection sites at segmental levels: sections were divided into either the L1 or the L3 injection groups. In three of the seven rats, CTb was injected into the L1 segment and one injection was confined mainly to the medial motor nuclei (figure 3.2A), while the other two were in lateral motor nuclei (figure 3.2B-C). In the other four animals, CTb was injected into the L3 segment and two of the injections were located in medial motor nuclei (figure 3.2D-E), while the other two were in lateral motor nuclei (figure 3.2F-G).

3.3.2 Aim 1: The distribution of short ascending propriospinal interneurons projecting to L1 or L3 segments in both sides of the L5 segment

Each of the 7 CTb injections resulted in extensive retrograde labelling of neurons on both sides of the L5 segment. Separate cell counts were made for the locations as described in the experimental procedures section, and representative photomicrographs of retrogradely labelled neurons in these locations are shown in figure 3.3. The overall distribution of the retrogradely labelled cells from 8 sections per experiment is shown as a series of cell plots in figure 3.4 and expressed as cell counts in figure 3.5.

In all 7 experiments, the majority of neurons located in the contralateral side to the injection site were concentrated in lamina VIII. Fewer cells were present in the deep dorsal horn and intermediate zone (laminae V-VII and X). Only a small number of labelled neurons was scattered in the remaining laminae of the contralateral side. There was no significant difference in the distribution pattern in the contralateral L5 segment between the L1 and the L3 injection groups or between the medial and the lateral motor nuclei injection groups. The mean percentage (\pm SD) of contralateral lamina VIII neurons expressed as a proportion of the total number of contralaterally located neurons of the 7 experiments was $54.9\% \pm 5.5\%$ and this was significantly higher than the percentages of contralateral cells in other laminae (ANOVA, $p < 0.01$; Figure 3.5, *). However, in contrast to the contralateral side, only a small population of CTb labelled cells was found in ipsilateral lamina VIII in all 7 animals. In the medial motor nuclei injection group, the largest population in the ipsilateral side at the L5 segmental level was in the medial dorsal horn, concentrated mainly in laminae V-VI, and

extending dorsally into laminae III-IV. The percentage of ipsilateral cells in laminae V-VI was significantly higher than the percentages of ipsilateral cells in other laminae (ANOVA, $p < 0.01$; [Figure 3.5](#), *). Whereas, in the lateral motor nuclei injection group, most ipsilateral cells were found in lamina VII, and the number of cells gradually decreased from laminae V-VII to laminae I-II. The percentage of ipsilateral cells in lamina VII was significantly higher than the percentages of ipsilateral cells in other laminae (ANOVA, $p < 0.01$; [Figure 3.5](#), *). There was no significant difference between the L1 and L3 injection group.

By quantifying and comparing the average number of CTb retrogradely labelled neurons per 100 μ m of length in the L5 segment, two significant differences (Student's *t*-test, $p < 0.05$; [Table 3.2](#), *) were found between the medial and the lateral motor nuclei injection groups: (1) On the contralateral side, the mean density of all CTb labelled cells and the mean densities of CTb labelled cells in laminae III-IV, V-VI, VII and X were significantly greater in the medial motor nuclei injection group. (2) On the ipsilateral side, the mean densities were significantly greater for laminae I-II, III-IV and V-VI but were significantly lower for lamina VII in the medial motor nuclei injection group. No obvious difference was found between the L1 and the L3 injection group.

3.3.3 Aim 2: The neurochemical properties of short ascending propriospinal interneurons projecting to L1 or L3 segments in both sides of the L5 segment

Calbindin and calretinin immunoreactivities

In all 7 experiments, CTb retrogradely labelled neurons with calbindin and/or calretinin immunostaining were present within both the contralateral and ipsilateral sides of L5 segments ([Figure 3.6-3.9](#)). The average percentage (\pm SD) of these neurons expressed as a proportion of the total number of CTb labelled neurons was 25% \pm 3.5% (rang from 21% to 30%). There was no obvious difference between the L1 and L3 injection groups or between the medial and the lateral motor nuclei injection groups.

CTb labelled calbindin positive cells were mainly distributed within the ipsilateral side of the L5 segment especially within the ipsilateral dorsal horn; whereas cells in the contralateral side were more widely dispersed ([Figure 3.6B](#), [3.7](#), [3.10A](#)). The number of cells per 100 μ m were significantly greater on the ipsilateral (average \pm SD; 40 \pm 9.3) than on the contralateral side

(average \pm SD; 20 ± 8.4) in all 7 experiments (Student's *t*-test, $p < 0.05$). In contrast, fewer CTb labelled calretinin positive cells were present in the ipsilateral side (Figure 3.6C, 3.8, 3.10B). The average number (\pm SD) of the CTb and calretinin positive cells per 100 μ m was 17 ± 6.1 and 15 ± 3.8 on the contralateral side and the ipsilateral side, respectively. Nevertheless, there were clear distribution patterns on both sides of L5 segments. Firstly, the great majority of CTb labelled calretinin cells in the contralateral side were located in lamina VIII, and the percentage of these cells (average \pm SD; $80\% \pm 10.8\%$) in contralateral lamina VIII was significantly higher than the percentages of contralateral cells in other laminae (ANOVA, $p < 0.05$; Figure 3.10B, *). On the other hand, the largest population of ipsilateral CTb cells with calretinin immunoreactivity was found in the deep dorsal horn (laminae V-VI), while the superficial dorsal horn (laminae I-II) had fewer or no CTb and calretinin positive cells. The percentage of CTb/calretinin positive cells (average \pm SD; $43\% \pm 5.9\%$) located in ipsilateral laminae V-VI was significantly higher than the percentages of those located in other ipsilateral laminae (ANOVA, $p < 0.05$; Figure 3.10B, *). There was a $2\% \pm 1.1\%$ (average \pm SD) population of CTb labelled cells which were immunopositive for both calbindin and calretinin (Figure 3.6D, 3.9, 3.10C). This type of cell was found mainly on the ipsilateral side although examples were noted in all laminae of both sides. The number of these cells in the ipsilateral side was significantly higher than that in the contralateral side (Student's *t*-test, $p < 0.01$) and the average (\pm SD) density per 100 μ m was 4 ± 4.5 and 15 ± 6.6 (contralateral and ipsilateral side, respectively).

The distribution of CTb labelled neurons with calbindin and/or calretinin immunostaining within laminae was also investigated in this study. Figure 3.11 compares the distribution of the four types of CTb labelled neurons within laminae at the L5 segmental level, and Table 3.3 presents the average number and proportion of CTb labelled cells with calbindin and/or calretinin immunoreactivity per 100 μ m within each lamina. No significant differences were found between the L1 and the L3 injection group or between the medial and the lateral injection group. As only one fourth of CTb retrogradely labelled neurons in the L5 segment was immunoreactive for calbindin and/or calretinin, the overwhelming majority of component cells in most of the laminae were positive for CTb only. However, the largest number of calbindin positive/ CTb cells were found in the contralateral superficial dorsal horn (laminae I-II) and both contralateral- and ipsilateral-LSNs.

ChAT immunoreactivity

A group of CTb labelled cells with ChAT immunoreactivity was observed in this study. This group of cells was consistently present in both sides of lamina X, surrounding the central canal of the L5 segment in all 7 experiments (Figure 3.12A). Moreover, a few CTb/ChAT double labelled cells were also found in contralateral lamina VIII (in 5 of 7 experiments) and ipsilateral laminae VI-VII (in 6 of 7 experiments; Figure 3.12B&C). However, there was no particular pattern related to segmental injection location or lamina injection location.

3.3.4 Aim 3: The proportion of excitatory and inhibitory CIN axons terminating in contralateral lateral motor nuclei of L5 segments

Following CTb injections into the L1 or L3 motor nuclei, large numbers of anterogradely labelled axon terminals were encountered in the grey matter of the L5 segment, both ipsilateral and contralateral to the site of tracer application. Despite the substantial ipsilateral labelling, attention was focused exclusively on axon terminals that were labelled in the contralateral lateral motor nuclei at L5 segmental level because nearly all of these terminals should be CIN terminals. Initially, a series of triple labelling experiments were performed (Table 3.1 group D) on each animal to determine the percentage of excitatory and inhibitory labelled terminals in the L5 contralateral-lateral motor nuclei. This group of sections were reacted with: CTb+VGAT+VGLUT1+VGLUT2. In total, 4155 axon terminals in the lateral motor nuclei of the contralateral side were examined (range = 300 to 1000 terminals for each experiment). Confocal microscope images revealed that nearly 3/4 (average \pm SD, 74.4% \pm 8.36 %) of the terminals examined were positive for VGLUT but negative for VGAT immunoreactivity, and 24.5% \pm 7.87 % were positive for VGAT but negative for VGLUT immunostaining (Table 3.4, Figure 3.13A-D, 3.14A). Thus, about 1% of selected terminals were not labelled for either VGLUTs or VGAT. The proportion of excitatory and inhibitory terminals was not significantly different between the L1 and the L3 injection groups or between the medial and the lateral motor nuclei injection groups.

Sequential immunocytochemistry with a fourth antibody against ChAT enabled us to determine whether the terminals examined formed contacts with motoneurons (Figure 3.13A'-D'). The results showed that among the CTb/VGLUT positive terminals, 6.4% \pm 2.42% and 80.3% \pm 7.79% (average \pm SD) made contacts with cell bodies and dendrites of ChAT labelled

motoneurons, respectively (Table 3.4, Figure 3.14B). A similar distribution was also found for CTb/VGAT positive terminals, where $6.3\% \pm 3.21\%$ and $78.9\% \pm 12.01\%$ (average \pm SD) formed synapses with cell bodies and dendrites of motoneurons, respectively (Table 3.4, Figure 3.14B). The remaining $13.3\% \pm 7.39\%$ of VGLUT terminals and $14.9\% \pm 12.01\%$ of VGAT terminals did not make contacts with ChAT positive cells (Table 3.4, Figure 3.14B). The distribution of CTb labelled VGLUT positive/ VGAT negative terminals and CTb labelled VGAT positive/VGLUT negative terminals was not significantly different between the L1 and the L3 injection groups or between the medial and the lateral motor nuclei injection groups.

In order to clarify further which neurotransmitters were contained in these terminals, we performed another two series of triple labelling experiments by incubating sections in: CTb+GAD+VGLUT1 (Table 3.1, group E) or CTb+GlyT2+VGLUT2 (Table 3.1, group F). In group E, a total of 2949 CTb labelled axon terminals in the lateral motor nuclei of the contralateral side of the L5 segment were examined (range = 300 to 1000 terminals in each experiment). Confocal microscope images revealed that approximately 3/4 (average \pm SD, $76.4\% \pm 8.05\%$) of terminals were negative for both VGLUT1 and GAD, while $23.6\% \pm 8.05\%$ were positive for GAD but negative for VGLUT1 (Table 3.5, Figure 3.15, 3.17A). Only occasional CTb labelled terminals were immunoreactive for VGLUT1 (Figure 3.15C). None of the terminals examined was positive for both VGLUT1 and GAD immunoreactivities. The proportion of GAD/VGLUT1 negative terminals and GAD positive/ VGLUT1 negative terminals were not significantly different between the L1 and the L3 injection groups or between the medial and the lateral motor nuclei injection groups.

In group F, a total of 3104 CTb labelled axon terminals in the lateral motor nuclei of the contralateral side was examined (ranged from 300 to 1000 terminals in each experiment). Confocal microscope images revealed that about $71.5\% \pm 5.05\%$ (average \pm SD) of terminals were positive for VGLUT2 but negative for GlyT2, while $25.6\% \pm 6.08\%$ were positive for GlyT2 but negative for VGLUT2 (Table 3.5, Figure 3.16A-B, 3.17B). A small population ($2.9\% \pm 2.57\%$; average \pm SD) of terminals was found to be negative for both VGLUT2 and GlyT2, and only occasional CTb labelled terminals were immunoreactive for both VGLUT2 and GlyT2 (Table 3.5, Figure 3.16C-D). The proportion of VGLUT2 positive/GlyT2 negative terminals and GlyT2 positive/VGLUT2 negative terminals was not significantly different

between the L1 and the L3 injection groups or between the medial and the lateral motor nuclei injection groups.

There were two further comparisons between the proportions of terminals. The first was a comparison of the percentage of three populations of terminals: (i) the terminals with VGLUT1/2 immunoreactivity but without VGAT immunostaining (in group D), (ii) the terminals that were negative for both VGLUT1 and GAD (in group E), and (iii) the terminals labelled by VGLUT2 but not GlyT2 (in group F). The second was a comparison of the percentage of terminals with VGAT immunoreactivity but without VGLUT1/2 immunostaining (in group D), the percentage of the terminals that were positive for GAD but negative for VGLUT1 (in group E), and the percentage of the terminals labelled by GlyT2 but not VGLUT2 (in group F). Following ANOVA analysis, it was found that there was no significant difference between the three populations in the first group or in the second group.

3.4. Discussion

3.4.1 Labelling of short ascending propriospinal interneurons and CIN axon terminals

It is well established that CTb is a reliable tracer for both anterograde and retrograde neuronal labelling (Chen and Aston-Jones, 1995; Ericson and Blomqvist, 1988; Lindh et al., 1989; Rivero-Melian et al., 1992). CTb is taken up by axon terminals, dendrites and cell bodies, and is transported in both anterograde and retrograde directions to label both axon terminals and the somatodendritic compartment of neurons. In this study, all the injection sites were in the lateral or medial motor nuclei and extended to the grey and white matter of the L1 or L3 segment, except for one experiment in which CTb was injected into the border of laminae V-VII but also spread to the lateral motor nucleus of the L1 segment (see [Figure 3.2C](#)). Various constituents of the spinal neuronal structures are located within the areas of tracer spread, such as cell bodies and dendrites of motoneurons, along with axon terminals, dendrites and cell bodies of various spinal interneurons. Consequently, in the L5 segment, the great majority of the cells retrogradely labelled by CTb should be short ascending propriospinal interneurons whose axons terminate in the injection area and those located in the contralateral side of injection site should be predominately CINs. In addition, because the injection sites were in

motor nuclei, a high proportion of these labelled cells are likely to be premotor interneurons. However, CTb may also be taken up by fibres of passage, especially those damaged by the needle during injections (Birinyi et al., 2003; Chen and Aston-Jones, 1995), resulting in a proportion of stained neurons which are not short ascending propriospinal interneurons. In this study, CTb spread into the ventral funiculus or ventrolateral funiculus of the spinal white matter, where spinoreticular tracts, spinothalamic tracts, and fibres ascending to midbrain reticular formation run. The neurons whose axons compose the above ascending pathways are located in lamina I, III, IV, VII, and VIII contralateral to their axonal terminations and bilaterally in laminae V, VI, X and the lateral spinal nucleus (Tracey, 1995). Although, it can not be ruled out that some of the retrograde labelling in these locations may be a consequence of uptake by fibres of passage or damaged axons, the vast majority of CTb labelled neurons in the L5 segment are very likely to be propriospinal interneurons.

Similarly, injected CTb was taken up by interneurons located in the injection areas through their dendrites and cell bodies and transported anterogradely into their axons. Many of these axons projected contralaterally and gave rise to collaterals forming rich terminal arbors in the lateral motor nuclei of the contralateral grey matter. Therefore, the great majority of terminals examined in this study should originate from CINs with cell bodies located in the L1 or L3 segment ipsilaterally to the injection site. Nevertheless, a few of the axon terminals may be derived from other potential sources. Firstly, contralateral CINs were also retrogradely labelled, thus terminals examined in the contralateral L5 segment may arise from the axon collaterals of these CINs. However, it has been reported that few CIN axons gave off collaterals ipsilaterally to their cell bodies before crossing the midline in the rat spinal cord (Birinyi et al., 2001), which is supported by the present findings (see below discuss). Therefore, it seems that the probability of labelling terminals originating from contralateral CINs is very low. Secondly, the examined axon terminals could originate from those supraspinal neurons whose axons course in the ventral or ventrolateral funiculus, give off collaterals at spinal level, cross the central canal and reach the ventrolateral part of the ventral horn. These descending pathways include corticospinal tract, coeruleospinal tract, reticulospinal tract, raphe-spinal tract and vestibulospinal tract (Tracey, 1995). However, the number of terminals originating from these fibres is very likely to be limited (if any) because only a few descending fibres are known to decussate in spinal cord. There are two further lines of evidence to rule out this possibility. Firstly, in rat spinal cord, very few axon terminals of

corticospinal tract are found in lamina IX and even fewer form direct contacts with motoneurons (Brosamle and Schwab, 1997). Secondly, characterization of vesicular glutamate transporters in the rat corticospinal tract terminals showed that of all these terminals in laminae V-VI, only 58% contain VGLUT1 but none contain VGLUT2, suggesting either they may use another vesicular glutamate transporter or they may not be exclusively glutamatergic (unpublished dissertation of Emma Reid). Consequently, if a sizeable proportion of labelled terminals in the lateral motor nuclei were given off by the corticospinal tract, then a considerable percentage of examined terminals should either be VGLUT1 immunoreactive or negative for both VGLUT and VGAT. Nevertheless, the results here show very few terminals were VGLUT1 immunoreactive and only 1% terminals were negative for VGLUT1/2 and VGAT. Axon terminals of the remaining descending pathways are less likely to be labelled because they have been shown to mainly contain noradrenaline, serotonin or peptides. However, some of raphe-spinal neurons and vestibulospinal neurons may contain amino acids, such as glutamate and GABA (Tracey, 1995). In conclusion, it is fair to assume that the vast majority of terminals examined in the contralateral lateral motor nuclei at the L5 segment originate from CINs whose cell bodies located in the injection areas, although it can not be ruled out that there may be a limited number of terminals originating from other sources.

3.4.2 Distribution of short ascending propriospinal interneurons

Previous studies have demonstrated that premotor spinal interneurons are located mainly in lamina VIII contralaterally and laminae V-VII ipsilaterally to the injection site (Barajon et al., 1990; Harrison et al., 1984; Jankowska and Skoog, 1986; Puskar and Antal, 1997). This distribution pattern has been confirmed by the present study, which also extended the range of short ascending propriospinal interneurons that were labelled. On the contralateral side, CTb labelled cells are concentrated within lamina VIII which are well known as a subgroup of CINs. Because few labelled cells were found in ipsilateral lamina VIII, this suggests that lamina VIII CINs rarely give off collaterals ipsilaterally to their cell bodies, and this is consistent with previous results (Bannatyne et al., 2003; Birinyi et al., 2001). On the ipsilateral side, the largest population of CTb labelled neurons was located in laminae V-VI following medial motor nuclei injections; however, with lateral motor nuclei injections, more cells were concentrated within lamina VII. This finding may indicate that the subgroups of short

ascending propriospinal interneurons that project to motoneurons innervating different muscle groups are distributed in different areas of the rat spinal cord.

Results obtained from a study where biotinylated dextran amine (BDA) was injected into the medial and lateral motor columns of the lumbar spinal cord showed that the proportion of contralateral labelled premotor interneurons was strikingly higher than that in the injections performed in the present study (Puskar and Antal, 1997). However, a more detailed comparison of the density of CTb labelled cells in separate laminae revealed that this statistical difference in the density of labelled cells mainly exists in the deep dorsal horn and intermediate zone (laminae III-IV, V-VI, VII and X) of the contralateral side. In contrast to the contralateral side, the total number of labelled cells on the ipsilateral side was not significantly different between the medial and the lateral motor nuclei injection groups, although medial motor nuclei injections produced a significantly greater proportion of cells in ipsilateral laminae I-II, III-IV, and V-VI than lateral motor nuclei injections. The lateral motor nuclei injections produced significantly larger numbers of labelled cells in ipsilateral lamina VII than medial injections. Moreover, regardless of the location of the injection site, Puskar and Antal (1997) compared the number of BDA labelled premotor interneurons of the two sides of the spinal cord in each experiment, and they found that the vast majority of labelled cells were located ipsilaterally. However, the quantitative data presented here shows that the proportion of CTb labelled neurons distributed in ipsilateral and contralateral sides are similar. There are two possible explanations of this discrepancy: 1) the number of ipsilateral cells labelled by CTb was smaller than those labelled by BDA; or 2) the number of contralateral cells labelled by CTb was larger than those labelled by BDA. The first possibility seems unlikely because CTb was injected into and spread out of motor nuclei so that CTb labelled cells include both premotor and non-premotor interneurons, while the injection of BDA was confined into motor nuclei. Therefore, fewer non-premotor cells were labelled by BDA, and the greater number of CTb labelled contralateral cells was due to the increased labelling of non-premotor CINs. Accordingly, the difference between the present study and Puskar & Antal's study suggests that the target cells of the short ascending CINs in the L5 segment include both motoneurons and interneurons located in the rostral lumbar segment.

3.4.3 The neurochemical properties of short ascending propriospinal interneurons

Previous studies in rats have demonstrated that the two calcium-binding proteins calbindin and calretinin were widely distributed throughout the grey matter of spinal cord. Calbindin immunoreactive cells were most abundant in the superficial dorsal horn, while many cells in laminae V-VI and VII-VIII exhibited intense calretinin labelling (Antal et al., 1990; 1991; Ichikawa et al., 1994; Ren et al., 1993; Ren and Ruda, 1994). It was also reported that cells double-labelled for calbindin and calretinin were observed throughout the length of the spinal cord but they were more numerous at cervical and lumbar levels (Morona et al., 2006; Ren and Ruda., 1994). A similar distribution pattern was observed in this study (Figure 3.6a), but more importantly, about 25% of CTb labelled short ascending propriospinal interneurons displayed calcium-binding protein immunoreactivity. There is a differential distribution of calbindin and calretinin. For example, CTb/calbindin cells were concentrated on the ipsilateral side predominantly in the dorsal horn; whereas, CTb/calretinin cells were mainly present in contralateral lamina VIII and ipsilateral laminae V-VI. In addition, a small proportion of propriospinal interneurons were found to be immunoreactive for both calbindin and calretinin and located bilaterally in the L5 segment, although a greater number of cells were ipsilateral to the injection site. Many studies suggest that calbindin and calretinin immunoreactive cells have diverse properties and can not be simply grouped into any specific neuron type in terms of morphology and neurotransmitter content (Fahandejsaadi et al., 2004; Grkovic et al., 1997; Morona et al., 2006). However, the subgroup of short ascending propriospinal interneurons expressing these calcium-binding proteins may indicate they play a certain role in the whole network since more recent investigations have proposed essential role of calretinin and calbindin in Ca^{2+} homeostasis (Blatow et al., 2003; Cheron et al., 2004; Schwaller et al., 2002), and this is discussed later.

Borges and Iversen (1986) have described the distribution of ChAT immunoreactive neurons in rat spinal cord and they found ChAT was contained in neurons located in almost all grey laminae, but were particularly abundant in laminae III and VIII-X in lumbar segments. At least five different types of cholinergic neurons have been identified, including motoneurons, preganglionic autonomic neurons, small dorsal horn neurons (laminae III-V), partition neurons (lamina VII) and central canal cells (lamina X; Barber et al., 1984; Borges and Iversen, 1986; Houser et al., 1983; Phelps et al., 1984; Sherriff and Henderson, 1994). The last two groups are involved in short range (less than 6 segments) propriospinal cholinergic circuitry (Sherriff

and Henderson, 1994). The present findings show that a small number of CTb labelled cells was ChAT-positive and they were found in ipsilateral laminae VI-VII and bilaterally in lamina X. However, in addition to these two areas, CTb/ChAT cells were also observed in contralateral lamina VIII. This may indicate that a small proportion of lamina VIII CINs are cholinergic and form contralateral cholinergic projections. Moreover, because no ChAT-positive CTb labelled cells were found in the dorsal horn, it was confirmed that small dorsal horn cholinergic cells projected only to the neighbouring laminae within the same segment (Sherriff and Henderson, 1994).

3.4.4 The proportion of excitatory and inhibitory CIN axons terminating in contralateral lateral motor nuclei of L5 segments

It is well established that excitatory neurons use glutamate as a neurotransmitter, while GABA and glycine are the main inhibitory neurotransmitters in the rat spinal cord. In the present study a series of immunocytochemical experiments were performed with antibodies raised against specific transmitter-related proteins to determine the neurotransmitter phenotypes of CINs. VGLUT1 and VGLUT2 antibodies are generally accepted as specific markers for glutamatergic axon terminals (Bai et al., 2001; Todd et al., 2003; Varoqui et al., 2002), while the VGAT antibody immunolabels both GABAergic and glycinergic synaptic vesicles in inhibitory terminals (Aubrey et al., 2007; Burger et al., 1991; Chaudhry et al., 1998; McIntire et al., 1997; Wojcik et al., 2006). Therefore, co-localization of CTb-labelling with immunoreactivity for VGLUT1/2 indicates excitatory CIN terminals, whereas inhibitory CIN terminals were identified by the presence of both CTb and VGAT immunostaining.

The results show that of the total number of inputs originating from the L1 or L3 CINs to contralateral lateral motor nuclei of the L5 segment, approximately 75% were excitatory, while only about 25% were inhibitory. In addition, about 80% of these excitatory and inhibitory terminals formed direct synapses on dendrites of contralateral motoneurons in the lateral motor nuclei; that is, among the total number of those terminals contacting motoneurons, 75% were excitatory. Study of neonatal rat spinal cord showed that the proportion of excitatory and inhibitory CIN terminals in the ventral horn were 27% and 58%, respectively (Weber et al., 2007). Studies on cat spinal motor nuclei revealed that a majority of the terminals contacting motoneurons were inhibitory (Ornüng et al., 1996; 1998). These

results differ from the present findings but this discrepancy may be explained by the following. Firstly, CIN terminals examined in the present study were exclusively confined to lateral motor nuclei, while those examined in the neonatal rat spinal cord were selected within a random location from the whole ventral horn. Secondly, the present results are based on terminals from contralateral CINs only, but the terminals examined in the cat studies were from premotor neurons which include ipsilateral interneurons and contralateral CINs. Therefore, if the previous results and the present findings are taken together (ignoring the potential differences between species and developmental stage), it might be suggested that the direct innervation from CINs to contralateral motoneurons is predominantly excitatory, while inhibitory CINs may often act via contralateral interneurons. This conclusion is supported by the work of Butt and Kiehn (2003), who demonstrated that the excitatory pathways from premotor CINs in L2 segments projecting to contralateral L4 motor neurons were exclusively monosynaptic, while inhibitory connections are formed via both monosynaptic and polysynaptic pathways *in vitro* preparations of neonatal rat spinal cord.

It is well known that VGLUT1 and VGLUT2 are expressed by largely non-overlapping populations of terminals and VGLUT1 is present mainly in primary afferent terminals while VGLUT2 is found in interneuron axon terminals in the rat central nervous system (Todd et al., 2003; Varoqui et al., 2002). However, there is no statistical difference between the percentage of CIN terminals with VGLUT2 immunolabelling (Table 3.1 group F), the percentage of CIN terminals immunoreactive for VGLUT1/2 (Table 3.1 group D), and the percentage of CIN terminals negative for both VGLUT1 and GAD (Table 3.1 group E). Therefore, these three groups of terminals are likely to belong to the same population of terminals that are glutamatergic and contain VGLUT2. This is consistent with the prediction that the examined terminals originate from interneurons (Todd et al., 2003; Varoqui et al., 2002), although it can not be ruled out that there may be a small portion of VGLUT1/GAD negative terminals containing glycine but not VGLUT2.

GAD and GlyT2 are known to be markers of GABAergic and glycinergic neurons, respectively, and antibodies against them have been used in a variety of studies (Bannatyne et al., 2003; Rousseau et al., 2008; Todd et al., 2003; Varoqui et al., 2002; Weber et al., 2007). Therefore, GABAergic terminals and glycinergic terminals are identified by the co-localization of CTb with GAD and CTb with GlyT2, respectively. The results here show no

statistical difference between the percentage of CIN terminals immunoreactive for VGAT (in group D), for GAD (in group E) and for GlyT2 (in group F), and indicate that these three groups of terminals are likely to belong to the same population. Numerous investigations have demonstrated that coexistence of GABA and glycine is frequently observed in axon terminals in the rat spinal cord (Mackie et al., 2003; Ornüing et al., 1994, 1996, 1998; Taal and Holstege, 1994). However, the proportions of the GABA/glycine terminals of the total number of inhibitory terminals varied with their origination, location and the animal age and species. For example, Todd and Sullivan (1990) found that in the dorsal horn of adult rat spinal cord, nearly all of the glycinergic cells were also GABA immunoreactive. In the ventral horn of neonatal rat spinal cord, however, Weber et al. (2007) reported that CIN terminals containing both GABA and glycine were fewer than those that only contain one of the two inhibitory amino acids. Contradictory results were obtained from studies of terminals contacting motoneurons in adult cat spinal cord, which showed that almost all of the GABAergic terminals contained glycine (Ornüing et al., 1996, 1998). Nevertheless, the results of present study suggest that in the contralateral lateral motor nuclei of adult rat spinal cord, most of the inhibitory terminals from ipsilateral CINs contain both GABA and glycine. However, this suggestion is only based on a statistical argument and has not been shown directly. To obtain direct evidence, further experiments should be performed by reacting sections with antibodies against GAD and glyT2.

In addition, several CTb labelled terminals displayed unexpected immunocytochemical characteristics. For example, in group E, occasional CTb terminals (less than 0.1%) were observed to be positive for VGLUT1 (Figure 3.15) and as discussed above, these terminals may be from descending tract cells labelled by the passage of fibres, such as raphe-spinal tract (Todd et al., 2003). Moreover, about 1% of CTb terminals were neither labelled by VGLUT1/2 nor VGAT in group D (Figure 3.13) and this result is similar to a previous study reporting that about 6% nerve terminals forming synapses with dendrites in the cat spinal motor nuclei were not enriched for glutamate, glycine or GABA (Ornüing et al., 1998). These “negative” terminals may not originate from CINs and they utilize some other types of neurotransmitters. For example, Shupliakov et al (1993) have shown that some terminals in the lamina IX of the cat spinal cord may contain putative neurotransmitters, such as aspartate and taurine. Another likely explanation might be that the concentration of antigen in these terminals was very low, and the antibodies did not reveal them. Similarly, in group F, 2.9% of

CTb terminals were found to be negative for both GlyT2 and VGLUT2 (Figure 3.16C), and these terminals may be immunoreactive for GABA only. In addition, a cluster of CTb terminals that were both GlyT2 and VGLUT2 immunoreactive was observed in group F (Figure 3.16D). This coexistence was not quantified because it was a very rare observation. Nevertheless, cells containing a mixture of excitatory and inhibitory neurotransmitters have been reported in spinal cord and hippocampus of adult animals by several studies (Gutierrez 2005; Sandler and Smith, 1991; Todd et al., 2003). It remains to be investigated whether this colocalization of excitatory and inhibitory neurotransmitters in the same terminal is due to a genetic mistake during cell development or it has a functional significance. However, it is worth keeping in mind that not all the neurotransmitters contained in an axon terminals act on the postsynaptic profile as their action depends on whether the corresponding receptor is present on the postsynaptic profile.

3.4.5 Functional considerations

The CPG has been generally accepted to be a neuronal network that generates rhythmic motor behaviours. However, observations on distribution of CPGs are not consistent. For example, *in vitro* preparations of neonatal rats showed that the hindlimb locomotor CPG is confined only to upper lumbar segments (Cazalets et al., 1995; Wheatley et al., 1994), while others reported that the ability to generate rhythmic activities in hindlimb muscles was distributed through out all lumbar segments (Kjaerulff and Kiehn, 1996; Kudo and Yamada, 1987). Irrespective of whether or not interneurons in lower lumbar segments are components of the hindlimb CPG, the present study clearly demonstrates a strong neuronal connection between the L5 and the L1/L3 segments on both sides of the spinal cord. Functionally speaking, the connectivity patterns of the short ascending propriospinal interneurons in the L5 segment to rostral lumbar segments are different. As discussed above, dorsal horn and lamina VII neurons located in the L5 segment predominantly projected to medial and lateral motor nuclei in the L1/L3 segments, respectively. This might suggest that these two populations of neurons may have different functions. One possibility could be that although interneurons located in dorsal horn and intermediate zone participate in both trunk and hindlimb movements, those located in ipsilateral dorsal horn, especially in deep dorsal horn, may be preferentially responsible for postural adjustment, whereas those located in ipsilateral lamina VII are tend to be involved in hindlimb movements. In contrast with ipsilateral neurons, similar proportions of CINs in

contralateral lamina VIII were labelled from medial and lateral motor nuclei injections. This may indicate that a similar proportion of CINs are required for coordinating left/right movements of hindlimb and trunk. Lamina VIII CINs are known to constitute the main group of neurons forming synaptic contacts with contralateral motoneurons (Alstermark and Kummel, 1990; Harrison et al., 1986; Hoover and Durkovic, 1992; Jankowska et al., 2003) and are considered to be fundamental parts of locomotor CPGs (Kiehn and Butt, 2003). Two subpopulations of CINs have been identified in lamina VIII, receiving monosynaptic input either from medial longitudinal fasciculus (MLF) or from group II muscle afferents (Jankowska et al., 2005). Both of them are involved in locomotion and determining different patterns of crossed reflexes (Armstrong, 1988; Deliagina et al., 2002; Jankowska et al., 2005; Mori et al., 2001; Noga et al., 2003), but they are modulated differently by descending monoamine systems (Hammar et al., 2004). Whether these two subgroups have different effects on coordination of hindlimb and trunk movements is not clear; therefore, it might be worth investigating the populations of lamina VIII CINs responsible for hindlimb and trunk movements by injecting different tracers into lateral and medial motor nuclei in the same segment. More detailed functions of CINs are discussed in the next chapter.

About 25% short ascending propriospinal interneurons in the L5 segment contain calbindin and/or calretinin, which are two of the most well described calcium binding proteins. In supraspinal levels of the central nervous system, their neuronal functions have been studied, for example in cortical neurons and hippocampal neurons (Mattson et al., 1991; Mockel and Fischer, 1994; Terro et al., 1998). Little is known about the exact function of neurons containing calbindin/calretinin in the spinal cord. However, because of their obvious role in buffering intracellular Ca^{2+} fluxes and resistance to Ca^{2+} induced excitotoxicity, cells expressing them might have higher resistance to degeneration during prolonged excitation (Airaksinen et al., 1997; Andressen et al., 1993; Edmonds et al., 2000). In addition, calbindin and calretinin are known as fast calcium buffer proteins, and provide cells with physiological features different to those containing slow calcium buffer proteins, such as parvalbumin (Bastianelli, 2003; Schwaller et al., 2002). For example, the presence of slow calcium buffer proteins and the absence of fast calcium buffer proteins provide the cerebellar stellate and basket cells the ability to fire at very high repetitive levels by keeping calcium level at near resting level (Bastianelli, 2003). Therefore, those propriospinal interneurons expressing the fast calcium buffers, calbindin and/or calretinin, may have more stabilized dynamics than

other cells without these proteins. Moreover, the different locations of calbindin and calretinin short ascending propriospinal interneurons indicates that at the neuronal level, they may contribute to particular roles in the network.

A small proportion of the total population of short ascending propriospinal interneurons in the L5 segment are cholinergic. It has been suggested that those ChAT cells located in lamina VI-VII and X, the so called partition and central canal cells, are the origin of “C boutons” (Miles et al., 2007). C boutons are known to make direct contacts with somata and proximal dendrites of motoneurons and are responsible for the increased motoneuron excitability during locomotor-related activity (Arvidsson et al., 1997; Hellstrom et al., 1999; 2003; Li et al., 1995; Nagy et al., 1993; Welton et al., 1999; Wilson et al., 2004). It can thus be suggested that these partition and central canal cells facilitate motoneurons to fire at a sufficient level so that appropriate muscle contraction is induced while excitatory input to motoneurons is kept to a minimal level. In addition, a strong relationship between cholinergic spinal interneurons and production of fictive locomotion has been reported by Huang et al. (2000), who found that an increased number of cholinergic neurons located in the medial laminae VII-VIII express c-fos during fictive locomotion. Hence, it could be hypothesised that these ChAT-positive propriospinal interneurons play prominent role in the generation of rhythmic activity in the spinal cord, especially those cholinergic CINs providing propriospinal cholinergic innervation to coordinate activities between the two sides of the spinal cord.

In conclusion, the present results are of relevance to understanding the organization of networks involved in intra-segmental coordination of hindlimb movements. This study shows that L5 propriospinal interneurons, especially those located in contralateral lamina VIII and ipsilateral laminae V-VII, have extensive ascending projections to ipsilateral motor nuclei of the upper lumbar segments. Moreover, in the upper lumbar segments, both excitatory and inhibitory CINs give off axons descending to the contralateral lateral motor nuclei of the L5 segment and form contacts with motoneurons.

Figure 3.1. Photomicrograph of representative sections illustrating the injection site of CTb in the medial motor nuclei of the L1 segment (A) and the lateral motor nuclei of the L3 segment (B). The sections were reacted with an immunoperoxidase method to reveal CTb. The borders of the grey matters and the cytoarchitectonic laminae of the grey matter are indicated by grey lines. Roman numerals indicate the Rexed laminae of the grey matter. LSN, lateral spinal nucleus; cc, central canal. Scale bar = 500 μ m.

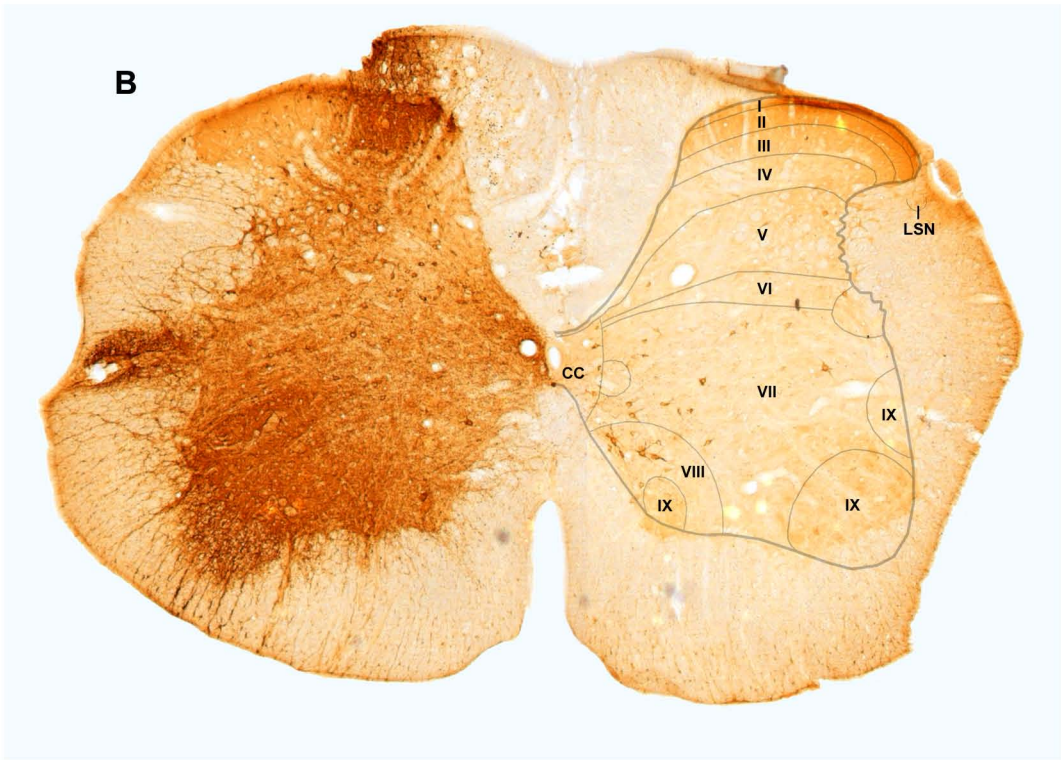
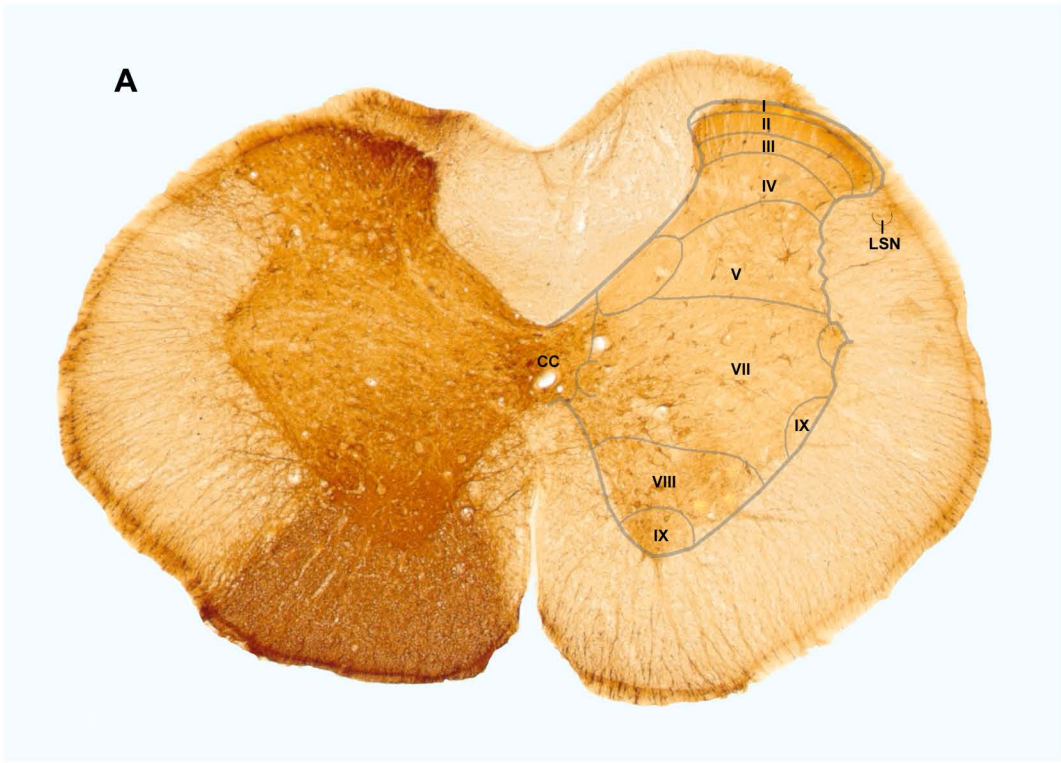
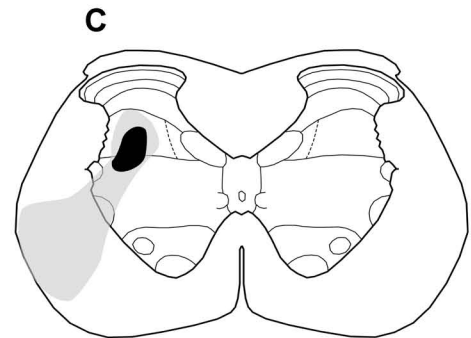
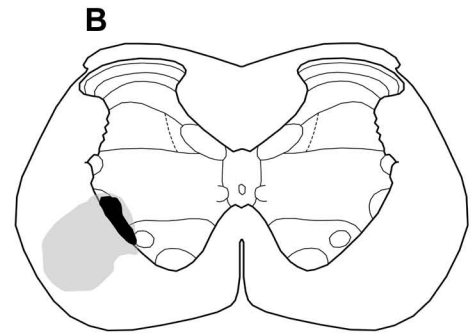
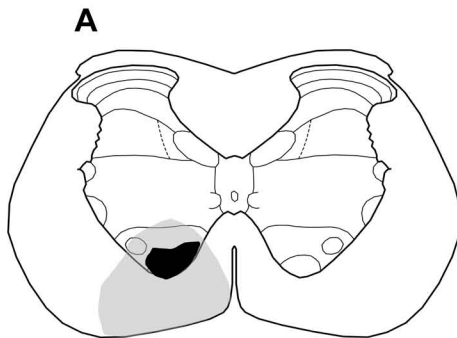


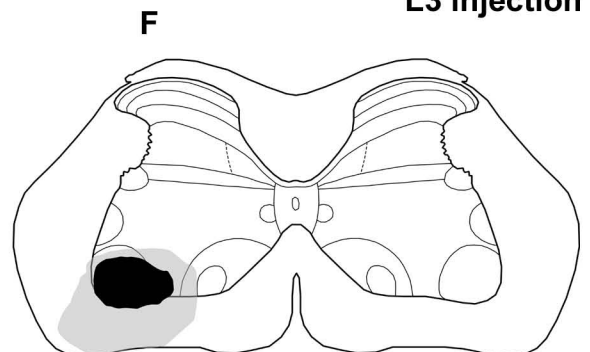
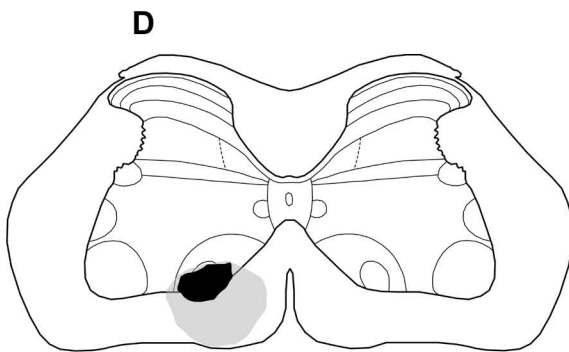
Figure 3.2. Reconstruction of the injection sites for all 7 experiments (A-G, corresponding to those in Table 3.4 and 3.5). The black shaded area shows the CTb injection site and the grey shaded area shows the maximum spread of CTb. Drawings are based on those in Paxions and Watson (1997). The dashed vertical and horizontal lines divide the experiments into the medial/lateral motor nuclei injection group and the L1/L3 injection group, respectively.

Medial motor nuclei injection vs. Lateral motor nuclei injection



L1 injection

vs.



L3 injection

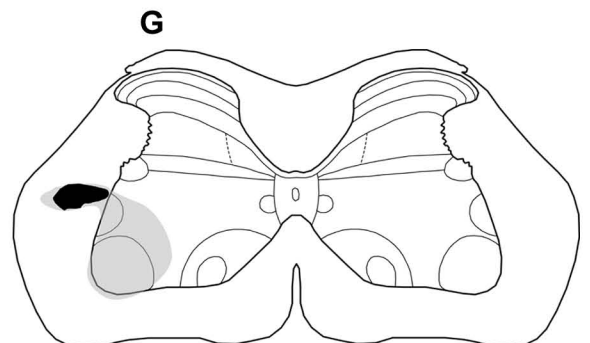
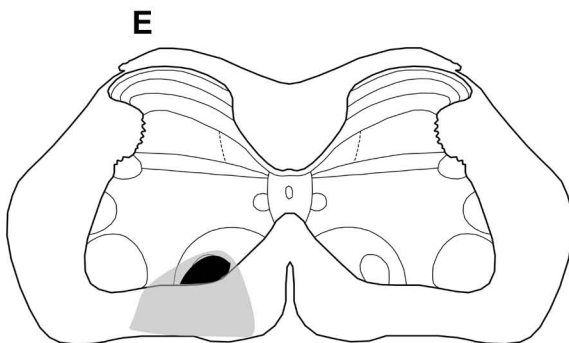
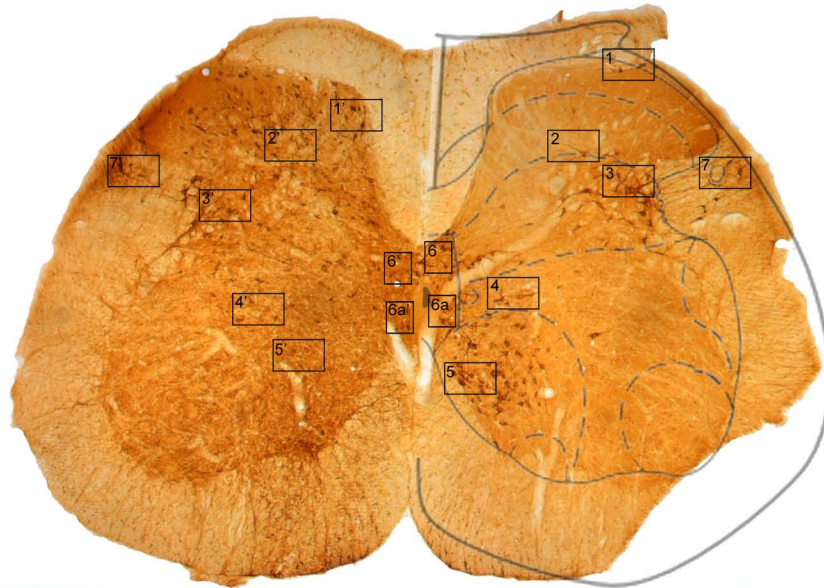


Figure 3.3. Retrograde labelling of neurons in the L5 segment following CTb injections in the L3 segment. The large photomicrograph on the top shows a general overview of the CTb retrogradely labelled cells after a reaction with immunoperoxidase. Details of areas demarcated by the boxes are shown in the small panels 1-7 and 1'-7'. The borders of the grey and white matter are represented by continuous lines. The cytoarchitectonic laminae of the grey matter for cell counting (corresponding to the laminae shown in small panels) are indicated by dashed lines. The right side of the section is contralateral to the side of CTb injection. Panels 1-7 and 1'-7' illustrate the soma and proximal dendrites of CTb labelled cells in the corresponding laminae. Scale bar = 250 μm (for the large panel); 50 μm (for all the small panels).

Ipsilateral side

Contralateral side



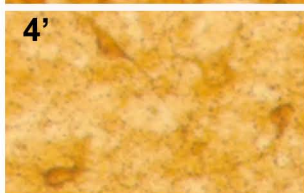
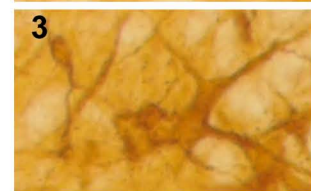
Laminae I-II



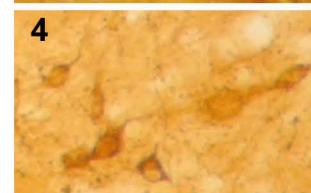
Laminae III-IV



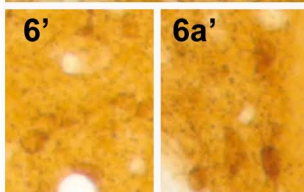
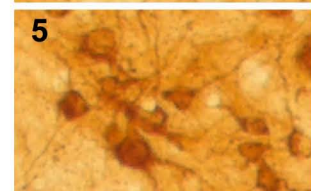
Laminae V-VI



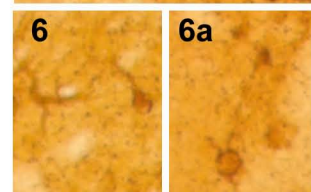
Lamina VII



Lamina VIII



Lamina X



LSN

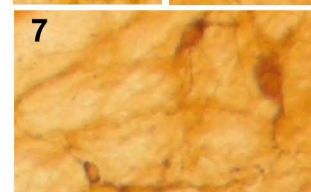


Figure 3.4. Distribution of cells retrogradely labelled by CTb in the L5 segment. Each section is a plot of all cells from each of the 8 sections selected from the L5 segment for each experiment (A-G, corresponding to those in Figure 3.2 and Table 3.4 and 3.5). The cells were plotted on the L5 section from the atlas of Paxions and Watson (1997). The right side of sections is contralateral to the side of CTb injection. The black dots represent cell bodies of CTb labelled cells. The dashed vertical and horizontal lines divided the experiments into the medial/lateral motor nuclei injection group and the L1/L3 injection group, respectively.

Medial motor nuclei injection vs. Lateral motor nuclei injection

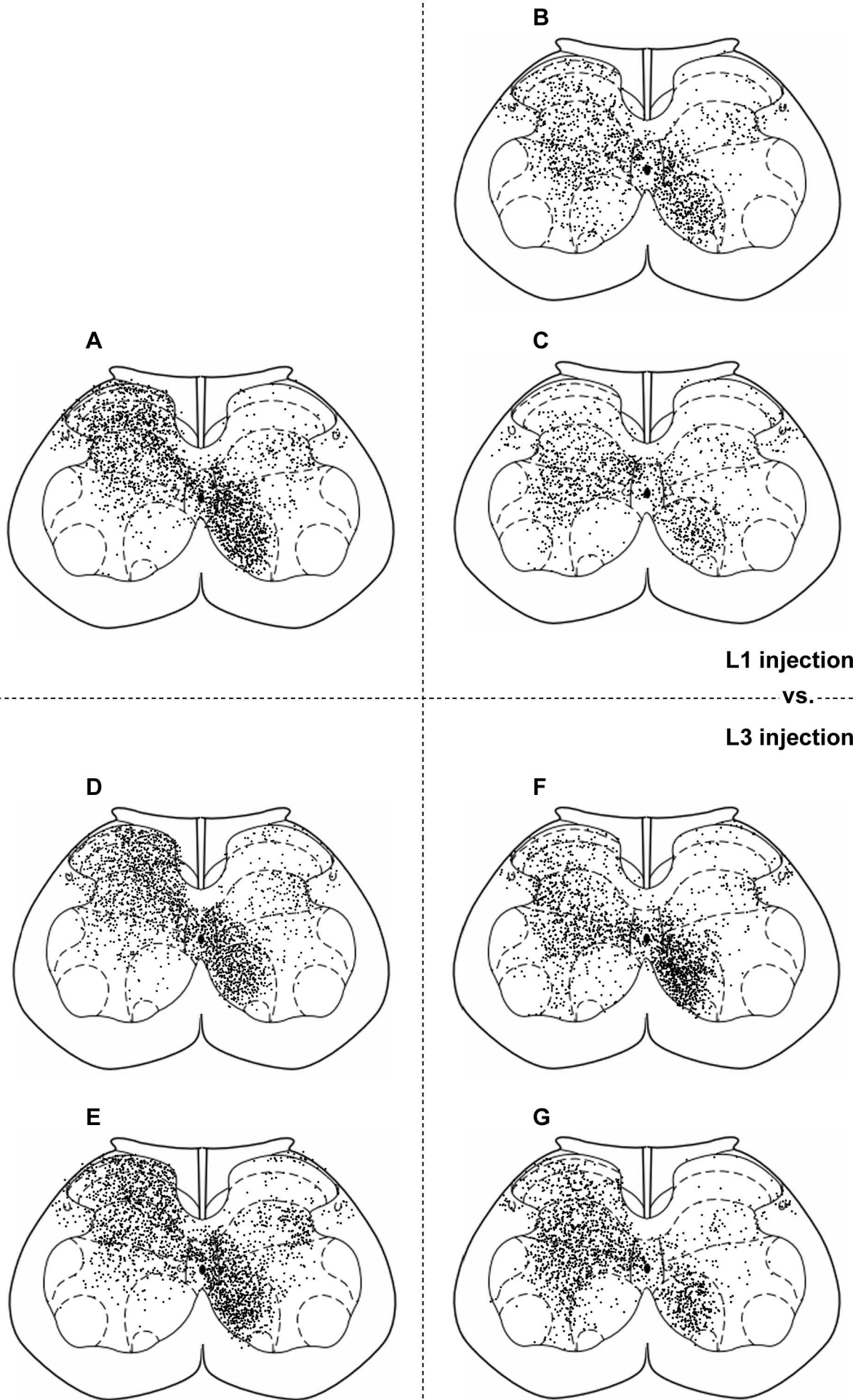


Figure 3.5. Laminar distribution of CTb retrogradely labelled cells in the L5 segment. Black asterisks and red asterisks indicate that the percentage of the cells in the corresponding lamina(e) are statistically significantly higher than those in other laminae of the contralateral side and the ipsilateral side, respectively (ANOVA, $p < 0.01$). Comparisons are made within the same side and unmarked differences are not significant. A-G correspond to those in Figure 3.2, 3.4 and Table 3.4, 3.5. The dashed vertical and horizontal lines divide the experiments into the medial/lateral motor nuclei injection group and the L1/L3 injection group, respectively.

Medial motor nuclei injection vs. Lateral motor nuclei injection

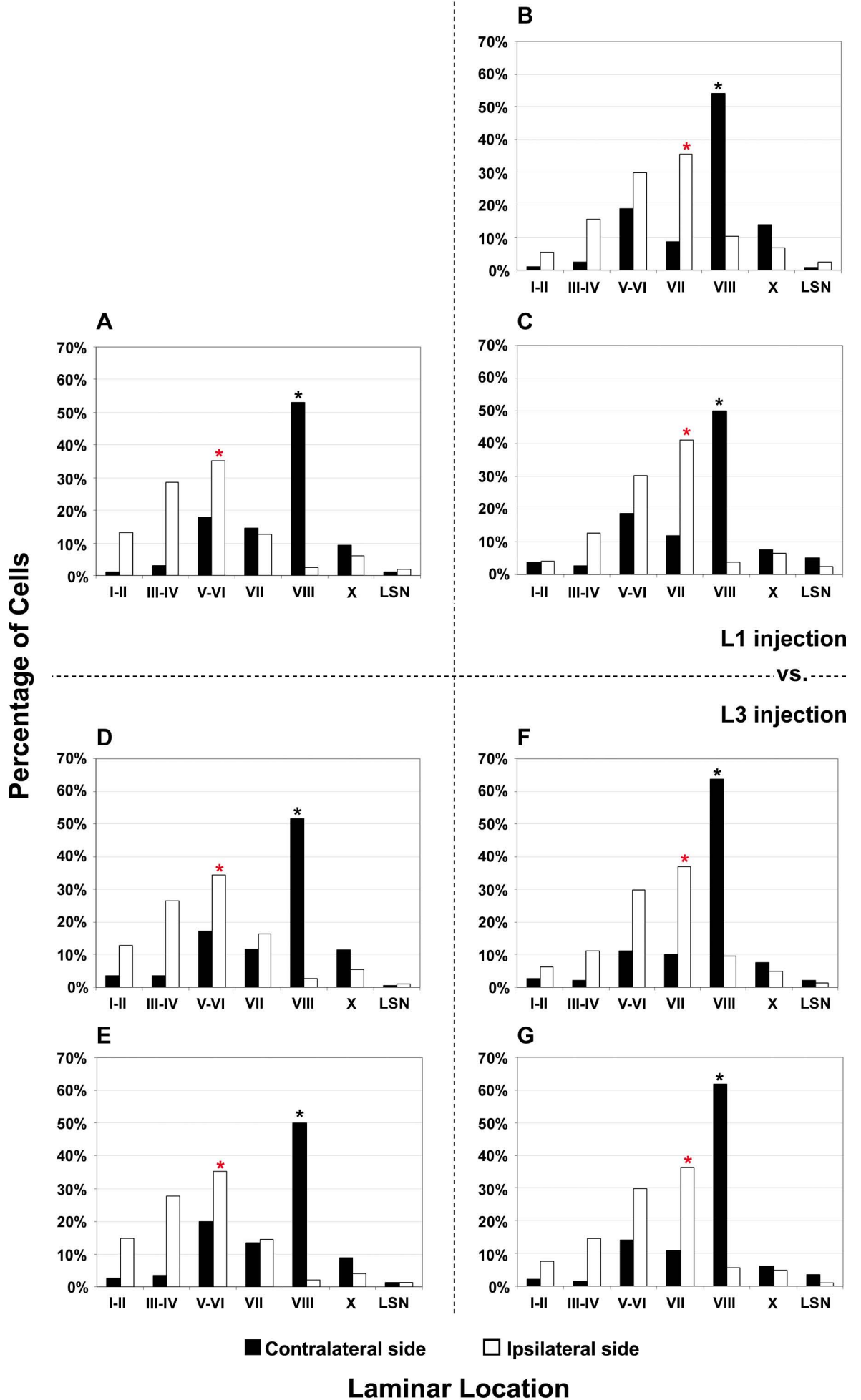


Figure 3.6a. Three colour confocal microscope images illustrating the distribution of CTb labelled cells and their immunoreactivities for calbindin and/or calretinin. (A) Reconstruction of an entire L5 section by a series of projected confocal images showing a general overview of CTb labelled cells (in red) with or without calbindin (in green) and/or calretinin (in blue) immunostaining. Details of the areas demarcated by the boxes are shown in Figure 6b (see the following page). Scale bar = 100 μm (A)

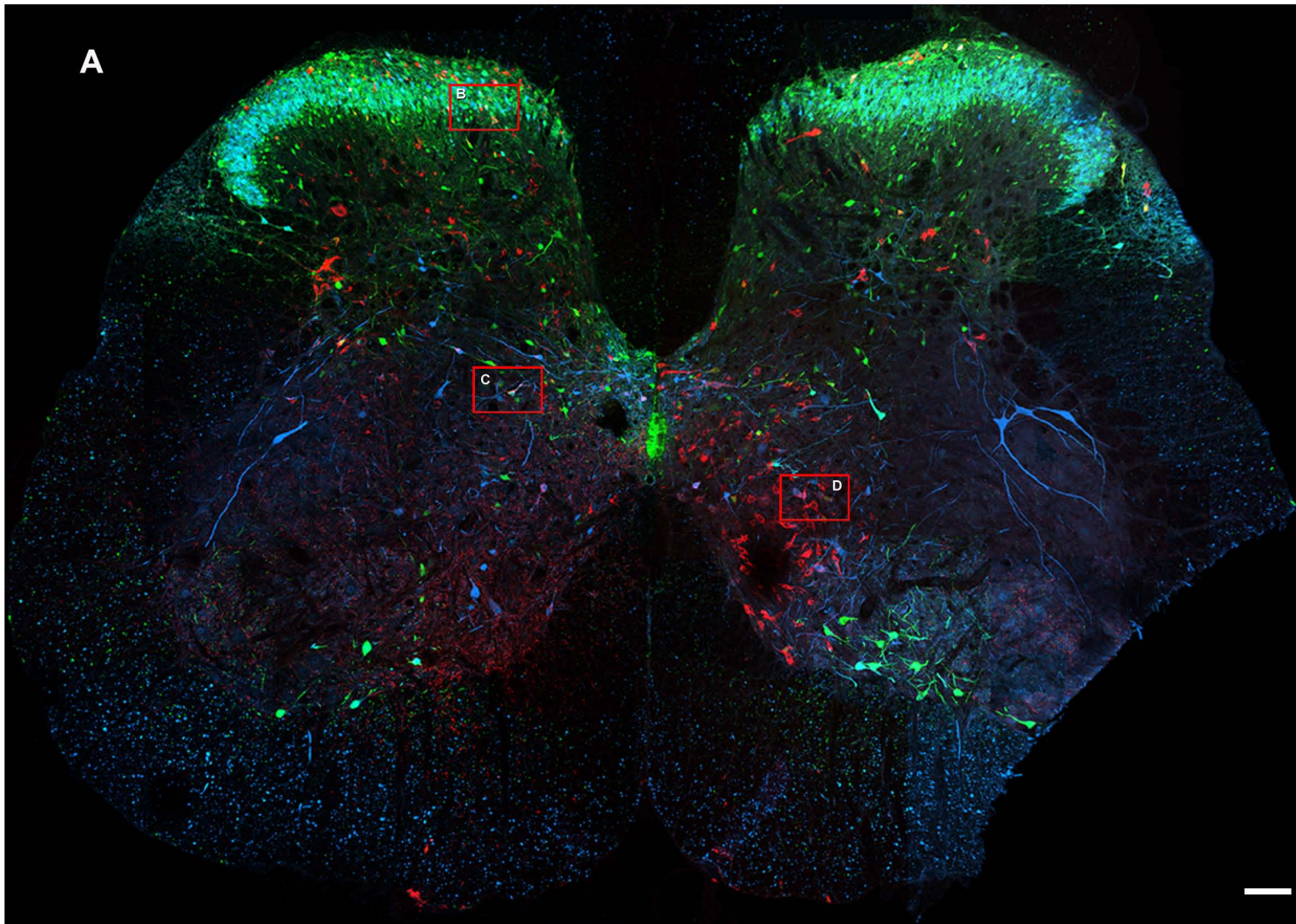


Figure 3.6b. Three colour confocal microscope images illustrating the distribution of CTb labelled cells and their immunoreactivities for calbindin and/or calretinin. (B1-B4, C1-C4, and D1-D4) are single optical sections and B4, C4, and D4 show merged images. Arrows in B1-B4 and D1-D4 indicate CTb labelled cells that were calbindin immunoreactive. Arrowheads in B1-B4 and C1-C4 indicate CTb labelled cells that were immunopositive for both calbindin and calretinin, and arrowheads in D1-D4 indicate CTb labelled cells that were immunopositive for calretinin. Asterisk in B1-B4 and D1-D4 indicate CTb labelled cells that were negative for both calbindin and calretinin. Scale bar = 10 μm (B1-B4, C1-C4, and D1-D4).

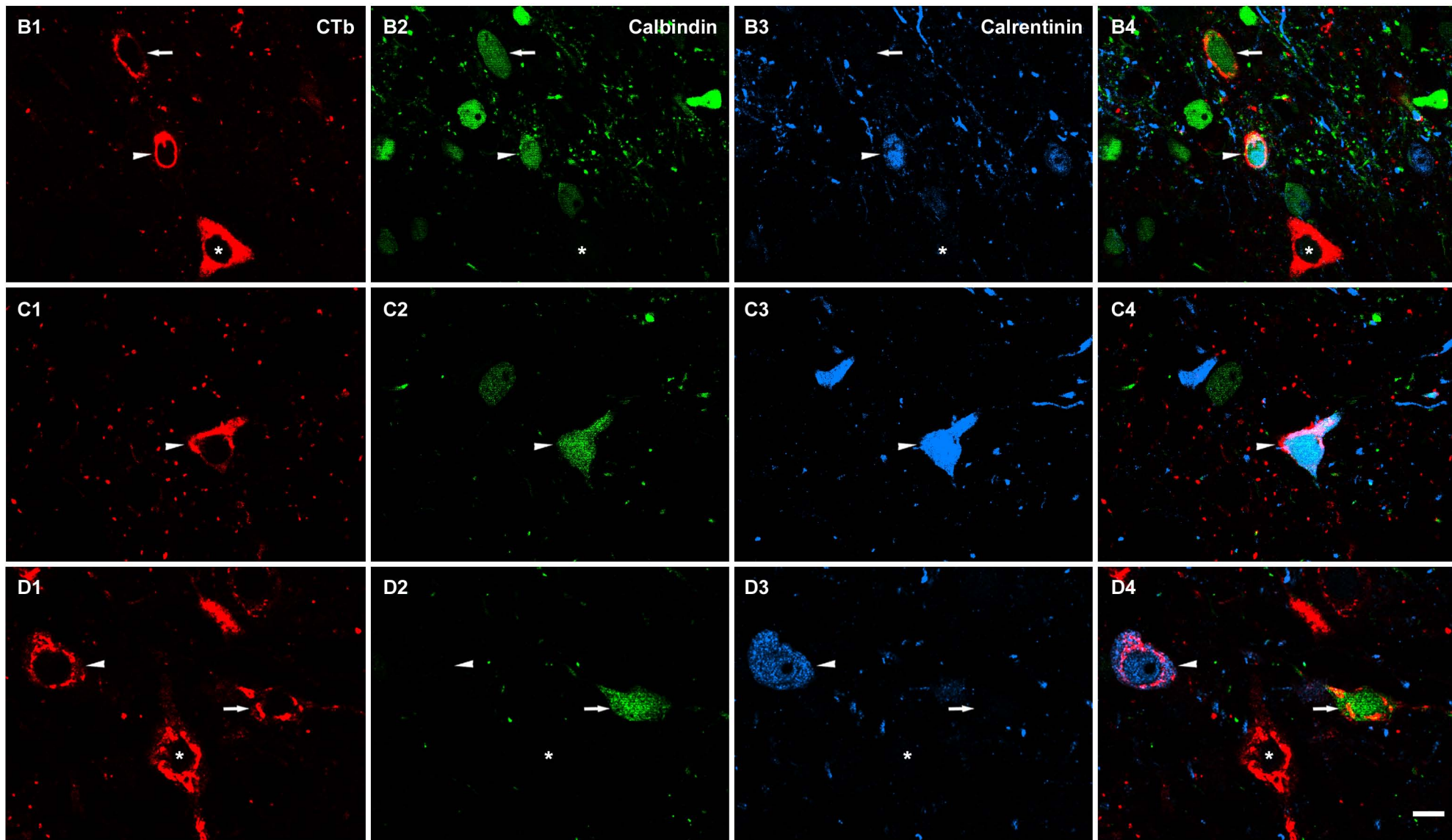
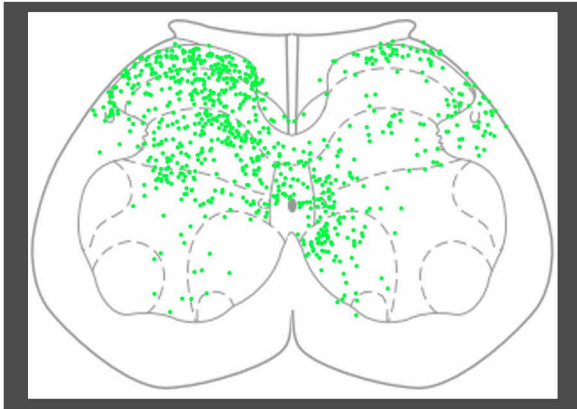
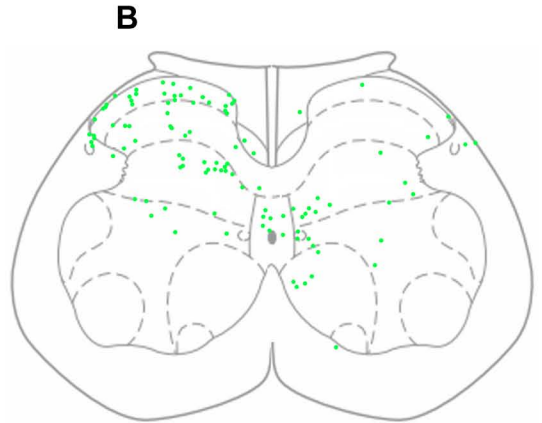
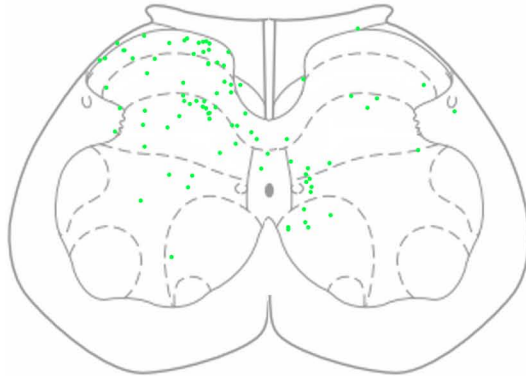


Figure 3.7. Distribution of CTb labelled cells with calbindin immunoreactivity in the L5 segment. The section in the box at top left is pooled data showing the overall distribution of CTb/calbindin immunoreactive cells plotted from 4 sections randomly selected from the L5 segment for all 7 rats. A-G (corresponding to those in Table 3.4 and 3.5) show the cell distribution for each experiment. The cells were plotted on the L5 section from the atlas of Paxinos and Watson (1997). The right side of sections is contralateral to the side of CTb injection. The green dots represent cell bodies of CTb cells with calbindin immunostaining. The dashed vertical and horizontal lines divided the experiments into the medial/lateral motor nuclei injection group and the L1/L3 injection group, respectively.

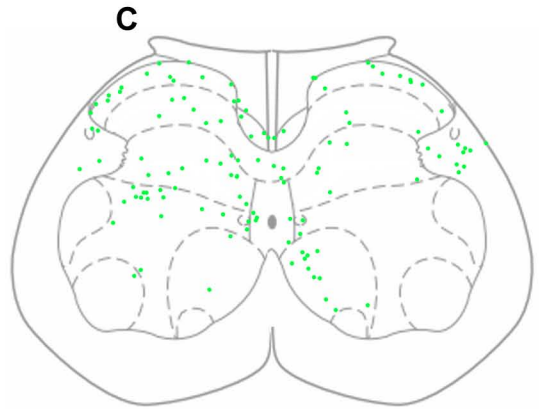
Medial motor nuclei injection vs. Lateral motor nuclei injection



A



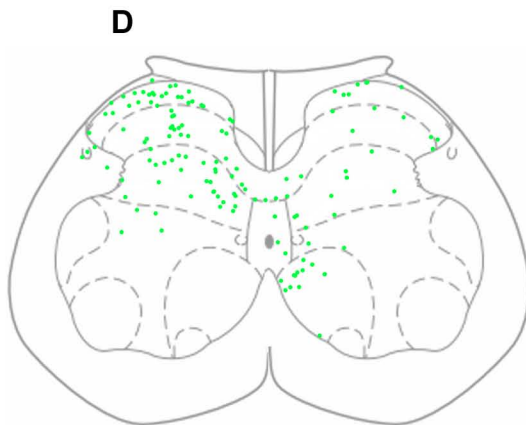
B



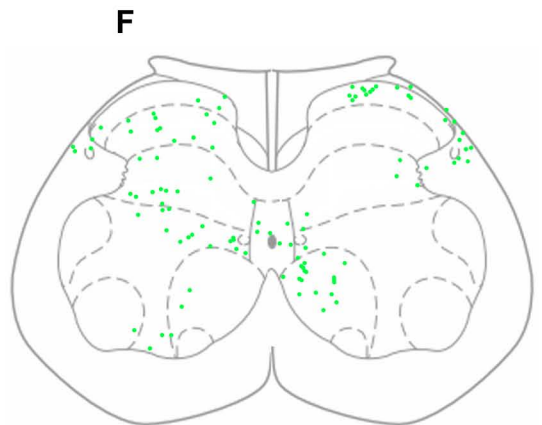
C

**L1 injection
vs.**

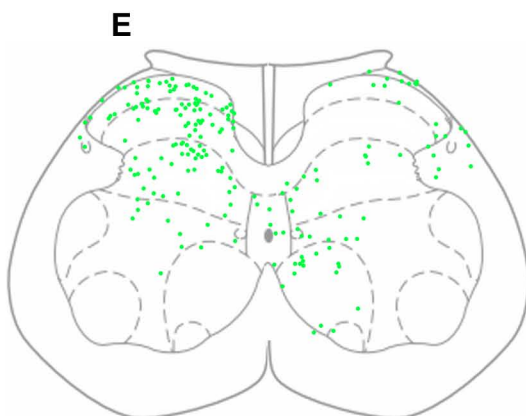
L3 injection



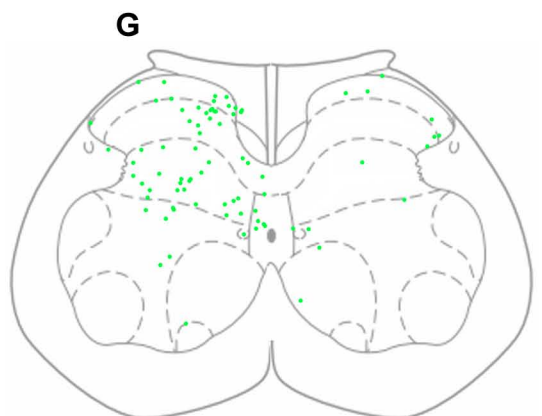
D



F



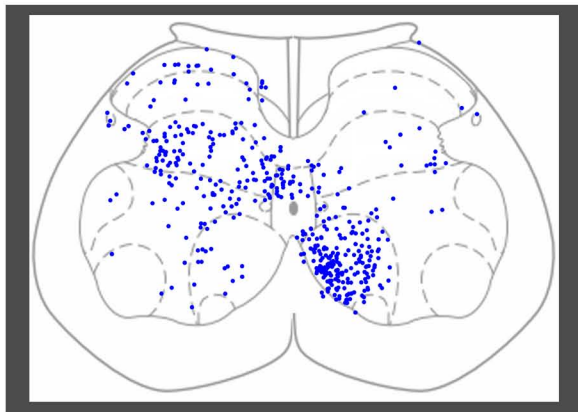
E



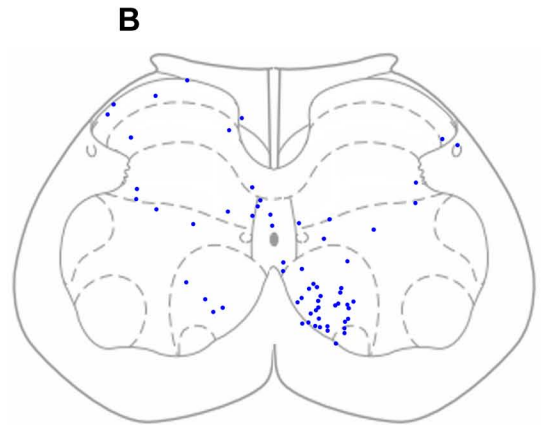
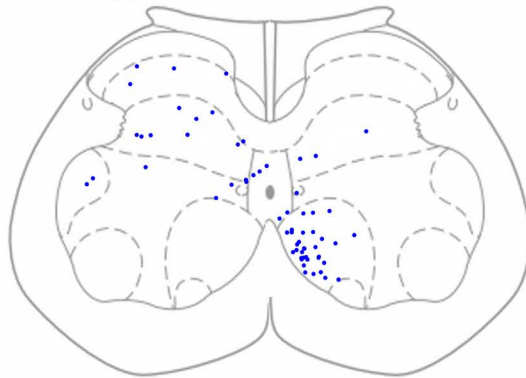
G

Figure 3.8. Distribution of CTb labelled cells with calretinin immunoreactivity in the L5 segment. The section in the box at top left is pooled data showing the overall distribution of the CTb/calretinin immunoreactive cells plotted from 4 sections randomly selected from the L5 segment for all 7 rats. A-G (corresponding to those in Table 3.1, 3.4, and 3.5) show the cell distribution for each experiment. The cells were plotted on the L5 section from the atlas of Paxinos and Watson (1997). The right side of sections is contralateral to the side of CTb injection. The blue dots represent cell bodies of CTb cells with calretinin immunostaining. The dashed vertical and horizontal lines divided the experiments into the medial/lateral motor nuclei injection group and the L1/L3 injection group, respectively.

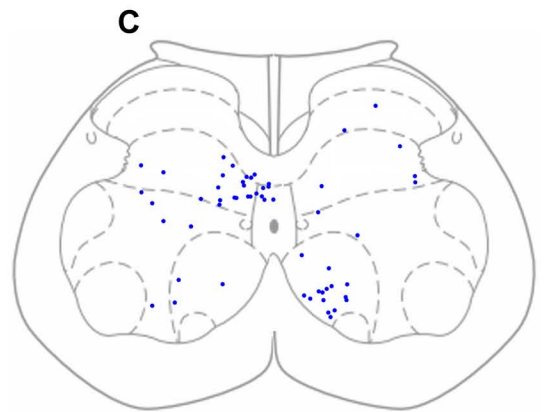
Medial motor nuclei injection vs. Lateral motor nuclei injection



A



B



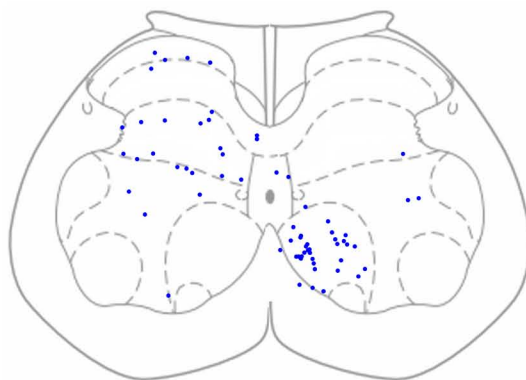
C

L1 injection

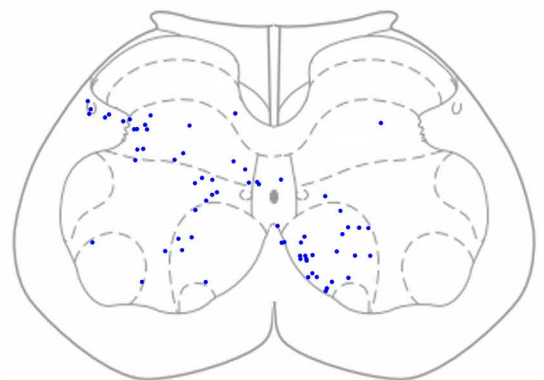
vs.

L3 injection

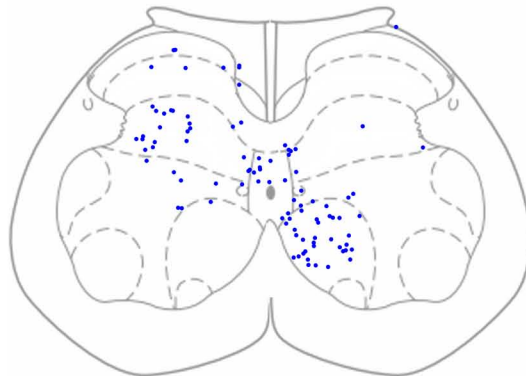
D



F



E



G

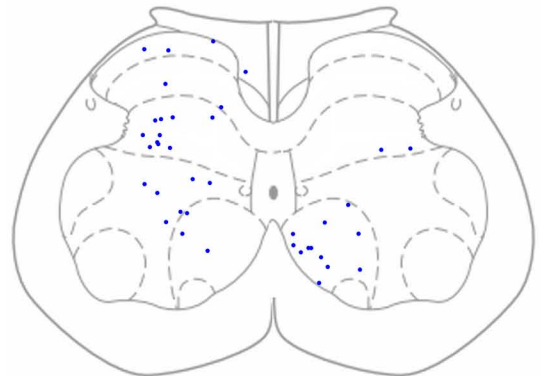
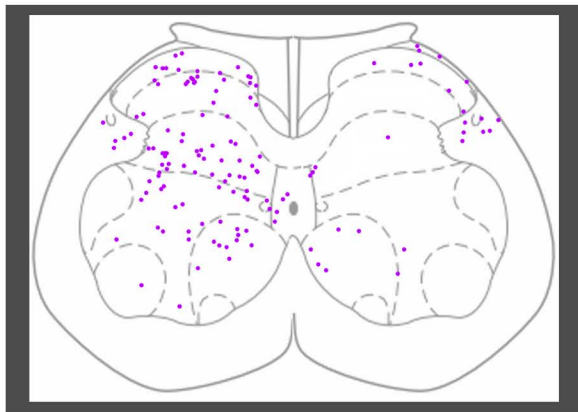
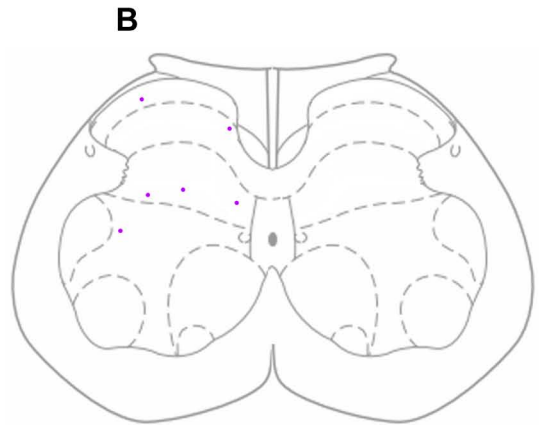


Figure 3.9. Distribution of CTb labelled cells with both calbindin and calretinin immunoreactivity in the L5 segment. The section in the box at top left is pooled data showing the overall distribution which compiles all the CTb cells positive for both calbindin and calretinin immunoreactivity plotted from 4 sections randomly selected from the L5 segment for all 7 rats. A-G (corresponding to those in Table 3.1, 3.4, and 3.5) show the cell distribution for each experiment. The cells were plotted on the L5 section from the atlas of Paxinos and Watson (1997). The right side of sections is contralateral to the side of CTb injection. The purple dots represent cell bodies of CTb cells with both calbindin and calretinin immunostaining. The dashed vertical and horizontal lines divided the experiments into the medial/lateral motor nuclei injection group and the L1/L3 injection group, respectively.

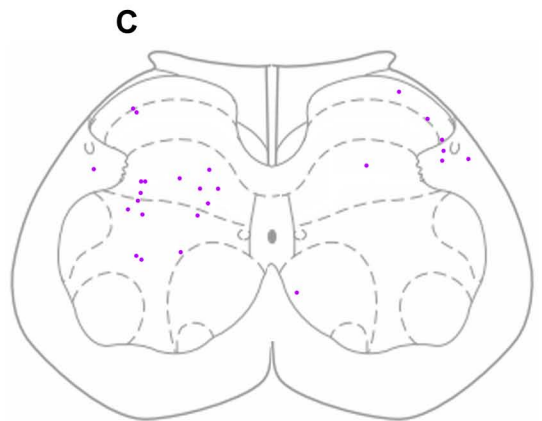
Medial motor nuclei injection vs. Lateral motor nuclei injection



A



B

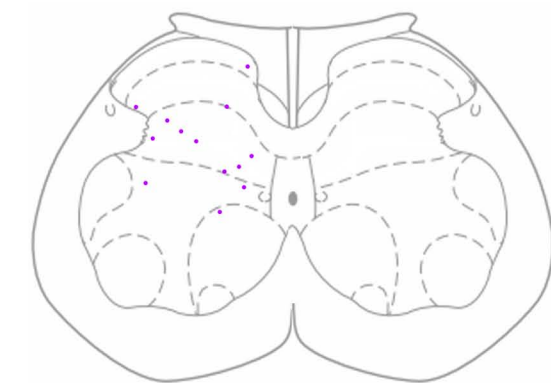


C

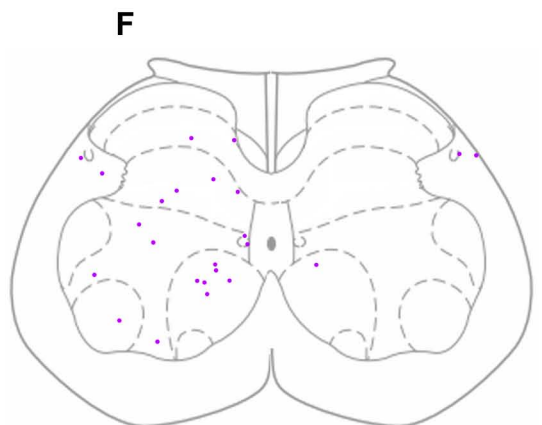
L1 injection

vs.

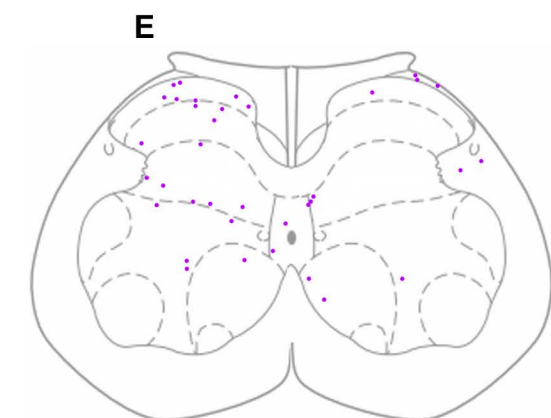
L3 injection



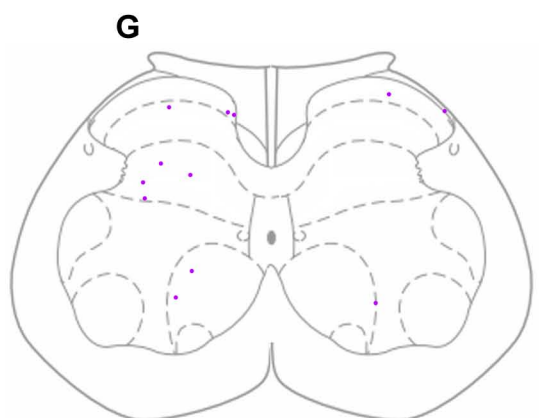
D



F



E



G

Figure 3.10. Laminar distribution of CTb labelled cells with calbindin immunoreactivity (A), calretinin immunostaining (B), and both calbindin and calretinin immunoreactivity (C) in the L5 segment for the 7 experiments. Error bars are standard deviations. Black asterisks and red asterisks indicate the percentage of the cells in the corresponding lamina(e) are statistically significant higher than those in other laminae of the contralateral side and the ipsilateral side, respectively (ANOVA, $p < 0.05$). Comparisons are made within the same side and unmarked differences are not significant.

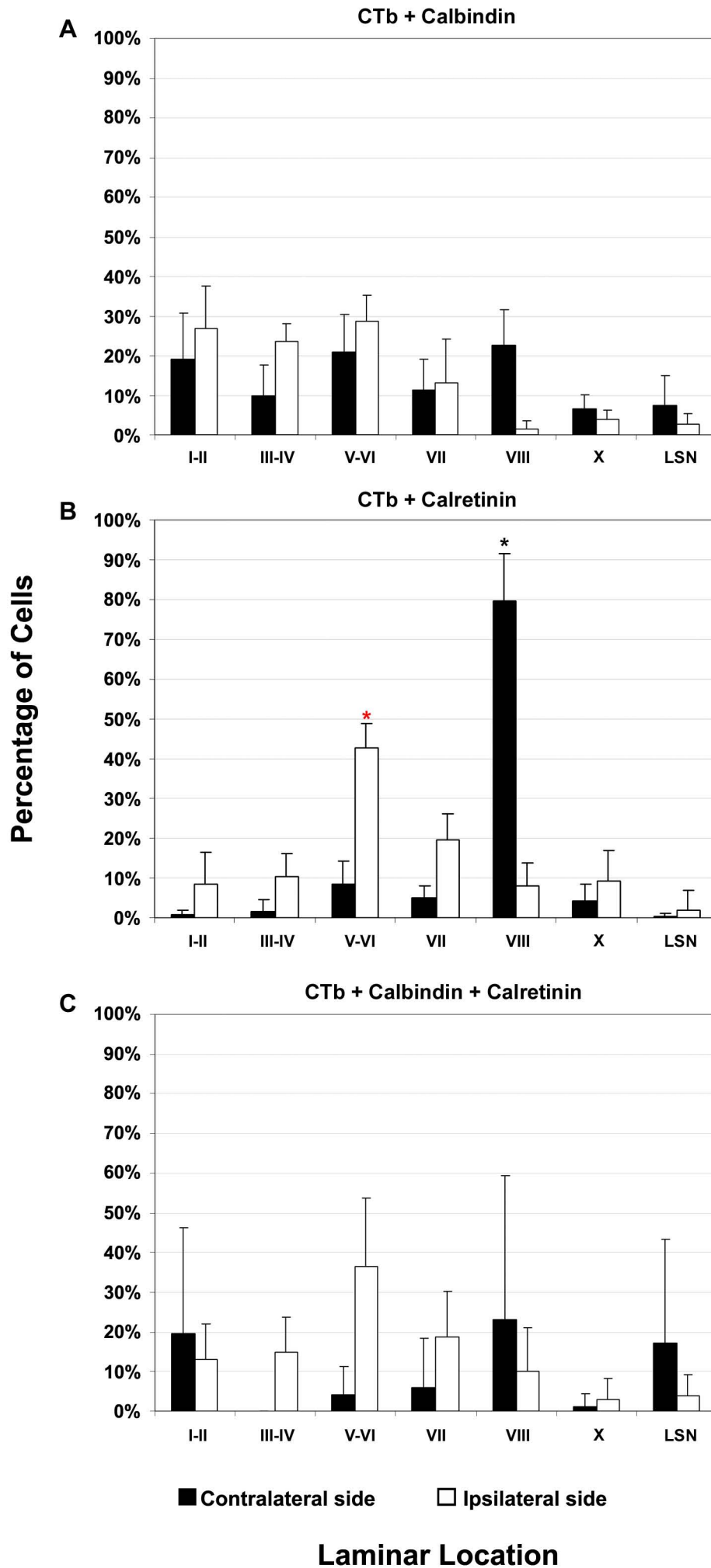


Figure 3.11. Distribution of cells within laminae at the L5 segmental level for the 7 experiments. Error bars are standard deviations. The red, green, blue and purple bars represent cells labelled by CTb alone, cells labelled by CTb and calbindin, cells labelled by CTb and calretinin, and CTb labelled cells immunopositive for both calbindin and calretinin, respectively.

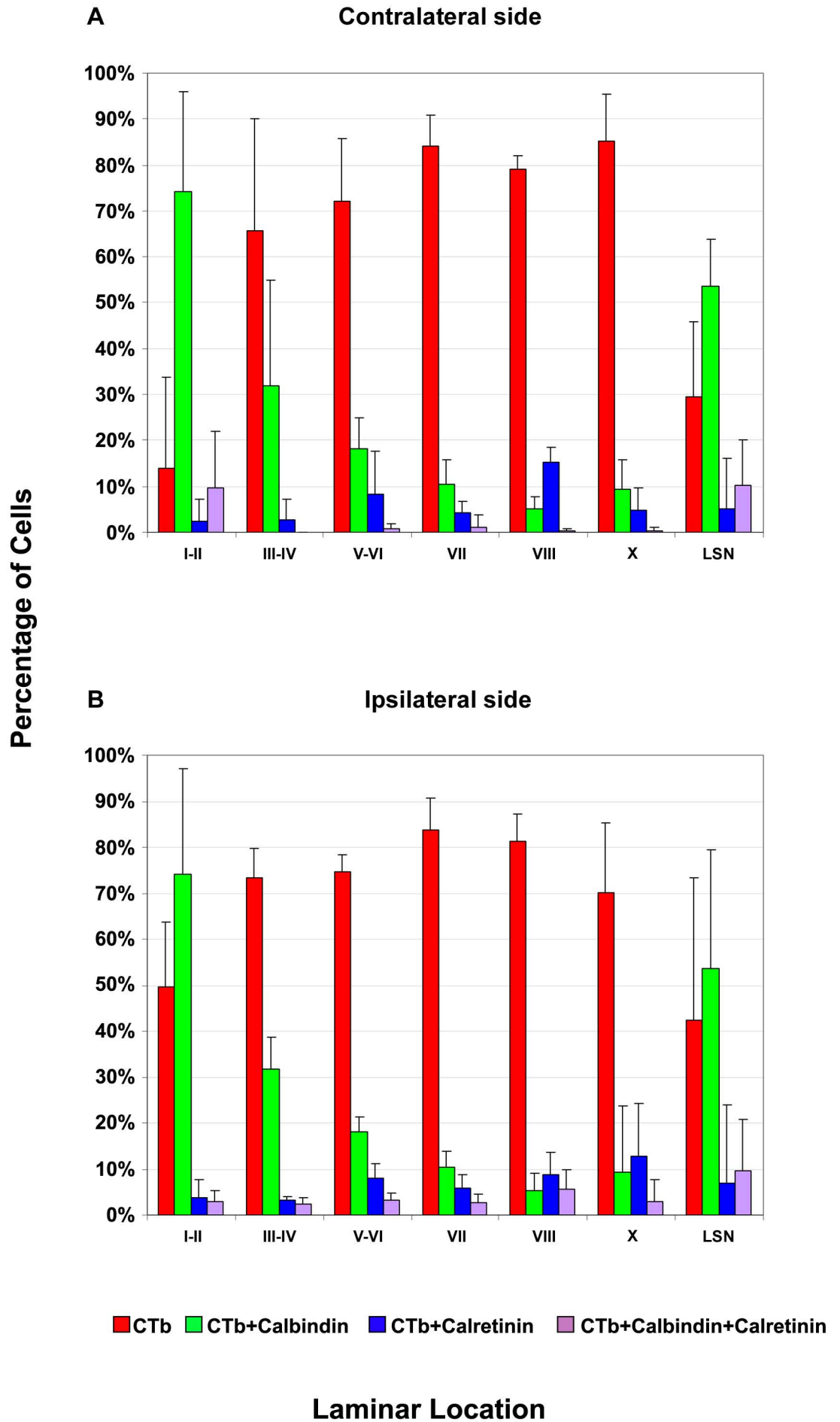


Figure 3.12A. Single optical sections illustrate CTb labelled neurons that were immunopositive for ChAT located in bilaterally in laminae X around the central canal. CTb labelled cells are shown in red (A1 and A4), ChAT immunoreactivity in green (A2 and A5). A3 and A6 show merged images confirming the double labelling of CTb and ChAT. Arrows indicate CTb labelled cells that were also ChAT immunoreactive. The right hand side of the central canal is the contralateral side to the injection site. *cc*, central canal. Scale bar = 20µm.

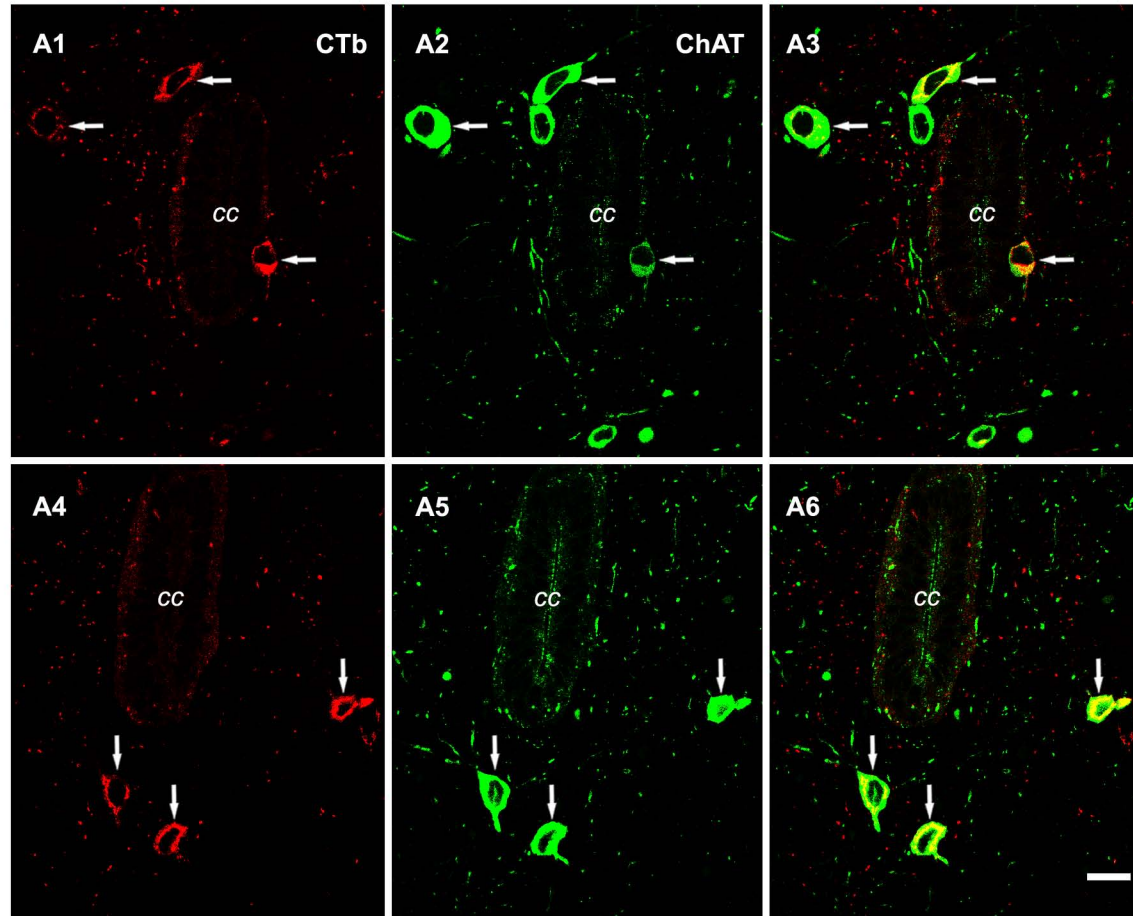


Figure 3.12B, C. Single optical sections illustrating CTb labelled neurons that were immunopositive for ChAT located in ipsilateral laminae VI-VII (B) and contralateral lamina VIII (C). CTb labelled cells are shown in red, ChAT immunoreactivity in green. The areas demarcated by boxes in B and C are shown in B1-B3 and C1-C3. Arrows in B and C indicate another two CTb labelled cells that were also ChAT immunoreactive. B3 and C3 show merged images confirming the double labelling of CTb and ChAT. The right hand side of the central canal is the contralateral side to the injection site. *cc*, central canal. Scale bar = 50µm (B, C), 5 µm (B1-B3, C1-C3).

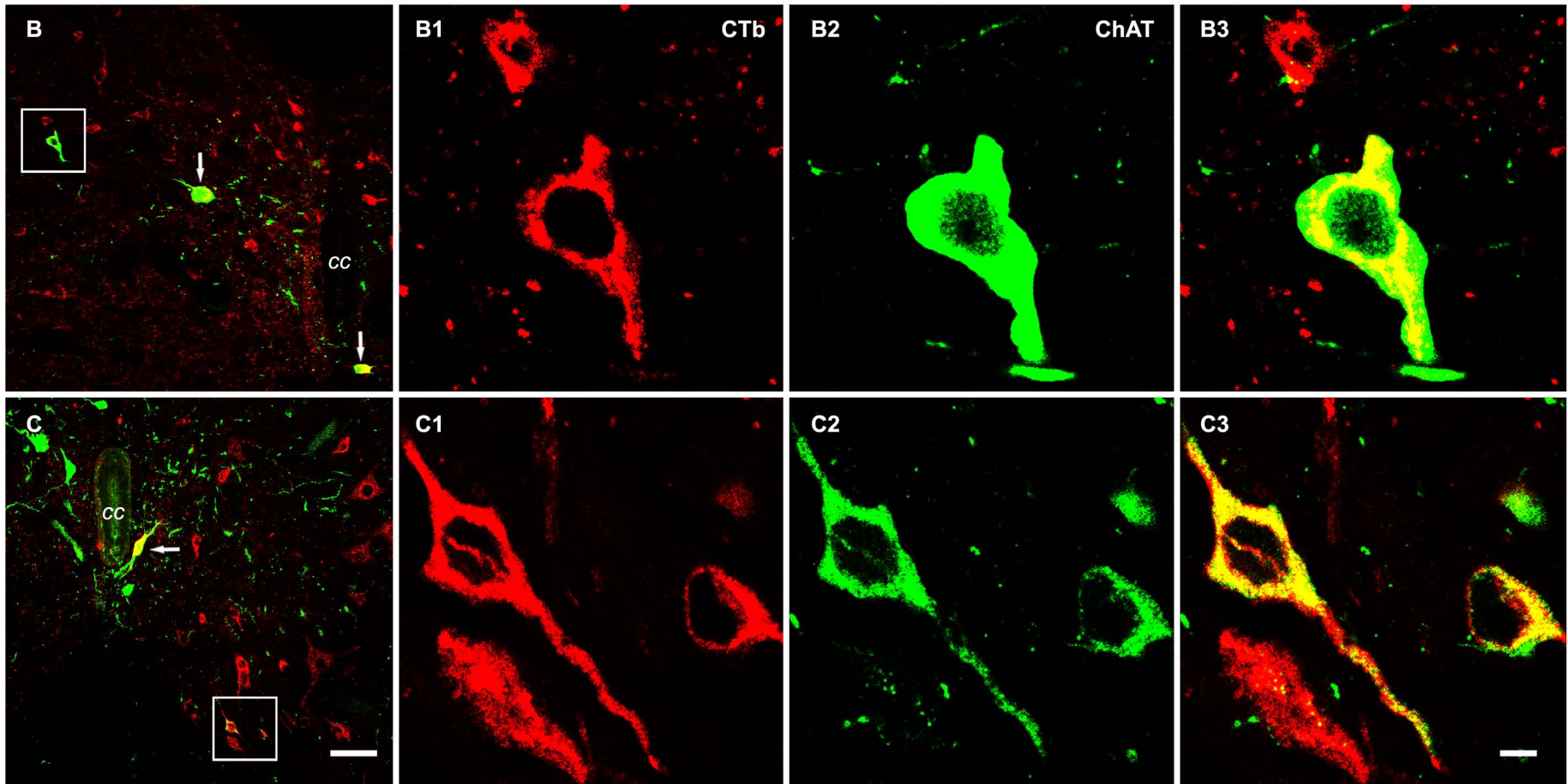


Figure 3.13a. Sequential immunocytochemistry for CTb labelled terminals with VGLUT1/2 or VGAT immunoreactivity. (A and A') A general overview of CTb labelled terminals and their neurotransmitter content before (A) and after (A') a reaction with a fourth antibody against ChAT. Details of the areas demarcated by the boxes are shown in B1-B4, and B1'-B4'. (B1-B4) Single optical sections illustrating the neurotransmitter content of terminals that were labelled by CTb (shown in red). Immunoreactivity for VGAT is shown in green, and immunoreactivity for VGLUT1 and VGLUT2 is in blue. B4 and B4' show merged images confirming the immunocytochemical characteristics of the examined terminals. Arrows in B1-B4 indicate CTb labelled excitatory terminals that were positive for VGLUT1/2 but negative for VGAT. Arrowheads in B1-B4 indicate CTb labelled inhibitory terminals that were positive for VGAT but negative for VGLUT1/2. The larger arrows in B1-B4 indicate a CTb labelled terminal without immunolabelling for either VGAT or VGLUT. (B1'-B4') Single optical sections of the same terminals that were rescanned after sequential incubation with a fourth antibody against ChAT. The extra green labelling present in B2' which is absent in B2 corresponds to additional ChAT immunostaining which labels motoneurons. Therefore, arrows (D) and arrowhead (D) in B4' indicate excitatory and inhibitory terminals in contact with motoneuron dendrites, respectively. The arrow (S) in B4' indicates the terminals making contact with a motoneuron cell body. The unattributed arrows and arrowheads in B4' indicate excitatory and inhibitory terminals that were not in contact with motoneurons, respectively. Scale bar = 10 μm (A, A'); 5 μm (B1-B4, B1'-B4').

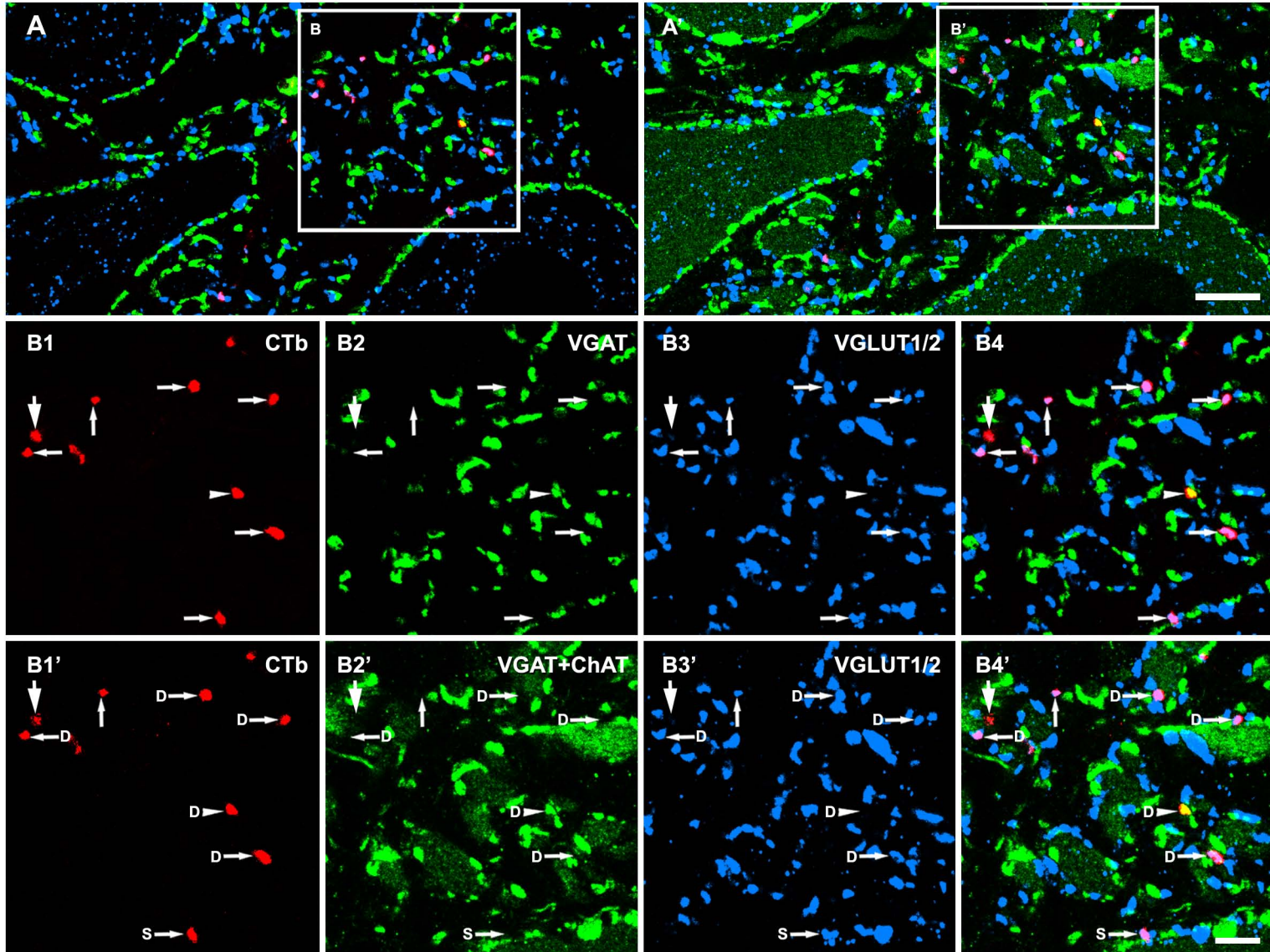


Figure 3.6a. Three colour confocal microscope images illustrating the distribution of CTb labelled cells and their immunoreactivities for calbindin and/or calretinin. (A) Reconstruction of an entire L5 section by a series of projected confocal images showing a general overview of CTb labelled cells (in red) with or without calbindin (in green) and/or calretinin (in blue) immunostaining. Details of the areas demarcated by the boxes are shown in Figure 6b (see the following page). Scale bar = 100 μm (A)

Figure 3.6b. Three colour confocal microscope images illustrating the distribution of CTb labelled cells and their immunoreactivities for calbindin and/or calretinin. (B1-B4, C1-C4, and D1-D4) are single optical sections and B4, C4, and D4 show merged images. Arrows in B1-B4 and D1-D4 indicate CTb labelled cells that were calbindin immunoreactive. Arrowheads in B1-B4 and C1-C4 indicate CTb labelled cells that were immunopositive for both calbindin and calretinin, and arrowheads in D1-D4 indicate CTb labelled cells that were immunopositive for calretinin. Asterisk in B1-B4 and D1-D4 indicate CTb labelled cells that were negative for both calbindin and calretinin. Scale bar = 10 μm (B1-B4, C1-C4, and D1-D4).

Figure 3.12A. Single optical sections illustrate CTb labelled neurons that were immunopositive for ChAT located in bilaterally in laminae X around the central canal. CTb labelled cells are shown in red (A1 and A4), ChAT immunoreactivity in green (A2 and A5). A3 and A6 show merged images confirming the double labelling of CTb and ChAT. Arrows indicate CTb labelled cells that were also ChAT immunoreactive. The right hand side of the central canal is the contralateral side to the injection site. *cc*, central canal. Scale bar = 20µm.

Figure 3.12B, C. Single optical sections illustrating CTb labelled neurons that were immunopositive for ChAT located in ipsilateral laminae VI-VII (B) and contralateral lamina VIII (C). CTb labelled cells are shown in red, ChAT immunoreactivity in green. The areas demarcated by boxes in B and C are shown in B1-B3 and C1-C3. Arrows in B and C indicate another two CTb labelled cells that were also ChAT immunoreactive. B3 and C3 show merged images confirming the double labelling of CTb and ChAT. The right hand side of the central canal is the contralateral side to the injection site. *cc*, central canal. Scale bar = 50 μ m (B, C), 5 μ m (B1-B3, C1-C3).

Figure 3.13a. Sequential immunocytochemistry for CTb labelled terminals with VGLUT1/2 or VGAT immunoreactivity. (A and A') A general overview of CTb labelled terminals and their neurotransmitter content before (A) and after (A') a reaction with a fourth antibody against ChAT. Details of the areas demarcated by the boxes are shown in B1-B4, and B1'-B4'. (B1-B4) Single optical sections illustrating the neurotransmitter content of terminals that were labelled by CTb (shown in red). Immunoreactivity for VGAT is shown in green, and immunoreactivity for VGLUT1 and VGLUT2 is in blue. B4 and B4' show merged images confirming the immunocytochemical characteristics of the examined terminals. Arrows in B1-B4 indicate CTb labelled excitatory terminals that were positive for VGLUT1/2 but negative for VGAT. Arrowheads in B1-B4 indicate CTb labelled inhibitory terminals that were positive for VGAT but negative for VGLUT1/2. The larger arrows in B1-B4 indicate a CTb labelled terminal without immunolabelling for either VGAT or VGLUT. (B1'-B4') Single optical sections of the same terminals that were rescanned after sequential incubation with a fourth antibody against ChAT. The extra green labelling present in B2' which is absent in B2 corresponds to additional ChAT immunostaining which labels motoneurons. Therefore, arrows (D) and arrowhead (D) in B4' indicate excitatory and inhibitory terminals in contact with motoneuron dendrites, respectively. The arrow (S) in B4' indicates the terminals making contact with a motoneuron cell body. The unattributed arrows and arrowheads in B4' indicate excitatory and inhibitory terminals that were not in contact with motoneurons, respectively. Scale bar = 10 μm (A, A'); 5 μm (B1-B4, B1'-B4').

Figure 3.13b. Sequential immunocytochemistry for CTb labelled terminals with VGLUT1/2 or VGAT immunoreactivity. (C and C') A general overview of CTb labelled terminals and their neurotransmitter content before (C) and after (C') a reaction with a fourth antibody against ChAT. Details of the areas demarcated by the boxes are shown in D1-D4, and D1'-D4'. (D1-D4) Single optical sections illustrating the neurotransmitter content of terminals that were labelled by CTb (shown in red). Immunoreactivity for VGAT is shown in green, and immunoreactivity for VGLUT1 and VGLUT2 is in blue. D4 and D4' show merged images confirming the immunocytochemical characteristics of the examined terminals. Arrows in D1-D4 indicate CTb labelled excitatory terminals that were positive for VGLUT1/2 immunoreactivity but negative for VGAT. Arrowheads in D1-D4 indicate CTb labelled inhibitory terminals that were positive for VGAT but negative for VGLUT1/2. (D1'-D4') Single optical sections of the same terminals that were rescanned after sequential incubation with a fourth antibody against ChAT. The extra green labelling present in D2' was absent in D2, and this corresponds to additional ChAT immunostaining which labels motoneurons. Therefore, the arrow (D) in D4' indicates an excitatory terminal in contact with motoneuron dendrite. The unattributed arrows and arrowheads in D4' indicate excitatory and inhibitory terminals that were not in contact with motoneurons, respectively. Scale bar = 10 μ m (C, C'); 5 μ m (D1-D4, D1'-D4').

Figure 3.15. Single optical sections illustrating neurotransmitter content of CTb labelled terminals. Immunoreactivity for CTb is shown in red, GAD in green and VGLUT1 in blue. The far right column shows merged images confirming the immunocytochemical characteristics of the examined terminals. Arrows indicate CTb labelled GABAergic terminals that were GAD immunoreactive but negative for VGLUT1. Arrowheads indicate CTb labelled terminals that were negative for both GAD and VGLUT1 immunoreactivity. Arrows (*) in C1-C4 indicate a CTb labelled VGLUT1 positive terminal which was negative for GAD. Scale bar = 5 μ m.

Figure 3.16. Single optical sections illustrating neurotransmitter content of CTb labelled terminals. Immunoreactivity for CTb is shown in red, GlyT2 in green and VGLUT2 in blue. The far right column is merged images confirming the immunocytochemical characteristics of the examined terminals. Arrows indicate CTb labelled glutamatergic terminals that were VGLUT2 immunoreactive but negative for GlyT2. Arrowheads in A1-A4 and B1-B4 indicate CTb labelled glycinergic terminals that were positive for GlyT2 immunoreactivity. Arrowheads in C1-C4 indicate CTb labelled terminals that were negative for both GlyT2 and VGLUT2. Arrowheads in D1-D4 indicate CTb labelled terminals that were immunopositive for both GlyT2 and VGLUT2. Scale bar = 5 μ m.

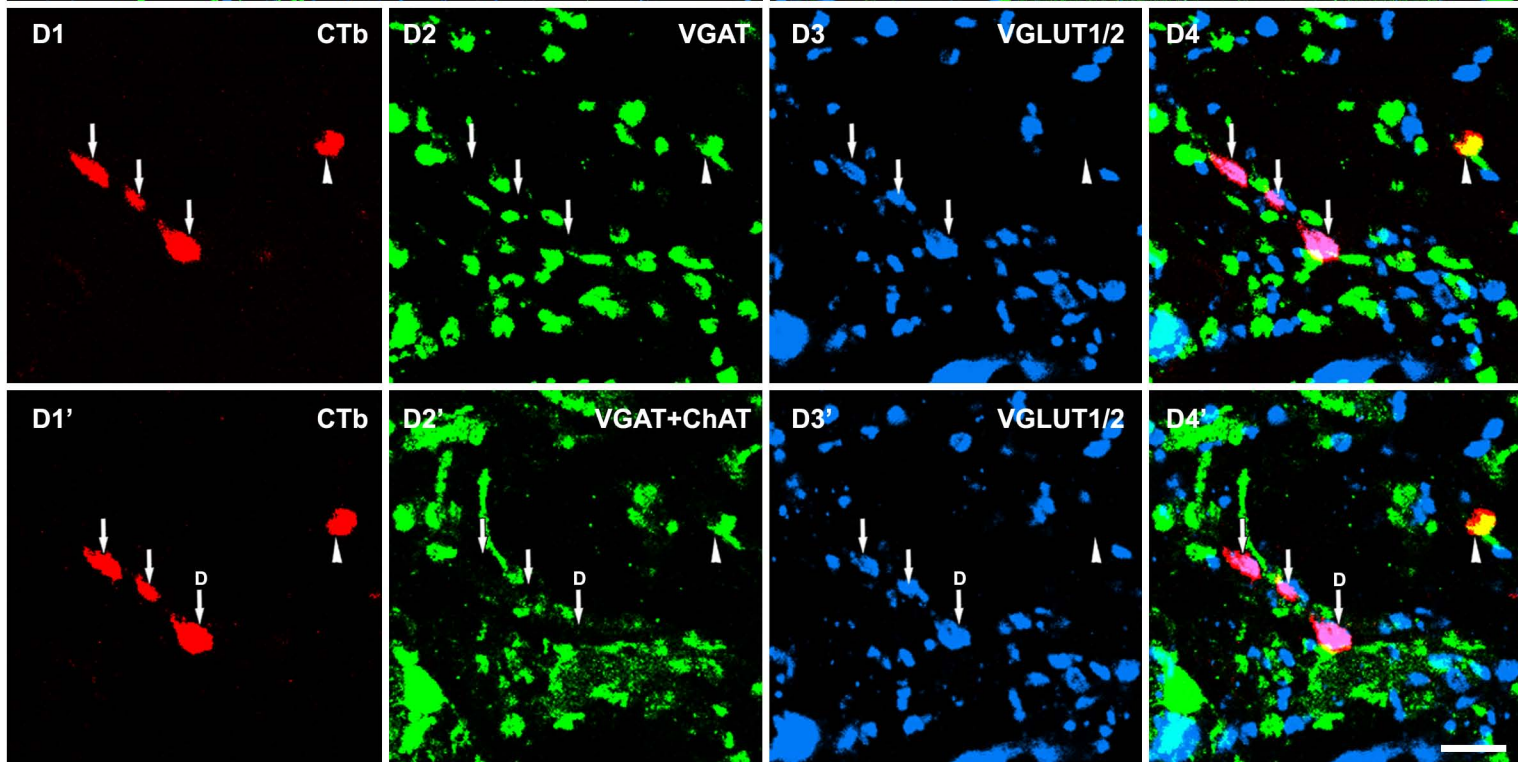
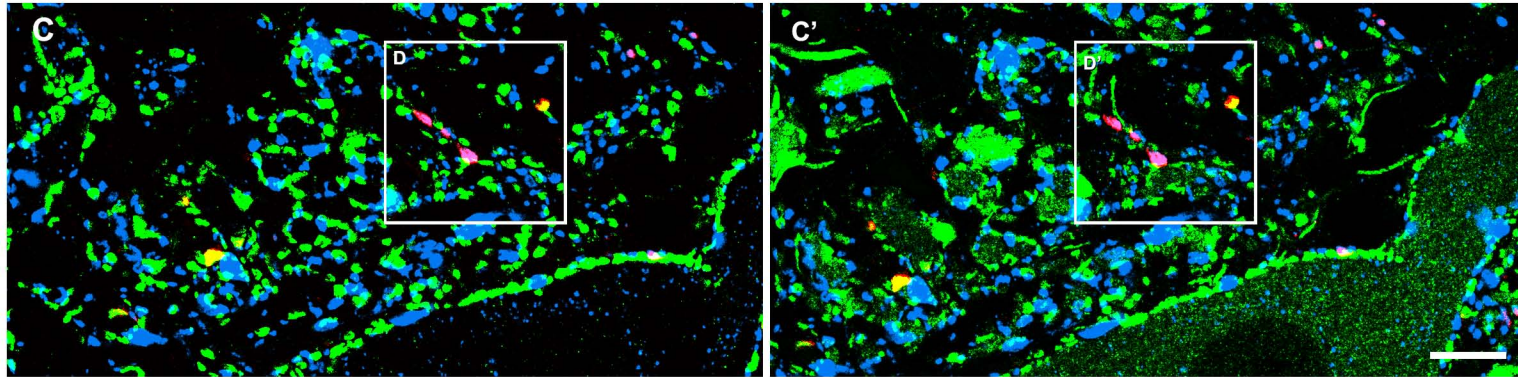


Figure 3.14. The proportions of excitatory and inhibitory CIN axon terminals in the lateral motor nuclei at L5 segmental level for all 7 experiments. (A) The average percentage of CTb anterogradely labelled terminals with VGLUT immunoreactivity, with VGAT immunostaining, or without VGLUT/VGAT labelling expressed as a proportion of the total number of CTb terminals. (B) The average percentage of VGLUT terminals in contact with motoneuron cell bodies, dendrites or unidentified neurons of the total number of excitatory terminals, and the average percentage of VGAT terminals in contact with motoneuron cell bodies, dendrites or unidentified neurons of the total number of inhibitory terminals. Error bars are standard deviations.

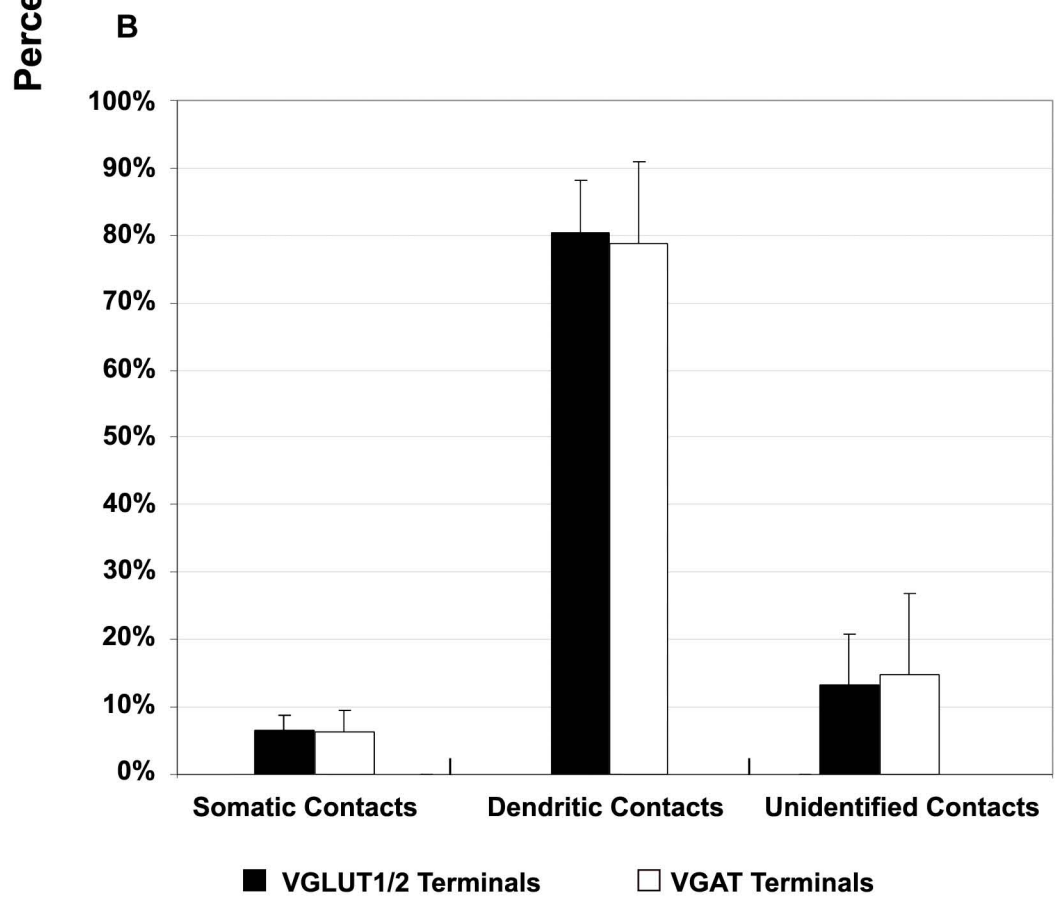
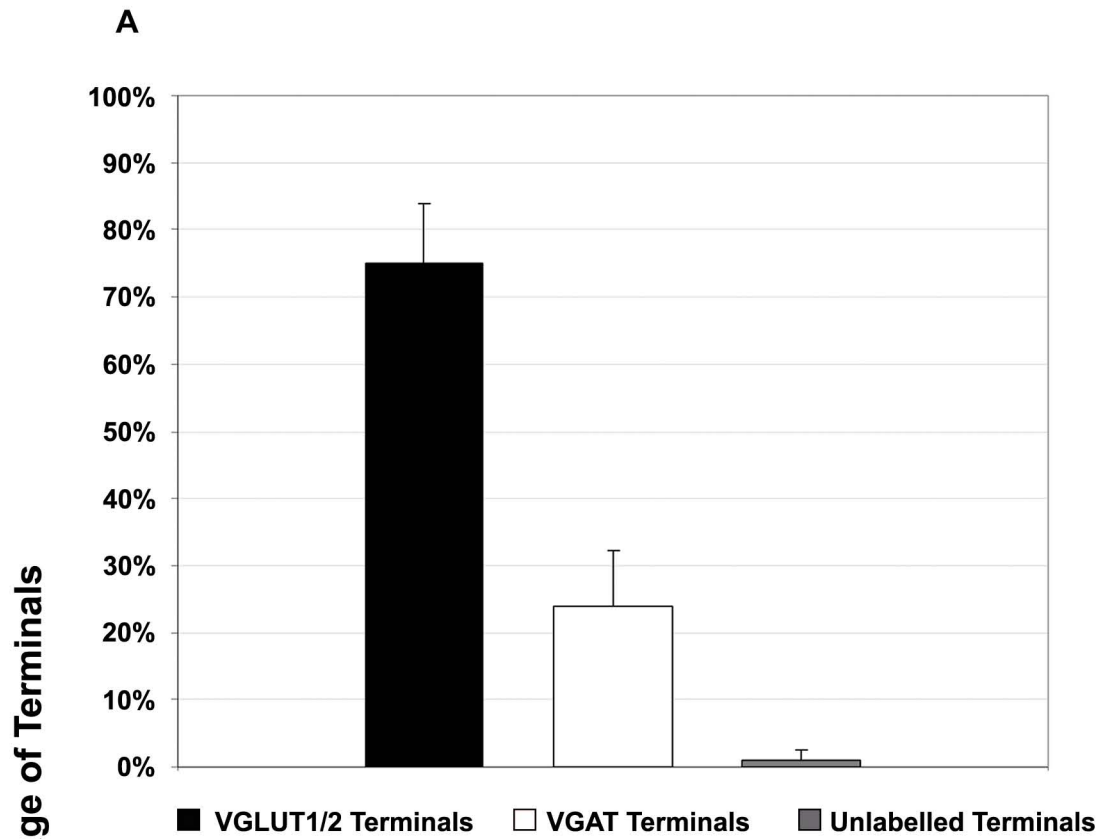


Figure 3.15. Single optical sections illustrating neurotransmitter content of CTb labelled terminals. Immunoreactivity for CTb is shown in red, GAD in green and VGLUT1 in blue. The far right column shows merged images confirming the immunocytochemical characteristics of the examined terminals. Arrows indicate CTb labelled GABAergic terminals that were GAD immunoreactive but negative for VGLUT1. Arrowheads indicate CTb labelled terminals that were negative for both GAD and VGLUT1 immunoreactivity. Arrows (*) in C1-C4 indicate a CTb labelled VGLUT1 positive terminal which was negative for GAD. Scale bar = 5 μ m.

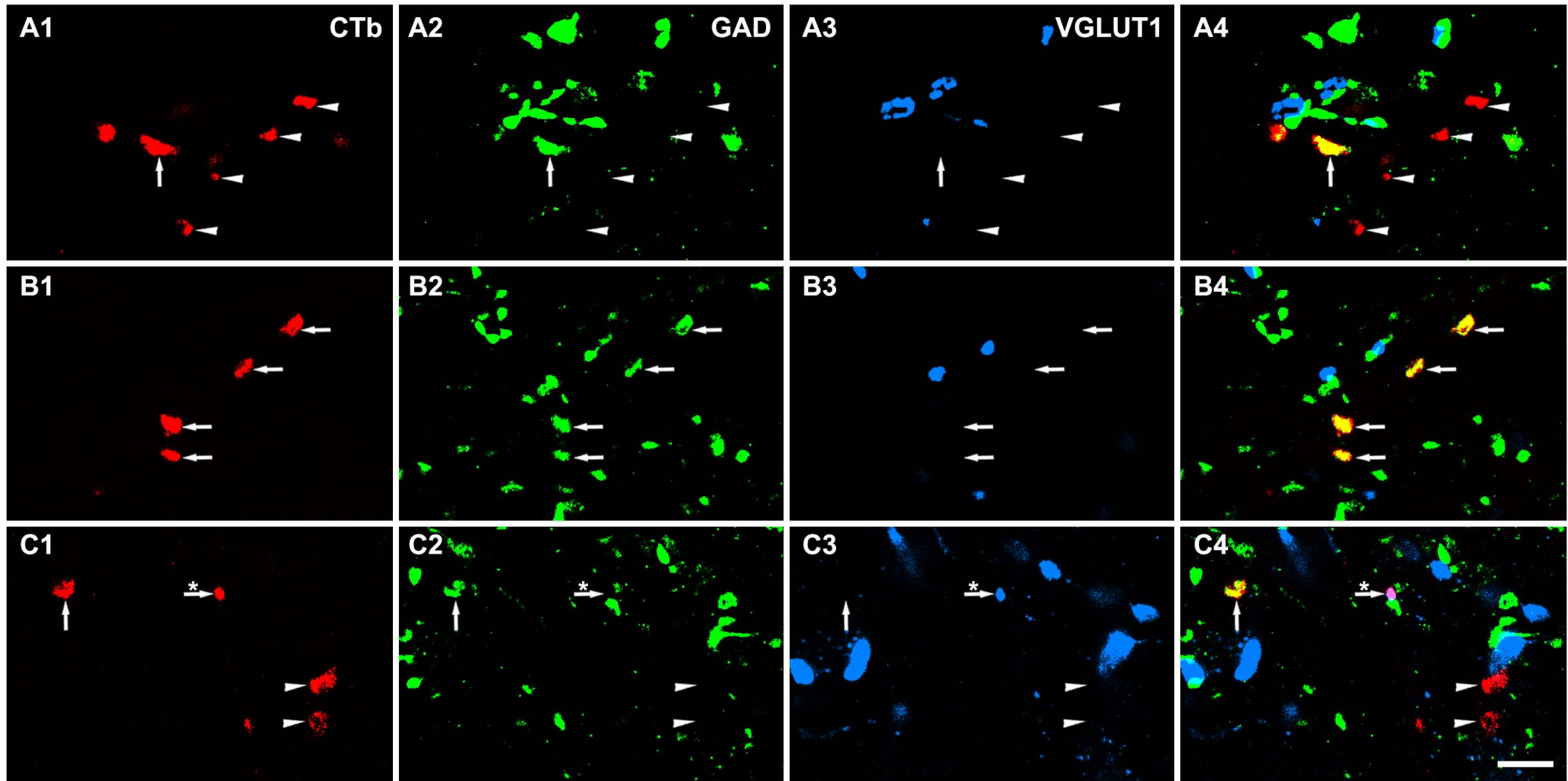


Figure 3.16. Single optical sections illustrating neurotransmitter content of CTb labelled terminals. Immunoreactivity for CTb is shown in red, GlyT2 in green and VGLUT2 in blue. The far right column is merged images confirming the immunocytochemical characteristics of the examined terminals. Arrows indicate CTb labelled glutamatergic terminals that were VGLUT2 immunoreactive but negative for GlyT2. Arrowheads in A1-A4 and B1-B4 indicate CTb labelled glycinergic terminals that were positive for GlyT2 immunoreactivity. Arrowheads in C1-C4 indicate CTb labelled terminals that were negative for both GlyT2 and VGLUT2. Arrowheads in D1-D4 indicate CTb labelled terminals that were immunopositive for both GlyT2 and VGLUT2. Scale bar = 5 μ m.

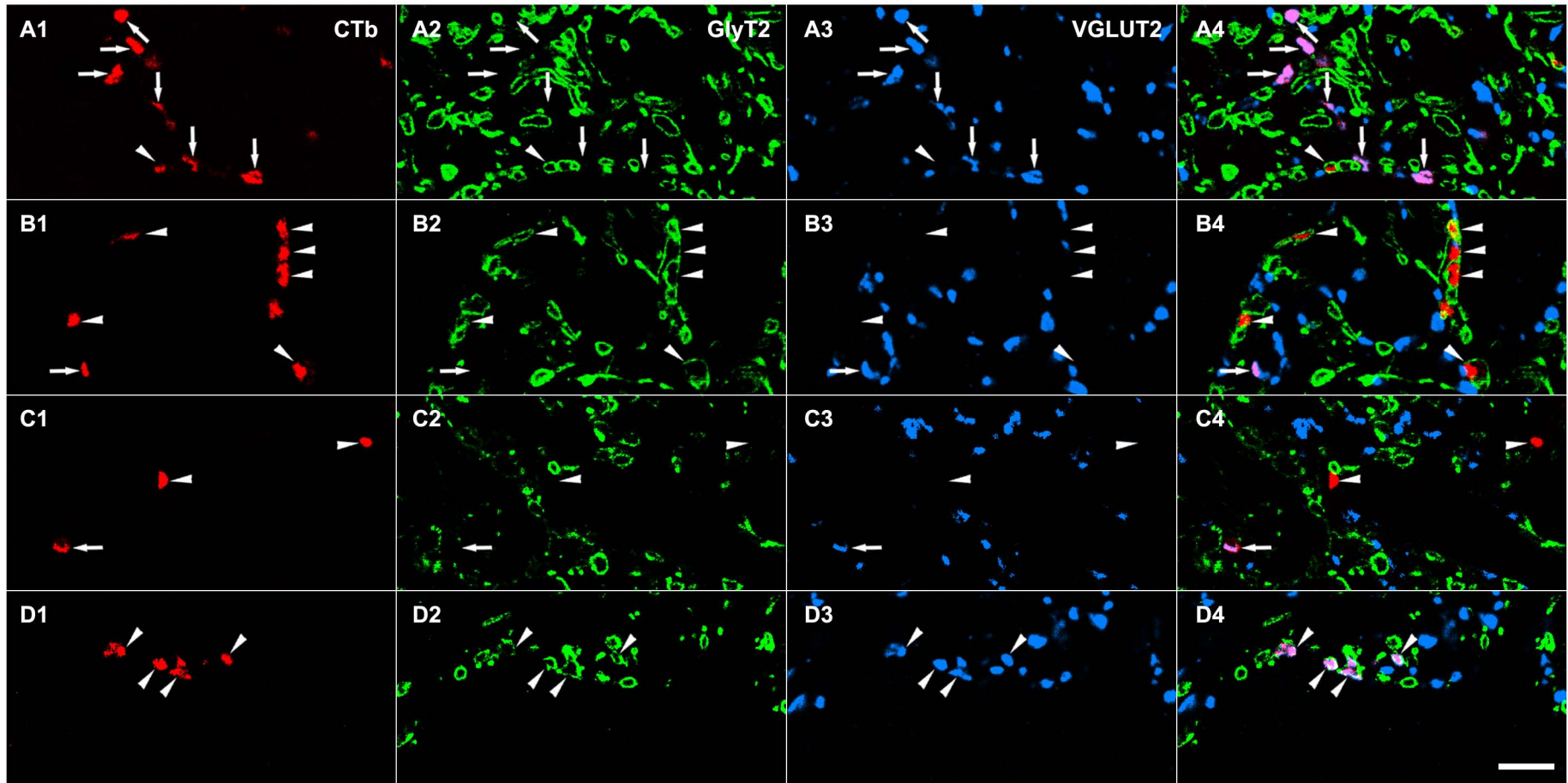


Figure 3.17. The neurotransmitter content in CIN axon terminals in the lateral motor nuclei at L5 segmental level for all 7 experiments. (A) The average percentage of CTb anterogradely labelled terminals without VGLUT1/GAD labelling and with GAD immunostaining of the total number of CTb terminals examined. (B) The average percentage of VGLUT2 positive terminals, GlyT2 positive terminals and unidentified terminals of the total number of CTb terminals examined. Error bars are standard deviations.

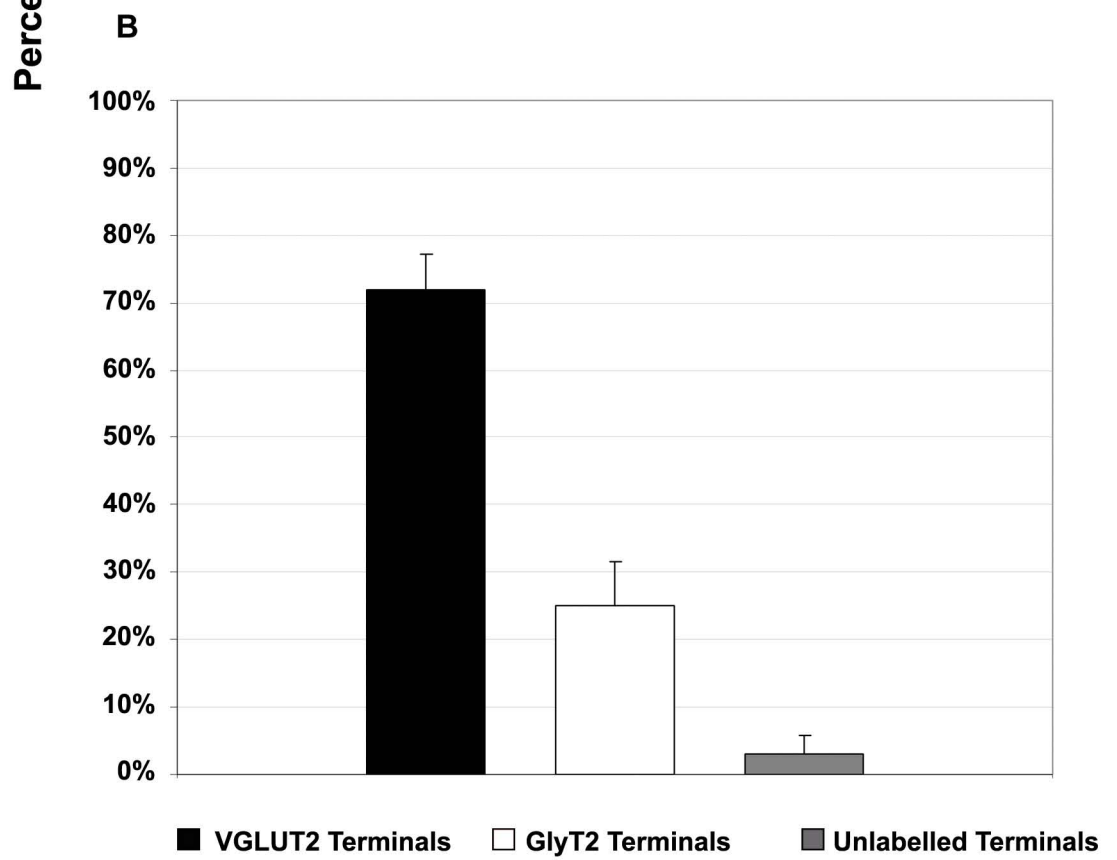
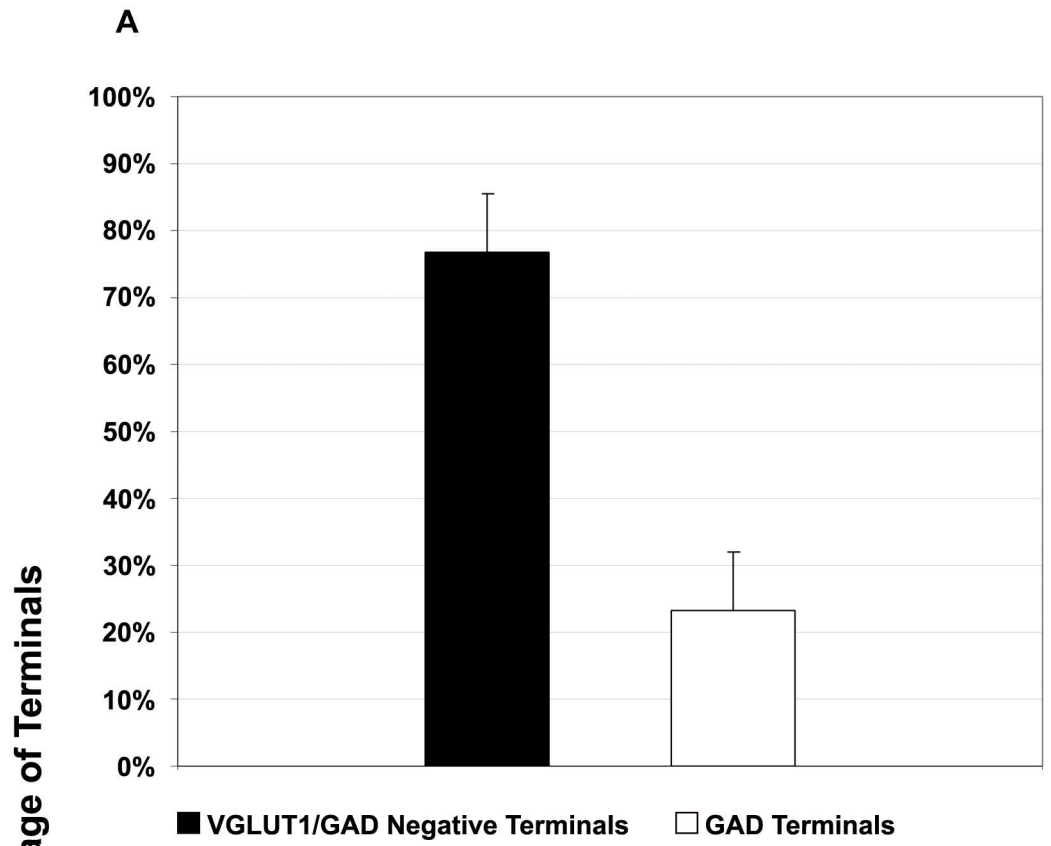


Table 3.2

	I-II	III-IV	V-VI	VII	VIII	X	LSN	Total
M-I Contra	5±2.64	* [7±1.10	* [35±6.24	* [26±3.05	99±8.48	* [19±3.09	2±0.93	* [192±21.67
L-I Contra	3±1.58	[3±1.07	[17±4.92	[12±3.50	65±27.24	[10±5.41	3±1.55	[113±38.46
M-I Ipsi	* [31±3.70	* [62±4.97	* [79±8.64	* [33±8.25	6±1.34	12±2.47	3±0.63	226±26.79
L-I Ipsi	[10±6.13	[23±7.07	[52±12.60	[62±12.28	12±5.27	10±1.38	3±0.59	169±41.07

The average number of CTb retrogradely labelled cells per 100µm of length in different laminae of the L5 segment. The counts were grouped according to the medial motor nuclei injection (M-I) or the lateral motor nuclei injection (L-I). Numbers are average cell counts ± standard deviation (SD). Asterisks indicate significant difference between the contralateral (Contra) side or the ipsilateral (Ipsi) side of the medial and the lateral motor nuclei injection group (Student t-test, p<0.05).

Table 3.3

	I-II	III-IV	V-VI	VII	VIII	X	LSN	Total
Total Contra	6±3.74	5±3.58	23±11.47	20±7.58	90±32.68	16±7.56	3±3.35	162±55.65
CB+CTb Contra	4±2.41 (74.2%)	2±1.73 (31.8%)	4±1.76 (18.2%)	2±1.17 (10.3%)	5±2.66 (5.2%)	1±0.79 (9.4%)	2±1.91 (53.6%)	20±8.41 (12.4%)
CR +CTb Contra	0±0.24 (2.4%)	0±0.39 (2.6%)	1±0.91 (8.3%)	1±0.67 (4.2%)	13±4.77 (15.2%)	1±1.03 (5.0%)	0±0.19 (5.0%)	17±6.09 (10.5%)
CB+CR+CTb Contra	1±0.85 (9.5%)	0±0.00 (0.0%)	0±0.39 (0.7%)	0±0.24 (1.2%)	0±0.38 (0.4%)	0±0.19 (0.3%)	1±0.65 (10.3%)	2±2.26 (1.3%)
Total Ipsi	56±35.63	94±42.81	156±31.52	112±34.69	26±14.26	22±5.86	5±4.18	474±67.55
CB+CTb Ipsi	22±9.04 (50.8%)	19±8.08 (22.4%)	24±8.24 (14.9%)	9±5.87 (7.6%)	1±1.15 (4.1%)	3±1.51 (14.3%)	2±1.53 (41.0%)	79±18.84 (16.6%)
CR +CTb Ipsi	2±2.30 (3.7%)	3±1.53 (3.2%)	13±5.44 (8.1%)	6±2.38 (5.8%)	2±1.81 (8.8%)	3±2.52 (12.8%)	1±1.89 (6.9%)	30±8.28 (6.4%)
CB+CR+CTb Ipsi	2±1.95 (3.0%)	2±1.89 (2.4%)	5±2.34 (3.2%)	3±2.61 (2.8%)	2±2.07 (5.6%)	1±0.98 (2.8%)	1±0.95 (9.7%)	15±6.58 (3.2%)

The average numbers and proportions of CTb labelled cells with calbindin (CB) and/or calretinin (CR) immunostaining per 100µm within laminae at L5 segmental level. The counts were based on the 7 experiments. Numbers are average cell counts ± SD per 100µm, and numbers in parentheses show the average percentage of the cells within laminae. Total, the total number of CTb cells within the corresponding laminae; CB+CTb, CTb cells with CB immunostaining, CR+CTb, CTb cells with CR immunoreactivity; CB+CR+CTb, CTb cells with both CB and CR immunostaining; Contra, contralateral side; Ipsi, ipsilateral side; LSN, lateral spinal nucleus.

Table 3.4. The percentage of VGLUT- or VGAT-immunopositive CTb terminals in contralateral-lateral motor nuclei of the L5 segment

	Exp A	Exp B	Exp C	Exp D	Exp E	Exp F	Exp G	Average	±SD
Percentage of VGLUT terminals of total terminals	70.3%	70.8%	87.4%	71.5%	65.6%	69.9%	85.1%	74.4%	8.36%
Percentage of VGAT terminals of total terminals	28.6%	27.5%	12.6%	25.3%	34.4%	28.3%	14.9%	24.5%	7.87%
Percentage of VGLUT terminals with somatic contacts on MN of total VGLUT terminals	8.3%	3.8%	8.5%	5.4%	4.5%	9.5%	6.1%	6.4%	2.42%
Percentage of VGLUT terminals with dendritic contacts on MN of total VGLUT terminals	68.9%	75.9%	84.6%	82.7%	93.6%	76.4%	79.8%	80.3%	7.79%
Percentage of VGLUT terminals with unidentified contacts of total VGLUT terminals	22.9%	21.3%	6.9%	12.0%	1.9%	14.1%	14.0%	13.3%	7.39%
Percentage of VGAT terminals with somatic contacts on MN of total VGAT terminals	5.5%	6.0%	8.9%	5.9%	7.4%	9.9%	0.0%	6.3%	3.21%
Percentage of VGAT terminals with dendritic contacts on MN of total VGAT terminals	80.8%	54.8%	82.1%	84.2%	92.0%	73.3%	85.0%	78.9%	12.01%
Percentage of VGAT terminals with unidentified contacts of total VGAT terminals	13.7%	39.3%	8.9%	9.9%	0.6%	16.8%	15.0%	14.9%	12.01%

Table 3.5. The percentage of CTb labelled terminals with different immunoproperties in contralateral-lateral motor nuclei of the L5 segment

	Exp A	Exp B	Exp C	Exp D	Exp E	Exp F	Exp G	Average	±SD
Percentage of terminals negative for both VGLUT1 and GAD immunoreactivity of total CTb terminals	73.8%	75.3%	84.3%	74.1%	6.39%	74.4%	88.8%	76.4%	8.05%
Percentage of GAD terminals of total CTb terminals	26.2%	24.7%	15.7%	25.9%	36.1%	25.6%	11.3%	23.6%	8.05%
Percentage of VGLUT2 terminals of total CTb terminals	69.3%	74.4%	74.1%	70.8%	64.1%	68.0%	79.6%	71.5%	5.05%
Percentage of GlyT2 terminals with of total CTb terminals	28.1%	17.9%	24.5%	23.9%	34.1%	31.5%	18.9%	25.6%	6.08%
Percentage of terminals negative for both VGLUT2 and GlyT2 immunoreactivity of total CTb terminals	2.6%	7.6%	1.4%	5.3%	1.8%	0.5%	1.5%	2.9%	2.57%

Chapter 4

Investigation 2:

**Input properties of identified spinal interneurons
interposed in different pathways**

4.1. Introduction

The actions of primary afferent inputs on motoneurons are mainly mediated by spinal interneurons. The consequences of these actions are complex but the result in coordinated behaviours whose basic feature is expressed by the pattern of muscle contractions. Thus, spinal interneurons interposed in the primary afferent pathways have an important role in relaying information on muscle strength and length from primary afferents, and some of them may also be involved in initiation of movements from descending tract fibres. Therefore, regulation of these interneurons is essential to achieve appropriate reflex and locomotor movements, such as crossed extension accompanied by ipsilateral flexion, bilateral extension or bilateral flexion (Aggelopoulos et al., 1996; Armstrong, 1986; Grillner and Dubuc, 1988; Jankowska et al., 2005; Noga et al., 2003). These regulations are based on both excitatory/inhibitory actions and central/peripheral feedback loops and also include pre-/post-synaptic mechanisms; thus, the synaptic connections of interneurons are very complicated.

Firstly, spinal interneurons with inputs from primary afferents are excited not only by muscle afferents but also by cutaneous and joint afferents (Edgley and Jankowska, 1987a; Jankowska and Riddell, 1994). Secondly, they may also be interposed in the descending pathways to motoneurons. For instance, interneurons relaying information from flexor reflex afferent (FRA) pathways (including group II and III muscle afferents and high threshold muscle, joint and skin afferents) also mediate actions from supraspinal systems in feline (Davies and Edgley, 1994; Harrison and Jankowska, 1985; Leblond et al., 2001) and primate motoneurons (Iles and Pisini, 1992; Jankowska et al., 1976; Pauvert et al., 1998). Furthermore, spinal interneurons receiving monosynaptic input from descending tract fibres could also mediate mono- or polysynaptic actions from other primary afferents or descending fibres. For example, a subgroup of CINs located in lamina VIII of midlumbar segments of cats is known to receive direct inputs from the MLF in which axons of reticulospinal neurons descend (Bannatyne et al., 2003). These CINs could also be monosynaptically activated by stimulation of the vestibular nuclei (VN) or group I muscle afferents (Jankowska et al., 2005; Matsuyama and Jankowska, 2004). Besides the above direct activations, these CINs are also affected indirectly by group II muscle afferents via other interneurons, resulting in a facilitation or depression of the original actions (Cabaj et al., 2006; Jankowska et al., 2005). In addition to these centrally and/or peripherally evoked excitations, the activities of spinal interneurons are also adjusted by inhibitory control.

The inhibitory actions on the interneurons are mainly from two sources: (1) postsynaptic inhibition through disynaptic and polysynaptic pathways evoked by primary afferents and/or descending tract fibres (Edgley and Jankowska, 1987a; Jankowska and Riddell, 1994); and (2) presynaptic inhibition of primary afferent terminals forming axoaxonic synapses on their target cells (Maxwell et al., 1997; Maxwell and Riddell, 1999; Riddell et al., 1995).

The synaptic connections of several groups of interneurons in dorsal horn with inputs from primary muscle afferent and fibres descending in the MLF have been studied in detail (Bannatyne et al., 2006; Jankowska et al., 2008; Maxwell et al., 1997). However, given the considerable number of studies on the axonal projections and target cells of spinal intermediate zone and ventral horn interneurons in pathways from muscle afferents and descending tract fibres (Bannatyne et al., 2009; Jankowska et al., 2009), it is surprising that so few of the synaptic connections formed with these interneurons have been described. The aim of this study was fourfold: (1) to determine differences in axonal contact patterns on intermediate zone and ventral horn interneurons with and without monosynaptic primary afferent input; (2) to investigate if input patterns of the excitatory and inhibitory interneurons with monosynaptic primary afferent input are different; (3) to determine if there are differences in the presynaptic inhibitory control of the excitatory and inhibitory cells; and (4) to examine if there are differences in the input patterns of the lamina VIII CINs and dorsal horn CINs. The first three aims were achieved by using combinations of intracellular labeling of electrophysiologically identified cells with confocal microscopic and immunochemical labeling techniques to examine the contacts with these neurons in the cat spinal cord; the last investigation was performed in the rat spinal cord by using retrograde labeling and immunocytochemical methods to identify CINs and the synaptic contacts on them.

4.2. Experimental procedures

Experiments were performed on seven adult cats (weighing 2.5-3.5 kg) obtained from an accredited supplier to University of Göteborg and three adult male Sprague-Dawley rats (250-350g; Harlan, Bicester, UK). Cat experiments were approved by the University of Göteborg Medical Ethics Committee and comply with National Institutes of Health and European Union guidelines. Rat experiments were conducted according to British Home Office legislation and were approved by the University of Glasgow Ethics committee.

4.2.1 Surgical procedure and labeling of spinal interneurons

Cat experiments

General anaesthesia was induced with sodium pentobarbital (40-44 mg/kg, i.p.) and maintained with intermittent doses of α -chloralose as required to maintain full anaesthesia (Rhône-Poulenc Santé, France; doses of 5 mg/kg administered every 1-2 hours, up to 55 mg/kg, i.v.). The level of anaesthesia was monitored by continuous recording of blood pressure and heart rate and by observing pupil dilatation. Blood pressure was monitored via a carotid cannula and maintained at 100-130 mmHg. Additional doses of α -chloralose were given when increases in the blood pressure or heart rate were evoked by noxious stimulation or if the pupils dilated. During recordings, neuromuscular transmission was blocked by pancuronium bromide (Pavulon, Organon, Sweden; about 0.2 mg/kg/h, i.v.) and animals were artificially ventilated. The end-tidal concentration of CO₂ was maintained at about 4% by adjusting the parameters of artificial ventilation and the rate of a continuous infusion of a bicarbonate buffer solution with 5% glucose (1-2 ml/h/kg). Core body temperature was kept at about 37.5 °C by servo-controlled infrared lamps.

A laminectomy exposed the fourth to seventh lumbar (L4-L7) and low thoracic (Th11-Th13) segments of the cat spinal cord. Neurones in the lumbar segments were approached through small holes (about 1-2 mm²) made in the dura mater. At the Th12-13 level two pairs of stimulating electrodes were put in contact with the lateral funicle to identify and exclude neurones with axons ascending either ipsilaterally or contralaterally beyond this level by their antidromic activation. Two contralateral hindlimb nerves (the quadriceps, Q and Sartorius, Sart) and a number of ipsilateral nerves were transected and mounted on stimulating electrodes. The latter included Q, Sart, the posterior biceps and semitendinosus (PBST), anterior biceps and semimembranosus (ABSM), gastrocnemius and soleus (GS), plantaris (PI) and deep peroneus (DP) nerves. The nerves were stimulated by constant voltage 0.2 ms long current pulses, with intensity expressed in multiples of threshold (T) for the most excitable fibres in the given nerve. In most experiments the caudal part of the cerebellum was exposed by craniotomy and a tungsten electrode (impedance 40-250 k Ω) was placed in the ipsilateral MLF after having exposed the caudal part of the cerebellum. The electrode was inserted at an

angle of 30° (with the tip directed rostrally). The initial target was at Horsley-Clarke coordinates P9, L0.6, H-5 but its final position was adjusted on the basis of records of descending volleys from the surface of the lateral funiculus at the Th11 level.

Interneurons were searched for in the intermediate zone and ventral horn grey matter of L4-L7 segments at a depth where field potentials evoked by group I and/or group II afferents were maximal (Edgley and Jankowska, 1987a, b). Cells to be labelled were selected on the basis of monosynaptic activation either after stimulation of peripheral muscle nerves at sufficient intensities to recruit group I and/or group II muscle afferent fibres, or after stimulation of MLF. Peripheral nerves and MLF fibres were stimulated with constant voltage stimuli (0.2 ms duration, intensity expressed in multiples of threshold for the most sensitive fibres in the nerve) and constant current stimuli (0.2 ms, 100 μ A), respectively.

After identification, cells were labelled intracellularly with a mixture of equal parts of 5% tetramethylrhodamine-dextran (Molecular Probes, Inc, Eugene, Oregon, USA) and 5% Neurobiotin (Vector, UK) in saline (pH 6.5). The marker was applied by passing depolarizing constant current up to 5 nA for 5-8 minutes. New injection sites were a minimum of 100 μ m away from previous sites and the distance between each injected cell and its location was carefully recorded on a diagram of the lumbar segments. At the conclusion of the experiments, the animals were given a lethal dose of pentobarbital and perfused initially with physiological saline and subsequently with paraformaldehyde (4%) in 0.1 M PB (pH 7.4). Lumbar spinal cord containing labelled cells were removed and placed in the same fixative for 8 hours, and then were cut into segments (4, 5, 6 and 7).

Rat experiments

Three rats were deeply anesthetized with halothane under strict aseptic conditions. After a incision of dorsal midline at Th13 vertebra level, a small hole with a diameter of 1mm was made near the midline to expose the dorsal surface of upper lumbar segments of the spinal cord. The tip of the injection needle was inserted into the spinal cord and a 0.2 μ l volume of 1% CTb (Sigma-Aldrich, Co., Poole, UK) in distilled water was microinjected at the target site. The needle was left in place for 5 min following the injection and then removed. The wound was sutured closed and all animals recovered uneventfully. Following a 5-day survival period,

the rats were reanesthetized with pentobarbitone (1 ml i.p.) and perfused through the left ventricle. The entire spinal cord was removed and post-fixed for 8 hours at 4 °C. The spinal cord was then dissected into C1 to L6 segments according to the dorsal roots. The detailed procedures were described in the methods section of Chapter 3.

The L4-L7 segments of cats and the L5 segments of rats were rinsed several times in 0.1 M PB. All the segments were cut into 50 µm thick transverse sections with a Vibratome (Oxford instruments, Technical products international Inc. USA) and sections of cat segments were collected in strict serial order to enable reconstruction of labelled cells. All sections were placed immediately in an aqueous solution of 50% ethanol for 30 minutes to enhance antibody penetration. Following this treatment, cat sections were mounted in serial order on glass slides with Vectashield (Vector Laboratories, Peterborough, UK) and examined with a fluorescence microscope. Sections containing labelled interneurons were reacted firstly with avidin-rhodamine (1:1000; Jackson Immunoresearch, Luton, UK) and rescanned with a fluorescence microscope.

4.2.2 Immunocytochemical processing of tissue

Sections were incubated in the combinations of primary antibodies listed [Table 4.1](#). All antibodies were diluted in PBST and incubated for 72 hours. They were rinsed in PBS and incubated for 3 hours in solutions of secondary antibodies coupled to fluorophores before mounting with anti-fade medium (see [Table 4.1](#) for details).

Selected cat sections containing axon terminals from each labelled cell were reacted with one of the following antibodies: mouse anti-gephyrin and guinea pig anti-VGLUT1; or rabbit anti-GAD and guinea pig anti-VGLUT2 (see [Table 4.1](#), cat sections containing terminals). Cat sections containing labelled cell bodies and dendrites were reacted with rabbit GAD and guinea-pig VGLUT1 firstly. VGLUT1 and VGLUT2 terminals should be distinguishable from each other, but the antibody that was used to label VGLUT2 terminals was also from guinea-pig. Therefore, a sequential incubation was performed on the sections containing somata and dendrites. When the reactions of the initial combination of both primary and secondary antibodies were complete, these sections were re-incubated with VGLUT2 antibody ([Table 4.1](#), cat sections containing cell bodies and dendrites). As a result, VGLUT1 terminals were purple

Table 4.1. Summary of primary and secondary antibody combinations and concentrations used in the current study

	Section containing	Primary antibody combination	Primary antibody concentration	Supplier	Secondary antibodies	Sequential immunoreaction	Secondary antibodies
cat	axon terminals	mo. gephyrin gp. VGLUT1	1:100 1:5000	Connex, Martinsried, Germany Chemicon, Harrow, UK	Alexa488 Cy-5		
	axon terminals	rbt GAD gp VGLUT2	1:2000 1:5000	Sigma, Poole, UK Chemicon, Harrow, UK	Alexa488 Cy-5		
	Soma & dendrite	rbt GAD gp VGLUT1	1:2000 1:5000		Alexa488 Cy-5	gp VGLUT2	Rh.Red
rat	dh/VIII CIN	mo. CTb	1:250	A. Wikström, University of Gothenburg Chemicon, Harrow, UK	Rh.Red		
		rbt VGLUT2	1:5000		Alexa488		
		gp VGLUT1	1:5000		Cy-5		

All secondary antibodies were raised in donkey and conjugated to Rhodamine Red (Rh. Red; 1:100), or Cyanine 5.18 (Cy-5; 1:100; both supplied by Jackson ImmunoResearch, West Grove, USA), or Alexa-fluor 488 (Alexa488; 1:500; Molecular Probes, Eugene, USA). CIN, commissural interneuron; dh, dorsal horn; VIII, lamina VIII; GAD, glutamic acid decarboxylase; VGLUT vesicular glutamate transporter; CTb, B-subunit of cholera toxin; mo., mouse; rbt, rabbit; gp, guinea pig.

in colour as a consequence of the extra red labelling on the original blue labelling, while VGLUT2 terminals were present in red only. Dorsal horn and lamina VIII CINs obtained from rat experiments were identified by the contralateral location and the presence of transported CTb from injection sites (the detailed explanations were discussed in the previous chapter). Triple immunofluorescence was performed on these sections with rabbit anti-VGLUT2 and guinea-pig anti-VGLUT1 antibodies (rat sections in [Table 4.1](#)).

4.2.3 Confocal microscopy, reconstruction and analysis

All sections from both cats and rats were mounted in a glycerol-based antifade medium and examined with a Bio-Rad MRC 1024 confocal laser scanning microscope.

Cat sections containing labelled cells and their dendrites were initially imaged at a low magnification (X10 lens; zoom factor 2). These images were used as a frame of reference for the location of labelled processes within each section and to make preliminary reconstructions of the cells. Each cell was then examined systematically at a higher magnification by using a X40 oil immersion lens at zoom factor of 2. Series of three-colour confocal images were gathered at intervals of 0.5 μm and their locations were determined by using the corresponding low-power reference image so that a montage was constructed for each section. Usually 10 to 20 series of images were collected from each section and processes of cells were contained within four or five sections. Sections containing axonal terminals of labelled cells were scanned by using a 60Xoil lens, zoom factor 3 or 4 at 0.5 μm intervals.

Cells were reconstructed three-dimensionally and VGLUT1, VGLUT2 and presynaptic GAD contacts on labelled cells were recorded with appropriate markers by using NeuroLucida for confocal software (MicroBrightField, Colchester, VT, USA), teamed with confocal assistant software. Reconstructions always started from the stacks of single optical sections containing the cell body, and then the axon and dendritic processes were systematically added from the next stacks until reconstruction of the axon or the dendritic tree was complete. To avoid bias, contacts were viewed in their own individual channels in a single optical section initially, and counted in merged image stacks showing all three channels and switching through different channels (if necessary). The NeuroLucida program provides information about the distribution of contacts over the dendritic tree; therefore, a three-dimensional Sholl analysis was

performed to show absolute numbers of contacts and numbers of contacts/100 μm of dendritic length contained within concentric spheres at standard distances from the centre of the cell body of each cell. By using this program, the density of contacts per unit area ($100 \mu\text{m}^2$) of cell membrane was estimated. The equivalent diameter of each labelled cell body was measured from projected confocal images obtained from all seven cats by using Image J software (National Institutes of Health, USA).

Rat sections from the L5 segment were examined within the dorsal horn (lamina V-VI) and lamina VIII contralateral to the injection site. Sections containing labelled CINs were scanned by using a $\times 40$ oil immersion lens with a zoom factor of 2 at $0.5 \mu\text{m}$ intervals. The stacks of images were analyzed with Neurolucida for Confocal software. Cells were reconstructed three-dimensionally and VGLUT1 as well as VGLUT2 contacts on labelled cells were recorded with appropriate markers. The analysis of contacts formed with these CINs was performed in the same way described above for cat material.

Two-group comparisons were made by using a Student's *t*-test, and multi-group comparisons were made by ANOVA followed by a *post hoc* Tukey's analysis. A $p < 0.05$ was considered to be statistically significant.

4.3. Results

4.3.1 Cat experiments

In cat experiments, seventy six spinal interneurons that were monosynaptically excited by primary afferents or MLF were intracellularly labelled. However, cells that were weakly labelled, without identifiable terminals, or had burst somata were excluded from the sample. Therefore, a total of 21 interneurons that were sufficiently well labelled from the 7 adult cats (2-5 cells from each animal) were reconstructed and the terminals contacting them were analysed in detail.

According to their electrophysiological properties, the 21 interneurons were classified into two groups. [Figure 4.1](#) shows a series of electrophysiological records illustrating functional identification criteria for each of the 21 cells used in the morphological analysis. Group A

includes 17 interneurons (cell 1 to cell 17) that were monosynaptically activated by stimulation of peripheral nerves, while the remaining 4 interneurons (cell 18 to cell 21) belong to group B that were directly excited by stimulation of MLF and do not have any monosynaptic input from peripheral nerves.

All the cells were located within the L4 to the L7 segments. The location of the cell bodies of the 17 cells in group A distributed in the intermediate zone (laminae VI-VII), while the cell bodies of the 4 cells in group B were exclusively concentrated in Lamina VIII (shown in [Figure 4.2](#)). The diameters of the equivalent circle of cell bodies of the 17 cells in group A had a wider range (from 22 to 64 μ m) than those of the 4 cells in group B ([Figure 4.3](#)). The diameters of the equivalent circle of the 3 cells (cell 19 to cell 21) are similar, which are 33, 34 and 35 μ m, respectively, while the remaining one (cell 18) had a bigger soma with a diameter of 53 μ m. In addition, cells in group A included both ipsilateral and contralateral projecting neurons, whereas all the 4 cells in group B were exclusively lamina VIII CINs projecting to the contralateral side. [Figure 4.4](#) illustrates the axonal projections of these 21 cells. All the 21 cells had radial dendritic arbors; however, the cells with monosynaptic primary afferent input had more extensively spread dendrites (up to 1000 μ m from soma) than the cells without monosynaptic primary afferent input (up to 625 μ m). The reconstructions of the 21 cells and the distribution of the contacts on them are shown in [Figures 4.5-4.7](#), and the morphological and neurochemical properties are summarised in [Table 4.2](#).

Aim 1: Are there differences in axonal contact patterns on interneurons with and without monosynaptic primary afferent input?

One of the major findings was that the two groups of interneurons received different VGLUT1 and VGLUT2 axonal contact patterns. [Figure 4.5](#) shows an example of the confocal microscope images of VGLUT1 and VGLUT2 immunoreactive axon terminals in contact with the two cells from each group (cell 1 and cell 21). VGLUT1 contacts were doubled-labelled with blue and red, while VGLUT2 contacts were red. This is because, in addition to VGLUT1 and VGLUT2, axonal terminals containing GABA were also examined by using GAD immunocytochemical labelling (in green and will be shown later) and the antibodies to label VGLUT1 and VGLUT2 terminals were both from guinea pig. Therefore, VGLUT1 terminals were not pure blue but displayed a purple colour and VGLUT2 terminals were red which was

the same colour used for labelling postsynaptic cells. [Figure 4.5](#) illustrates the reconstructions of these two cells showing the considerable differences in distribution of VGLUT1 and VGLUT2 contacts on these two cells (cell 1 and cell 21) from each group.

Confocal microscope analysis revealed that the majority terminals contacting the cells in group A which had monosynaptic primary afferent input were VGLUT1 positive, and the density of VGLUT1 terminals per $100\ \mu\text{m}^2$ was significantly higher than VGLUT2 terminals (Student *t*-test, $p < 0.001$). The average number (\pm SD) of VGLUT1 and VGLUT2 contacts per $100\ \mu\text{m}^2$ of these 17 cells was 1.04 ± 0.66 and 0.09 ± 0.16 , respectively. The reconstructions in [Figure 4.6A](#) and [Figure 4.7](#) show the distribution of contacts on these cells. In contrast to the cells in group A, those cells in group B received strikingly less VGLUT1 input but much more VGLUT2 input and all these differences were significant (Student *t*-test, $p = 0.01$). The average density (\pm SD) of VGLUT1 and VGLUT2 contacts on the group B cells were 0.10 ± 0.06 and 0.39 ± 0.18 , respectively. Moreover, group B cells were further divided into two subpopulations. The densities of VGLUT1 terminals contacting cell 18 and cell 19 (the first subgroup) were higher than those contacting cell 20 and cell 21 (the second subgroup). In contrast, the densities of VGLUT2 contacts on the cells in the first subgroup were lower than those on the cells in the second subgroup. The average densities (\pm SD) of VGLUT1 and VGLUT2 contacts per $100\ \mu\text{m}^2$ were 0.16 ± 0.01 and 0.23 ± 0.04 for the first subgroup, respectively; but were 0.05 ± 0.03 and 0.54 ± 0.02 for the second subgroup, respectively. However, because of the small sample number, no statistical comparison was performed between these two subgroups. [Figure 4.6B](#) and [Figure 4.8](#) illustrate the distribution of the contacts on group B cells. The detailed data about the density of VGLUT1 and VGLUT2 contacts per $100\ \mu\text{m}^2$ and the total surface (μm^2) for each of these cells are shown in [Table 4.3](#).

In addition, the general distribution patterns of VGLUT1 and VGLUT2 axonal terminals contacting the two groups of interneurons are also different. Firstly, the distribution of VGLUT1 terminals on the cells in group A decreased with the distance from cell body. This was confirmed by performing a Sholl analysis for numbers of contacts per unit ($100\text{-}\mu\text{m}$) dendritic length contained within concentric shells with radii which increase in $25\ \mu\text{m}$ units from the centre of the cell body for all 17 cells and taking average number of contacts in each unit length ([Figure 4.9A](#)). The average number of VGLUT1 contacts per $100\ \mu\text{m}$ of dendritic length contained in the first two $25\ \mu\text{m}$ concentric units was higher than 20 contacts (24.1 and

24.8 contacts/100 μ m, respectively), but it decreased significantly to less than 15 contacts and 10 contacts when the radius of concentric shells increased to 100 μ m and to 200 μ m, respectively. VGLUT2 terminals were not the majority contact type on the cells in group A and their frequency was much less than that of VGLUT1 terminals, therefore their distribution pattern is not discussed here. However, both VGLUT1 and VGLUT2 contacts on the cells in the MLF group (group B) appear to be evenly distributed over the whole dendritic tree on proximal, intermediate and distal dendrites (Figure 4.9B&C).

Aim 2: Are input patterns of excitatory and inhibitory interneurons with monosynaptic primary afferent input different?

In the 17 interneurons of group A, the neurotransmitter present in their terminals was identified by using immunocytochemical analysis. Axon terminals of the seven neurons (cell 1 to cell 7) were VGLUT2 immunoreactive and hence are glutamatergic. Figure 4.10A shows a series of Neurobiotin-labeled terminals from cell 5 that were immunoreactive for VGLUT2 but not for GAD. The remaining ten cells (cell 8 to cell 17) possessed axon terminals that were apposed to gephyrin and were therefore glycinergic. Figure 4.10B illustrates gephyrin labelling associated with terminals from cell 10 and there is no immunoreactivity for VGLUT1 in their terminals.

Although there was no statistical difference between the input patterns of excitatory and inhibitory interneurons with monosynaptic primary afferent input, confocal microscopic analysis revealed that glutamatergic cells tended to receive more VGLUT1 contacts than glycinergic cells. The average number (\pm SD) of VGLUT1 contacts on the excitatory and inhibitory cells were 729 ± 442.4 and 262 ± 185.8 , respectively, and the average packing densities of VGLUT1 terminals in contact with the excitatory and inhibitory cells were $1.24 \pm 0.70/100\mu\text{m}^2$ and $0.85 \pm 0.57/100\mu\text{m}^2$, respectively. In addition, the distribution of VGLUT1 contacts on each individual dendritic branch within an interneuron with monosynaptic primary afferent input was not always even. Table 4.4 shows the highest and lowest density of VGLUT1 contacts on individual dendritic branches within a cell and the mean density of VGLUT1 contacts on the cell.

Aim 3: Are there differences in presynaptic inhibitory control of the interneurons with monosynaptic group I/II afferent input?

Some of the VGLUT1 terminals forming synaptic contacts with labelled interneurons were themselves postsynaptic to other axon terminals immunopositive for GAD. This type of axoaxonic arrangement was found on dendrites of all 17 interneurons with monosynaptic input from primary afferents. In addition, it was very often the case that more than one presynaptic terminal made contact with the same postsynaptic axon terminal. [Figure 4.11](#) shows an example of several presynaptic GAD terminals (in green) that were in contact with three VGLUT1 terminals (in blue) which were also presynaptic to a part of a dendrite of the labelled neuron. The general distribution pattern of VGLUT1 terminals with (represented by blue open triangles) and without (represented by blue filled triangles) associated presynaptic GAD terminals is shown in [Figure 4.6A](#) and [Figure 4.7](#). The mean density (\pm SD) of VGLUT1 contacts associated with presynaptic GAD terminals was $1.01 \pm 0.70/100\mu\text{m}^2$ for glutamatergic cells and $0.62 \pm 0.51/100\mu\text{m}^2$ for glycinergic cells. So, the average percentage (\pm SD) of the above densities expressed as a proportion of the density of the total number of VGLUT1 contacts were $74.3\% \pm 12.97\%$ and $68.3\% \pm 8.69\%$ for glutamatergic and glycinergic cells, respectively. However, there was no statistical difference between the excitatory and inhibitory neurons. Detailed data are shown in [Table 4.3](#). Furthermore, the average numbers of total VGLUT1 contacts and VGLUT1 contacts associated with presynaptic GAD terminals was calculated for both glutamatergic and glycinergic cells per 100 μm units of the dendritic length on proximal (defined as $<100\mu\text{m}$ from the soma), intermediate (between 100 and $300\mu\text{m}$) and distal ($>300\mu\text{m}$) dendrites (Jankowska et al., 1997b). For excitatory neurons, these values were 30.0, 12.9, and 3.6 contacts/ $100\mu\text{m}$ for all VGLUT1 contacts and 26.8, 10.3, and 2.2 contacts/ $100\mu\text{m}$ for VGLUT1 contacts associated with presynaptic GAD terminals on proximal, intermediate and distal dendrites, respectively. For inhibitory neurons, these values were 12.5, 8.3, and 5.7 contacts/ $100\mu\text{m}$ for all VGLUT1 contacts and 10.1, 5.5, and 3.9 contacts/ $100\mu\text{m}$ for VGLUT1 contacts associated with presynaptic GAD terminals on proximal, intermediate and distal dendrites, respectively.

4.3.2 Rat experiments

In rat experiments, CINs were retrogradely labelled by injection of the tracer CTb into motor nuclei of three rats. In total, 30 dorsal horn CINs (in lateral laminae V; 10 cells from each rat) and 60 lamina VIII CINs (20 cells from each rat) located in the contralateral L5 segment were examined. Detailed information of these CINs, such as soma location and axonal projection, is described in chapter 3.

Aim 4: Are there differences in the input patterns of CINs located in dorsal horn and lamina VIII?

By comparing the density of VGLUT1 and VGLUT2 immunoreactive terminals contacting the CINs located in laminae V-VI and lamina VIII, two highly significant differences (Student's *t*-test, $p < 0.01$) were found: (1) the density of VGLUT2 contacts was significantly higher than the density of VGLUT1 contacts on dorsal horn CINs, and this was also true for lamina VIII CINs; (2) the density of VGLUT2 contacts on dorsal horn CINs was significant higher than that on lamina VIII CINs, and this was also the case in the density of VGLUT1 contacts. [Figure 4.12 and 4.13](#) show an example of the confocal microscope images of VGLUT1 and VGLUT2 immunoreactive axon terminals in contact with the CINs located in lamina VIII and lamina VI, respectively. The mean densities of VGLUT2 and VGLUT1 terminals forming contacts with lamina VIII CINs were $5.04 \pm 2.62/100\mu\text{m}^2$ and $0.15 \pm 0.16/100\mu\text{m}^2$, respectively; while those corresponding values for dorsal horn CINs were $10.98 \pm 4.36/100\mu\text{m}^2$ and $2.21 \pm 1.25/100\mu\text{m}^2$, respectively. Moreover, very occasionally, terminals forming contacts with lamina VIII CINs were immunoreactive for both VGLUT1 and VGLUT2 ([Figure 4.12](#)).

4.4. Discussion

The present study combined electrophysiological and immunocytochemical methods to address a specific anatomical question concerning the input patterns of intermediate zone and lamina VIII interneurons with or without monosynaptic inputs from group I/II muscle afferents in cat spinal cord. In addition, the study is also focused on CINs because of their crucial role in coordinating the motor activity on the two sides of the spinal cord during locomotion. This part of study was restricted to an examination of the input terminals contacting dorsal horn and lamina VIII CINs in the L5 segment of rat spinal cord.

4.4.1 Classification of intracellularly labelled interneurons and quantitative analysis of the synaptic contacts on these interneurons

The intracellularly labelled interneurons were classified into two distinct groups, one with monosynaptic input from group I/II afferents and the other with monosynaptic input from MLF but without direct input from group I/II. The validity of this classification depends critically on the reliability of the criteria for EPSPs evoked mono- and disynaptically. Jankowska et al (2005) have discussed these criteria in detail, thus, generally speaking, three features of EPSPs were used to differentiate monosynaptic from disynaptic EPSPs: (1) monosynaptic EPSPs had a fixed range of segmental latencies following the first positive peak of the afferent/descending volleys (0.5-1ms, 1.8-2.8ms, and 0.4-0.9ms for group I afferents, group II afferents, and MLF, respectively); (2) monosynaptic EPSPs were evoked successfully by each single stimulus and were of similar amplitude; (3) there was no or minimal temporal facilitation of effects of successive stimuli in a train.

There are three issues that must be considered in relation to the validity of the conclusions presented here. Firstly, because intracellular recording from interneurons deep in the grey matter is difficult and intracellular labelling of interneurons is required at a high quality, the samples of neurons on which the analysis is based are relatively small (samples of 17 neurons with monosynaptic input from primary afferents and a smaller sample of 4 interneurons with monosynaptic input from MLF). Secondly, the muscle nerves examined are the main source of group I/II afferent inputs to laminae VI-VIII interneurons (Edgley and Jankowska, 1987b); but it can not be ruled out that there might be primary afferent inputs from those muscles that were not tested. In addition, it is not known whether the interneurons investigated also received inputs from other peripheral afferents such as skin and joint nerves; thus, these identified interneurons can not be simply considered to mediate information from only one class of primary afferent. Thirdly, because of the technical limitations stated in results sections, the intracellularly labelled interneurons and the VGLUT2 terminals contacting them are both present in red. This might led to an underestimate of the number of VGLUT2 contacts especially when the cell was very strongly labelled and VGLUT2 contacts were in the middle of dendrite/soma. Nevertheless, the criteria to identify VGLUT2 contacts in all these cells are consistent, so the potential error is likely also to be consistent.

4.4.2 Different contact patterns on interneurons with and without monosynaptic primary afferent input

The most striking observations made in the present study were the significant differences in axonal contact patterns on interneurons with and without monosynaptic input from primary afferents. It was shown that the vast majority terminals contacting cells monosynaptically activated by group I/II muscle afferents (thereafter referred as group I/II cells) were VGLUT1 positive, while much fewer or no VGLUT2 contacts were on these cells. In contrast to group I/II cells, contacts formed with those interneurons that received monosynaptic input from MLF but not primary afferents (thereafter referred as MLF cells) were mainly VGLUT2 positive. It is well established that all of the primary afferent terminals in the grey matter of lumbar spinal cord except those in lamina I are VGLUT1 immunoreactive, while VGLUT2 immunoreactivity is frequently present in axon terminals that are likely to be derived from intrinsic spinal interneurons (Todd et al., 2003; Varoqui et al., 2002). Therefore, the above findings are consistent with the electrophysiological properties of these cells; i.e. stimulations of muscle afferents evoke monosynaptic EPSP in the group I/II cells but not in the MLF cells (Figure 4.1). In addition, the results obtained from anatomical studies suggest that group I/II intermediate zone interneurons less frequently receive excitatory inputs from other interneurons. This indication is supported not only by the electrophysiological features of these cells but also by a recent anatomical study (Bannatyne et al., 2009). Firstly, the electrophysiological records show that following the monosynaptic EPSP induced by stimulation of primary afferents, usually a disynaptic IPSP appeared, but a di-/poly-synaptic EPSP was seldom recorded. These IPSPs represent the disynaptic actions of the stimulated afferents which were mediated via monosynaptically excited inhibitory group I/II cells. Whereas, the absence of a di-/poly-synaptic EPSP represents no excitatory action from other spinal interneurons that were mono-/poly-evoked by stimulation of muscle afferents. Moreover, a recent study by Bannatyne (2009) has shown that inhibitory intermediate zone interneurons in pathways from group I and II afferents contacted cells with high concentrations of VGLUT1 terminals on proximal dendrites, indicating these postsynaptic cells were very likely to be group I/II cells. However, excitatory group I/II interneurons formed contacts with unidentified neurons, which were located in regions outside motor nuclei and had no or very low concentrations of VGLUT1 contacts associated with them (Bannatyne

et al., 2009); therefore, they were not likely to receive inputs from primary afferents. Taken together, the two sets of findings strongly suggest that the excitatory drive to group I/II cells in the intermediate zone is mainly from primary afferents, while the inhibitory control to these group I/II cells is, at least partly, from inhibitory group I/II cells (Figure 4.14). However, the present study did not allow a precise identification of the primary muscle afferents monosynaptically contacting the group I/II interneurons. Thus it is worth bearing in mind that these inputs could be from group Ia, Ib and/or II afferents, and also, that these afferents may be distributed to several subpopulations of group I/II cells responsible for distinct functions. For instance, interneurons receiving monosynaptic inputs from both group I afferents are known to mediate non-reciprocal inhibition of motoneurons (Jankowska et al., 1981); nonetheless, interneurons mediating reciprocal inhibition mainly receive primary afferent inputs from group Ia (Jankowska, 1992). This issue will be discussed further in section 4.4.3.

A subpopulation of CINs located in lamina VIII has been identified and they mediate disynaptic actions of reticulospinal neurons on contralateral motoneurons, i.e. they are monosynaptically activated by stimulation of MLF and in turn monosynaptically excite or inhibit contralateral motoneurons (e.g. see: Bannatyne et al., 2003; Jankowska et al., 2003; 2005). Although this subgroup of CINs exclusively have no monosynaptic group II inputs, some of them were found to receive monosynaptic input from group I muscle afferent (Jankowska et al., 2005). In the present study, all the MLF cells should belong to this subgroup because they were CINs located in lamina VIII; however, none of them received monosynaptic input from either group I or group II afferents. Since CINs are highly non-homogeneous interneurons (e.g. see: Bannatyne et al., 2003; Birinyi et al., 2003; Butt and Kiehn, 2003; Matsuyama et al., 2004; Stokke et al., 2002), this discrepancy may suggest that even within the same general subgroup of MLF CINs, functional differences may exist. In addition, the results presented here show that two out of four MLF CINs received more VGLUT1 contacts than the remaining two CINs. As reported by Jankowska et al. (2005), some but not all CINs in the MLF subgroup also received monosynaptic input from lateral vestibulospinal (VS) tract and Cai et al. (2008) have found that some vestibular descending pathways contain VGLUT1. Therefore, these two MLF CINs with more VGLUT1 contacts may mediate monosynaptic actions of VN fibres. Moreover, there are some other potential sources of VGLUT1 terminals contacting MLF cells. For example, Scheibel and Scheibel (1966) have illustrated a fan-shaped axonal termination of corticospinal tract in cat spinal cord,

with a small portion of PT fibres terminating in lamina VIII. A previous study reported that corticospinal axons contain VGLUT1 (Fremeau et al., 2001), thus some VGLUT1 terminals contacting MLF CINs could originate from pyramidal tract cells. Besides descending tract fibres, VGLUT1 (both mRNA and protein) was also found in a small population of spinal neurons located in the dorsomedial part of the intermediate zone, near the central canal (Kullander et al., 2003; Oliveira et al., 2003). Accordingly, these VGLUT1-expressing cells may be another potential source of the VGLUT1 terminals forming contacts with lamina VIII MLF CINs.

Most of the previous studies showed that MLF CINs did not have ipsilateral projections in adult cats (Bannatyne et al., 2003; Jankowska, 2008), although occasional bilateral projections have been reported by Matsuyama (2006), who showed that of 34 lamina VIII neurons, only one had a bilateral projecting axon. However, the present study showed that three out of the four examined MLF CINs projected bilaterally and one of them has possible bilateral contacts with motoneurons (Figure 4.4 cell 19-21). This might suggest that this population of CINs may directly act on motoneurons bilaterally and they may also influence the activity of motoneurons indirectly by acting through interneurons on both sides of grey matter. Based on the previous studies of the axonal projections of intermediate zone interneurons relaying information from muscle afferents and/or reticulospinal tract fibres (Bannatyne et al., 2003; 2009; Jankowska et al., 2005; 2009), and also the combined electrophysiological and morphological results in the present study, it is possible to summarize that the putative synaptic connections of interneurons relaying information from group I/II afferents and from the MLF to motoneurons (Figure 4.14). The distinct network connections of the MLF CINs suggest several significant functional differences with group II CINs. Firstly, direct and indirect evidence indicate that centrally initiated locomotion by stimulation of the mesencephalic locomotor region (MLR) is relayed by reticulospinal interneurons (Armstrong, 1988; Deliagina et al., 2002; Matsuyama et al., 2004; Mori et al., 2001; Norga et al., 2003; Shefchyk and Jordan, 1985). Secondly, MLF CINs also mediate trisynaptic actions from both ipsilateral and contralateral pyramidal tract (PT) fibres, i.e. they are disynaptically excited by PT fibres via reticulospinal neurons; thus, they may be also responsible for initiating voluntary movements (Cabaj et al., 2006; Edgley et al., 2004; Jankowska et al., 2006). Furthermore, since some of these CINs receive monosynaptic input from VS tract as well, they could be incorporated in networks for postural adjustments (Krutki et al., 2003). In addition, fastigial

neurons disynaptically activate MLF CINs via VS tract, indicating these CINs contribute to motor control and cerebellum initiated-learning processes (Matsuyama and Jankowska, 2004). Moreover, MLF CINs could also receive inputs from interneurons with monosynaptic primary afferent input, and thus are interposed in polysynaptic reflex pathways (Cabaj et al., 2006; Jankowska, 2008).

Among the 21 group I/II cells, cell 8 was an anomalous neuron because the density of VGLUT1 and VGLUT2 terminals in contact with it were similar and not significantly different (Figure 4.8E and Table 4.2). This differs from the finding that the majority contacts on the group I/II cells were formed by VGLUT1 terminals. However, this could be explained by the electrophysiological properties of cell 8. Firstly, as shown in Figure 4.1 (cell 8), when the strength of stimulus was at 1.7 and 2 times threshold (the intensity ensured to active all group I afferents; Jankowska et al., 2005), a group I EPSP was evoked with a latency of 1.25 ms. Because the latency of group I monosynaptic EPSPs was defined as 0.5-1.0 ms and disynaptic EPSPs was 1.4-1.8 ms, then a latency of 1.25 ms was more likely to be a disynaptic EPSP. This indicates cell 8 might be activated disynaptically by group I afferents via other group I/II cells. Secondly, when the strength of stimulus was increased to 5 times threshold (the intensity ensured to active all group II afferents; Jankowska et al., 2005), following the group I EPSP, a group II monosynaptic EPSP was evoked. This means that cell 8 received monosynaptic input from group II afferents. In contrast to cell 8, the electrophysiological records of the remaining group I/II cells show that all of the disynaptic PSPs induced by group I/II afferents were inhibitory and there was no group I disynaptic EPSP. Taken together, the electrophysiological and the input properties of cell 8 suggest that this cell may represent a subpopulation of group I/II interneurons which also receive input from other group I/II cells.

4.4.3 Postsynaptic excitation from and presynaptic inhibition of group I/II afferents monosynaptically contacting excitatory and inhibitory intermediate zone interneurons

Postsynaptic excitation The results show that in the intermediate zone, the glutamatergic group I/II interneurons tend to receive more VGLUT1 contacts than glycinergic cells, although the difference was not significant. This is possibly due to the limited number of cells examined. If the sample size was increased, then the difference may prove to be significant.

There are two possible interpretations of this finding. One is that group I and/or II muscle afferents have stronger monosynaptic inputs to excitatory than inhibitory intermediate zone interneurons. In other words, stimulation of these primary afferent fibres will monosynaptically activate more excitatory cells than inhibitory cells. At first glance, it seems that this arrangement may break the balance between excitatory power and inhibitory power. However, if the whole network connections are taken into account (Figure 4.14), the recruitment of a larger number of glutamatergic rather than glycinergic interneurons in group I and II pathways might actually balance the excitatory and inhibitory actions of the network. This is because inhibitory group I/II cells seem to have a wider range of target cells, including group I/II cells themselves than excitatory group I/II cells. In addition, because the VGLUT1 terminals contacting these interneurons could originate from all kinds of proprioceptive myelinated afferents including group Ia, Ib, II and III afferents (Todd et al., 2003), these interneurons could be interposed in different spinal reflex pathways or integrate information from different sources. Therefore, the alternative possibility is that the convergence of different classes of primary afferent occurs less frequently on inhibitory rather than on excitatory interneurons. This arrangement may provide flexibility of neuronal networks, which allows the same neuron to be interposed in different pathways. Thus, opposite actions from the same source, such as phase- or state-dependent reversal of spinal reflexes, could be selected to complete appropriate activities (Figure 4.15A); or information from separate sources, such as FRA pathways, could be integrated to achieve coordinated actions (Figure 4.15B).

Presynaptic inhibition Several studies have demonstrated that almost all the terminals that form axoaxonic synapses with group I and II afferents are GABAergic and some of these presynaptic boutons could also contain glycine as a co-neurotransmitter (Maxwell et al., 1990; 1997; Maxwell and Riddell, 1999; Watson and Bazzaz, 2001). Only one study found that there were 5% of presynaptic inhibition terminals immunoreactive for glycine but not GABA (Watson and Bazzaz, 2001); however, pharmacological evidence suggests that glycine has a postsynaptic role only and is not responsible for presynaptic afferent modulation because strychnine (an antagonist of glycine) has no effect on presynaptic inhibition (Watson and Bazzaz, 2001). Therefore, by using GAD immunoreactivity to identify presynaptic terminals at axoaxonic contacts, virtually all axoaxonic presynaptic terminals should be labelled. Quantitative analyses indicates that most VGLUT1 terminals contacting excitatory and inhibitory group I/II cells are associated with presynaptic GAD terminals and the targeted

group I/II interneurons are potentially subject to strong presynaptic inhibition. An additional point is that all of the intracellularly labelled cells were glutamatergic or glycinergic and none of them contained GABA; therefore, it was unlikely that these cells were involved in presynaptic inhibition.

A previous observation has demonstrated that, in some axoaxonic arrangements, one group II afferent terminal was often associated with several GABAergic presynaptic terminals (Maxwell et al., 1997). More recently, Watson and Bazzaz (2001) reported that the mean number of axoaxonic contacts received per group Ia afferent terminal in the ventral horn and deep dorsal horn was 2.7 and 1.6, respectively. Consistent with these findings, it was quite often observed in the present study that more than one GABAergic boutons was presynaptic to the same VGLUT1 terminal forming contacts with intermediate zone interneurons (Figure 4.11). Furthermore, group II afferent terminals in intermediate zone are subject to stronger presynaptic inhibition than those within the dorsal horn (Jankowska et al., 2002; Riddell et al., 1995); thus, it is worth considering whether there is also differential presynaptic inhibition of the primary muscle afferents contacting excitatory and inhibitory interneurons within the same region of the grey matter of spinal cord. Immunocytochemical results show that in the intermediate zone, the proportion of group I/II terminals associated with GAD presynaptic terminals of the total group I/II terminals contacting the excitatory interneurons is not statistically different from those contacting inhibitory interneurons. Nevertheless, this does not mean the actions of group I/II afferents on their targeted excitatory and inhibitory interneurons are always equally affected by presynaptic inhibition. As discussed above, these group I/II interneurons may be shared by primary afferents from different nerves and be interposed in several reflex pathways. It is known that each type of afferent is differentially affected by presynaptic inhibition and their preferential evoking sources are also various. For example, presynaptic inhibition of Ia afferents is strongly present in those from both flexors and extensors, but is most effectively activated by flexor group I afferents; however, group Ib afferents from both flexor and extensor can be depolarized by Ib afferents (Rudomin and Schmidt 1999). Moreover, the degree of presynaptic inhibition is not invariant but changes according to the task to be performed. Duenas and Rudomin (1988) reported that the level of presynaptic inhibition of group I afferents was changing during the fictive locomotor cycle and it reached a maximal degree during the flexor phase. Therefore, the results of this study suggest that the intermediate zone interneurons that are interposed in group I and II reflex

pathways could be selectively activated and produce appropriate actions on motoneurons (an example see [Figure 4.15C](#), and also see [Figure 1.1D,E](#) in chapter 1). Presynaptic inhibition, consequently, is one of the effective modulatory mechanisms to achieve the flexibility of neuronal network.

4.4 VGLUT2 contacts form the majority excitatory inputs to both dorsal horn and lamina VIII CINs in rat spinal cord

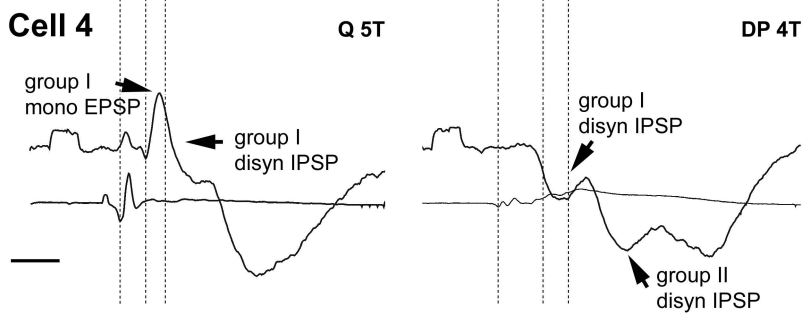
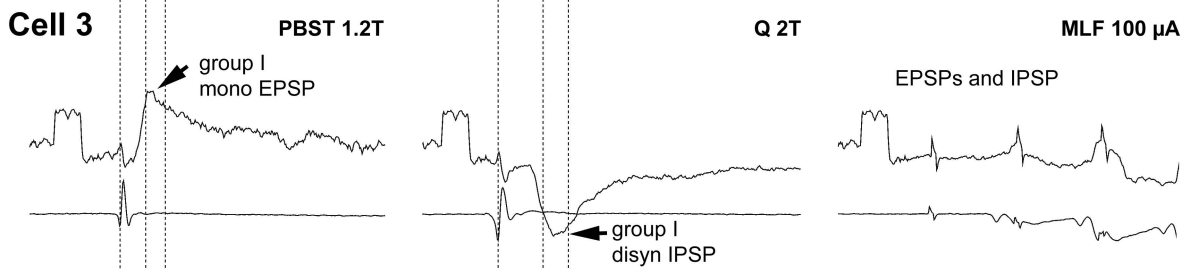
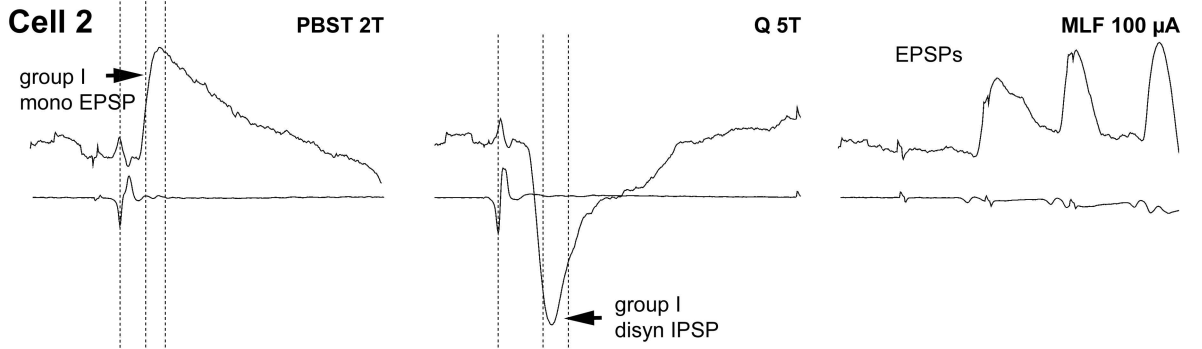
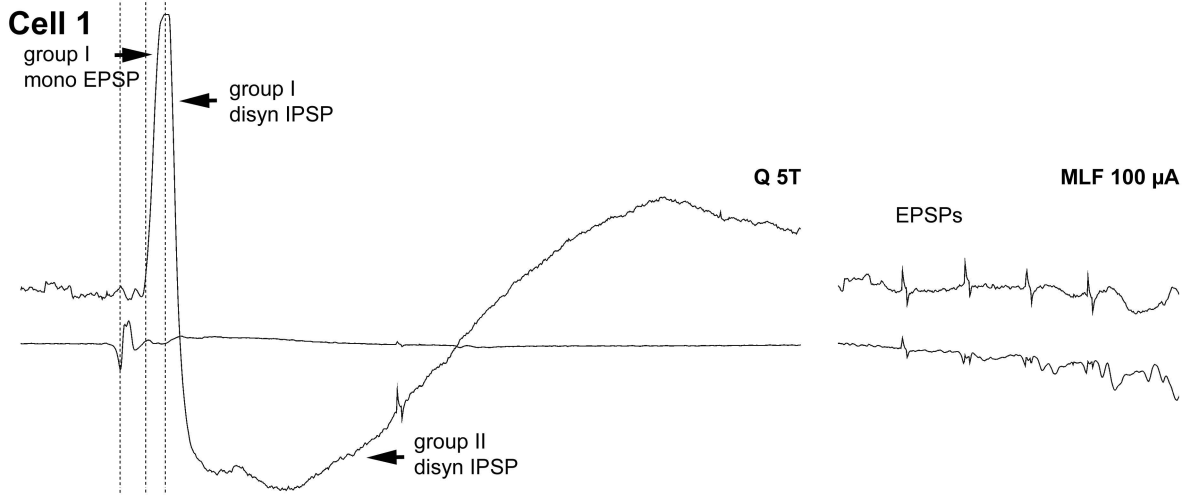
Similarly to the input pattern of cat lamina VIII CINs, VGLUT2 terminals formed the vast majority of contacts with CINs in both dorsal horn and lamina VIII of the rat spinal cord, suggesting that primary afferent fibres have no or very limited monosynaptic actions on these CINs. Moreover, dorsal horn CINs received significantly larger number of glutamatergic inputs than lamina VIII CINs. Most previous studies focused on the first and the last order interneurons in a neuronal network, as second or higher order interneurons are relatively difficult to identify and investigate. Therefore, the results presented here may provide some hints to fill the linkage of polysynaptic pathways from primary muscle afferents to motoneurons. First of all, the explanations should begin with the origin of the VGLUT1/2 terminals contacting these CINs. Although this can not be confirmed purely on the basis of anatomical labelling, potential sources still could be envisioned. The previous morphological and electrophysiological studies systematically investigated differential projections of interneurons with monosynaptic group I/II muscle afferents located in dorsal horn, intermediate zone, and ventral horn (Bannatyne et al., 2003; 2006; 2009; Jankowska et al., 2009). Their results showed that: 1) excitatory group I/II interneurons located in dorsal horn only project to ipsilateral dorsal horn and intermediate zone; 2) those located in intermediate zone project to both sides of grey matter except bilateral dorsal horn; 3) those in ventral horn lamina VIII exclusively project to contralateral ventral horn. Three conclusions could be deduced based on these findings: 1) excitatory CINs in dorsal horn are less likely to receive monosynaptic input from group I/II afferents, and this is consistent with the result of this study; 2) the VGLUT2 contacts on dorsal horn CINs originate from the ipsilateral dorsal horn interneurons but not from interneurons in intermediate zone and ventral horn; 3) the VGLUT2 contacts on lamina VIII CINs may have a wider origin, including bilaterally from intermediate zone and contralaterally from lamina VIII interneurons but not dorsal horn interneurons. A summary diagram is shown in [Figure 4.16](#). Accordingly, it seems that group I/II afferents

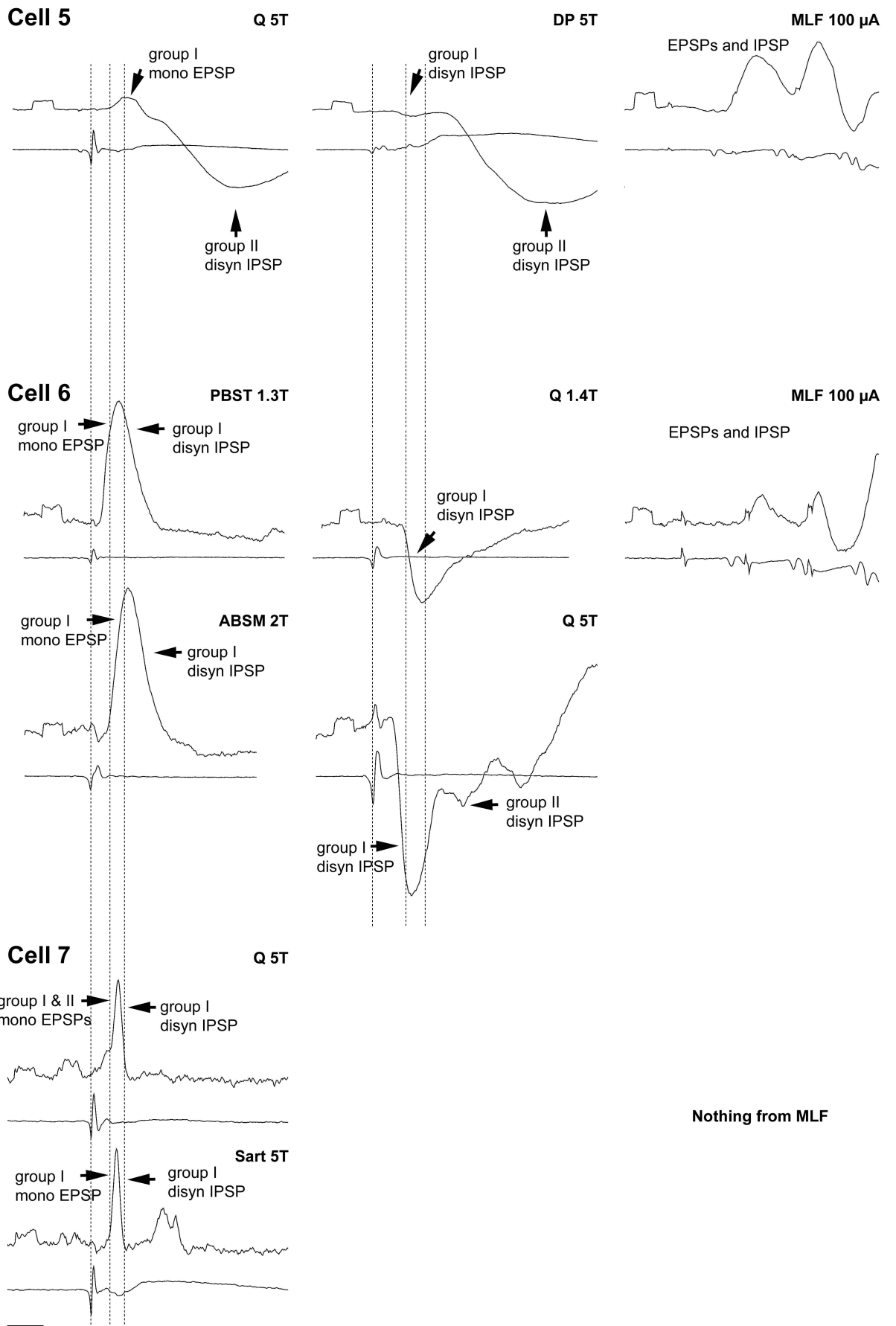
disynaptically activate dorsal horn and lamina VIII CINs through two separate pathways, i.e. activating dorsal horn CINs is via dorsal horn interneurons, while activating lamina VIII CINs is via cells in intermediate zone and ventral horn. Tri- and poly-synaptic actions of group II afferents on contralateral motoneurons have been demonstrated in previous studies (Arya et al., 1991; Edgley et al., 2003; Matsuyama and Mori, 1998) and both dorsal horn CINs and lamina VIII CINs are involved in these actions (Edgley et al., 2003; Eide et al., 1999; Stokke et al., 2002). Therefore, it may be suggested that these two subpopulations of CINs mediate different actions of primary muscle afferents or compose alternative pathways for the same actions. Nevertheless, these suggestions are confined to the neurons in group I/II afferent pathways; thus, it can not be ruled out that other excitatory interneurons which do not receive monosynaptic input from group I/II muscle afferents also project to these CINs.

In contrast to VGLUT2 contacts, VGLUT1 immunoreactive terminals were not major excitatory inputs to these CINs, and this was especially true for lamina VIII CINs. Although the results suggest that CINs are less likely to have powerful monosynaptic inputs from primary afferents, it can not be concluded that there are no inputs from these fibres. Group I and II muscle afferent terminals are known to be distributed in lamina V-VI but few of them are found in lamina VIII (Jankowska, 1992); therefore, this may explain the significantly higher density of VGLUT1 contacts on dorsal horn CINs when compared with lamina VIII CINs. Moreover, since the corticospinal axons also contain VGLUT1 (Fremeau et al., 2001), an alternative explanation might be that, in rat spinal cord, the corticospinal tract is branched profusely in intermediate regions corresponding to Rexed's laminae III-VI and only a small proportion was observed in lamina VIII (Brosamle and Schwab, 1997). Besides, low-threshold cutaneous afferent and proprioceptive myelinated afferent fibres could also be potential sources of VGLUT1 terminals forming contacts with these CINs (Todd et al., 2003). Moreover, as reported by Todd et al. (2003) and Sakata-Haga et al. (2001) that VGLUT1 and VGLUT2 are colocalized in some terminals in the spinal cord and forebrain of rat, in this study, terminals contacting lamina VIII CINs were occasionally found containing both transporters, also. However, the significance of this coexistence is unclear. In addition, it should be noticed also that the cells were retrogradely labelled and their distal dendrites were not revealed. Therefore, these results only apply to the cell bodies and proximal dendrites.

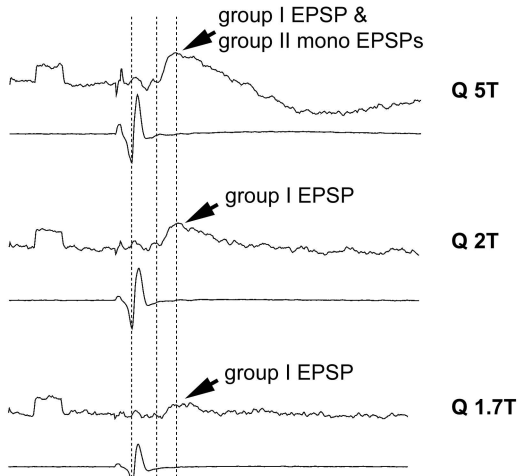
In conclusion, the present findings are of relevance to understanding the organization of interneurons involved in different pathways of group I/II muscle afferent and descending tract fibres. This study shows that the majority of excitatory inputs received by interneurons mediating monosynaptic actions of primary afferents are VGLUT1 immunoreactive, while those received by interneurons mediating monosynaptic actions of MLF are VGLUT2 immunoreactive. On average, excitatory group I/II interneurons receive more contacts than inhibitory neurons; however, the difference is not statistically significant. Both of these excitatory and inhibitory interneurons are strongly subject to presynaptic inhibitory control.

Figure 4.1. Examples of PSPs used to identify the 21 interneurons analysed morphologically. In each pair of traces, the upper trace is an intracellular record from the cell indicated and the lower is from the cord dorsum, (with negativity upward). The stimuli were applied to the quadriceps (Q), posterior biceps and semitendinosus (PBST) and deep peroneal (DP) nerves. The intensity of the stimuli is expressed in multiples of the threshold (T) for the most sensitive afferents in a given nerve. The stimuli were also applied to the medial longitudinal fasciculus (MLF) at intensity of 100 μ A. Arrows indicate monosynaptic (mono) and disynaptic (disyn) excitatory postsynaptic potentials (EPSPs) and inhibitory postsynaptic potentials (IPSPs), both on the basis of the threshold and the latency from incoming volleys (seen in the lower records). Dotted lines indicate the following: (1) afferent incoming volleys, (2) onset of group I or MLF monosynaptic EPSPs, (3) onset of group II monosynaptic EPSPs, (4) afferent incoming volleys, (5) onset of group I disynaptic IPSPs, and (6) onset of group II disynaptic IPSPs. Calibration pulses at the beginning of all microelectrode records are 0.2 mV, time calibration: 2 ms.

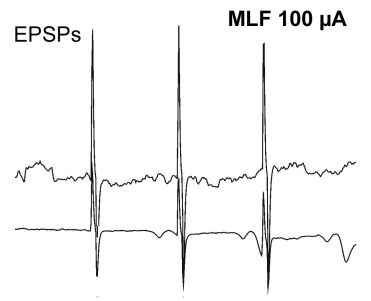
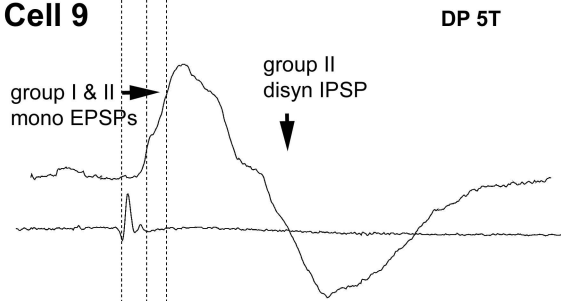




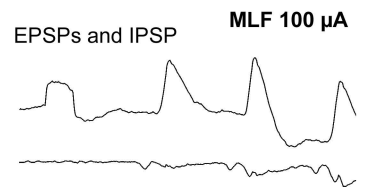
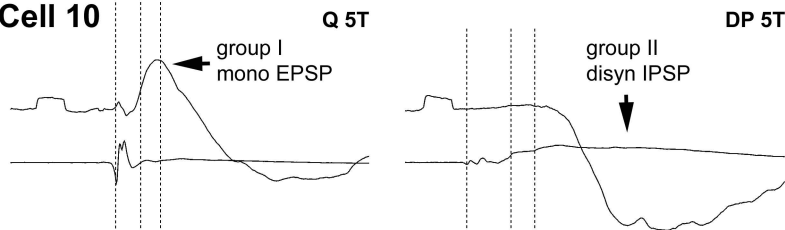
Cell 8



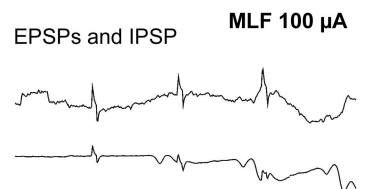
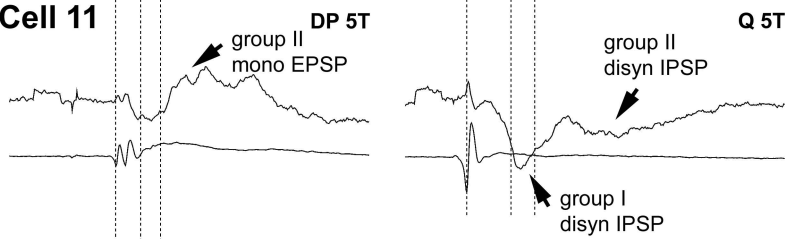
Cell 9



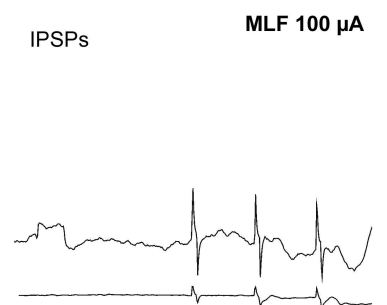
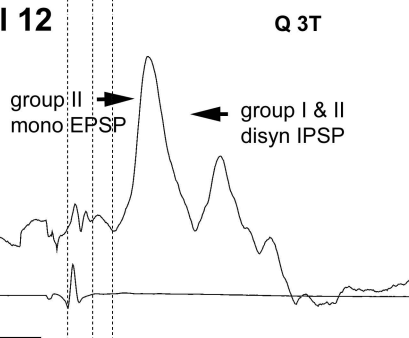
Cell 10



Cell 11

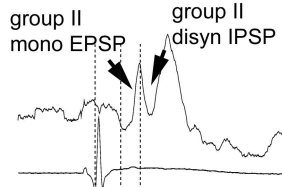


Cell 12



Cell 13

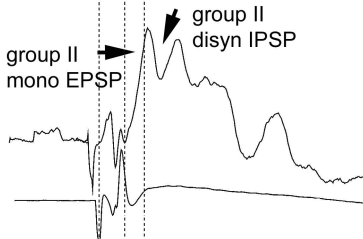
Q 5T



Nothing from MLF

Cell 14

Q 5T

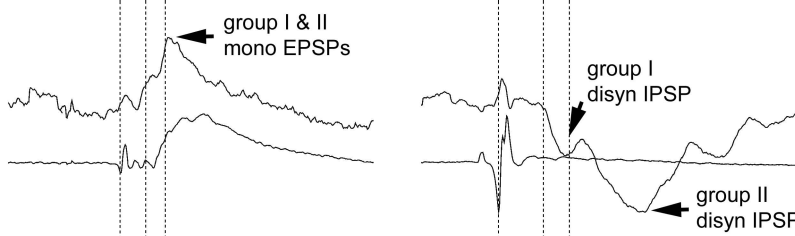


Nothing from MLF

Cell 15

DP 5T

Q 5T

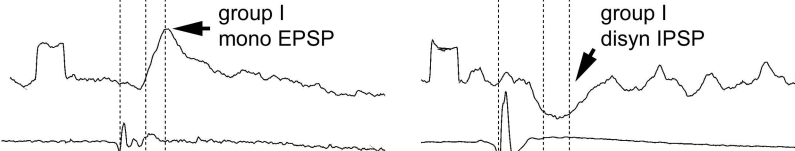


Nothing from MLF

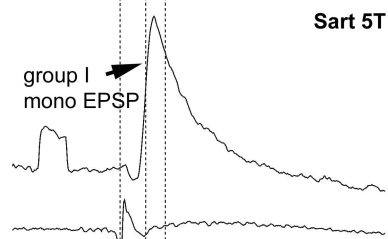
Cell 16

Sart 1.4T

Q 5T



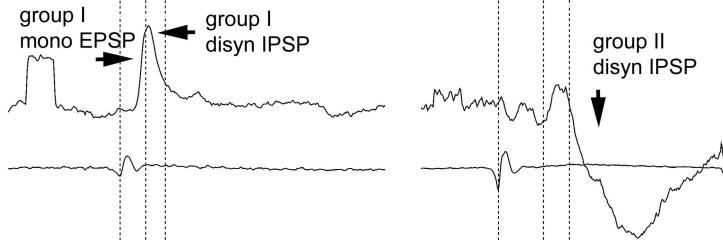
Nothing from MLF



Cell 17

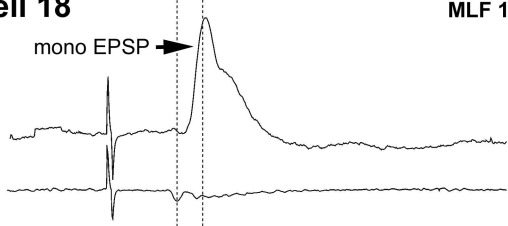
PBST 1.2T

Sart 5T

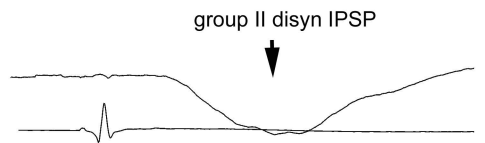


Nothing from MLF

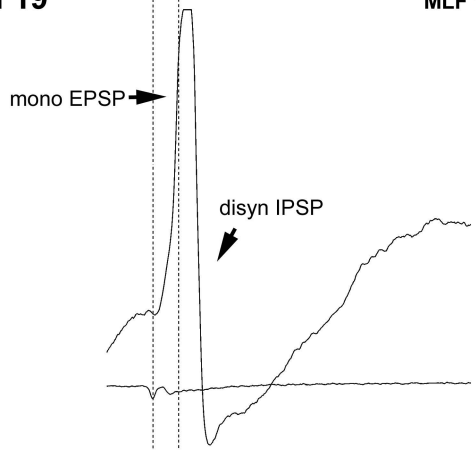
Cell 18 MLF 100 μ A



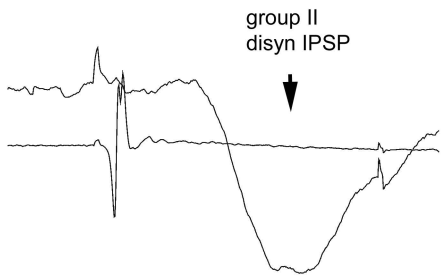
Q 5T



Cell 19 MLF 100 μ A



Q 5T



Cell 20 MLF 100 μ A



Nothing from peripheral nerves

Cell 21 MLF 100 μ A



Nothing from peripheral nerves

Figure 4.2. Location of identified spinal interneurons. (A) A low-power image showing the location of one of the cells (cell 2) in a transverse section of the L6 spinal cord. Note the cell body in lamina VII and dendrites which extend dorsally into lamina VI and ventrally into lamina VIII. (B) A diagram illustrating the locations of somata of all 17 cells with monosynaptic input from primary muscle afferent (circles). The green and red circles represent excitatory and inhibitory cells, respectively. Note all cells are distributed within laminae V-VII. (C) A diagram illustrating the locations of somata of all four cells with monosynaptic input from MLF (stars). Note all cells are located in lamina VIII. Scale bar = 300 μm .

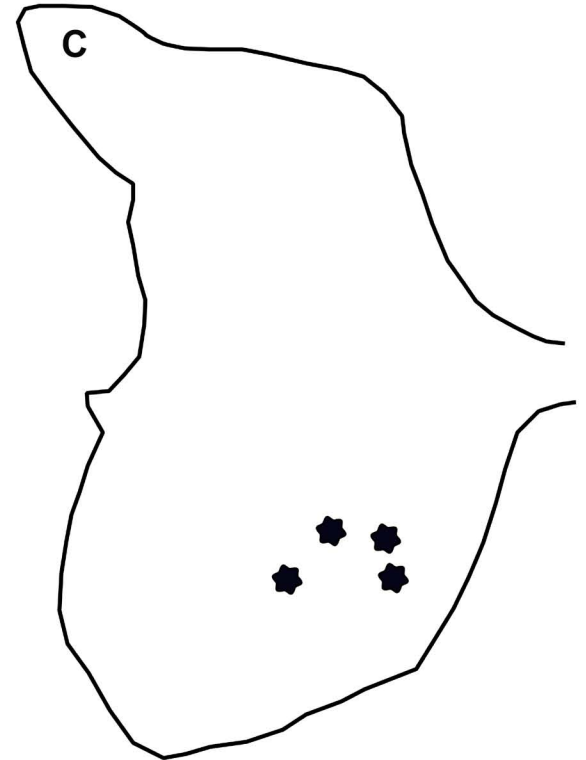
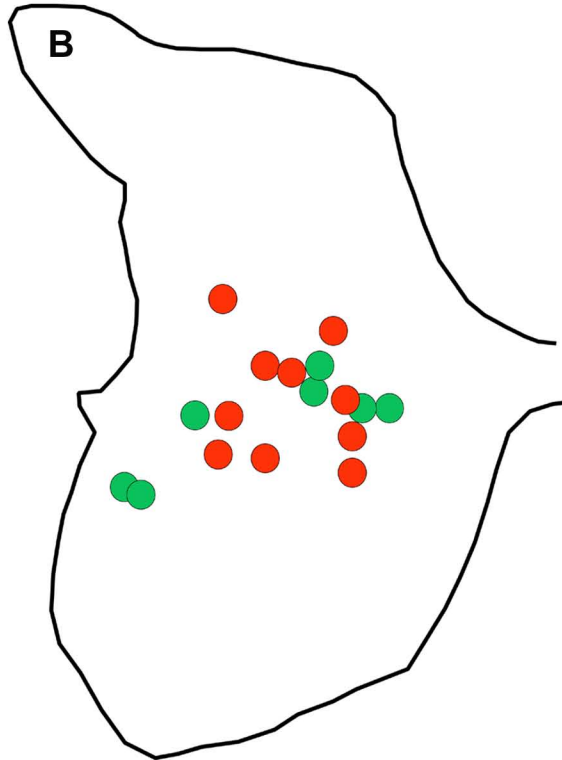
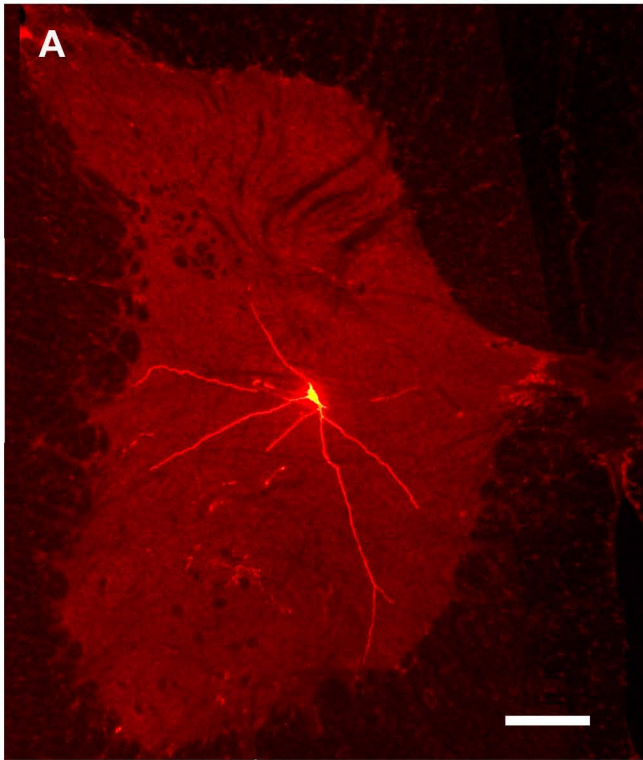


Figure 4.3. Cell body size distribution for the 21 cells examined. The diameters of equivalent circle were measured in projected confocal images of the 21 cells by using Image J software. Cells are divided into three groups: (1) excitatory cells in group A are the excitatory cells with monosynaptic primary afferent input; (2) inhibitory cells in group A are the inhibitory cells with monosynaptic primary afferent input; and (3) cells in group B are the cells without monosynaptic primary afferent input.

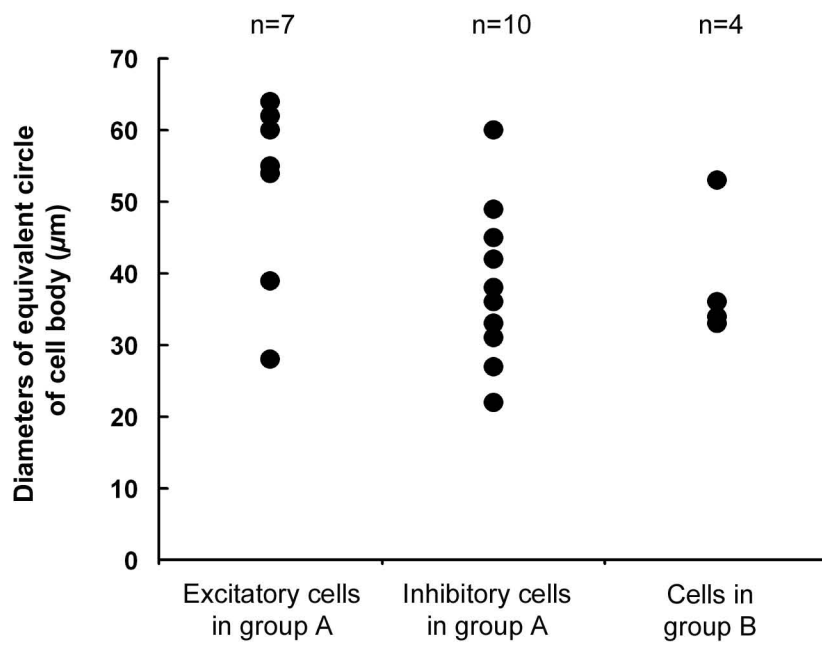
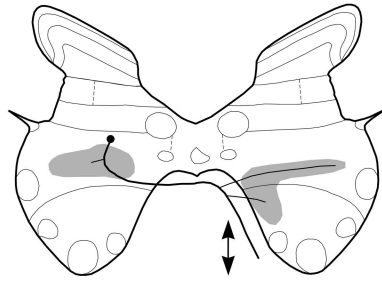
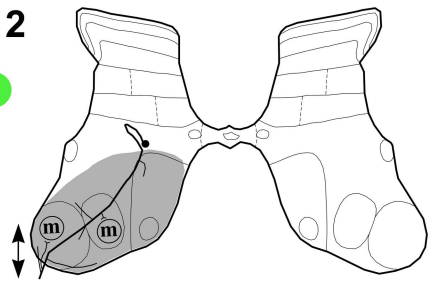


Figure 4.4. Axonal projections of glutamatergic and glycinergic interneurons. Cells bodies of interneurons are indicated by black circles, stem axons are indicated as thick lines, and the areas in which terminals were visualized are shaded in grey. Symbol  indicates possible contact with motoneurons. Rostral and caudal projections are indicated by upward and downward arrows, respectively. The green and red circles indicate the cells are excitatory and inhibitory respectively.

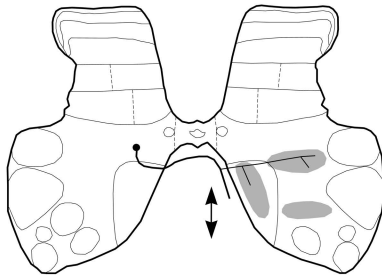
Cell 1



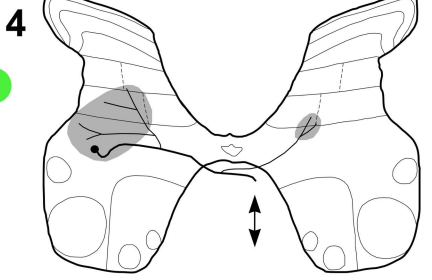
Cell 2



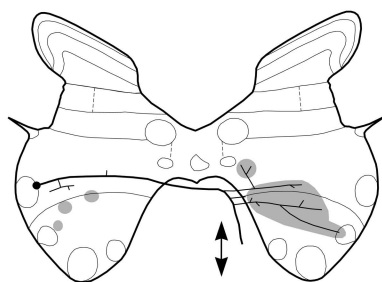
Cell 3



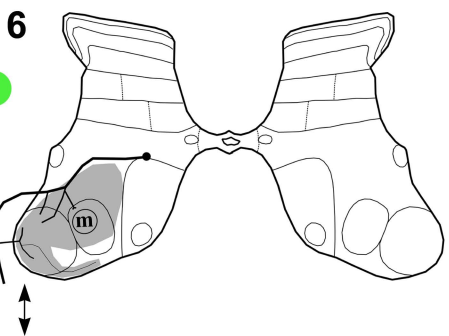
Cell 4



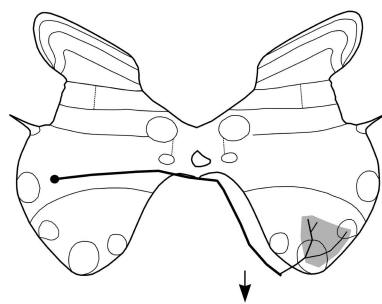
Cell 5



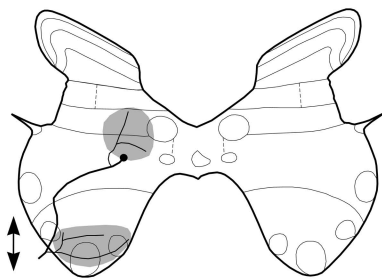
Cell 6



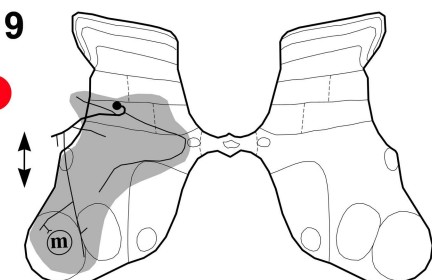
Cell 7



Cell 8



Cell 9



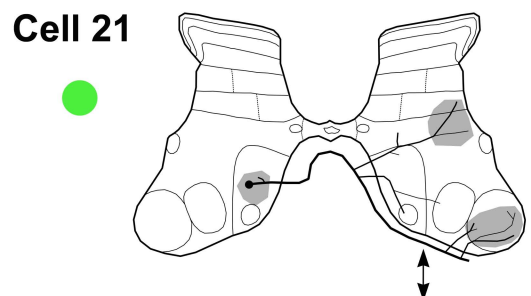
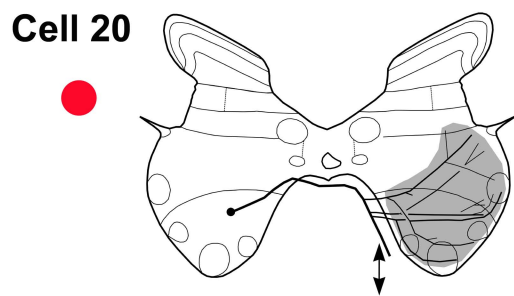
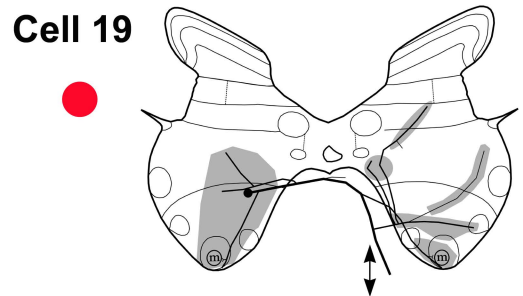
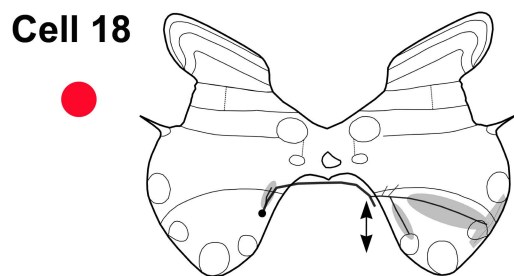
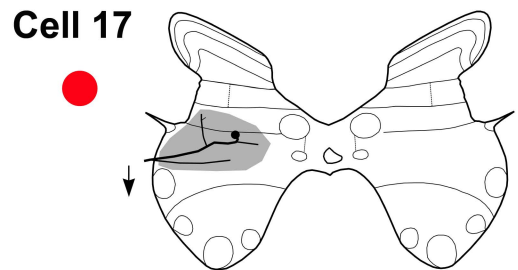
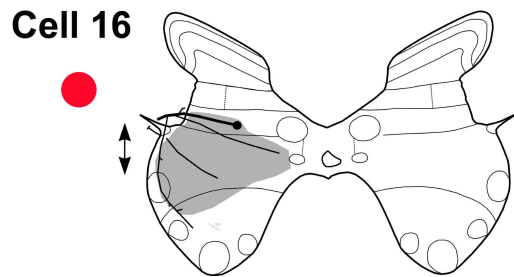
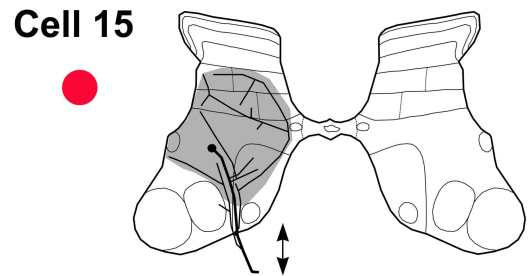
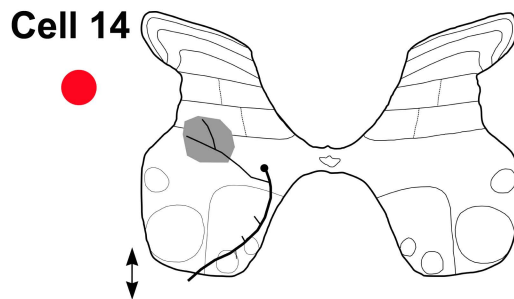
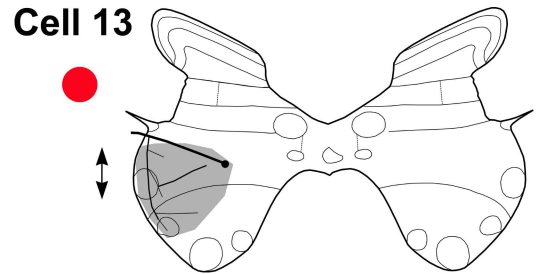
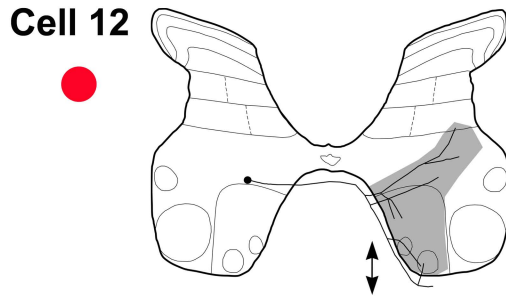
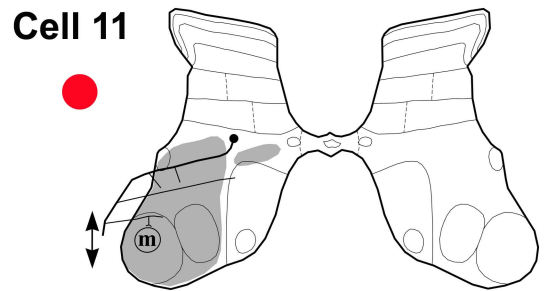
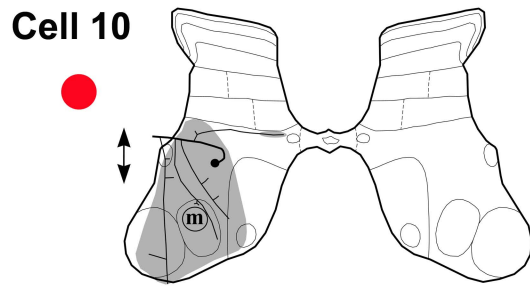
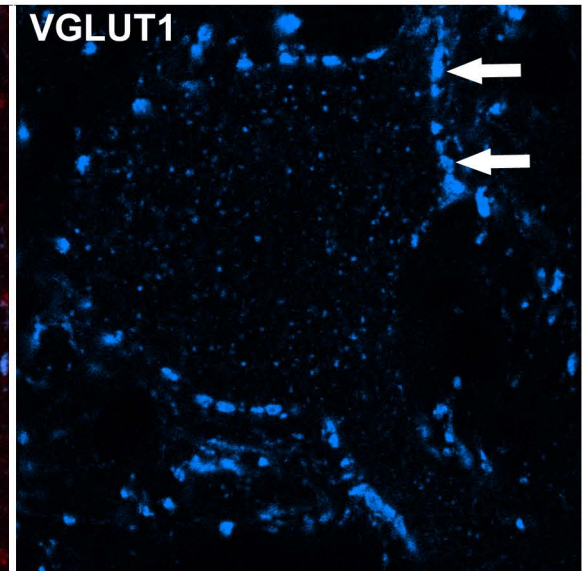
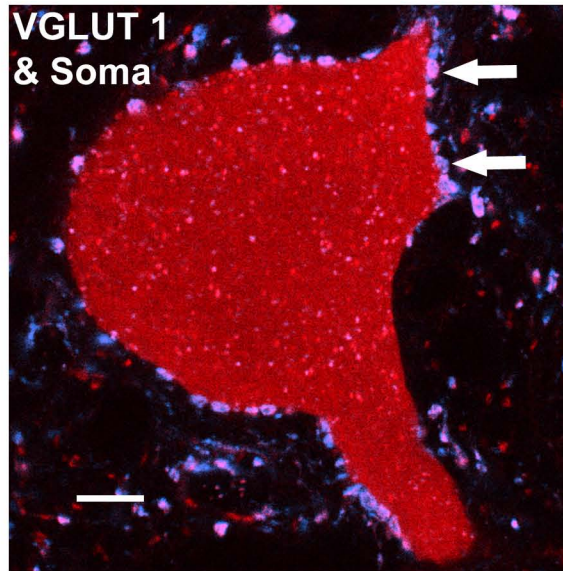


Figure 4.5. Morphology and immunocytochemical characteristics of VGLUT1 and VGLUT2 terminals in contact with postsynaptic interneurons. A series of single optical sections of confocal microscope images illustrating VGLUT1 and VGLUT2 immunoreactive axon terminals in contact with the cell (A, cell 1) with and (B, cell 21) without monosynaptic primary afferent input. The dendrite and soma of intracellularly labelled cells are in red, immunoreactivity for VGLUT1 in blue (arrows) and VGLUT2 in red (arrowheads). Scale bar = 10 μ m.

A



B

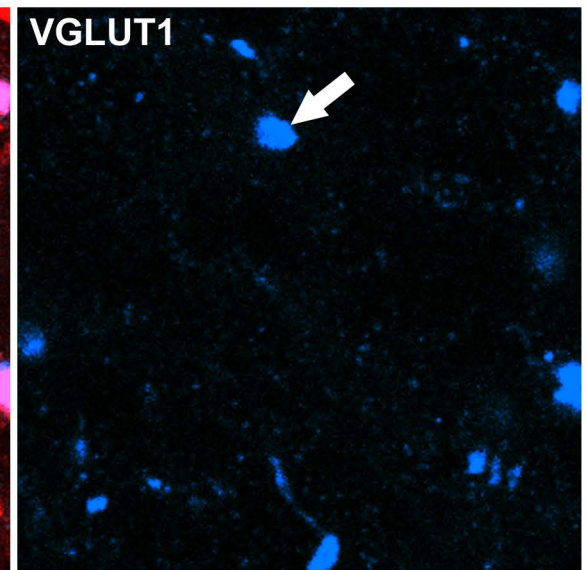
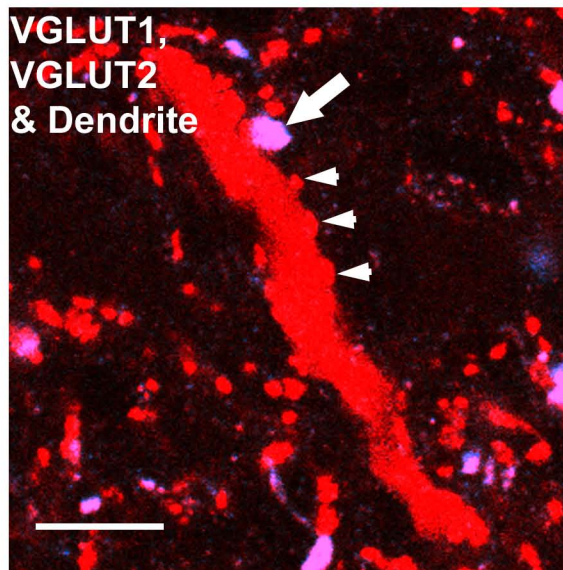
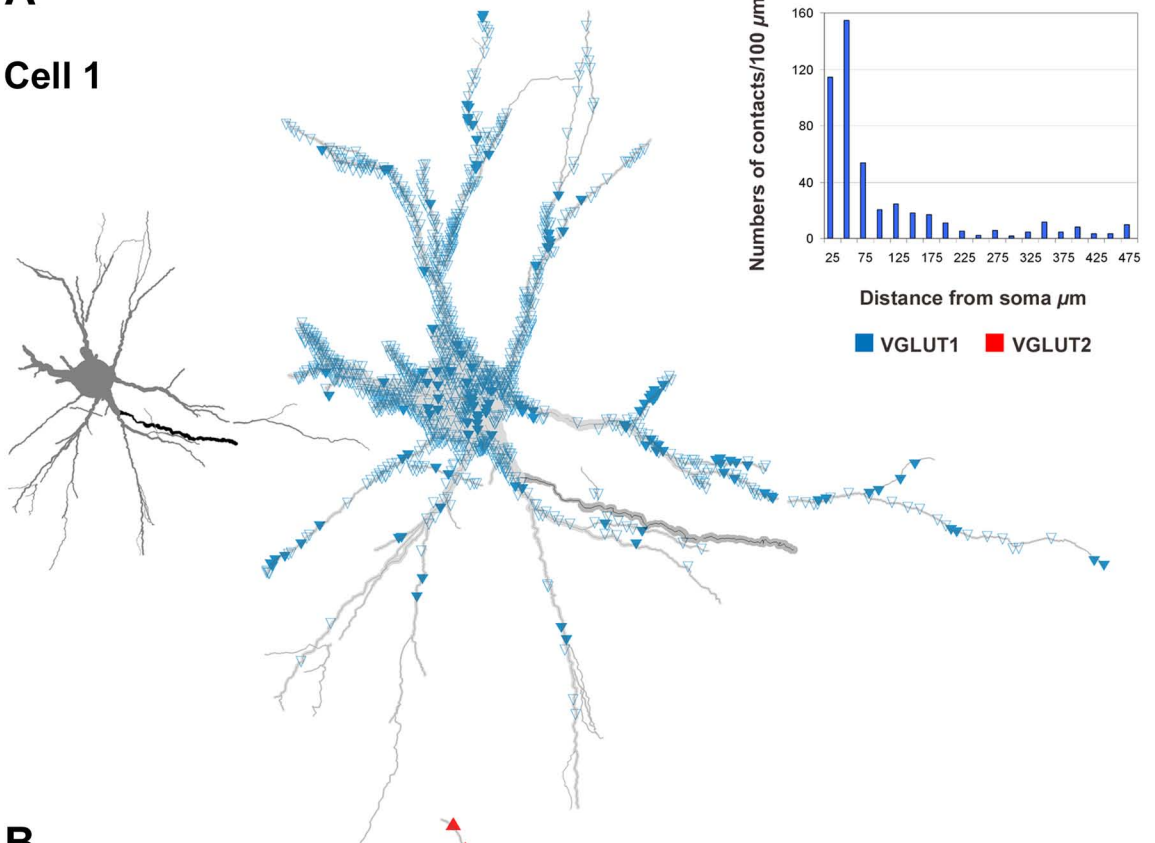


Figure 4.6. Reconstructions of cells with (A) and without (B) monosynaptic primary afferent input showing the distribution of VGLUT1 and VGLUT2 contacts. The reconstructions were made with NeuroLucica for Confocal. The two small images on the left without contacts plotted in figure A and B show the reconstructions of cell 1 and cell 21, respectively. Somata and dendrites are shown in grey and main axons in black. The two reconstructions in the middle show contacts on the two cells. The blue open triangles and blue filled triangles represent VGLUT1 terminals with and without associated presynaptic GAD terminals, respectively. The red triangles represent VGLUT2 terminals. The histograms are derived from Sholl analysis and show the numbers of contacts per 100 μm within 25- μm shells from the cell body of the two cells for each type. Scale bar = 50 μm .

A

Cell 1



B

Cell 21

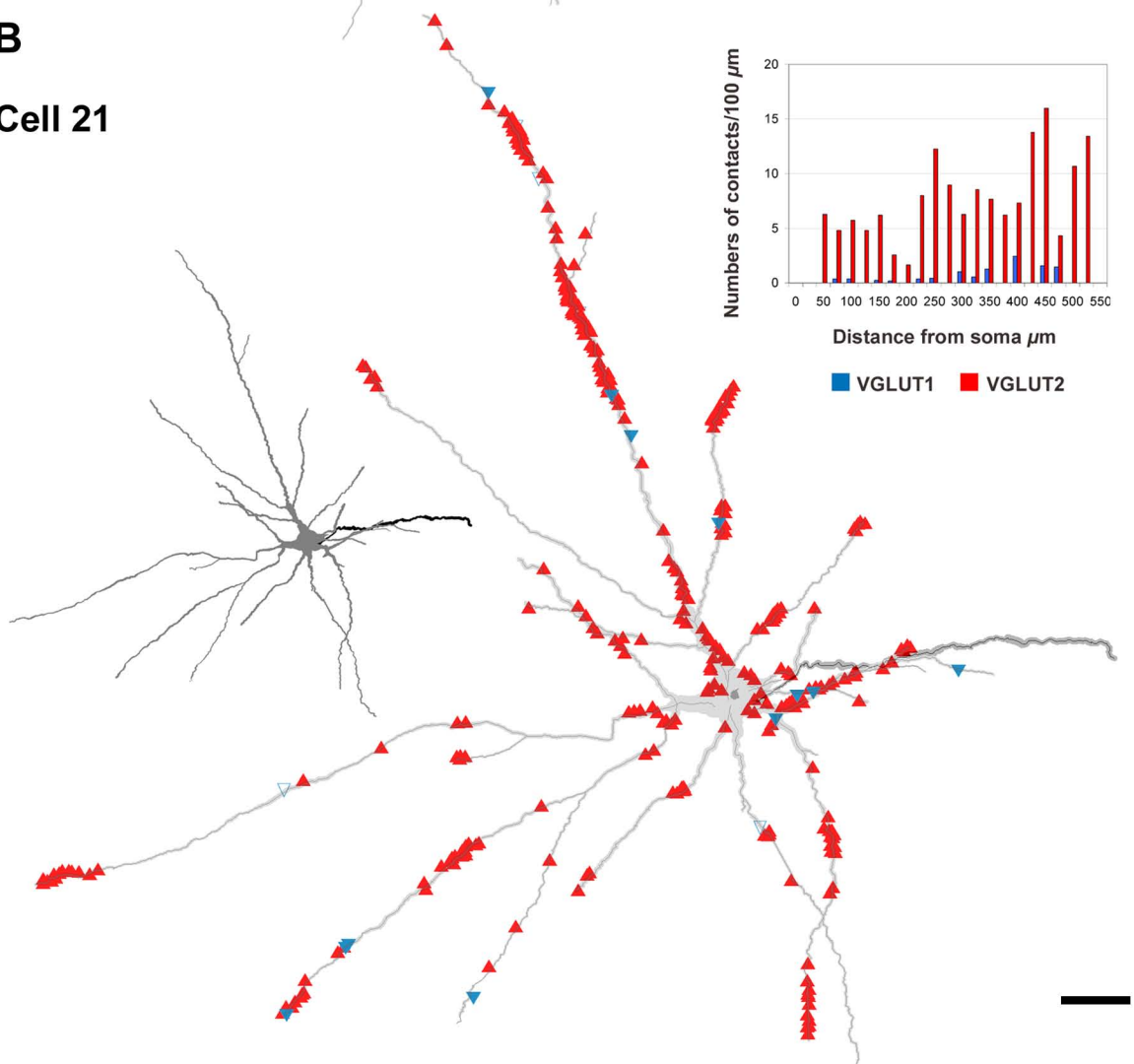
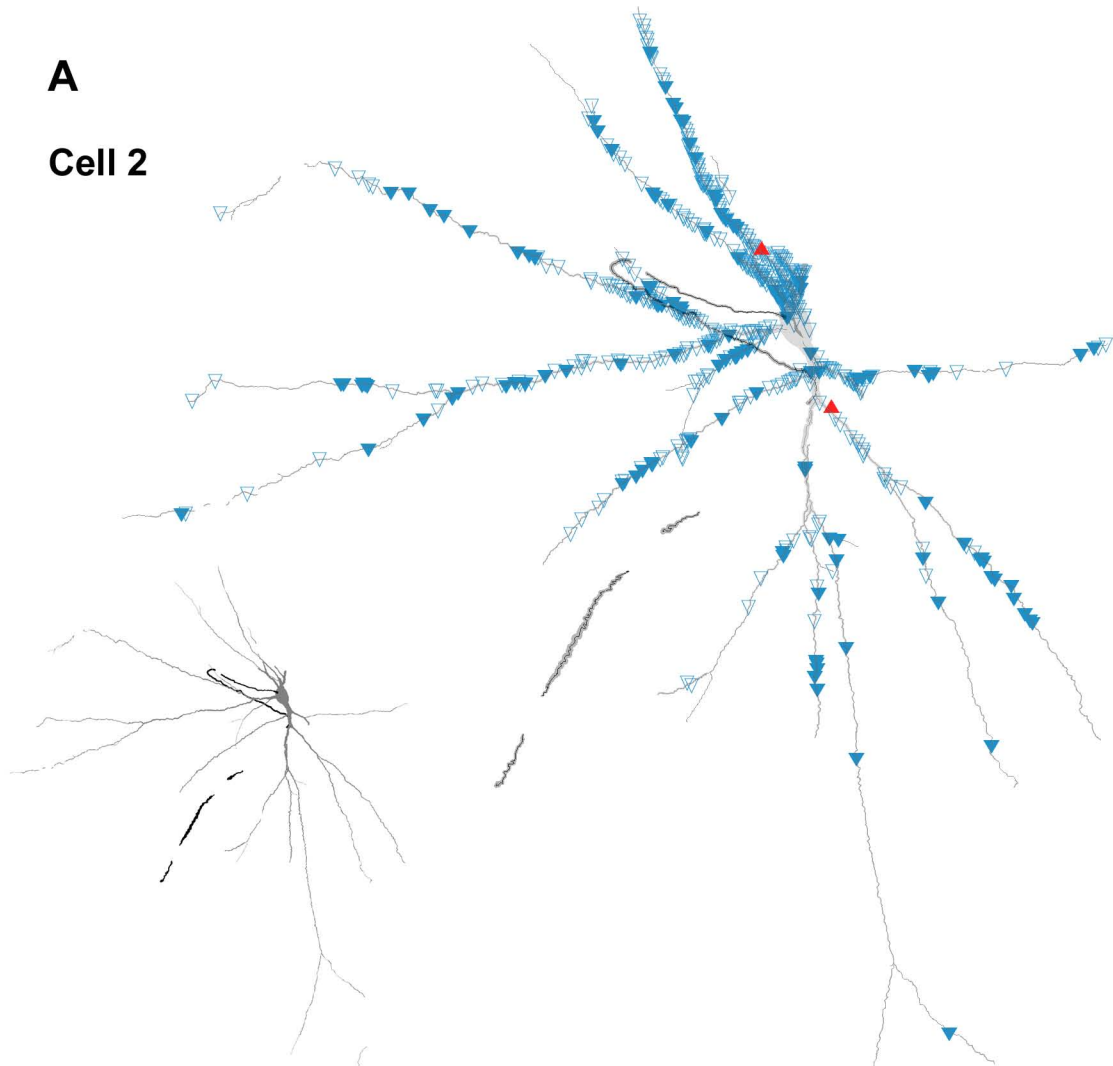
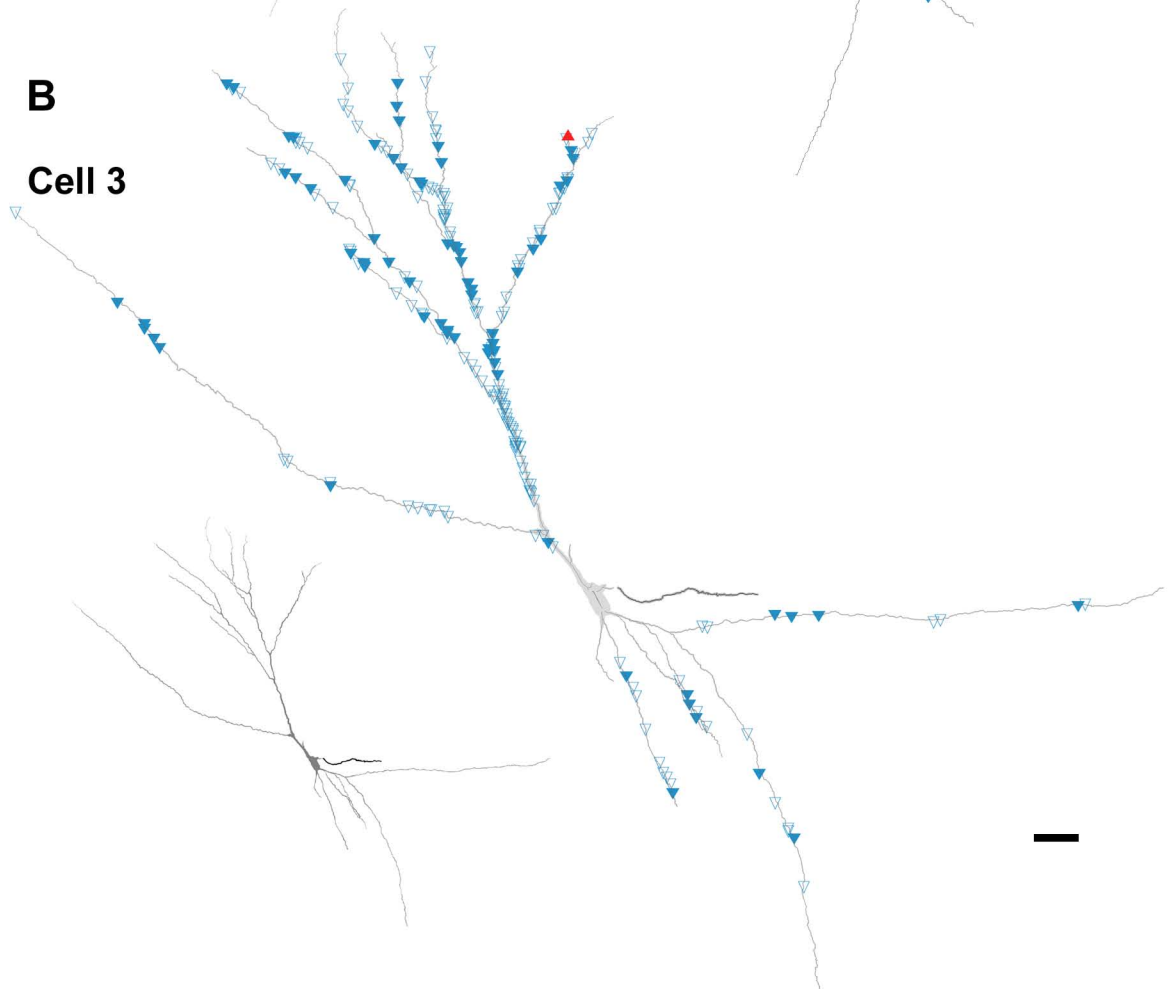


Figure 4.7. Reconstructions of cells with monosynaptic primary afferent input showing the distribution of VGLUT1 and VGLUT2 contacts. The reconstruction was made with NeuroLucida for Confocal. Figures A-F show excitatory cells (cells 2 to 7) and G-P show inhibitory cells (cells 8 to 17). All the small images without contacts plotted show the reconstructions of the 17 cells. Somata and dendrites are shown in grey and main axons in black. All the large reconstructions show distributions of contacts on these cells. The blue open triangles and filled triangles represent VGLUT1 terminals with and without associated presynaptic GAD terminals, respectively. The red triangles represent VGLUT2 terminals. Scale bar = 50 μm .

A
Cell 2

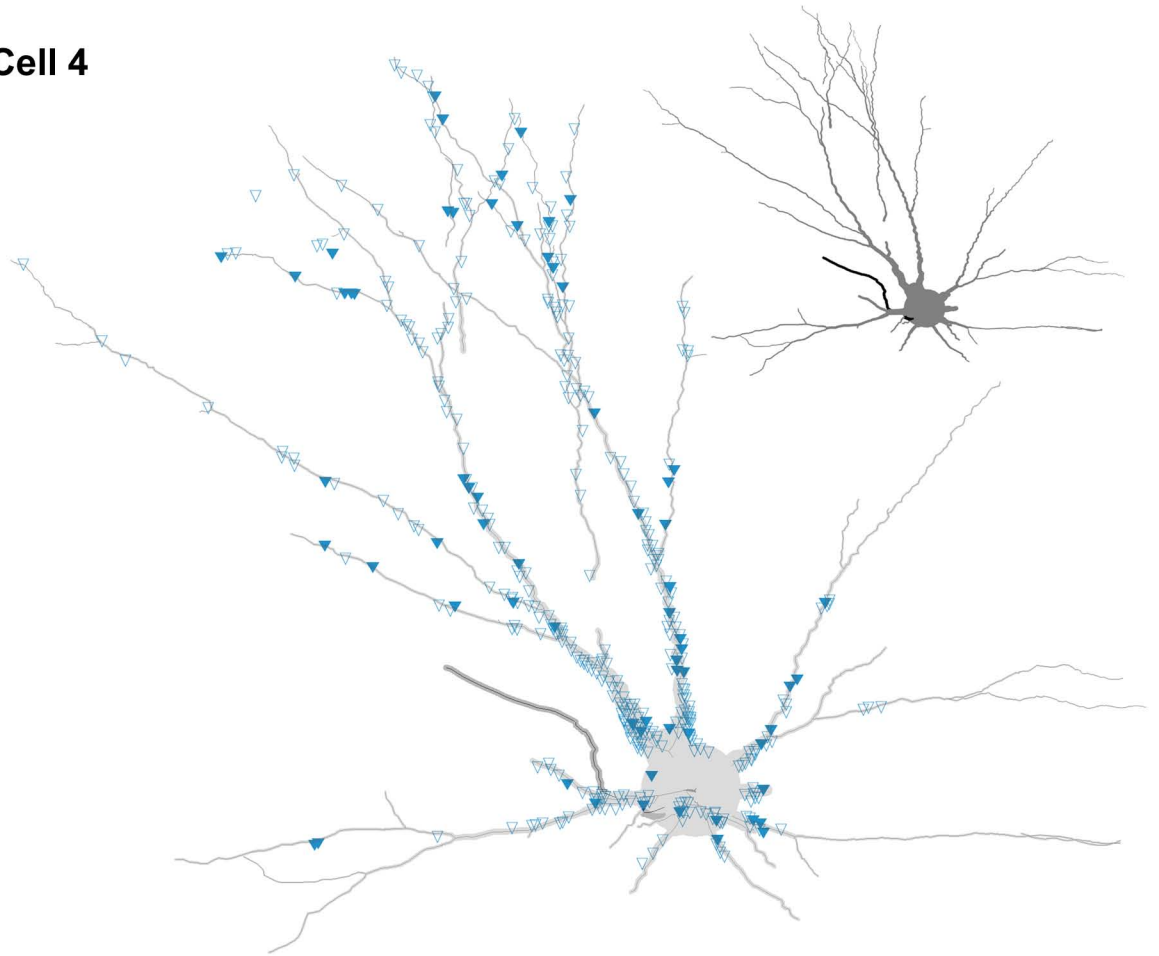


B
Cell 3



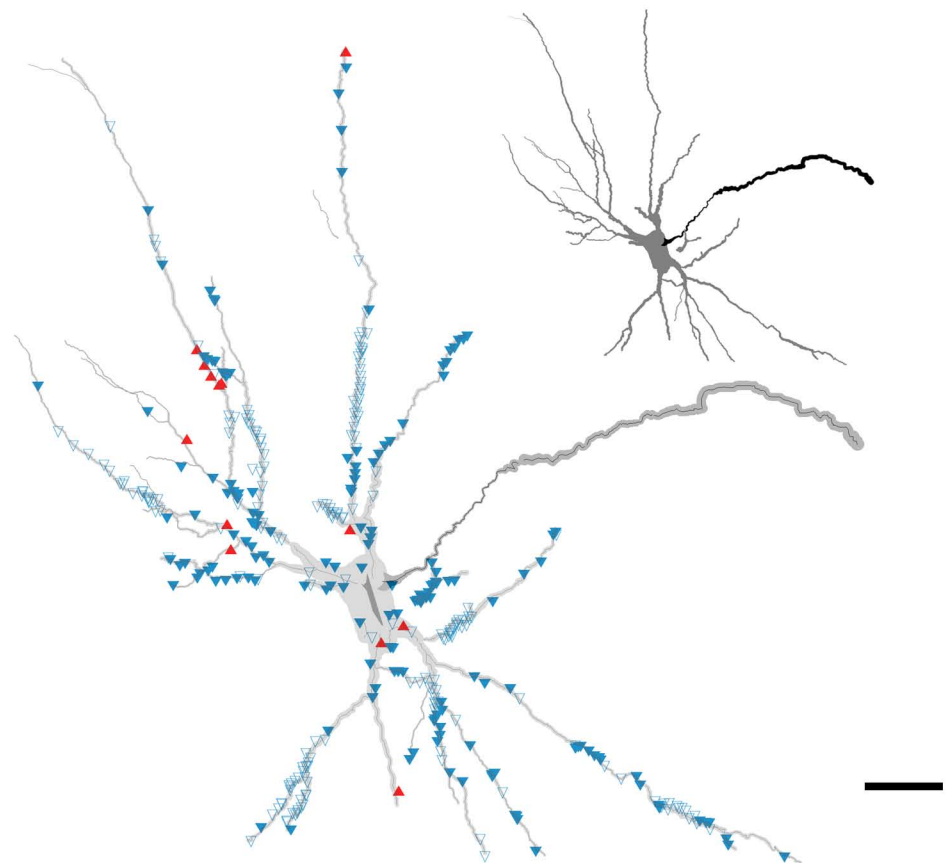
C

Cell 4



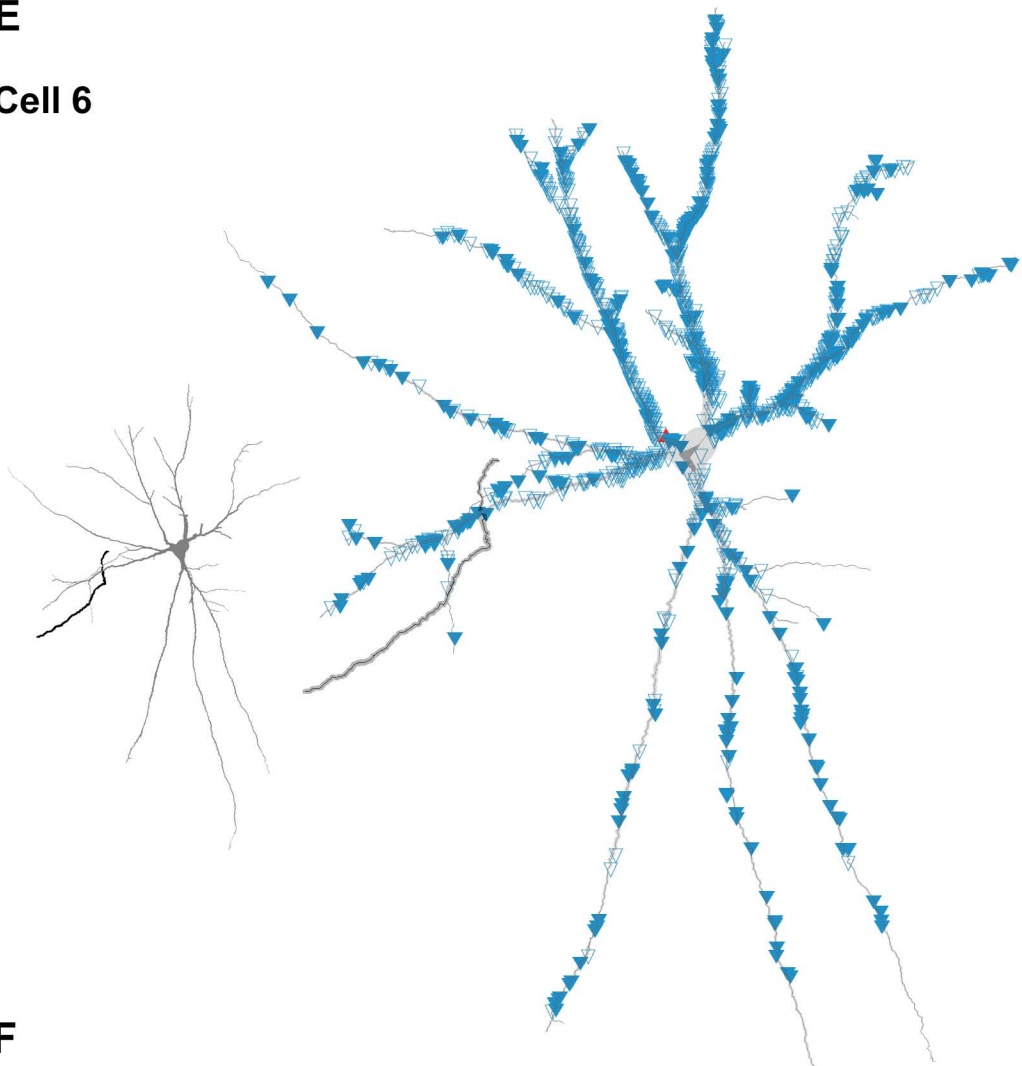
D

Cell 5



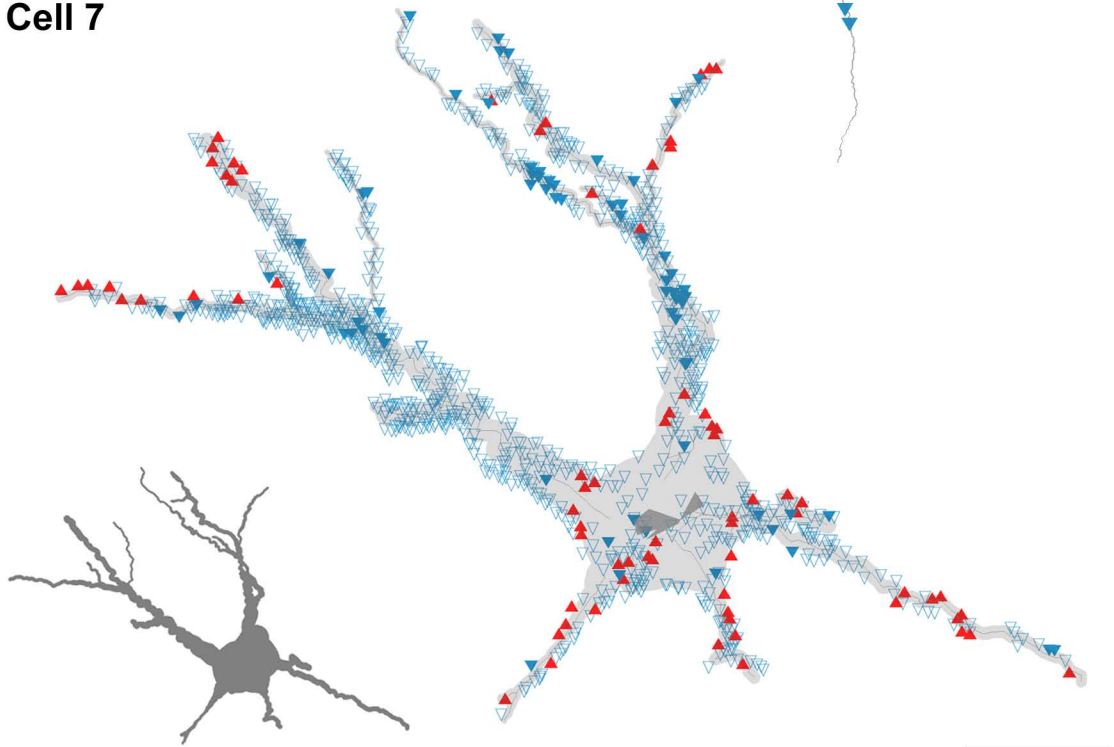
E

Cell 6



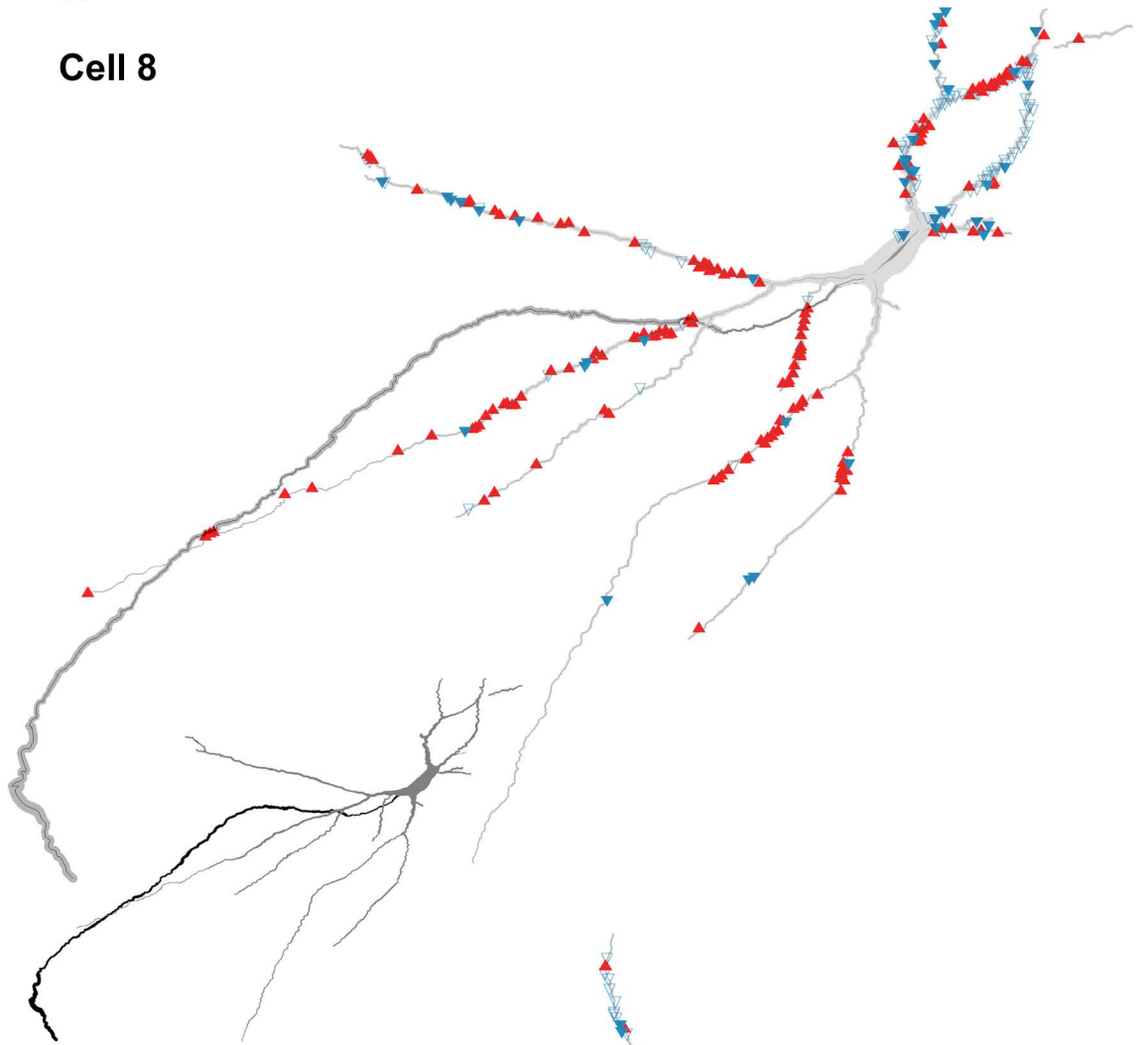
F

Cell 7



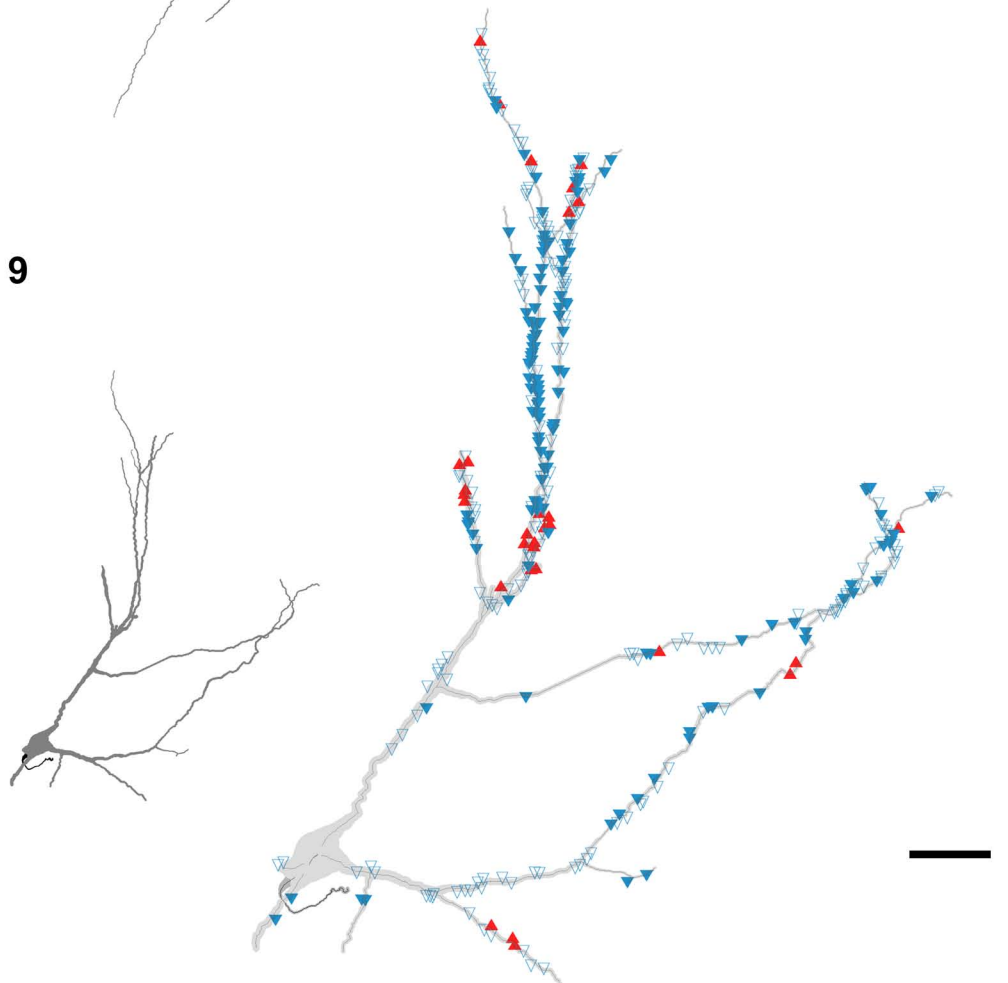
G

Cell 8



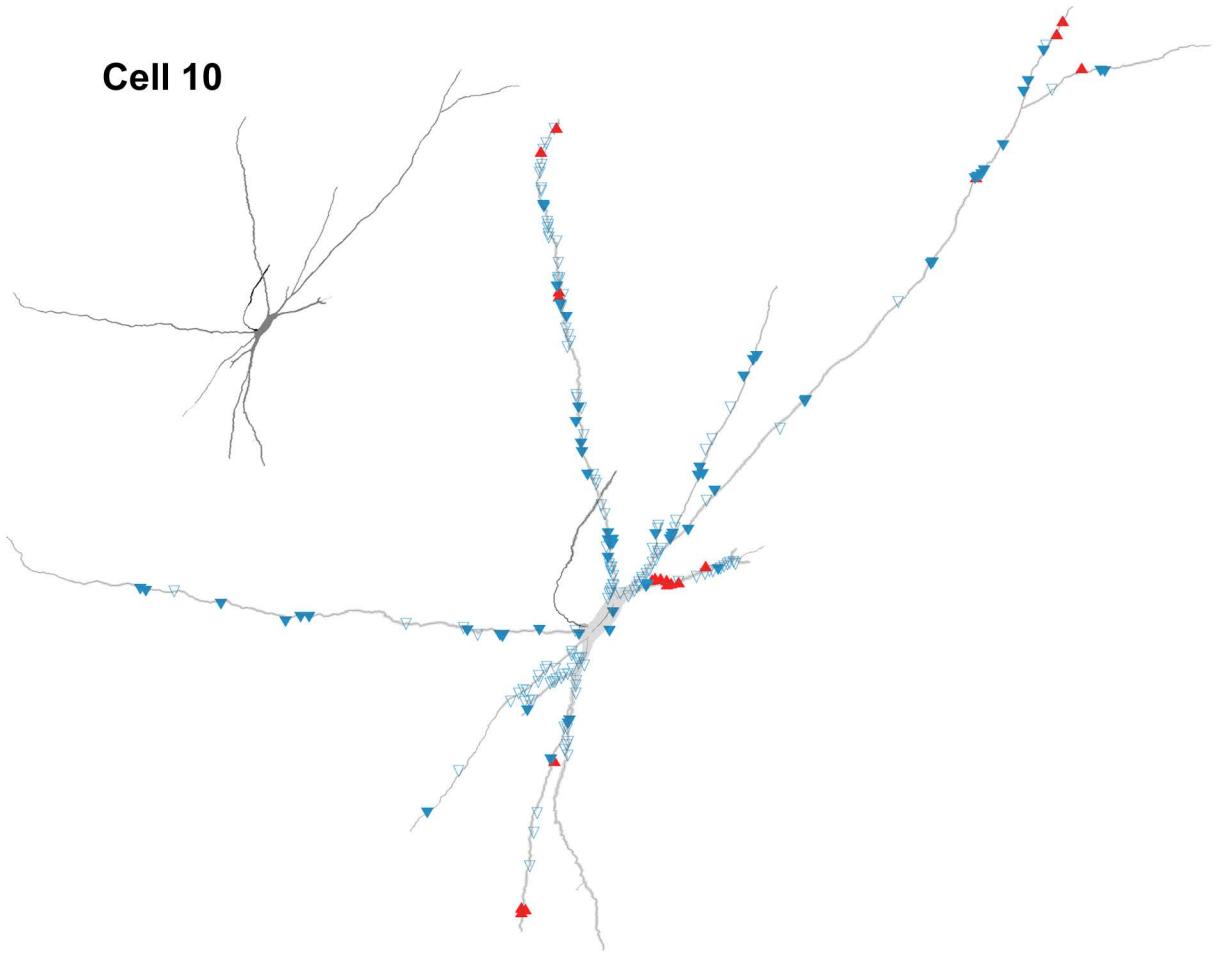
H

Cell 9



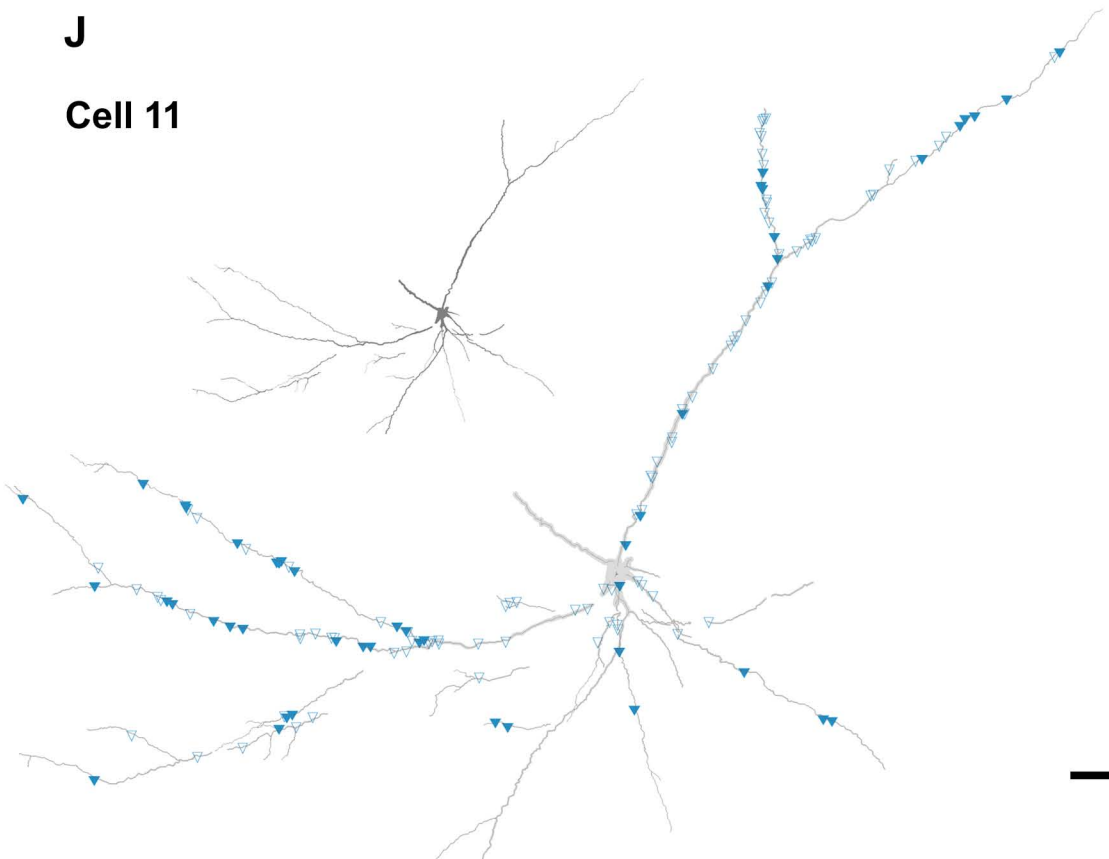
I

Cell 10



J

Cell 11

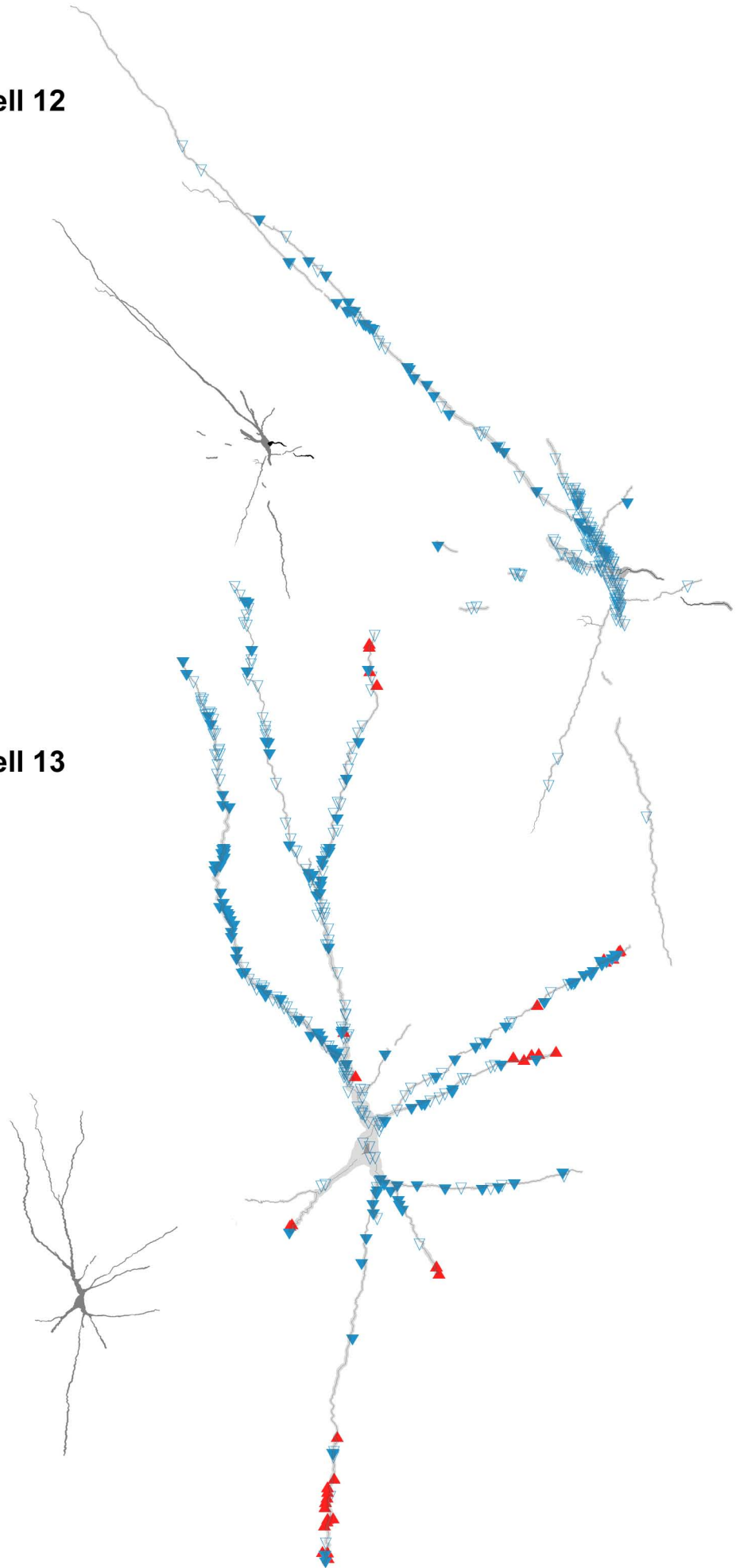


K

Cell 12

L

Cell 13



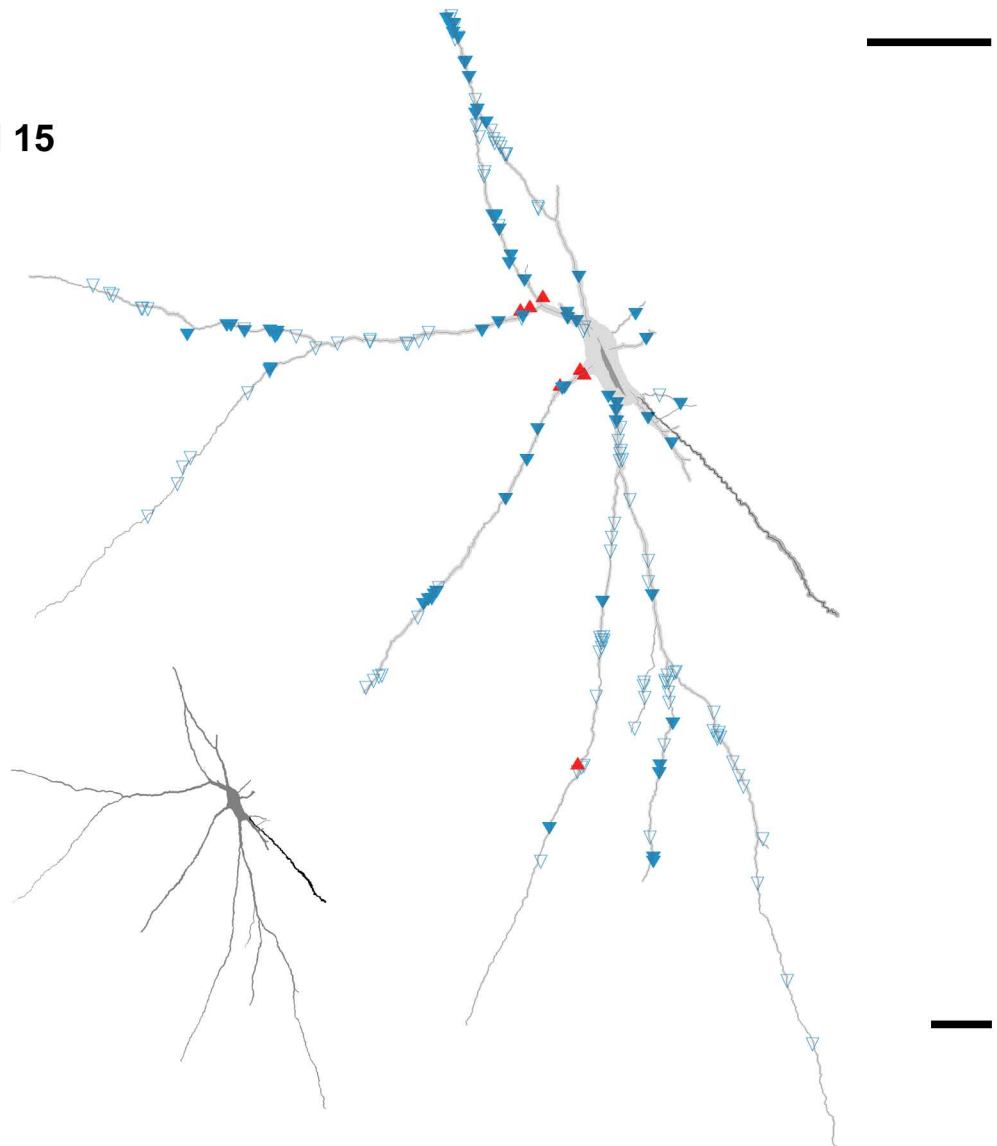
M

Cell 14



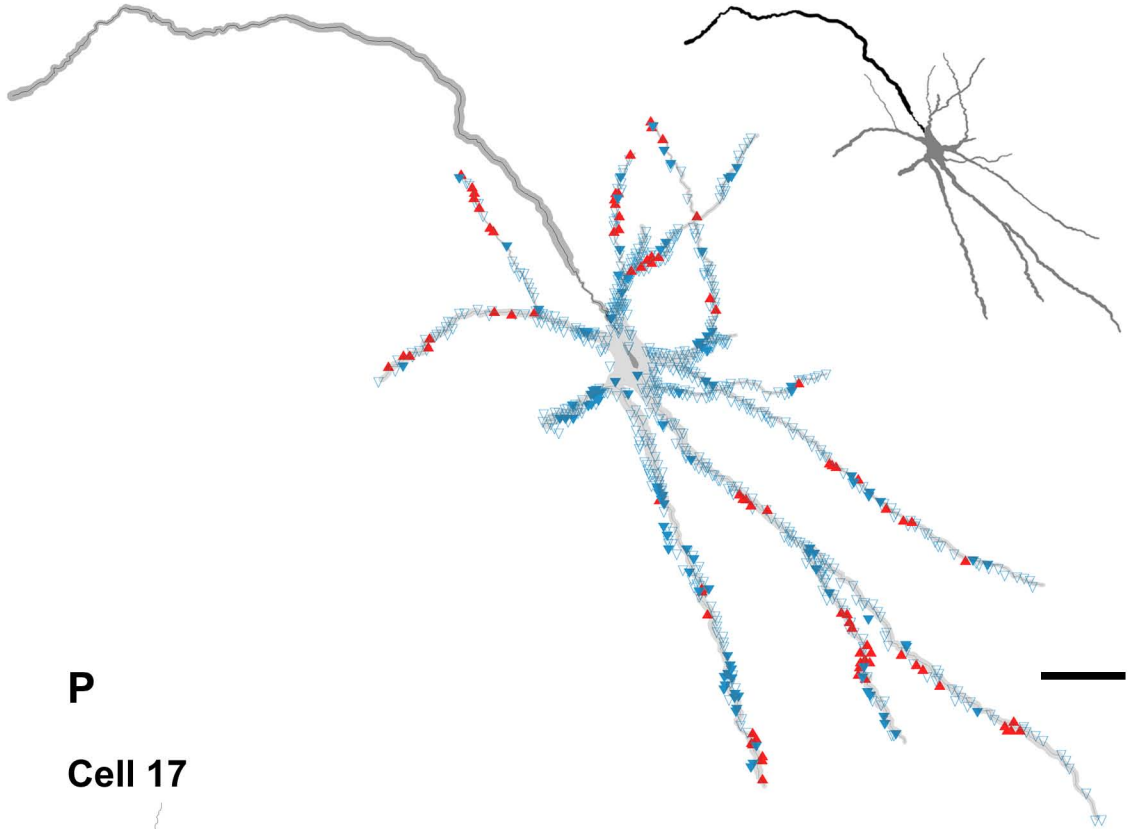
N

Cell 15



O

Cell 16



P

Cell 17

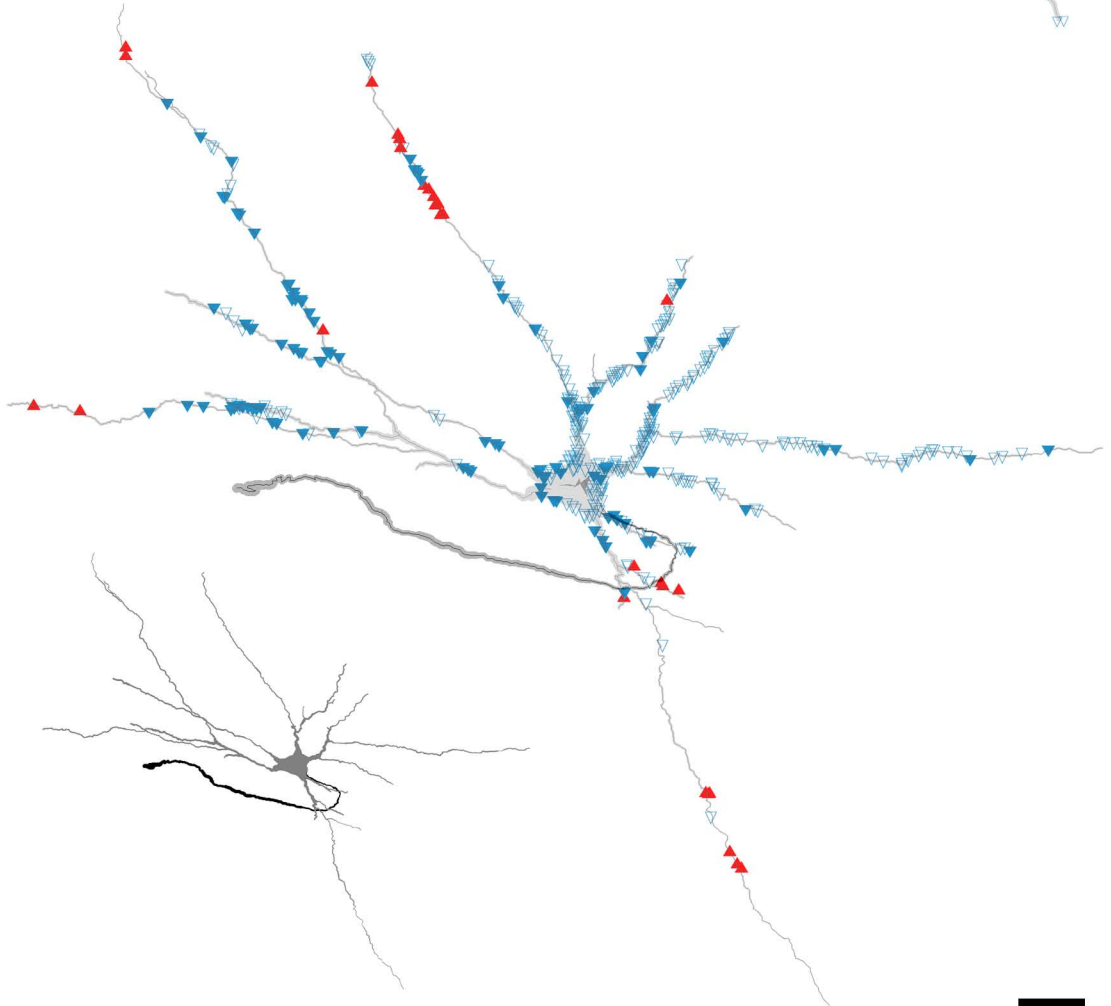
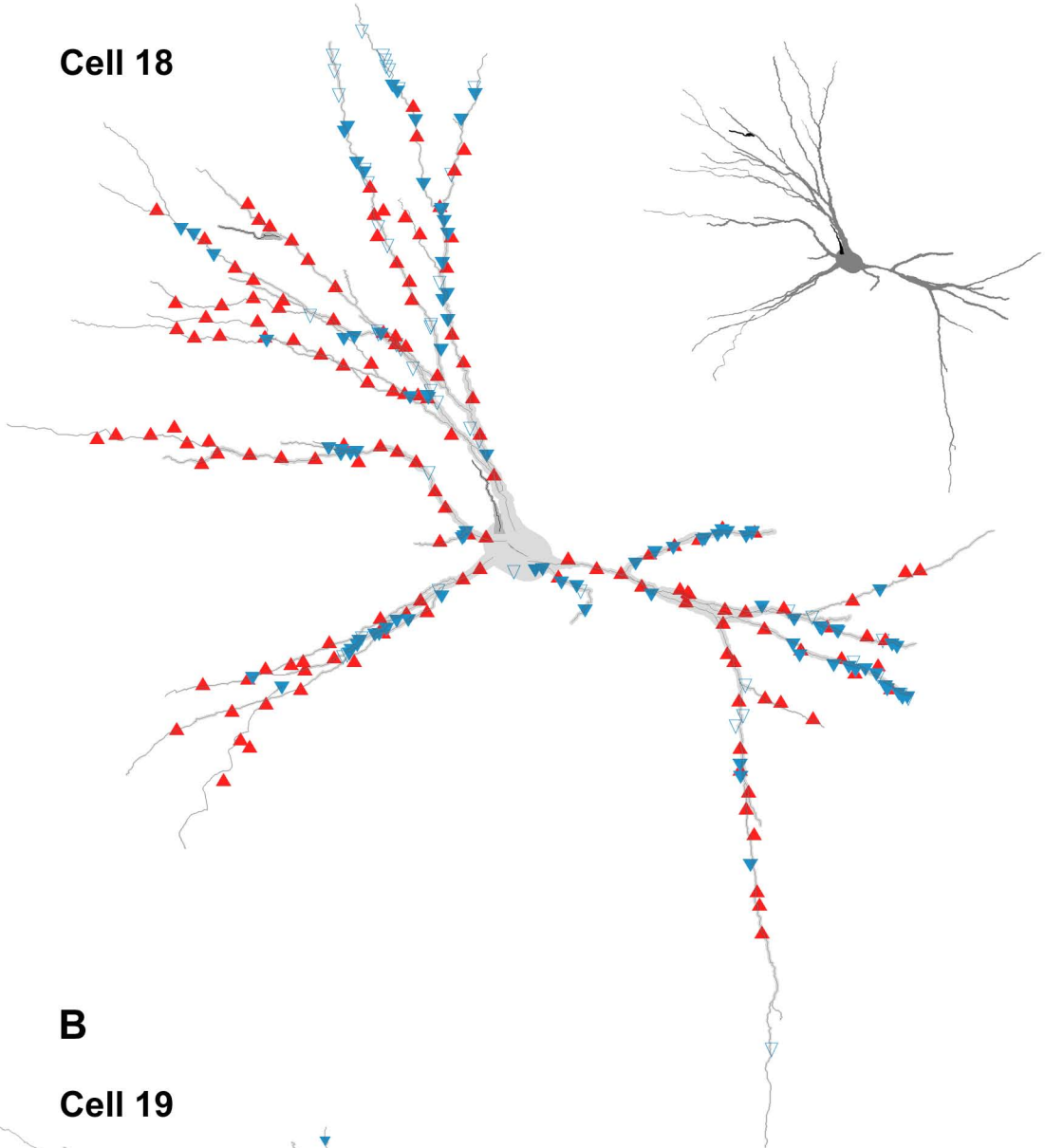


Figure 4.8. Reconstructions of cells without identified monosynaptic primary afferent input showing the distribution of VGLUT1 and VGLUT2 contacts. The reconstruction was made with NeuroLucida for Confocal. (A) and (B) show MLF cells with input from PT fibres (cells 18 and 19). (C) shows a MLF cell without input from PT fibres (cell 20). All the small images on the right without contacts plotted show the reconstructions of the three cells. Somata and dendrites are shown in grey and main axons in black. All the large reconstructions on the left show distributions of the contacts on these cells. The blue open triangles and filled triangles represent VGLUT1 terminals with and without associated presynaptic GAD terminals, respectively. The red triangles represent VGLUT2 terminals. Scale bar = 50 μm .

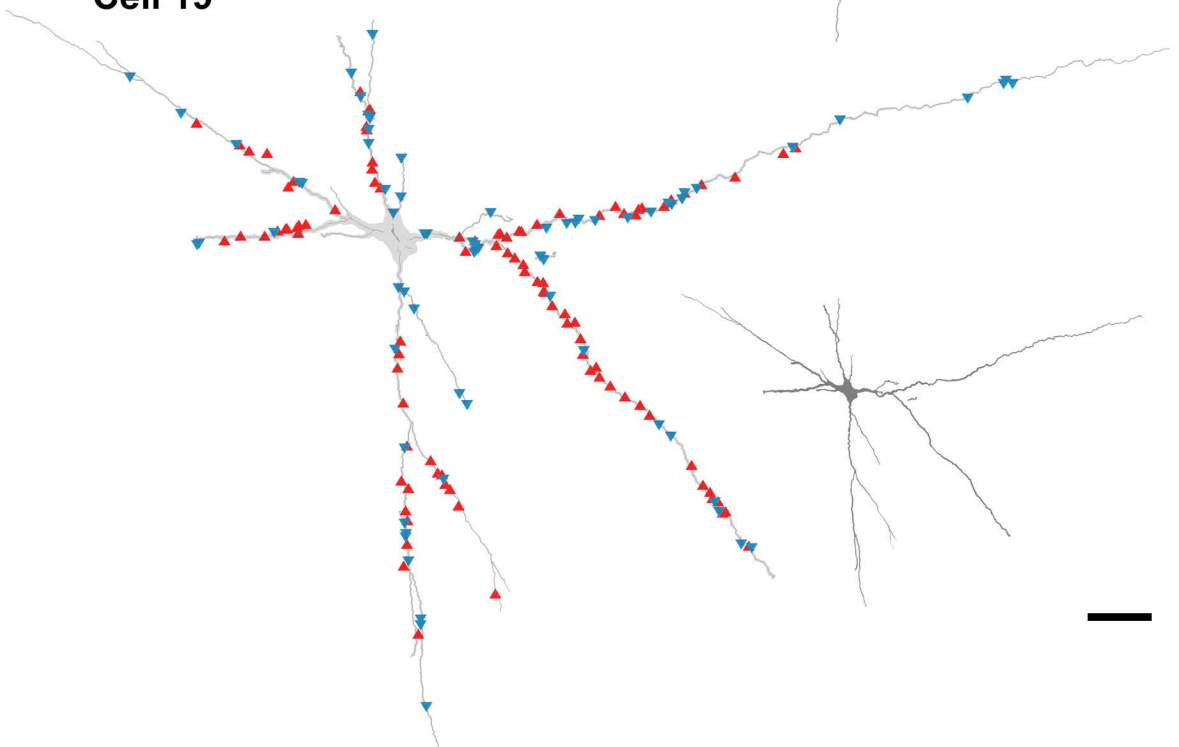
A

Cell 18



B

Cell 19



C

Cell 20

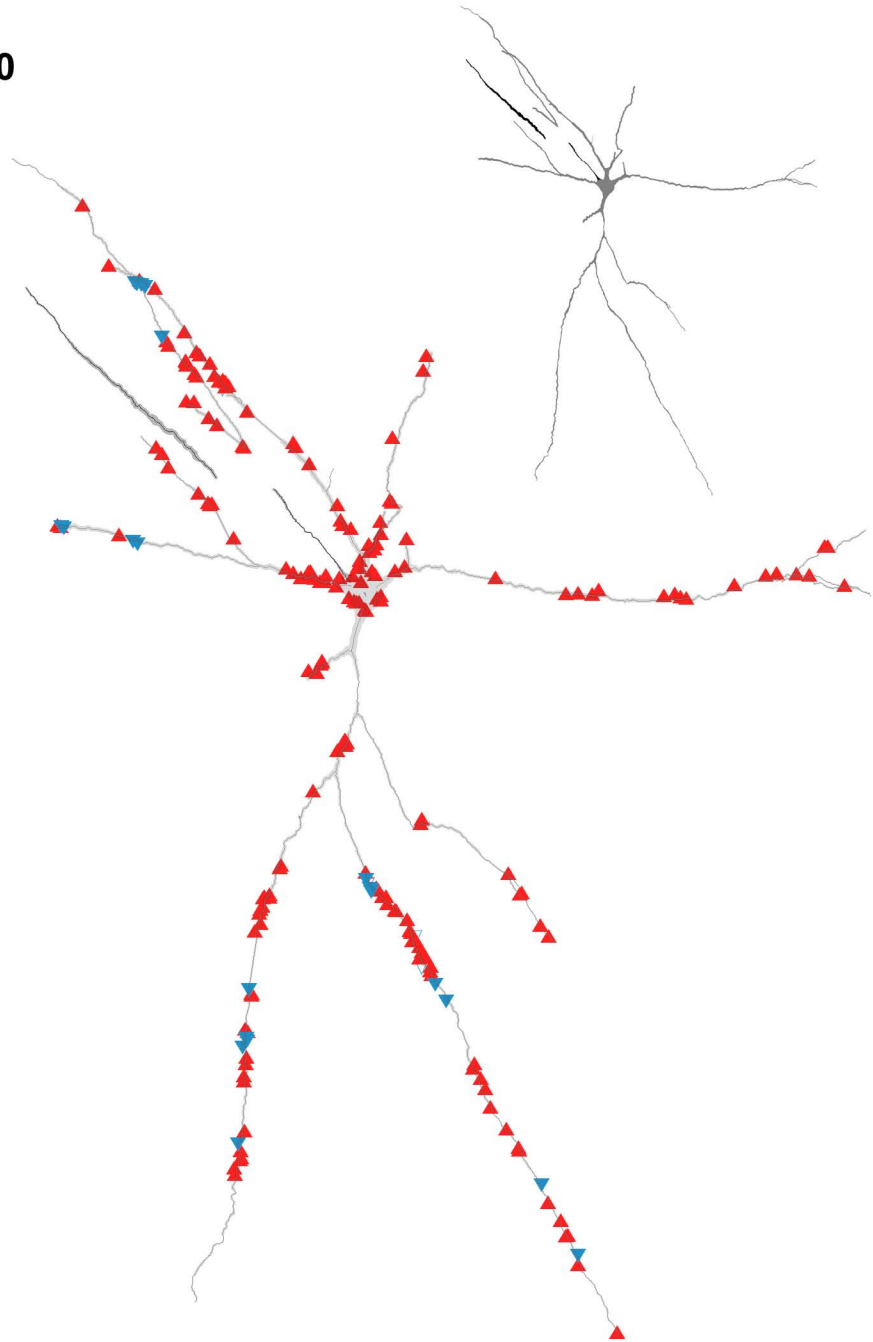


Figure 4.9. Comparison of the mean numbers of VGLUT1 and VGLUT2 terminals in contact with neurons (A) with or (B,C) without monosynaptic primary afferent inputs. The histograms show the mean numbers of contacts per 100 μm of dendritic length contained within concentric shells with radii which increase in 25- μm units from the centre of the cell body. (A) Group A cells (cells 1 to 17) received monosynaptic input from primary afferent inputs. (B) The first subgroup of cells (cells 18 and 19) received monosynaptic input from MLF. (C) The second subgroup of cells (cells 20 and 21) with monosynaptic input from MLF. Bars show standard deviations. Note that the scale in A is different with those in B and C.

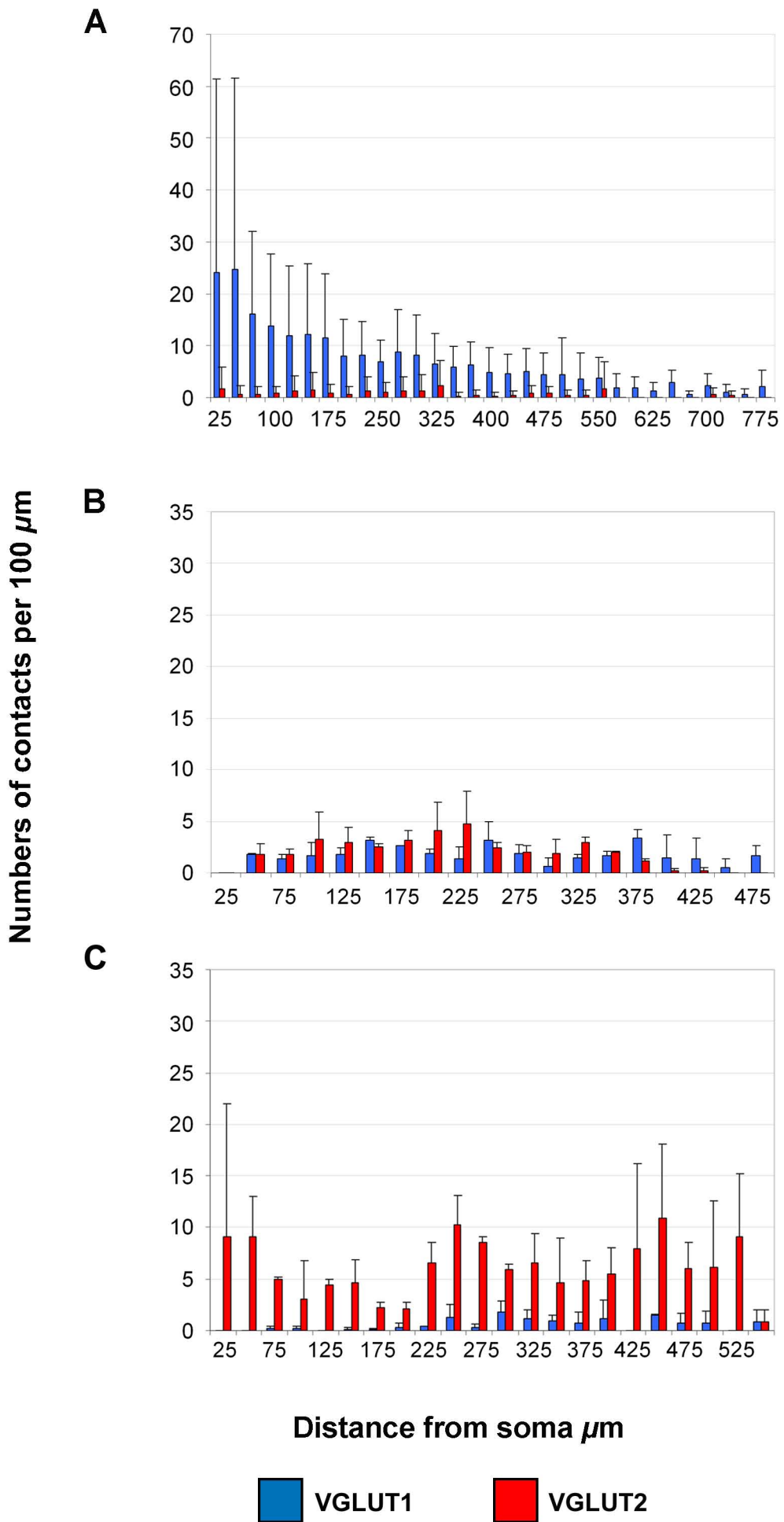


Figure 4.10. Immunocytochemical characteristics of a glutamatergic interneuron and a glycinergic interneuron. (A) A series of confocal microscope images illustrating neurotransmitter content of boutons originating from an excitatory neuron. The left panel shows projected images of two terminals of an excitatory neuron. The panels on the right show single optical sections through individual boutons. Axon terminals are shown in red (arrows), immunoreactivity for VGLUT2 in blue, and GAD in green. The merged image (far right) confirms that the terminals are immunoreactivity for VGLUT2. (B) The large panel on the left shows a projected image through a series of terminals of an inhibitory neuron. Additional small images are single optical sections through individual terminals (arrows). Axons are shown in red, immunoreactivity for gephyrin in green, and VGLUT1 in blue. The right panel of each series is a merged image confirming the association between gephyrin and the labelled interneuronal terminals. Scale bars = 10 μm .

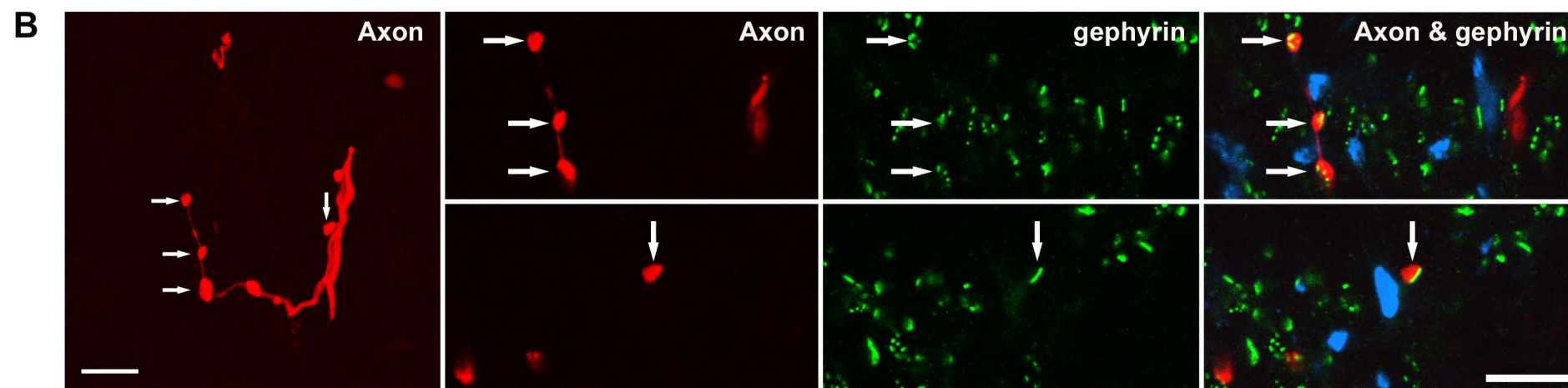
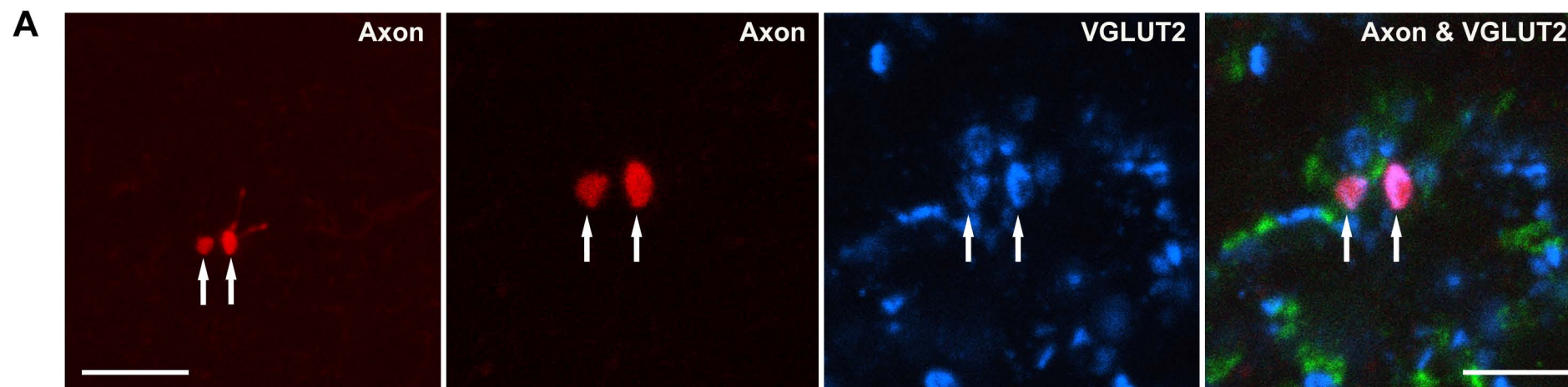


Figure 4.11. A series of confocal microscope images illustrating neurotransmitter content of terminals contacting the labelled interneuron and their relationship with GABA-containing terminals. The left two panels show single optical sections through individual boutons (arrowheads and arrows). The dendrite of the postsynaptic interneuron is shown in red, immunoreactivity for GAD in green and VGLUT1 in blue. The right two panels are merged images confirming that the VGLUT1 terminals are associated with presynaptic GAD terminals and are in turn presynaptic to the labelled interneuronal dendrite. Scale bar = 10 μ m.

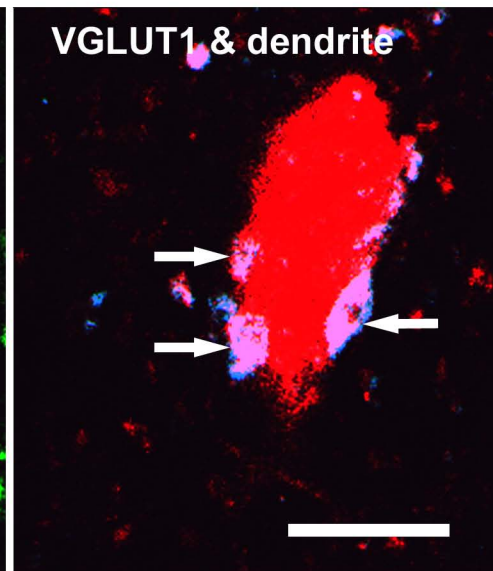
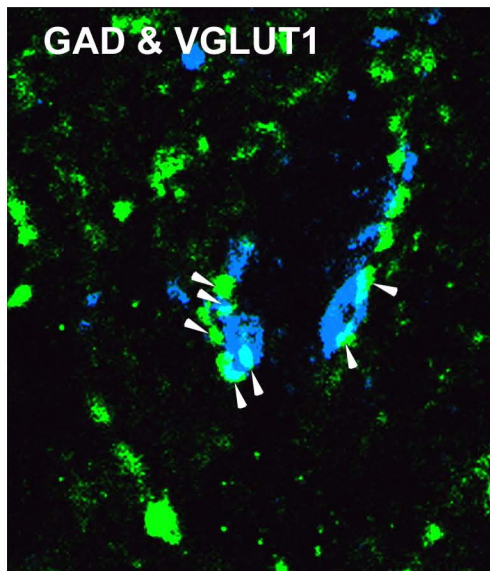
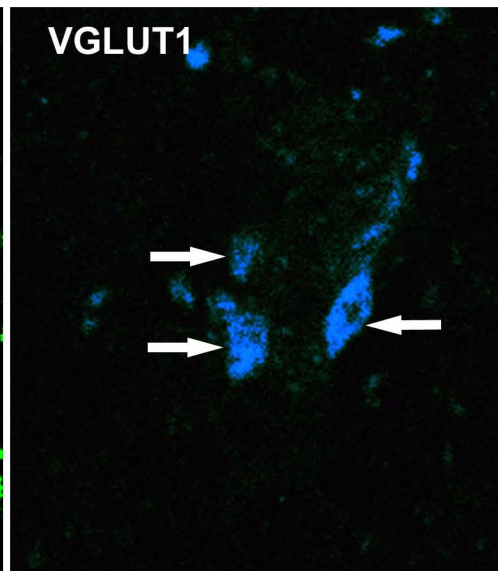
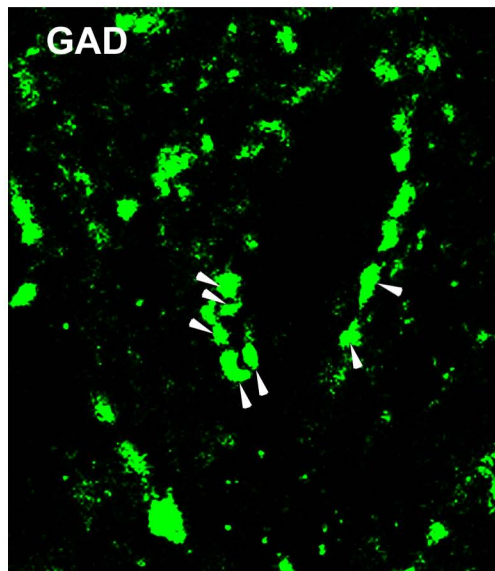


Figure 4.12. A series of confocal microscope images illustrating CTb retrogradely labelled CINs located in contralateral lamina VIII and neurotransmitter content of terminals contracting the labelled CINs. (A) A general overview of VGLUT1 and VGLUT2 terminals in contact with CTb labelled CINs in lamina VIII. Details of the areas demarcated by the boxes are shown in B1-B4, C1-C4 and D1-D4. (B1-B4 and C1-C4) Single optical sections illustrating the neurotransmitter content of terminals making synapses with the dendrites of the CIN. The labelled CINs are shown in red, immunoreactivity for VGLUT2 in green and VGLUT1 in blue. Arrows indicate VGLUT2 terminals in contact with the labelled CIN dendrites. The arrowhead indicates a VGLUT1 terminal contacting a dendrite. Asterisks indicate both VGLUT1 and VGLUT2 immunoreactive terminals contacting the CIN dendrite. (D1-D4) Single optical sections illustrating the neurotransmitter content of terminals making synapses with a cell body of a labelled CIN. Arrowhead indicates a VGLUT1 terminal in contact with the cell body. Scale bar = 10 μm (A), 5 μm (B1-B4, C1-C4, D1-D4).

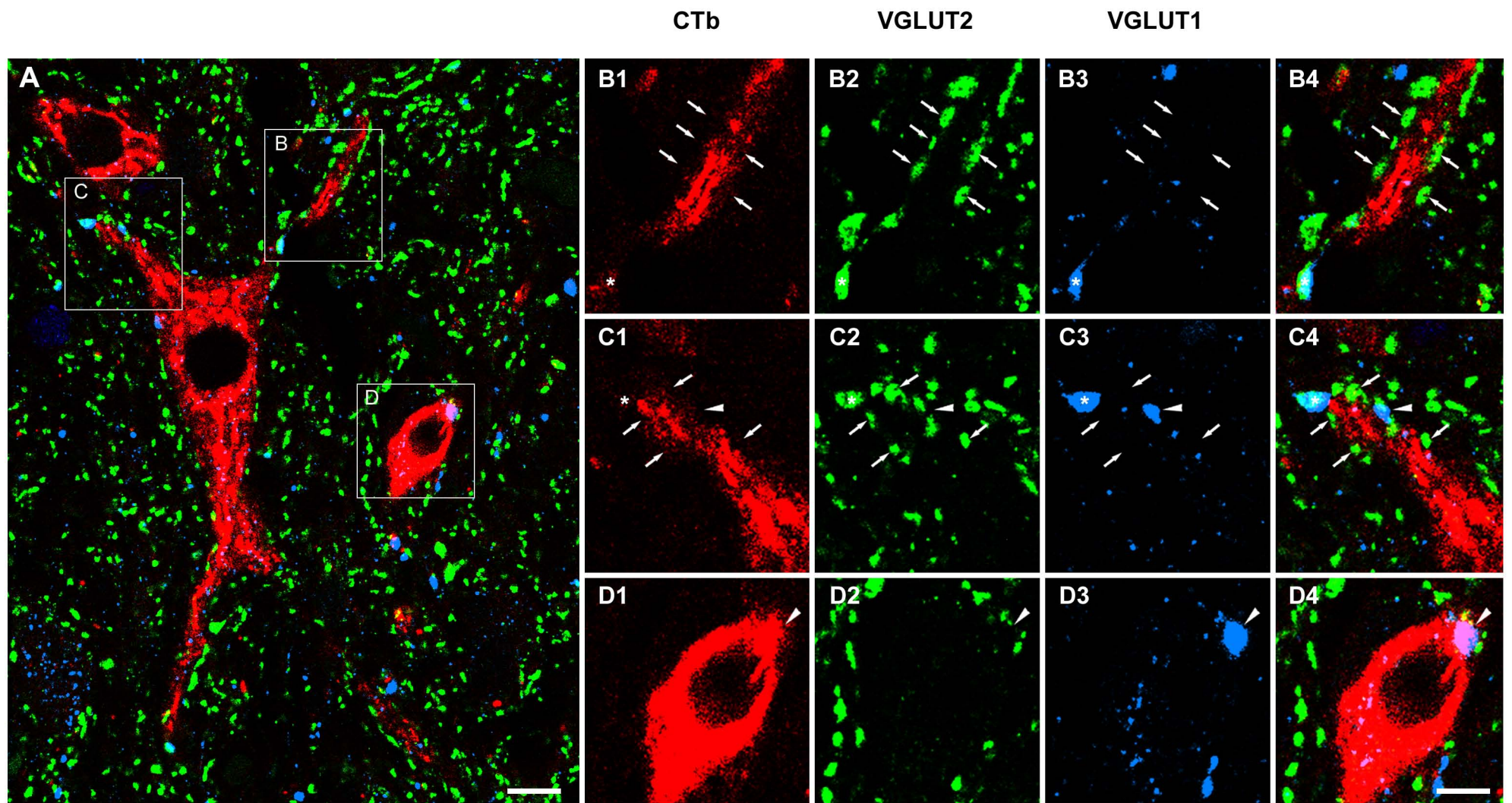


Figure 4.13. A series of confocal microscope images illustrating CTb retrogradely labelled CINs located in contralateral laminae V-VI and neurotransmitter content of terminals contracting the labelled CINs. (A) A general overview of VGLUT1 and VGLUT2 terminals in contact with CTb labelled CINs in laminae V-VI. Details of the areas demarcated by the boxes are shown in B1-B4 and C1-C4. (B1-B4 and C1-C4) Single optical sections illustrating the neurotransmitter content of terminals making synapses with the cell bodies of the CIN. The labelled CINs are shown in red, immunoreactivity for VGLUT2 in green and VGLUT1 in blue. Arrows indicate VGLUT2 terminals in contact with the cell bodies. Arrowheads indicate VGLUT1 terminals contacting the cell body. Scale bar = 10 μm (A), 5 μm (B1-B4, C1-C4, D1-D4).

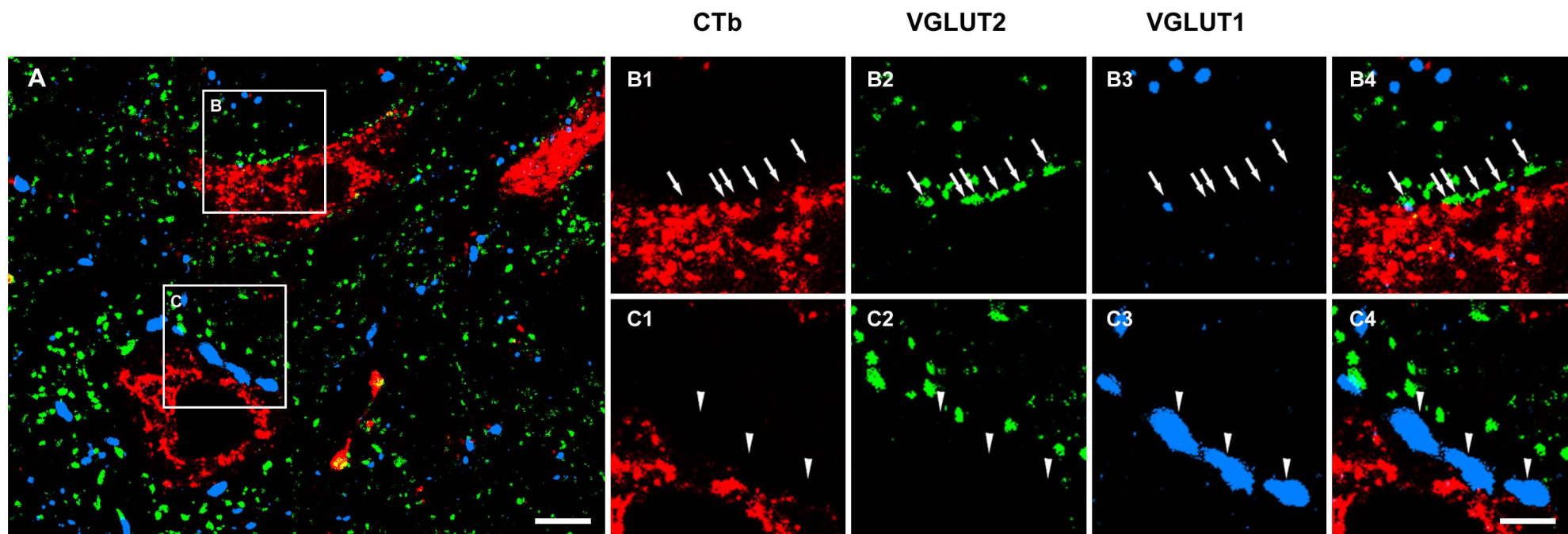


Figure 4.14. The synapses formed with the intermediate zone interneurons and by their axon collaterals. The axonal projections partly based on the morphological findings reported by Bannatyne et al., (2003, 2009), and Jankowska et al., (2005, 2009). The big green and red circles represent excitatory and inhibitory intermediate zone interneurons with monosynaptic group I and II muscle afferent input, respectively. The white circle represents lamina VIII commissural interneurons with monosynaptic input from MLF/vestibulospinal tract (VST) but without monosynaptic primary afferent input. The green, red and black lines with small circles at the end represent the axon projections of the corresponding cells. The blue, grey and dashed grey lines with small circles at the end represent group I/II afferents, MLF inputs, and VST fibres, respectively. The small red triangles indicate presynaptic terminals associated with the primary afferent terminals. INs, interneurons; MNs, motoneurons.

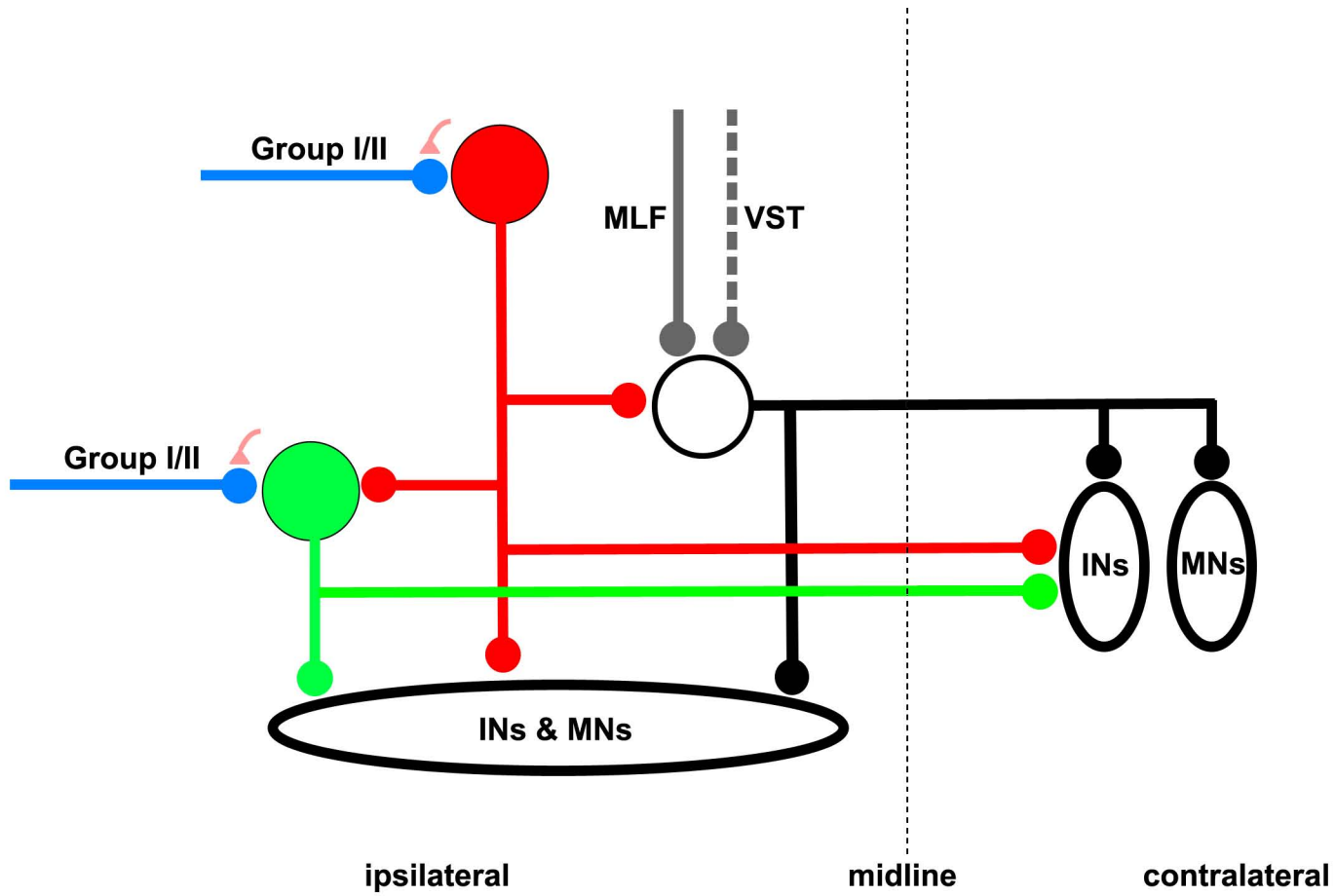


Figure 4.15. Schematic diagrams illustrating postsynaptic excitation and presynaptic inhibition in flexor reflex pathways. Green and red circles represent excitatory and inhibitory interneurons, respectively. Input lines with different colour (deep blue, light blue and grey) indicate different classes of primary afferents. White circles represent motoneurons. The small red triangles in image (C) indicate presynaptic terminals associated with primary afferent terminals. (A) Selection of opposite actions by an additional excitatory input. The pathway a1 is selected because of the facilitation from the convergent input b, resulting in the excitatory actions on motoneurons but not inhibitory actions. (B) Integration of information for coordinated activates. Interneurons interposed in different pathways (d and e, respectively) are excited by their common input c so that motoneurons innervating different muscles are activated together. (C) Selection of opposite actions by the modulation of presynaptic inhibition. Transmission of input f2 is depressed by presynaptic inhibition; thus motoneurons are activated by excitatory actions induced from pathway f1. Mn, motoneurons.

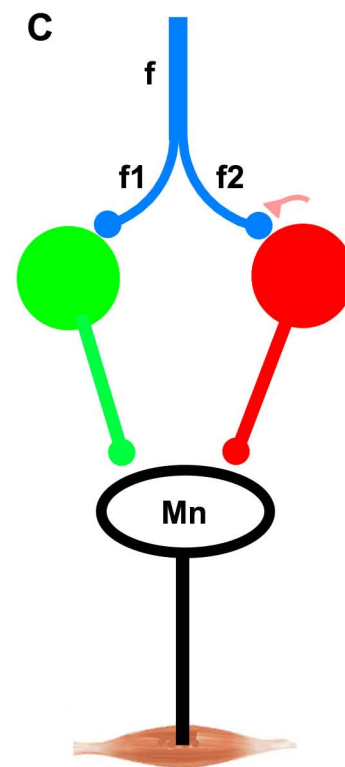
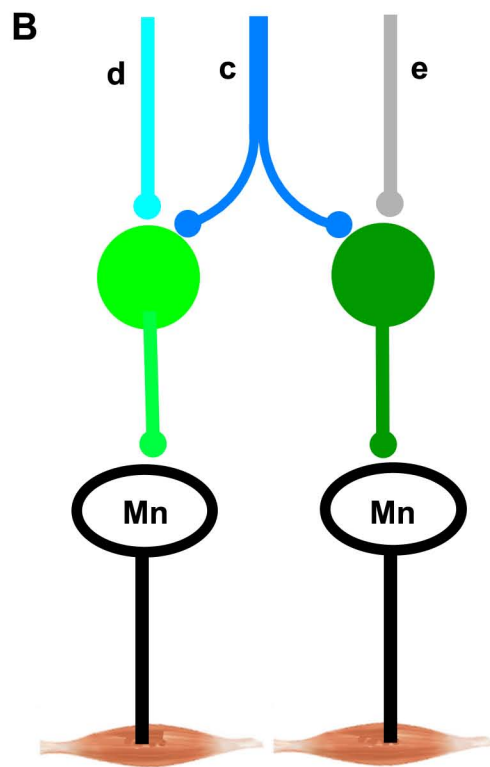
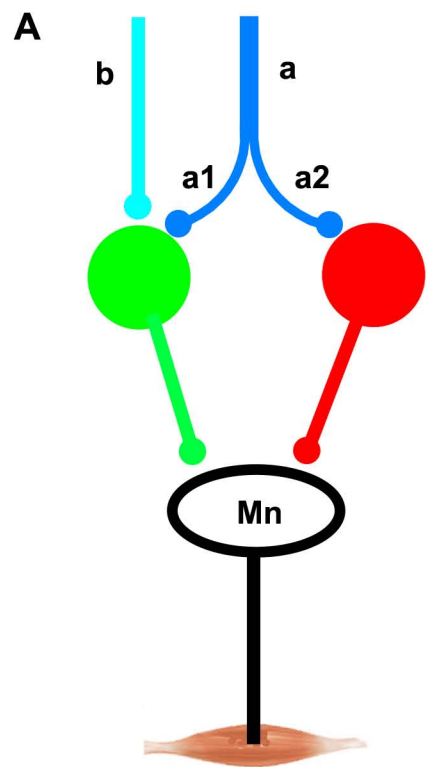


Figure 4.16. Summarized diagram illustrating the excitatory contacts to dorsal horn and lamina VIII CINs from interneurons with monosynaptic group I/II inputs. The white circles represent CINs located in dorsal horn (upper) and lamina VIII (lower), with axons (shown in black lines) projecting to contralateral side. The big green ovals represent excitatory interneurons with monosynaptic input from group I/II muscle afferents located in dorsal horn, intermediate zone and lamina VIII. The green lines with small circles at the end represent the axon projections to the corresponding cells. The projection areas of dorsal horn, intermediate zone and lamina VIII interneurons are from Bannatyne et al., (2006); (2009), and (2003) respectively.

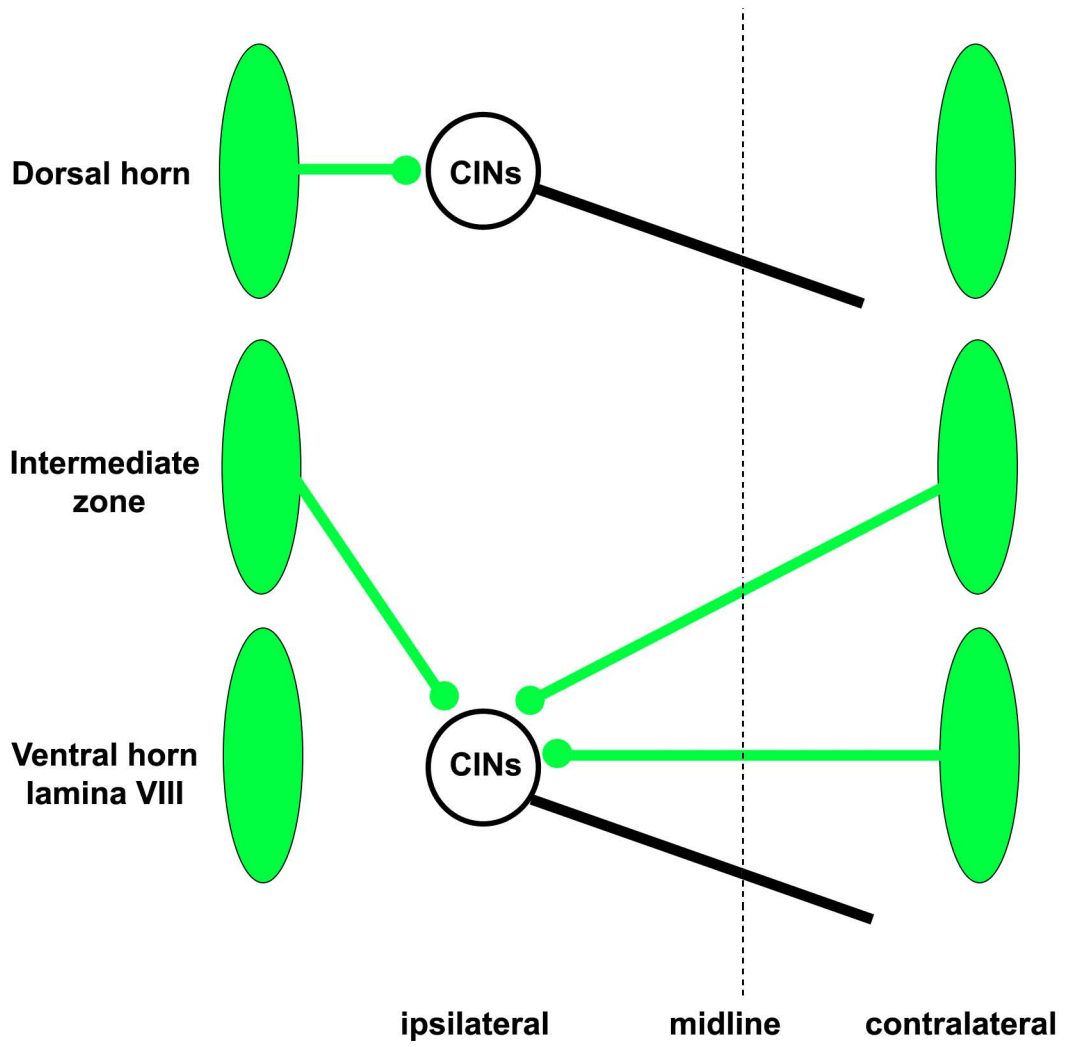


Table 4.2. Summary of morphological, neurochemical and electrophysiological data

	Morphology			Excitatory input	Immunocytochemical identify of terminals
	Segmental location	Soma position	Axonal projection		
Cell1	L4	Mid VII	Bilateral	I	VGLUT2
Cell 2	L6	Mid VII	Ipsilateral	I & MLF	VGLUT2
Cell 3	L7	Medial VII	Contralateral	I & MLF	VGLUT2
Cell 4	L5	VII	Bilateral	I	VGLUT2
Cell 5	L4	Lat VII	Bilateral	I & MLF	VGLUT2
Cell 6	L6	VII	Ipsilateral	I& MLF	VGLUT2
Cell 7	L4	Lat VII	Contralateral	I & II	VGLUT2
Cell 8	L4	Medial VII	Ipsilateral	I,II & MLF	gephyrin
Cell 9	L6	Lat VI	Ipsilateral	I, II	gephyrin
Cell 10	L6	Mid VII	Ipsilateral	I & MLF	gephyrin
Cell 11	L6	Mid VII	Ipsilateral	II	gephyrin
Cell 12	L5	Medial VII	Contralateral	II	gephyrin
Cell 13	L4	Mid VII	Ipsilateral	II	gephyrin
Cell 14	L6	Medial VII	Ipsilateral	II	gephyrin
Cell 15	L6	Mid VII	Ipsilateral	I & II	gephyrin
Cell 16	L4	Mid VI	Ipsilateral	I	gephyrin
Cell 17	L4	Mid VII	Ipsilateral	I & II	gephyrin
Cell 18	L4	VIII	Bilateral	MLF	gephyrin
Cell 19	L4	VIII	Bilateral	MLF	gephyrin
Cell 20	L4	VIII	Contralateral	MLF	gephyrin
Cell 21	L6	VIII	Bilateral	MLF	VGLUT2

Lat, lateral; Mid, central; I, group I afferent; II, group II afferent; MLF, medial longitudinal fasciculus

Table 4.3. The density of VGLUT1 and VGLUT2 contacts per 100 μm^2 of each cell

	Total surface of dendrite (μm^2)	Density of VGLUT1 terminals per 100 μm^2	Density of VGLUT2 terminals per 100 μm^2	Density of VGLUT1 terminals associated with GAD terminals per 100 μm^2	Percentage of VGLUT1 terminals associated with GAD terminals of total VGLUT1 terminals
Cell1	66628	1.90	0.00	1.56	82.1%
Cell 2	63565	0.86	0.00	0.64	74.4%
Cell 3	35957	0.64	0.00	0.44	68.8%
Cell 4	63263	0.66	0.00	0.55	83.3%
Cell 5	48830	0.74	0.03	0.40	54.1%
Cell 6	68064	1.87	0.00	1.21	64.7%
Cell 7	41549	2.43	0.18	2.25	92.6%
Cell 8	23975	0.51	0.65	0.33	64.7%
Cell 9	34631	0.89	0.10	0.53	59.6%
Cell 10	42852	0.46	0.05	0.31	67.4%
Cell 11	25751	0.54	0.00	0.33	61.1%
Cell 12	33569	0.55	0.00	0.43	78.2%
Cell 13	35055	0.81	0.10	0.47	58.0%
Cell 14	10413	1.09	0.02	0.77	70.6%
Cell 15	44856	0.38	0.02	0.25	65.8%
Cell 16	31988	2.29	0.26	1.97	86.0%
Cell 17	34204	1.08	0.08	0.77	71.3%
Cell 18	72897	0.15	0.20	N/A	N/A
Cell 19	38318	0.16	0.26	N/A	N/A
Cell 20	34965	0.07	0.53	N/A	N/A
Cell 21	54518	0.03	0.55	N/A	N/A

Table 4.4. Comparison of density of VGLUT1 terminals for each individual cell

	Average density of VGLUT1 terminals on the cell per 100 μm^2	The highest density of VGLUT1 terminals on a single dendritic branch per 100 μm^2	The lowest density of VGLUT1 terminals on a single dendritic branch per 100 μm^2	The ratio of the highest and lowest density of VGLUT1 terminals	Average density of VGLUT1 terminals associated with presynaptic GAD terminals on the cell per 100 μm^2	The highest density of VGLUT1 terminals associated with presynaptic GAD terminals on a single dendritic branch per 100 μm^2	The lowest density of VGLUT1 terminals associated with presynaptic GAD terminals on a single dendritic branch per 100 μm^2	The ratio of the highest and lowest density of VGLUT1 terminals associated with presynaptic GAD terminals
Cell 1	1.72	3.36	0.08	42.0	1.56	3.00	0.05	60.0
Cell 2	0.83	2.09	0.10	20.9	0.64	1.80	0.02	90.0
Cell 3	0.63	0.80	0.26	3.1	0.44	0.56	0.15	3.7
Cell 4	0.65	1.08	0.26	4.2	0.55	0.94	0.23	4.1
Cell 5	0.72	0.75	0.59	1.3	0.10	0.14	0.05	2.8
Cell 6	1.7	3.22	0.64	5.0	1.21	2.73	0.2	13.7
Cell 7	2.41	3.48	1.2	2.9	2.25	3.36	1.15	2.9
Cell 8	0.50	1.62	0.10	16.2	0.33	1.32	0.02	66.0
Cell 9	0.88	1.13	0.59	1.9	0.53	0.67	0.39	1.7
Cell 10	0.45	0.50	0.29	1.7	0.30	0.33	0.09	3.7
Cell 11	0.52	0.64	0.32	2.0	0.33	0.47	0.19	2.5
Cell 12	0.52	1.24	0.07	17.7	0.43	1.14	0.07	16.3
Cell 13	0.81	2.07	0.11	18.8	0.47	1.57	0.07	22.4
Cell 14	1.09	2.49	0.075	33.2	0.77	0.16	0.075	2.1
Cell 15	0.38	0.51	0.07	7.3	0.07	0.23	0.039	5.9
Cell 16	2.29	4.1	1.66	2.5	2	3.75	1.48	2.5
Cell 17	1.08	2.02	0.54	3.7	0.77	1.8	0.17	10.6

Chapter 5

Investigation 3:

**Cholinergic terminals in the ventral horn of adult rat and
cat**

5.1. Introduction

Since in 1954, Eccles et al. reported that di-hydro- β -erythroidine (DH β E), an antagonist of nicotinic receptors of acetylcholine (ACh), blocked most of the activation of the Renshaw cells by ventral root stimulation, ACh is generally accepted as the only neurotransmitter released at both central and peripheral synapses of somatic motoneurons (e.g. Curtis and Ryall, 1964; Eccles et al., 1954b Windhorst, 1996). However, this assertion has been challenged recently (Herzog et al., 2004; Mentis et al., 2005; Nishimaru et al., 2005). Firstly, both Eccles et al. and the following investigators found that cholinergic antagonists could not completely abolish the activation of Renshaw cells evoked by stimulation of motoneuron axon collaterals (Dourado et al., 2002; Eccles et al., 1954b Noga et al., 1987; Schneider and Fyffe, 1992). In addition, pharmacological studies, using *in vitro* preparations of young (P0-4) mouse spinal cord, show that this activation can be blocked if both cholinergic and glutamatergic antagonists were applied (Mentis et al., 2005; Nishimaru et al., 2005). More recently, Lamotte d'Incamps and Ascher (2008) analyzed the synaptic actions on Renshaw cells in the spinal cord slices of neonatal mice (P5-10) and they found that the synaptic current of Renshaw cells was mediated by two nicotinic receptors (responsible for the initial components) and two glutamate receptors (AMPA and NMDA; contribute to the later components).

Nevertheless, anatomical evidence supporting a role for glutamate as a co-transmitter with ACh is inconsistent in adult and young animals. Herzog et al. (2004) provided evidence that in adult rats, mRNA for both vesicular glutamate transporters 1 and 2 (VGLUT1; VGLUT2) was present in axon terminals in primary cultures of immunopurified motoneurons. In contrast, Kullander et al. (2003) and Oliveira et al. (2003) could not find mRNA for any of the three known vesicular glutamate transporters in motoneurons of adult rats (Kullander et al., 2003; Oliveira, et al., 2003). Similarly, studies in immunocytochemical studies have also produced conflicting evidence. Nishimaru et al. (2005), were unable to detect the presence of VGLUT1 or VGLUT3 in motoneuron axon collaterals but found some evidence for VGLUT2 co-localisation, but curiously only three cholinergic terminals (labelled with the vesicular cholinergic transporter, VACHT) in this region out of a sample of more than a thousand were positively labelled for VGLUT2. To some extent this is consistent with findings reported by Herzog et al. (2004) who proposed that VACHT and VGLUT2 were not co-localised in the same terminals but that individual collateral branches of motoneurons contained either one or

the other. On the other hand, Mentis et al. (2005) reported the absence of immunoreactivity for any of the vesicular glutamate transporters in motoneuron axon collaterals but nevertheless concluded that some terminals may be enriched with glutamate.

In summary, it seems that there is good pharmacological evidence to suggest that glutamate may be co-released along with acetylcholine at synapses formed between motoneurons and Renshaw cells in very young mice but anatomical evidence supporting this is inconsistent. Therefore, in order to determine if there was evidence to support the hypothesis that glutamate is co-localised in axon collaterals of mature animals and operates via an AMPA receptor, a series of anatomical studies were performed in the adult cat and rat. There were two principal aims of the study: 1) to determine if axon collaterals of adult motoneurons contain vesicular glutamate transporters; 2) to determine if axon collaterals of adult motoneurons are apposed to AMPA receptors. During the course of this study, a group of cholinergic axon terminals was identified in the ventral horn. These terminals did not originate from motoneurons but contained VGLUT2 and apposed AMPA receptors.

5.2. Experimental procedures

Experiments were performed on three adult rats (250-350 g; 10- 14 weeks old Harlan, Bicester UK) and one adult cat (3.6 kg; 6 months old) which was bred at the University of Göteborg. Rat experiments were conducted according to British Home Office legislation and were approved by the University of Glasgow Ethics Committee. The cat experiment was conducted according to NIH guidelines and was approved by the Göteborg University Ethics Committee.

5.2.1 Surgical procedure and labelling of motoneuron terminals

Cat experiments

The cat was deeply anaesthetised with sodium pentobarbital (40-44 mg/kg, i.p.) and supplemented with intermittent doses of α -chloralose as required to maintain full anaesthesia (Rhône-Poulenc Santé, France; doses of 5 mg/kg administered every 1-2 hours, up to 55 mg/kg, i.v.). A laminectomy was performed to expose lumbar (L4-L7) segments of the spinal

cord. Motoneurons were searched for in L6-L7 segments and identified on the basis of antidromic activation following stimulation of gastrocnemius and soleus nerves. Following identification, motoneurons were labelled intracellularly with a mixture of equal parts of 2% tetramethylrhodamine-dextran (Molecular Probes, Inc, Eugene, Oregon, USA) and 2% Neurobiotin (Vector, UK) in saline (pH 6.5). The marker was injected by passing depolarizing constant current 100-140 nA for 5-8 minutes. New injection sites were a minimum of 2 mm away from previous sites. At the conclusion of the experiment, the animal was given a lethal dose of pentobarbital and perfused, initially with physiological saline, and subsequently with paraformaldehyde (4%) in 0.1 M PB (pH 7.4). Lumbar segments of the spinal cord containing labelled cells were removed and placed in the same fixative for 8 hours at 4 °C. Axon collaterals from an intracellularly labelled excitatory interneuron (see Chapter 4 or Bannatyne et al., 2009) were obtained from the same animal for control material. For more detailed procedures, please chapter 4.

Rat experiments

Three Sprague-Dawley rats were deeply anaesthetised with halothane and the left sciatic nerve was exposed under strict aseptic conditions. A micropipette containing a 1% solution of the CTb (Sigma-Aldrich Co., Poole, UK) in sterile distilled water was inserted into the perineurium and 3-4 µl of this solution were pressure injected into the nerve. Following 3-5 days survival, the rats were anesthetized with pentobarbitone (1 ml i.p.) and perfused through the left ventricle with saline followed by a fixative containing 4% formaldehyde in 0.1 M phosphate buffer pH 7.4. L3 to L5 spinal cord segments were removed from each animal and post-fixed in the same fixative for 2-8 hours at 4 °C. Segments were then cut into two blocks.

The L7 segment of the cat and L3-L5 segments of rats were rinsed several times in 0.1 M PB. All the segments were cut into 50 µm thick transverse sections with a Vibratome (Oxford instruments, Technical products international Inc. USA) and sections of cat segments were collected in strict serial order to enable reconstruction of labelled cells. All sections were treated with an aqueous solution of 50% ethanol for 30 minutes to enhance antibody penetration. Following this treatment, cat sections were mounted in serial order on glass slides with Vesctashield (Vector Laboratories, Peterborough, UK) and examined with a fluorescence microscope. Sections containing labelled motoneurons were reacted firstly with avidin-

rhodamine (1:1000; Jackson ImmunoResearch, Luton, UK) and photographed with a digital camera attached to a fluorescent microscope. Sections containing labelled motoneuron axon terminals were then selected for further analysis.

5.2.2 Immunocytochemical processing of tissue

Aim 1: Do adult motoneuron axon collateral terminals contain vesicular glutamate transporters?

Sections were incubated in the combinations of primary antibodies listed in [Table 5.1](#). They were then incubated for 3 hours in solutions of secondary antibodies coupled to fluorophores before mounting with anti-fade medium (see [Table 5.1](#) for details). Sections containing axon terminals from the three labelled cat motoneurons were reacted with guinea pig anti-VGLUT1 and rabbit anti-VGLUT2. Motoneuron terminals obtained from rat experiments were identified by the presence of transported CTb from sciatic nerve injections (see above) which was co-localised with immunoreactivity for VACHT. Triple immunofluorescence was performed initially with VGLUT1, -2 and -3 antibodies (Groups A, B and C in [Table 5.1](#)). Also, as some cholinergic interneurons co-contain nitric oxide synthase (NOS; Miles et al., 2007), it was attempted to determine if any cholinergic axons that were positive for VGLUT2 (see below) originate from this source by reacting tissue with a combination of anti-NOS, anti-VACHT and anti-VGLUT2 antibodies (Group D in [Table 5.1](#)).

As motoneuron axon collaterals are known to form synapses with Renshaw cells and calbindin is thought to be a reliable marker for Renshaw cells (Alvarez et al., 1999; Carr et al., 1998), rat sections containing labelled collaterals were reacted with CTb and calbindin antisera along with one of the following: antibodies: VGLUT1 (Group E), VGLUT2 (Group F), or VACHT (Group G). Sequential immunocytochemistry on sections from groups F and G were performed. When analysis of sections with these initial combinations was complete, sections were re-incubated with a fourth antibody: goat anti-VACHT antibody (for group F) or guinea pig anti-VGLUT1 (for group G). The sections were remounted and the same field that had been scanned previously was identified and scanned again. By comparing labelling before and after the re-incubation in the VGLUT1 or VACHT antiserum, the additional staining could be

detected, which represents immunoreactivity for VACHT and VGLUT1 in groups F and G, respectively.

Aim 2: Are axon collaterals of adult motoneurons apposed to AMPA receptors?

An antigen unmasking method was used to reveal whether AMPA receptors subunits are associated with labelled motoneuron terminals. Sections containing axon collaterals from three motoneurons and one interneuron were processed. Pepsin treatment was performed by incubating sections at 37° C for 30 min in PBST, followed by 10 min in 0.2M HCl containing 1 mg/ml pepsin (Dako, Glostrup, Denmark) with continuous agitation. After rinsing, sections were incubated in a mouse anti-R2 subunit of the AMPA receptor (GluR2) antibody (1:300; Chemicon, Harlow, UK) for 72 hours at 4° C. Sections were then incubated in a species-specific donkey secondary antibody conjugated to Alexa488 (1:500; Molecular Probes, Eugene, Oregon, USA) for 24 hours.

Cholinergic terminals in rat tissue were examined to determine if they form associations with the GluR2 subunit of AMPA receptors. As GluR2 subunits are present in 98% AMPA-containing synapses in the rat spinal cord (Nagy et al., 2004), this subunit can be used as a general marker for this class of receptor. Before applying the antigen unmasking method to expose GluR2 subunits as described above, sections from three rats were incubated in goat anti-VACHT antibody (1:50000) for 72 hours and then subjected to a tyramide signal amplification (TSA) reaction in order to preserve labelling for VACHT following pepsin treatment. Sections were initially incubated for 4 hours in anti-goat horseradish peroxidase (HRP; 1:500; Jackson Immunoresearch, West Grove, PA, USA). The sections were then rinsed and processed with a tetramethylrhodamine fluorophore (diluted 1:50 in amplification diluent; PerkinElmer Life Sciences, Boston, MA) for 7 min (see Nagy et al., 2004 for details). Sections were rinsed, treated with pepsin, and incubated for 72 hours in mouse anti-GluR2 (1:300), followed by 24 hours in a species-specific donkey secondary antibody conjugated to Alexa488 (1:500). A control experiment was also performed to determine the association between glutamatergic boutons and GluR2 subunits. Sections from three rats were incubated for 72 hours in a combination of guinea pig anti-VGLUT1 (1:50000) and guinea pig anti-VGLUT2 (1:50000) antibodies. The sections were rinsed and placed in anti-guinea pig HRP (1:500; Jackson ImmunoResearch, West Grove, PA, USA) for 4 hours. They were processed

according to the TSA and pepsin treatment described above and incubated in mouse anti-GluR2 (1:300).

5.2.3 Confocal microscopy and data analysis

All sections were mounted in a glycerol-based antifade medium (Vectashield, Vector Laboratories, Peterborough, UK) and examined with a BioRad MRC 2100 confocal laser scanning microscope (BioRad, Hemel Hempstead, UK).

Cat sections with VGLUT markers were scanned by using a x60 oil-immersion lens at a zoom factor of 3.5 and at 0.5 μm steps in the z axis, while sections with GluR2 staining were examined with a x60 oil-immersion lens at a zoom factor of 2 and at 0.2 μm steps in the z axis. Image stacks were analyzed with Neurolucida for Confocal software (MBF Bioscience, Colchester, VT, USA). To avoid bias, all labelled motoneuron axon terminals and VGLUT markers (or GluR2 immunoreactivity) were viewed in individual channels for every single optical section initially and then examined in merged image stacks showing all three (or two) channels by switching between different channels. When scanning of immunoreactive boutons was complete, the sections were retrieved from the slides and rinsed in PBS. These sections together with the other sections containing soma and axons of labelled motoneurons were reacted with avidin-biotin-peroxidase complex technique (ABC technique). This involved an overnight incubation in a fresh solution of avidin-biotin-complex (Vector Laboratories Ltd, England) followed by a further rinse with PBS then PB. The sections were then placed in a solution containing hydrogen peroxide plus 3, 3'-diaminobenzidine (DAB; Sigma, Dorset, England) diluted in phosphate buffer for a period of approximately 4 minutes. During this time, the reaction was monitored constantly. Following the DAB reaction, sections were dehydrated in a series of ethanol solutions and mounted in serial order on gelatinised slides for cell reconstruction. This method provides a permanent record of the cells from which detailed reconstructions were made using a drawing tube.

Rat sections from the lumbar segments (L3-L5) were examined within the ventral region of lamina VII, between medial and lateral motoneuron pools, which contains most Renshaw cells (Carr et al., 1998). Sections reacted with antibodies against CTb, VAcHT and VGLUT (i.e. group A, B, and C) were scanned by using a x60 oil-immersion lens with a zoom factor of 2 at

0.5 μm intervals. The stacks of images were analyzed with NeuroLucida for Confocal software. Two hundred CTb labelled terminals that were also immunoreactive for VACHT were randomly selected from each rat. To avoid bias, a 100x100 μm grid was placed on the image and the terminal closest to bottom right corner of each grid square was selected. Selected terminals were then examined in the blue channel (representing the VGLUTs) to determine whether they were positive for VGLUT immunoreactivity. Sections reacted with antibodies for CTb, calbindin and VGLUT (i.e. group E and F) or CTb, calbindin and VACHT (i.e. group G) were scanned with a X40 oil-immersion lens and zoom factor of 2 at 0.5 μm intervals. Image stacks were analyzed with NeuroLucida to investigate the proportion of CTb-labelled terminals that made contact with Renshaw cells and were also immunolabelled for VGLUT1, VGLUT2 or VACHT in each group.

Sections reacted for VACHT and GluR2 were mounted in Vectashield anti-fade medium and scanned with the confocal microscope. Lamina VII of sections from each of the three rats was scanned by using a x60 oil-immersion lens with a zoom factor of 2 at 0.2 μm steps in the z-axis. In each section, two scanning fields were obtained from both sides with a 100x100 μm scanning area. By using NeuroLucida software, image stacks were initially viewed so that only VACHT immunoreactivity was visible. All VACHT immunoreactive boutons within the scanning box from each animal were selected for analysis. GluR2 staining was then examined, and it was determined whether VACHT terminals were apposed to GluR2 puncta. Control material reacted with a combination of VGLUT1 and 2 and GluR2 was analysed in exactly the same way.

In order to determine if axon terminals with different immunochemical characteristics belonged to different populations, a comparison was made between five groups of axon terminals. The equivalent diameter of axonal swellings that were double labelled for: (1) VACHT and GluR2; (2) VACHT and VGLUT2; (3) VACHT and no GluR2; (4) CTb and VACHT; and (5) CTb and VGLUT1 were measured from projected confocal images obtained from all three rats by using Image J software (National Institutes of Health, USA, <http://rsb.info.nih.gov/ij/>). A one-way ANOVA was used to determine if there were statically significant differences in the diameters of these groups ($p < 0.05$). This was followed by a Tukey's *post hoc* pairwise comparison to determine which groups were significantly different

from each other. Confocal microscope images were prepared by using Adobe Photoshop to adjust brightness and contrast.

5.3. Results

5.3.1 Aim 1: Do adult motoneuron axon collateral terminals contain vesicular glutamate transporters?

In total, 63 axon terminals obtained from 3 intracellularly labelled motoneurons from the cat experiment were analysed. Terminals that could not be traced back to the parent axon were excluded from the sample. Sections, which contained 11 motoneuron axon terminals, were reacted with antibodies against VGLUT1 and VGLUT2. Confocal microscope images showed that none of the 11 terminals were positive for either VGLUT1 or VGLUT2 immunoreactivity (Figure 5.1). The remaining 52 axon terminals were reacted for the presence of GluR2 (see below).

In rat experiments, both motoneuron axon terminals and primary afferent axons were labelled by injection of the tracer CTb. Retrogradely labelled motoneurons were found in lamina IX ipsilateral to the injection site of the L3 to L5 segments of the spinal cord. Initially, a series of three triple labelling experiments was performed on each animal to determine if VACHT and glutamate vesicular transporters were co-localised in motoneuron collateral terminals. Three groups of sections were reacted: A) CTb +VACHT +VGLUT1; B) CTb +VACHT +VGLUT2; and C) CTb +VACHT +VGLUT3. In each group, a total of 600 terminals, doubled-labelled for CTb and VACHT, were randomly selected from the three rats (200 from each rat). Confocal microscope images revealed that none of the selected terminals was positive for VGLUT1, VGLUT2 and VGLUT3 immunoreactivity (Figure 5.2A, B, and C). In addition, the equivalent diameter of 150 axon terminals, which were labelled by both CTb and VACHT but not VGLUT1, were also measured (50 from each rat), and the equivalent diameter of 150 presumed primary afferent terminals which were labelled by both CTb and VGLUT1 but not VACHT (50 from each rat). As predicted, there was a significant difference between these two types of terminal; the average (\pm SD) equivalent diameters of the motoneuron terminals and the primary afferent terminals were $1.99 \pm 0.51\mu\text{m}$ and $3.58 \pm 0.78\mu\text{m}$, respectively (See below).

In CTb +VAcHT +VGLUT2 (group B) experiments, it was not only found that there was no overlap of immunoreactivity for CTb and VGLUT2, but also a small population of VGLUT2-labelled axons with VAcHT staining was identified (Figure 5.2B). The equivalent diameter of VAcHT/ VGLUT2 terminals was $0.89 \pm 0.23\mu\text{m}$ (50 terminals from each rat). These were significantly smaller than the CTb/VAcHT and the CTb/VGLUT1 terminals (see below). In order to determine if these VAcHT/VGLUT2 terminals originated from the NOS-containing subgroup of cholinergic interneurons (see Miles et al., 2007), the relationship between these terminals and NOS was further investigated (Group D). A total of fifty VAcHT/VGLUT2 terminals were randomly selected but none of them displayed NOS immunoreactivity (Figure 5.2D).

Terminals which formed contacts with Renshaw cells identified by calbindin labelling (Alvarez et al., 1999; Carr et al., 1998) were investigated by performing immunoreactions with two antibody combinations: Group E) CTb +VGLUT1 + calbindin; and Group F) CTb +VGLUT2 + calbindin. For each combination, a sample of 15 calbindin labelled Renshaw cells (five from each of the three animals) located within ventral lamina VII between motor nuclei was analysed. Each of the scanning areas was $151\mu\text{m} \times 151\mu\text{m}$ and contained at least one cell body of a Renshaw cell and its proximal dendrites. In group E, a total of 285 CTb-labelled terminals which contacted Renshaw cells were recorded (average \pm SD, 19 ± 5.6 contacts per cell). Of these terminals, $99 \pm 3\%$ (281 out of 285) was found to be negative for VGLUT1 immunoreactivity (Figure 5.3A). Then the size of the remaining 1% (4 out of 285) terminals, which were immunoreactive for VGLUT1, was measured. Their equivalent diameters ranged from $3.65\mu\text{m}$ to $6.15\mu\text{m}$ (average \pm SD, $4.85 \pm 1.25\mu\text{m}$). In group F, a total of 339 CTb-labelled terminals (average \pm SD, 23 ± 3.5 per cell) which were apposed Renshaw cells was analyzed. None of the terminals that contacted Renshaw cells were labelled with VGLUT2 immunoreactivity (Figure 5.3B). By performing sequential immunocytochemistry with a fourth antibody against VAcHT, it was able to be confirmed that the CTb-positive VGLUT2-negative terminals originated from motoneurons as all VGLUT2-negative terminals were positively labelled for VAcHT immunoreactivity (Figure 5.3C). In sequential experiments, it was also noted that some VGLUT2 positive /CTb negative terminals were positive for VAcHT immunoreactivity but that they did not form contacts with Renshaw cells (not shown). These results suggest that some cholinergic terminals located in the deep ventral horn which do not originate from motoneurons contain glutamate.

To confirm the above findings, a further combination of CTb, VACHT and calbindin (Group G) was used. Another sample of 15 calbindin labelled Renshaw cells was examined (five from each of the three animals). In 151 μ m \times 151 μ m scanning fields, a total of 364 CTb labelled terminals which contacted Renshaw cells was analysed (average \pm SD, 24 \pm 5.6 per cell). Of these terminals, 97 \pm 4% (352 out of 364) was found to be positive for VACHT (Figure 5.4A, C). It was showed by sequential immunocytochemistry with a fourth antibody against VGLUT1 that the 12 VACHT-negative terminals were immunoreactive for VGLUT1. None of the 352 (out of 364) CTb/VACHT terminals was labelled for VGLUT1 (Figure 5.4B, D).

5.3.2 Aim 2: Are axon collaterals of adult motoneurons apposed to AMPA receptors?

The remaining 52 collateral terminals from the three cat motoneurons were used to investigate the relationship between labelled axon collateral swellings and GluR2 subunits in postsynaptic membrane receptors. Figure 5.5 shows an example of a reconstructed motoneuron and the organisation of its axon. Collateral axons from this cell were used in the analysis (Figure 5.6). No evidence of any obvious relationship between GluR2-immunoreactive puncta and motoneuron axon collaterals was found. However, all axon terminals from an interneuron which was labelled in the same animal as the motoneurons were apposed to GLUR2-immunoreactive puncta (Figure 5.7).

Associations between VACHT-labelled terminals and GluR2 immunoreactive puncta were also investigated in rat tissue. Confocal microscope images showed that although most VACHT immunoreactive boutons were not apposed to GluR2 puncta (Figure 5.8A-C), a small number of VACHT boutons were associated with GluR2 staining (Figure 5.8D-F). The average (\pm SD) equivalent diameters of the former group and the latter group were 1.95 \pm 0.53 μ m and 0.87 \pm 0.23 μ m, respectively. For comparison, the relationship between glutamatergic terminals (labelled with a combination of VGLUT1 and -2 antibodies) and GluR2 immunoreactive puncta in deep lamina VII was examined. Despite an intensive search, it was hard to detect any VGLUT immunoreactive axon terminal which was not apposed to GluR2-immunoreactive puncta (Figure 5.8G-I).

5.3.3 Comparison of equivalent diameters of populations of cholinergic and glutamatergic terminals in the rat

The equivalent diameters of five groups of terminals investigated in this study were compared. These five groups were: A) those that were labelled with VAcHT and were associated with GluR2; B) those that were labelled with VAcHT and VGLUT2; C) those that were labelled with VAcHT but were not associated with GluR2; D) those that were labelled with VAcHT and CTb; and E) those that were labelled with CTb and VGLUT1 (see Figure 5.9). Each group consisted of 50 randomly selected terminals obtained from each of the three rats. By using ANOVA analysis, it was found that there was a highly significant difference between these groups ($P < 0.0005$). A *post hoc* Tukey's pairwise comparison showed that there was no statistical difference between groups A and B or between groups C and D but that all other comparisons were significantly different.

5.4. Discussion

In the series of experiments reported here, it has been shown: 1) that axon collateral swellings of adult cat motoneurons do not contain the vesicular glutamate transporters VGLUT1 or VGLUT2 and have no obvious association with the GluR2 subunit of the AMPA receptor; 2) that axon collateral swellings of adult rat motoneurons also do not contain vesicular glutamate transporters VGLUT1, VGLUT2 or VGLUT3 and have no obvious association with the GluR2 subunit of the AMPA receptor; 3) that a group of cholinergic axon terminals within lamina VII of the rat spinal cord, contain VGLUT2 and form associations with the GluR2 subunit of the AMPA receptor.

5.4.1 Identification of labelled terminals

In the cat experiment, the analysis was confined to terminals which could be traced back to the parent axon and hence could be identified unequivocally as motoneuron collaterals. In rat experiments, terminals were classified into three distinct populations according to their immunocytochemical characteristics and equivalent diameters. Although there was some overlap in the distribution of terminal sizes between the three populations, statistical analysis

indicates that they form three distinct populations. (1) The first group of terminals are CTb labelled VACHT-immunoreactive terminals. The immunostaining of VACHT has been generally accepted as a reliable marker for cholinergic terminals (Alvarez et al., 1999); therefore, this group of terminals were identified as motoneuron axon collateral terminals. Their axons had intermediate-sized terminals (approximately 2 μ m in diameter) and made numerous contacts with Renshaw cells which were labelled with calbindin (Alvarez et al., 1999; Carr et al., 1998). Alvarez et al. (1999) also measured size of motoneurons terminals which were labelled by VACHT and made contacts with Renshaw cells and the size of other VACHT immunoreactive terminals scattered in the ventral horn, including C-boutons. Their results, which showed the mean diameter of motoneuron terminals ($2.26 \pm 0.94\mu$ m) as significantly different to other cholinergic terminals in the ventral horn, were similar to those described here. (2) The second group comprises CTb labelled non-cholinergic terminals that were immunopositive for VGLUT1. VGLUT1 is generally present in terminals of myelinated primary afferent axons but not in spinal interneurons (Todd et al., 2003; Varoqui, et al., 2002). Consequently, this group of terminals were classified as primary afferent terminals. These terminals were the largest of the three groups and had an average diameter of approximately 3.52 μ m. This is consistent with previous reports of the sizes of Group Ia afferent terminals (Watson and Bazzaz, 2001) which are likely to constitute the majority of primary afferents terminating in lamina VII (Brown, 1981). These terminals made occasional contacts with Renshaw cells (Figure 4C, D). (3) The third group of terminals was the most intriguing of all. This group comprised small cholinergic terminals (approximately 0.92 μ m in diameter) and were immunoreactive for VGLUT2 immunoreactivity. However, none of them were labelled with CTb and their axons apparently made no contacts with Renshaw cells. In addition, as reported by Alvarez et al. (1999), the average diameter of cholinergic terminals contacting Renshaw cells was larger than those of cholinergic terminals which did not form synapses with Renshaw cells in the ventral horn. Therefore, the third group of terminals are unlikely to be the recurrent collaterals of motor axons.

5.4.2 Motoneuron axon collateral terminals neither contain VGLUTs nor associate with AMPA receptors

Firstly, the results of the current study clearly demonstrate that cat and rat motoneuron axon collaterals do not contain VGLUTs. During the previous decade, the question about whether

glutamate is released from motoneuron terminals as a co-neurotransmitter with ACh has become controversial. For example, Herzog et al. (2004) and Nishimaru et al. (2005) shared the same opinion that VGLUTs were present in the central axon collaterals of motoneurons. However, Herzog et al. (2004) reported that both VGLUT1 and VGLUT2 were expressed only in the non-cholinergic motoneuron terminals of adult rats (i.e. glutamate and ACh were contained in separate populations of motoneuron terminals); while Nishimaru et al. (2005) found that glutamate and ACh were colocalized in the same population of motoneuron terminals in neonatal mice. In contrast to both of these studies, Mentis et al. (2005) could not detect immunoreactivity for any of the three VGLUTs in the central synapses of motoneuron terminals in young mice. Kullander et al. (2003) and Oliveira et al. (2003) also reported that the mRNAs for all three VGLUTs was absent in motoneurons and all the varicosities containing VGLUT1, VGLUT2 and VACHT in lamina IX were corresponding to distinct subgroups. Moreover, no evidence was found to show the arrangement suggested by Herzog et al. (2004) that motoneuron collaterals gave rise to axon branches which contained acetylcholine but not glutamate and *vice versa*. In fact, any CTb labelled terminals that were not immunoreactive for VACHT were invariably immunoreactive for VGLUT1 and were most probably terminals of primary afferent proprioceptors (see above).

Secondly, no obvious relationship was detected between cat or rat motoneuron terminals and immunoreactivity for the GluR2 subunit of the AMPA receptor. The GluR2 subunit is one of the four subunits of AMPA receptor and exists in almost all AMPA containing synapses (98%) in the rat spinal grey matter (Nagy et al., 2004). In addition, Poglar et al. (2008) investigated the relationship between AMPA receptors and PSD-95 (a major constituent of glutamatergic synapses) in rat spinal dorsal horn and their results suggested that AMPA receptors are present at nearly all glutamatergic synapses. Therefore, GluR2 can be considered to be a good marker for glutamatergic receptors, or at least, it marks virtually all AMPA receptors. In theory, there remains a small probability that synapses formed by motoneuron collaterals appose AMPA receptors that do not possess GluR2 subunit. However, both the present and previous studies provided evidence that suggests this hypothesis is an improbable explanation for the negative findings. In the present study, the control experiments showed that GluR2 subunits were abundant in deep lamina VII in rat and cat tissue and that, in the rat, VGLUT immunoreactive terminals were invariably associated with these subunits. In a previous study, Lamotte d'Inchamps and Ascher (2008) provided evidence that AMPA and NMDA receptors were

responsible for the later components of the current recorded between motoneurons and Renshaw cells in young mice. They also distinguished between AMPA and NMDA mediated components based on permeability to calcium. Therefore, it would be expected that GluR2 subunits are present at the synapses between motoneurons and Renshaw cells. Anatomical investigation of NMDA receptors is very limited because of the difficulties in immunocytochemical detection of them. Nevertheless, as discussed above, it might be true that AMPA receptors exist in practically all glutamatergic synapses; thus, absence of AMPA receptors may indicate absence of glutamatergic synapses. In the cat experiment, all axon terminals were incontrovertible motoneuron terminals because they could be traced to the parent motoneuron axon. In the rat experiment, it had to be confirmed by statistical analysis that the population of VAcHT terminals which did not appose GluR2 puncta belonged to the same population that were labelled for VAcHT and CTb (Group 1 discussed above), and belonged to a different population than those which appose GluR2 puncta did not belong to. The antigen retrieval method combined with TSA only enables two antibodies to be used on the same tissue and, for this reason, it was not possible to label these terminals for CTb in addition to VAcHT and GluR2. Also a previous study showed that motoneuron terminals could be distinguished from other populations of terminals in the ventral horn by statistical analysis of the terminal sizes (Alvarez et al., 1999). Therefore, taken together, the two sets of observations presented above suggest that glutamate is not co-localised with acetylcholine at central synapses of adult motoneurons and does not act through an AMPA receptor.

The pharmacological evidence which showed glutamate is co-released along with acetylcholine at motoneuron/ Renshaw cell synapses were obtained from neonatal mice (P0-10) by Mentis et al. (2005), Nishimaru et al. (2005) and Lamotte d'Inchamps and Ascher (2008). Therefore, a possible reason for differences in the findings of their studies and our anatomical observations may be related to the maturity of the experimental animals they used. For example, it has been suggested that glutamate is involved in a number of cerebral functions which are altered with age, such as learning, memory and motor functions (e.g. Segovia et al., 2001). On the other hand, the original observations of Eccles et al. (1954b) on adult cats indicated that cholinergic antagonists do not completely block transmission at motoneuron/Renshaw cell synapses and therefore it remains possible that another transmitter is co-released along with acetylcholine. The results of this study suggest that if glutamate is this transmitter, then it is not stored conventionally in vesicles and it does not act via AMPA

receptors. Mentis et al. (2005) reported that motoneuron central terminals did not contain vesicular glutamate transporters but that glutamate was enriched in them and argued that this was tentative evidence for a transmitter pool of glutamate. However, glutamate may be enriched in structures for a variety of reasons which are unrelated to transmitter function. For instance, a number of previous studies have found that in both brain and spinal cord, glutamate not only acts as an excitatory neurotransmitter, but also serves metabolic or other non-transmitter roles (e.g. Ji et al., 1991; Todd et al., 1994; Yingcharone et al., 1989). This point could be further supported by the finding that a considerable level of glutamate-like immunoreactivity was found in cell bodies of populations of GABAergic and glycinergic neurons (Ottersen and Storm-Mathisen 1985; Yingcharone et al., 1989). In addition, since GluR2 subunits directly represent AMPA receptors only, it is also possible that glutamate acts via kainate or activated NMDA receptors in the adult. However, the antagonist, 6-cyano-7-nitroquinoxaline-2, 3-dione (CNQX), used by Mentis et al. (2005) and Nishimaru et al. (2005) and the 2, 3-dihydroxy-6-nitro-7-sulfamoyl-benzo[f]quinoxaline-2, 3-dione (NBQX), used by Lamotte d'Inchamps and Ascher (2008) demonstrated a specific AMPA component of the current. Therefore, the most likely explanation of this discrepancy with the present findings is that the expression of AMPA receptors decreases during development to adulthood but further studies on young animals will be required to establish this.

5.4.3 Primary afferents contacting Renshaw cells and small cholinergic terminals containing VGLUT2 in deep ventral horn

Two further observations arose from this study. Firstly, we found evidence that a small number of primary afferent axons form contacts with Renshaw cells in adult rats. The classical view of Renshaw cells is that they are not monosynaptically activated by primary afferent axons (Eccles et al., 1954b; Renshaw 1946). However according to a recent report by Mentis et al. (2006), the density of primary afferent contacts on Renshaw cells decreases during development but the overall numbers of contacts remains approximately the same as a consequence of the enlargement of the cell. They suggest that there is a 'functional deselection' of such contacts during development and although such synapses are still present, they become less effective and have a limited influence on Renshaw cells in adulthood. Although, we did not attempt to quantify the numbers of CTb/VGLUT1 contacts on Renshaw

cells, our impression was that they were sparse in comparison to cholinergic contacts which would be consistent with a limited influence in adulthood.

The second observation was perhaps the most novel of all. It was found that a population of cholinergic axons in lamina VII were immunoreactive for VGLUT2 and also formed associations with GluR2 subunit immunoreactivity. These axon terminals were considerably smaller than those originating from motoneurons and were not seen to make contacts onto Renshaw cells. At present it is not possible to determine the origin of these axons but it seems very unlikely that they originate from descending systems or primary afferents as neither of these groups of neuron uses acetylcholine as a neurotransmitter (e.g. Rustioni and Weinberg, 1989). However, it is highly likely that this group of terminals originates from local interneurons (Barber et al., 1984) or propriospinal neurons (Sheriff and Henderson, 1994) which are known to be cholinergic. Previous studies showed that spinal cholinergic interneurons are mainly composed of three populations in the spinal cord: partition cells in lamina VII, central canal cells in lamina X, and small dorsal horn cells in lamina III-V (Barber et al., 1984; Sheriff and Henderson, 1994). Although it is difficult to confirm the precise origin of these VAcHt/VGLUT2 terminals at present, they are not likely to come from the small dorsal horn cells. This is because most of cholinergic dorsal horn cells contain NOS and/or GABA (Laing et al., 1994; Miles et al., 2007; Todd, 1991), while the VAcHt/VGLUT2 terminals are lack of NOS. In addition, anatomical evidence reported by Miles et al. (2007) suggested that some of medial partition cells without NOS were the origin of the large 'C-terminals' on motoneurons; therefore, these partition neurons could also be excluded as the source of the small terminals observed in the present study. Consequently, the small cholinergic terminals containing VGLUT2 may be from subpopulations of the central canal cells and/or the remaining partition cells. Besides the above three groups of spinal interneurons, preganglionic neurons form a large proportion of the total population of cholinergic neurons in the spinal cord (Sheriff and Henderson, 1994). Immunohistochemical evidence produced by Ito et al. (2005) demonstrated that VGLUT2-immunoreactivity was present in some of the cholinergic terminals originating from preganglionic neurons; however, they also found all these VGLUT2/VAcHt terminals were immunopositive for NOS. Therefore, the small VGLUT2/VAcHt terminals found in this study do not likely originate from these preganglionic neurons.

In conclusion, the results of this study does not provide any evidence to support the proposition that glutamate is co-localised in central synapses of adult motoneurons and acts via an AMPA receptor. However, some small cholinergic terminals which probably originate from interneurons are likely to use glutamate as a co-transmitter and act via AMPA receptors.

All secondary antibodies were raised in donkey and Rhodamine Red (Rh. Red; 1:100), or Cyanine 5.18 (Cy-5; 1:100; all three supplied by Jackson ImmunoResearch, West Grove, USA), and Alexa-fluor 488 (Alexa488; 1:500; Molecular Probes, Eugene, USA). CB, calbindin; CTb, B-subunit of cholera toxin; VGLUT vesicular glutamate transporter; mo., mouse; rbt, rabbit; gt, goat; gp, guinea pig; shp, sheep.

Table 5.1. Summary of primary and secondary antibody combinations and concentrations used in the current study

Group	Primary antibody combination	Primary antibody concentration	Supplier	Secondary antibodies	Sequential immuno-reaction	Secondary antibodies
Cat	gp VGLUT1 rbt VGLUT2	1:5000 1:5000	Chemicon Chemicon	Alexa488 Cy-5		
Rat A	mo. CTb gt VACHT gp VGLUT1	1:250 1:5000 1:5000	A. Wikström, University of Gothenburg Millipore, USA	Rh.Red Alexa488 Cy-5		
B	mo. CTb gt VACHT gp VGLUT2	1:250 1:5000 1:5000	Chemicon	Rh.Red Alexa488 Cy-5		
C	mo. CTb gt VACHT gp VGLUT3	1:250 1:5000 1:5000	Chemicon,	Rh.Red Alexa488 Cy-5		
D	shp NOS gp VACHT rbt VGLUT2	1:200 1:5000 1:5000	P.Emson, University of Cambridge	Rh.Red Alexa488 Cy-5		
E	mo. CTb gp VGLUT1 rbt CB	1:250 1:5000 1:2000	Swant, Bellizona, Switzerland	Rh.Red Alexa488 Cy-5		
F	mo. CTb gp VGLUT2 rbt CB	1:250 1:5000 1:2000		Rh.Red Alexa488 Cy-5	gt. ChAT	Cy-5
G	mo. CTb gt VACHT rbt CB	1:250 1:1000 1:5000		Rh.Red Alexa488 Cy-5	gp VGLUT1	Cy-5

Figure 5.1. A reconstruction of a cat motoneuron and its axon collaterals that was intracellularly labelled with Neurobiotin (A) and a series of confocal microscope images illustrating the absence of VGLUT1 and -2 immunoreactivity within the motoneuron axon terminals (B-D). (A) The soma and axonal arborisation are shown in black and dendrites in grey. The thinner grey line represents the outline of the grey matter and the central canal; the thicker grey line represents the border of the spinal cord. The axon terminals illustrated in B-D are taken from the area outlined by the box in A. (B) A projected image through a series of terminals originating from a motoneuron shown in A. (C1-C4) Single optical sections and (D1-D4) projected images of two individual terminals (arrows). (C4 and D4) Merged images confirming the absence of overlap of immunoreactivity for VGLUT1 and VGLUT2 and labelled motoneuron terminals. Scale bars= 200 μ m (large panel in A); 10 μ m (small panel in A and B); 5 μ m (C1-C4 and D1-D4).

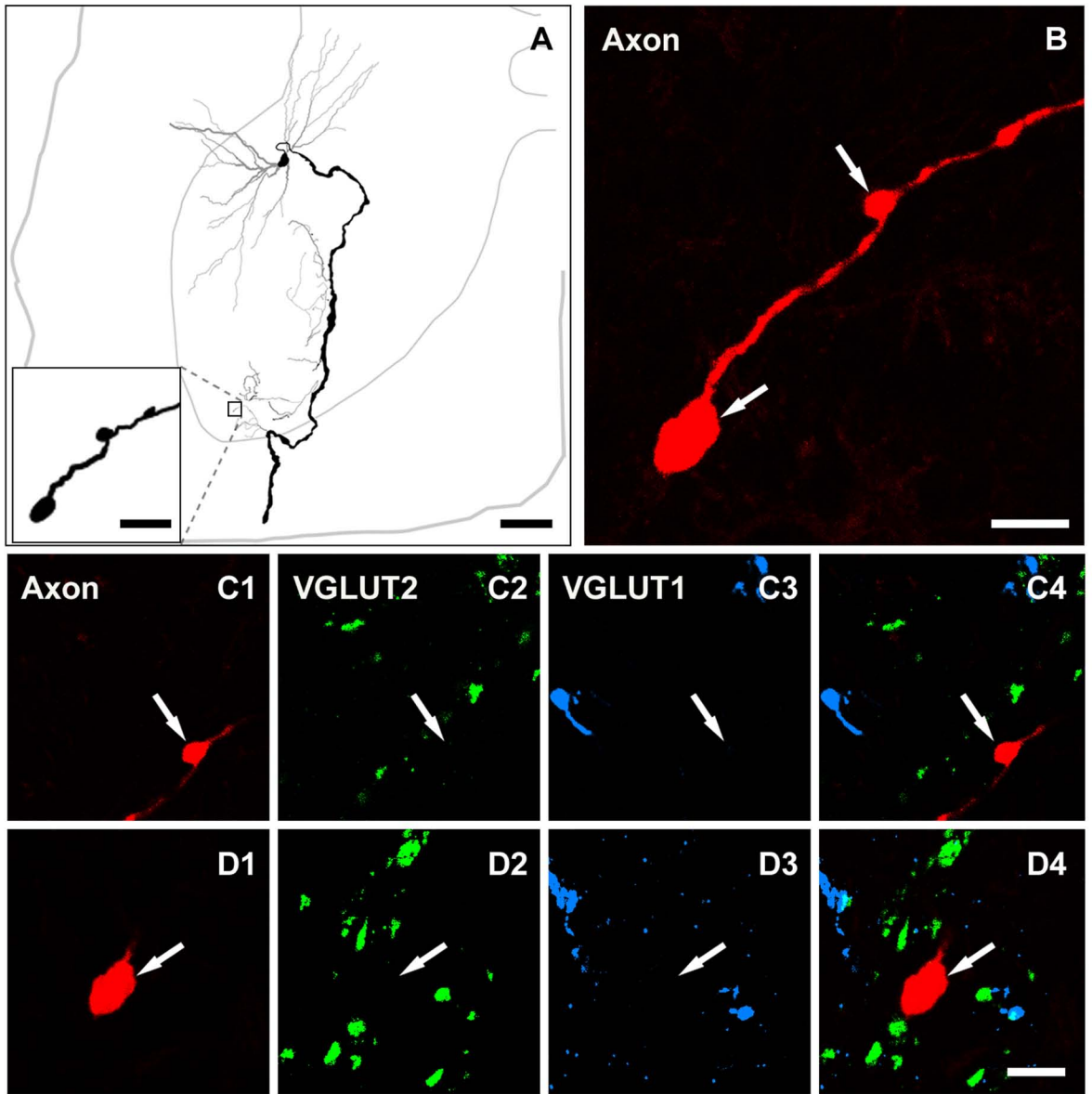


Figure 5.2A, B. Three colour confocal images showing CTb labelled rat motoneuron terminals that are positive for VACHT-immunoreactivity but are negatively labelled for both VGLUT1 and VGLUT2. (A1-A4 and B1-B4) Projected images of three single optical sections. Arrows indicate CTb labelled motoneuron terminals that were VACHT immunoreactive. Arrowheads in A indicate VGLUT1 immunoreactive terminals also labelled by CTb that are likely to originate from proprioceptive primary afferent fibres. Arrowheads in B indicate VGLUT2 immunoreactive terminals that also contain VACHT staining but are not labelled with CTb. (A4 and B4) Merged images. Scale bar = 5 μ m

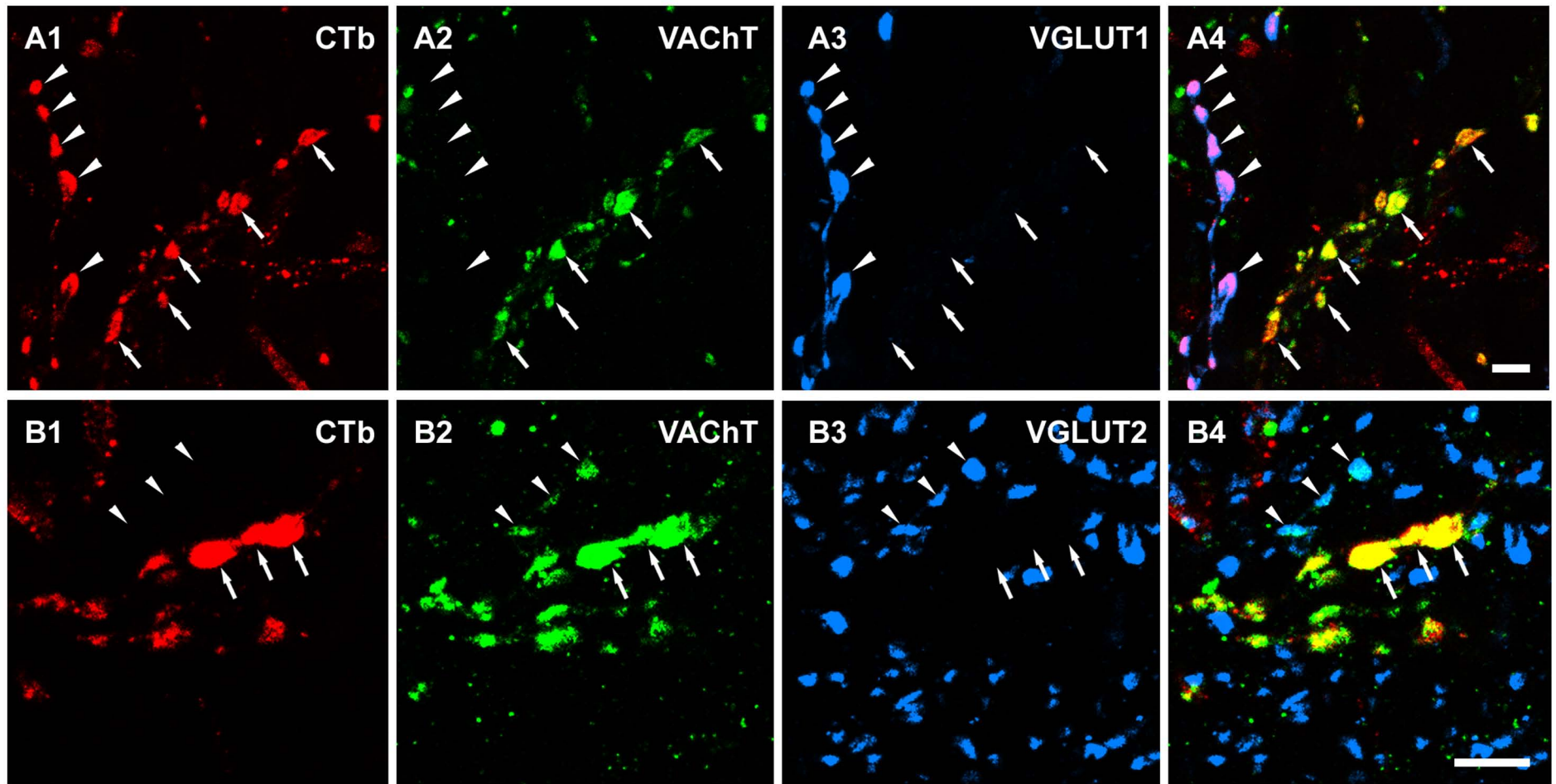


Figure 5.2C, D. Three colour confocal images showing CTb labelled rat motoneuron terminals that are positive for VACHT-immunoreactivity but are negatively labelled for VGLUT3 (C) and the relationship of VACHT/VGLUT2 double labelled terminals with NOS immunoreactivity (D). (C1-C4 and D1-D4) are single optical sections. Arrows in C indicate CTb-labelled motoneuron terminals that were VACHT immunoreactive, and arrows in D indicate terminals that were immunopositive for both VACHT and VGLUT2. Arrowheads in C indicate VGLUT3 terminals. Arrowheads in D indicate NOS immunopositive terminals that were also labelled by VACHT. (C4 and D4) are merged images. Scale bar = 5 μ m.

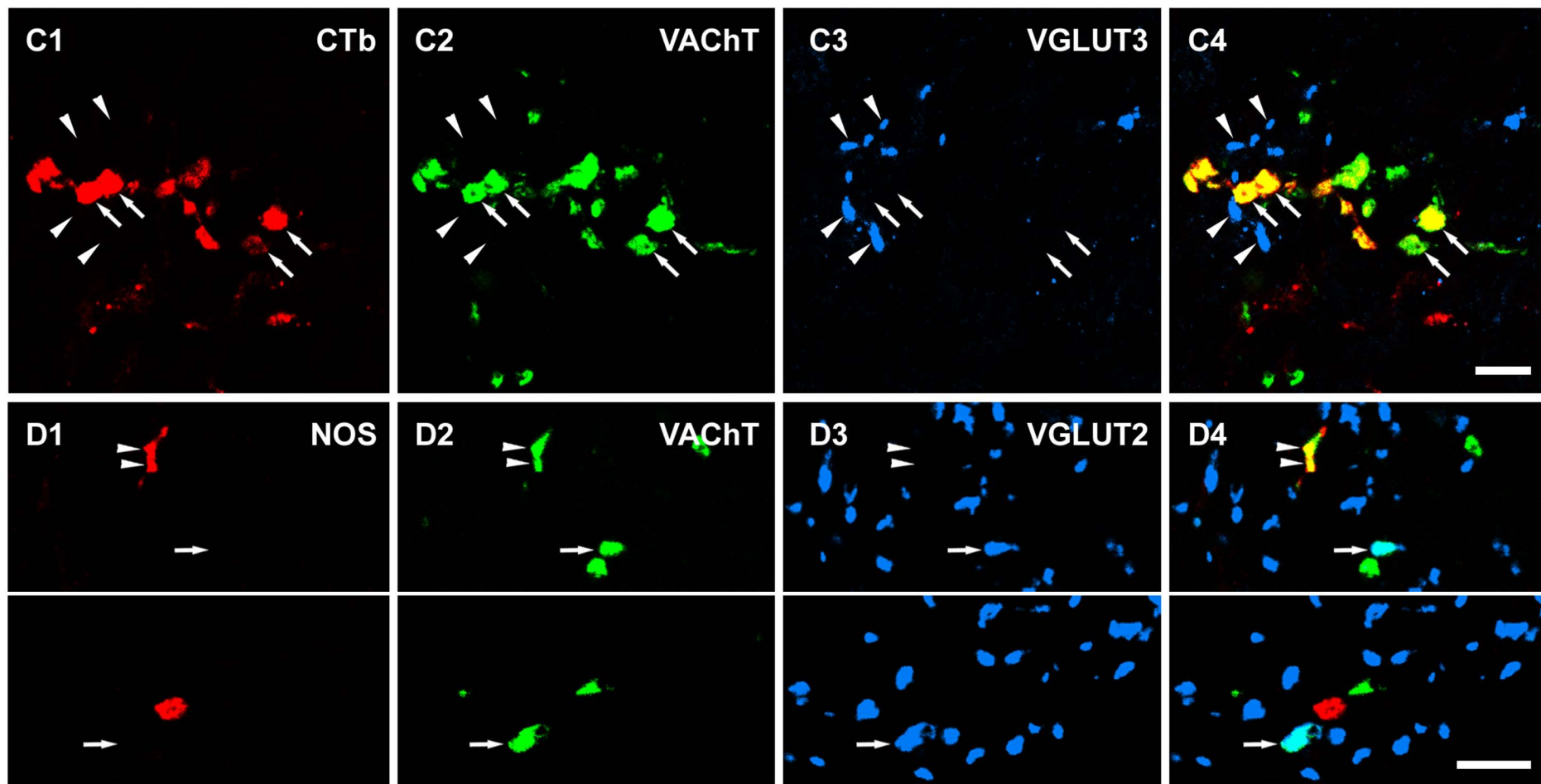


Figure 5.3. Single optical sections illustrating CTB-labelled rat motoneuron terminals in contact with Renshaw cells. (A1-A4 and B1-B4) All of the CTb-labelled motoneuron terminals making contact with two calbindin-labelled cells were negative for VGLUT1- and VGLUT2-immunoreactivity, respectively. Arrows indicate selected motoneuron terminals which contact the calbindin-labelled cells. Arrowheads indicate VGLUT1 and VGLUT2 terminals in A and B, respectively. (C1-C4) Single optical sections of the same area shown in B1-B4 that have been rescanned after sequential incubation with a fourth antibody for VACHT. The extra labelling present in C3 (indicated by arrows), which was absent in B3, corresponds to the additional VACHT-immunostaining. Note that all CTb terminals that form contacts with the Renshaw cell are immunoreactive for VACHT (profiles indicated by arrows in C4, merged image on the right) and hence can be confirmed to be motoneuron axon terminals. (A4, B4 and C4) Merged images. Scale bar = 10 μ m.

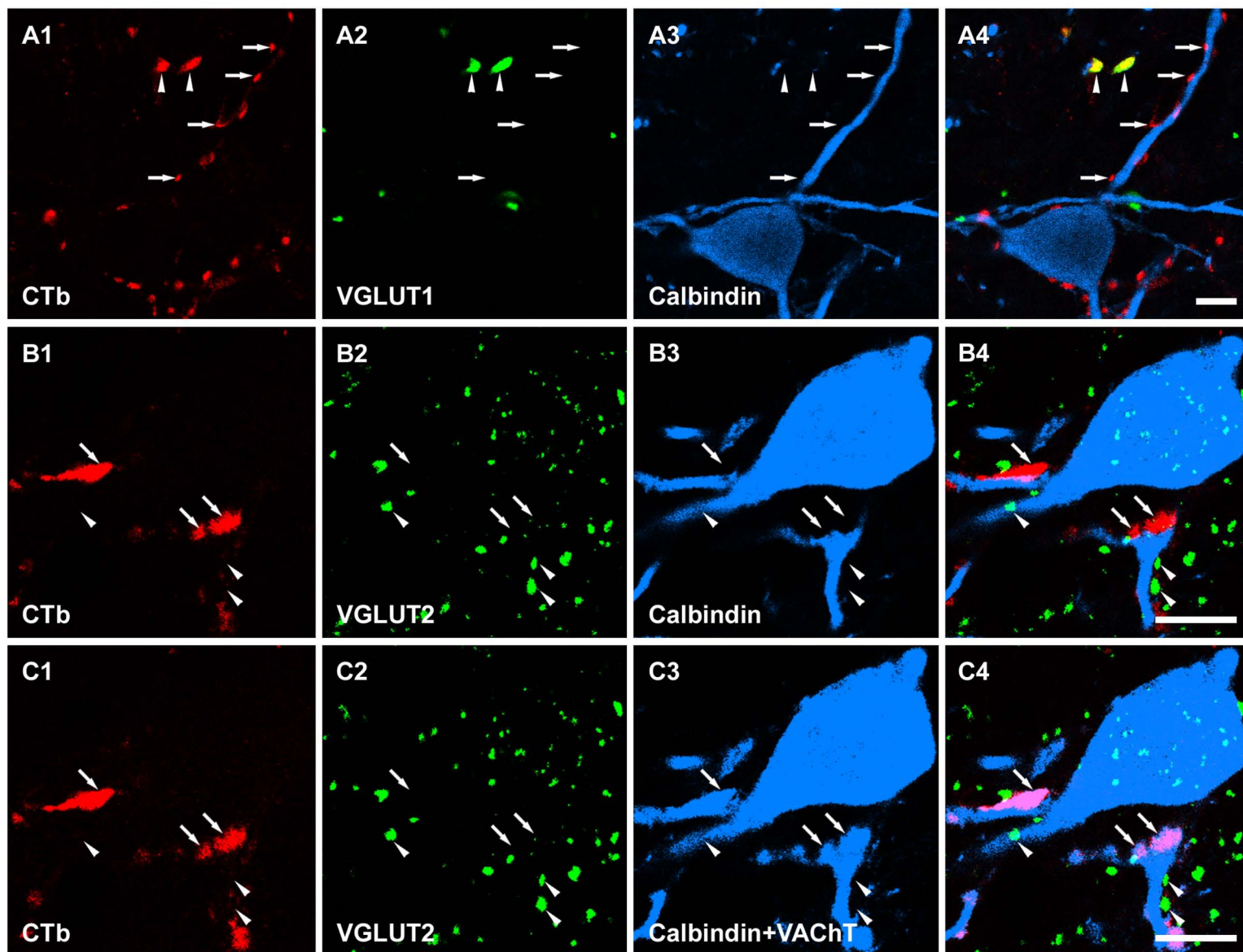


Figure 5.4. Sequential immunocytochemistry for CTb-labelled terminals in contact with a Renshaw cell in rat. (A, B) A general overview of CTb-labelled terminals in contact with a calbindin-labelled cell before and after a reaction with a fourth antibody against VGLUT1. Details of the areas demarcated by the boxes are shown in C1-C4 and D1-D4. (C1-C4) Single optical sections illustrating that most of the CTb-labelled terminals in contact with the calbindin cell were positive for VACHT. Arrows indicate double-labelled CTb axon terminals with VACHT staining. The arrowhead indicates a single CTb-labelled terminal on the Renshaw cell that was negative for VACHT. (D1-D4) Single optical sections of the same terminals that were rescanned after sequential incubation with a fourth antibody against VGLUT1. The extra labelling present in D3 (indicated by arrowhead), which was absent in C3, corresponds to additional VGLUT1-immunostaining (see D4). Note that this VGLUT1 positive terminal, which forms an apposition with the Renshaw cell, is bigger than CTb-labelled motoneuron terminals, and is likely to be a primary afferent terminal. A, B, C4 and D4 are merged images. Scale bar = 10 μ m.

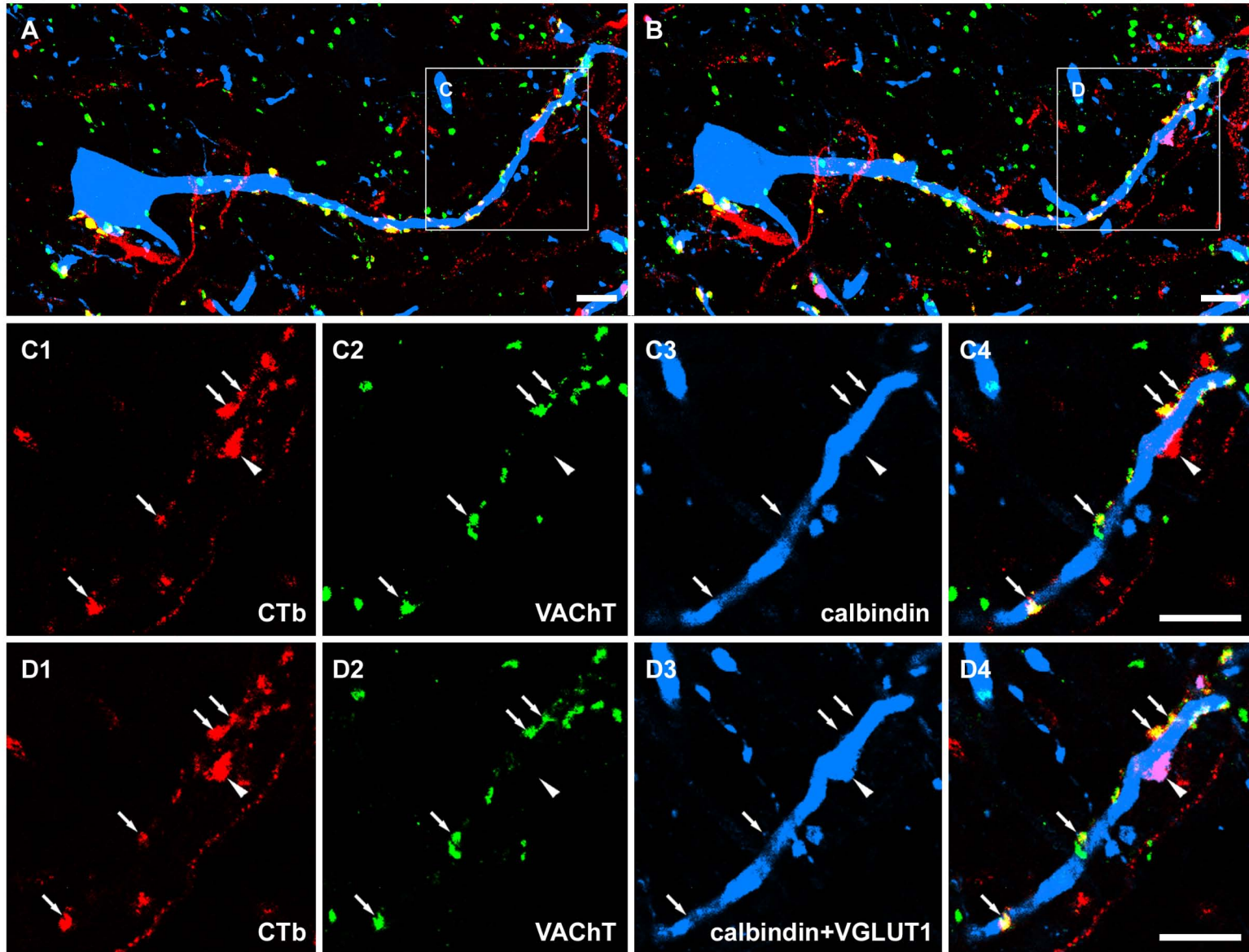


Figure 5.5. Reconstruction of a cat motoneuron and its axon collaterals that was intracellularly labelled with neurobiotin. The soma and axonal arborisation are shown in black and dendrites in grey. The thinner grey line represents the outline of the grey matter and the central canal; the thicker grey line represents the border of the spinal cord. The axon terminals illustrated in [Figure 5.6](#) are taken from the area outlined by the box. Scale bar = 200 μm (in big panel), 10 μm (in small panel).

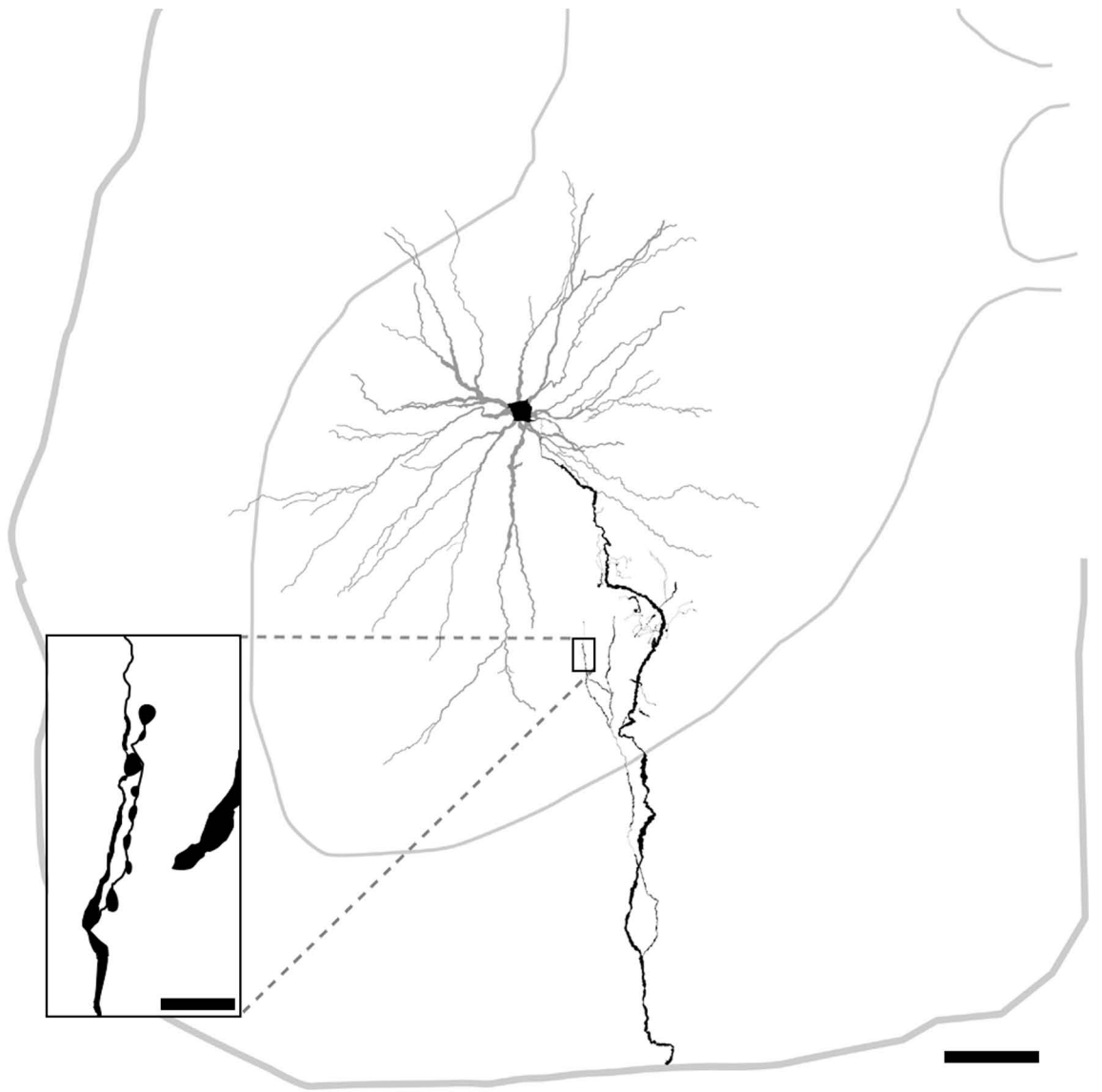


Figure 5.6. Relationship between intracellularly labelled cat motoneuron axon terminals and immunoreactivity for the GluR2 subunit of the AMPA receptor following antigen unmasking with pepsin. The large panel on the left (A) shows a projected image of a series of terminals originating from a motoneuron. (B-C) There is no obvious association between motoneuron axon terminals and GluR2 immunoreactivity. Details of the areas demarcated by the boxes in A are shown in B1-B3 and C1-C7. (B1-B3) Motoneuron axon terminals (B1), GluR2 (B2), and a merged image (B3) of the same single optical section. (C1-C7) A series of merged single optical sections through the motoneuron terminals taken at intervals of 0.3 μm . scale bar = 5 μm (A, B1-B3), 1 μm (C1-C7).

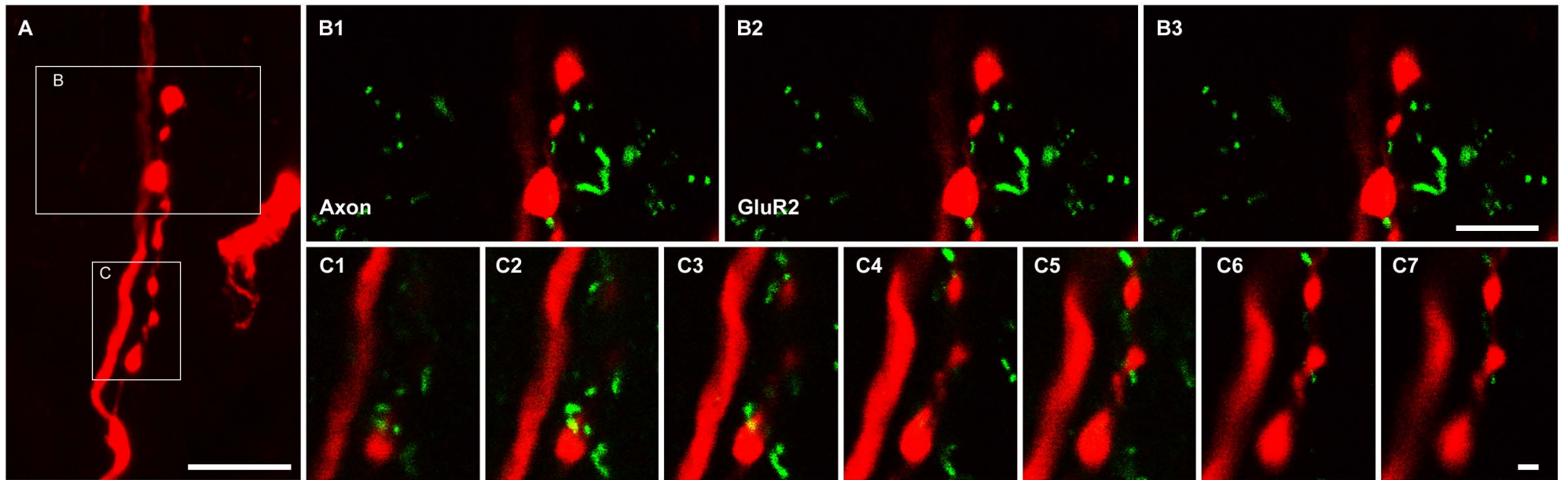


Figure 5.7. Relationship between intracellularly labelled cat interneuron axon terminals and immunoreactivity for the GluR2 subunit of the AMPA receptor following antigen unmasking with pepsin. The large panel on the left (A) shows a projected image of a series of terminals originating from an excitatory interneuron. (B-C) Associations between interneuronal axon terminals and GluR2 immunoreactivity. Details of the areas demarcated by the boxes in A are shown in B1-B3, C1-C7 and D1-D7. (B1-B3) Interneuron axon terminals (B1), GluR2 (B2), and a merged image (B3) of the same single optical section. (C1-C7 and D1-D7) Series of merged single optical sections through the interneuron terminals taken at intervals of 0.2 μm . scale bar = 5 μm (A, B1-B3), 2 μm (C1-C7, D1-D7).

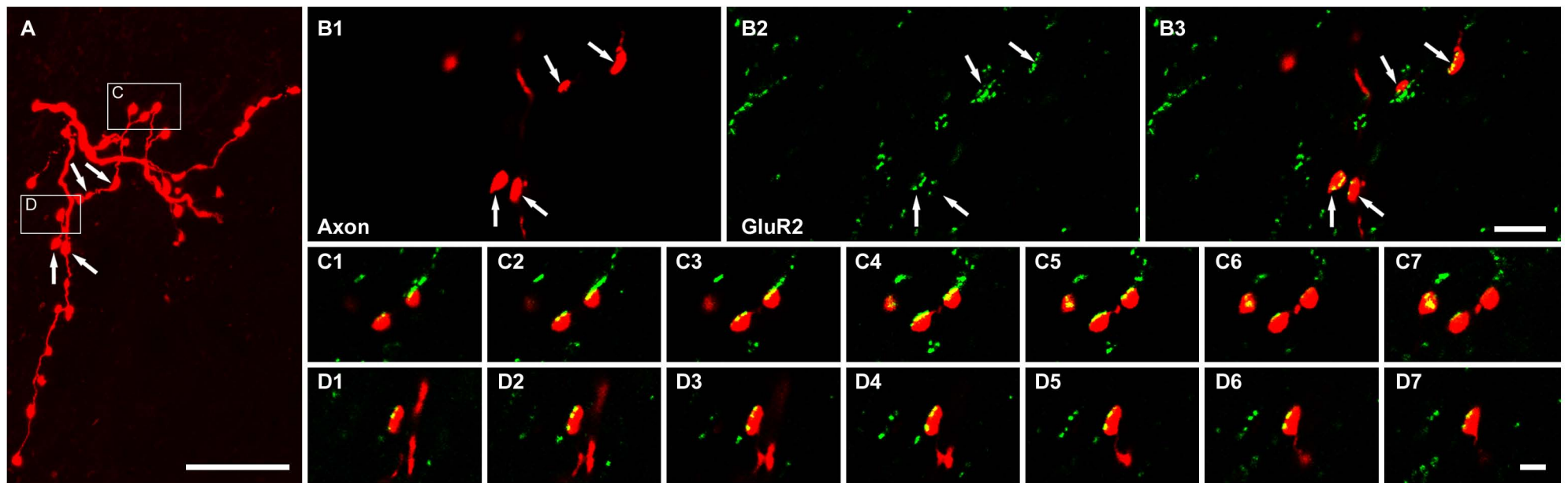


Figure 5.8. Relationships between VACht-labelled terminals and VGLUT-labelled terminals and immunoreactivity for the GluR2 subunit of the AMPA receptor following antigen unmasking with pepsin in rat. (A, D) General overviews of groups of VACht-immunostained terminals (red) and their relationships with GluR2-immunoreactive puncta (green). (G) A general overview of a group of VGLUT1 and VGLUT2 immunoreactive terminals in lamina VII and their relationship with GluR2-immunoreactive puncta. Details of the areas demarcated by the boxes are shown in B1-B3, C1-C4, E1-E3, F1-F4, H1-H3, and I1-I4. (B1-B3, E1-E3, H1-H3) VACht terminals (B1, E1), VGLUT1 and VGLUT2 terminals (H1), GluR2 puncta (B2, E2, H2), and merged images (B3, E3, H3) of the same single optical sections. (C1-C4, F1-F4 and I1-I4) Series of merged single optical sections through the selected terminals taken at intervals of 0.2 μm . Note that the VACht terminals which lack any association with GluR2 puncta (B, C), are bigger than the terminals which form appositions with GluR2 puncta (E, F). Scale bar = 5 μm (A, D, and G); 1 μm (B, C, E, F, H, I).

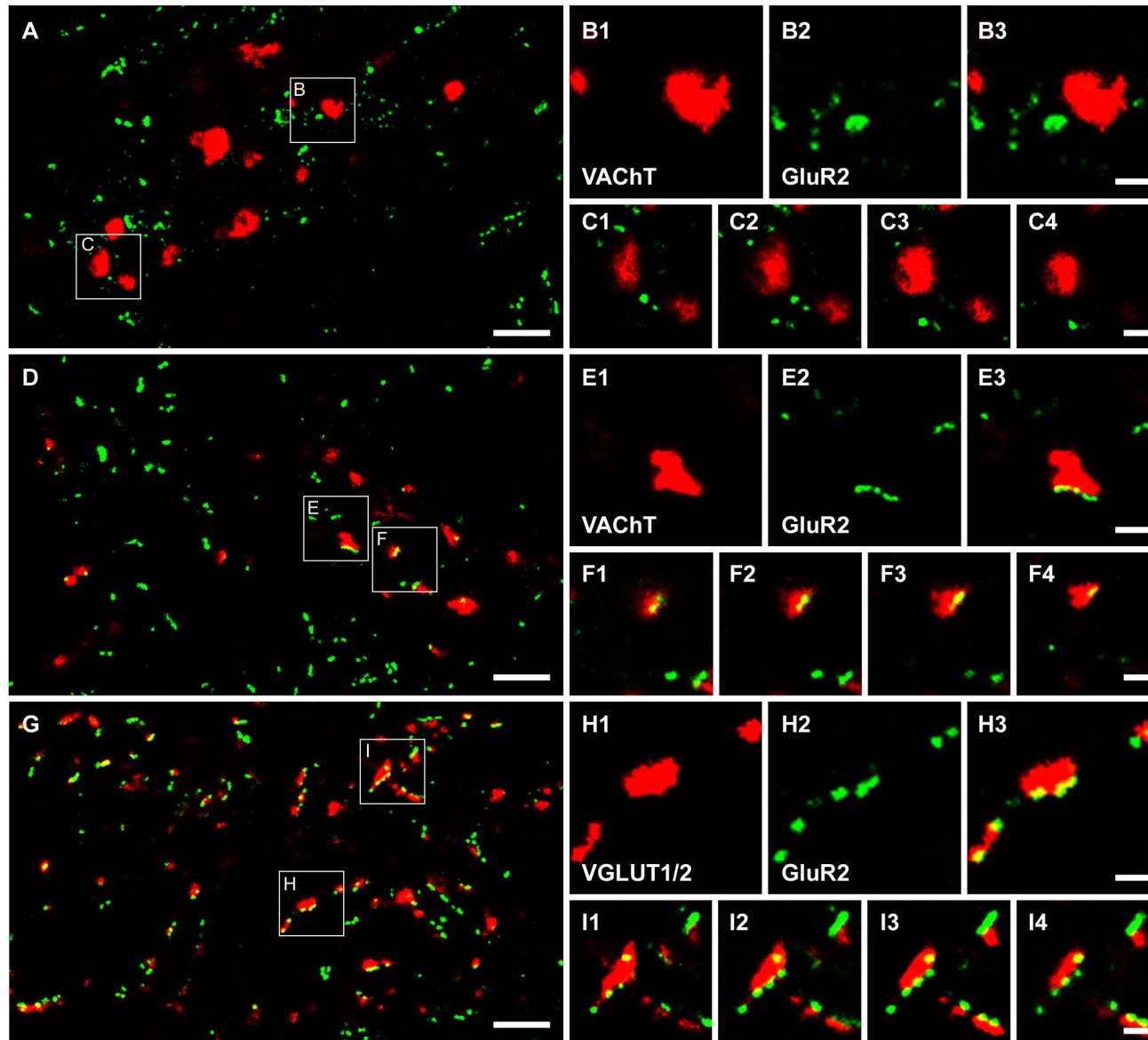
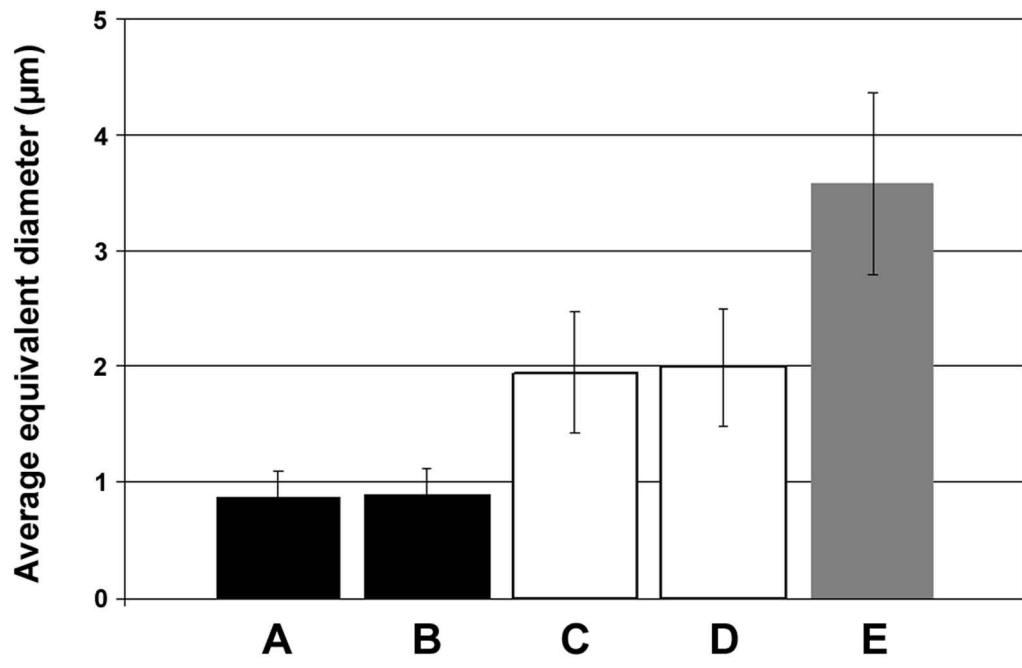


Figure 5.9. Comparison of the average equivalent diameters of five groups of terminals. (A, B) The average equivalent diameters of VACHT terminals with GluR2 association and with VGLUT2 labelling, respectively. (C, D) The average equivalent diameters of VACHT terminals without association with GluR2 and with CTb labelling, respectively. (E) The average equivalent diameters of CTb terminals with VGLUT1 immunoreactivity. One way ANOVA showed that there was a significant difference between these groups and a post hoc comparison showed no difference between groups A and B and between groups C and D. all other comparisons were significantly different. Bars show standard deviations.



Chapter 6
General Discussion

Neurons in the locomotor CPG are activated by inputs from descending locomotor commands and generate the rhythm and pattern of muscle contraction; however, CPG activity is subject to adaptation by a variety of sensory control mechanisms, which are likely to be an inherent part of CPGs and affect the overall motor output. Therefore, the current studies are focused on those spinal interneurons involved in sensorimotor integration, and in summary, three conclusions can be derived. (1) The first investigation shows that propriospinal interneurons in the L5 segment extensively project both contralaterally and ipsilaterally to rostral lumbar segments (L1/L3) and some of these ascending neurons are cholinergic or express calcium-binding proteins. On the other hand, in rostral lumbar segments (L1/L3), there is a population of CINs descending to the motor nuclei in the L5 segments and the majority of terminals originating from these CINs are glutamatergic. (2) The second study demonstrates that spinal interneurons with and without monosynaptic primary afferent inputs receive distinct contacts. The neurons with monosynaptic inputs from primary afferents were mainly contacted by VGLUT1-positive terminals, while the majority contacts on the cells with monosynaptic inputs from MLF but not primary afferents were VGLUT2 immunoreactive. In addition, the excitatory and inhibitory interneurons with monosynaptic input from primary afferents receive a similar proportion of excitatory drive and both types are subject to strong presynaptic inhibitory control of their primary afferent input. (3) The third investigation shows that a group of small cholinergic terminals located in the deep ventral horn contains glutamate as a co-neurotransmitter. However, these terminals do not originate from motoneurons.

If we synthesise and reorganize the above results, all the identified interneurons could be classified as either CINs or ipsilaterally projecting interneurons, both of which include excitatory and inhibitory cells. It has been proposed that ipsilateral excitatory networks are involved in the rhythm generation during locomotion, while ipsilateral inhibitory networks are responsible for the alternation between flexor and extensor motoneurons on the same side (Kiehn, 2006). The evidence to support these suggestions is that rhythmic activity still can be generated by hemi-sected spinal cord in the absence of inhibition (e.g., with application of strychnine or bicuculline); however, flexor and extensor motoneurons on the same side are activated in synchrony rather than alternation (Kiehn, 2006). The coordination between left-right sides is achieved by the CIN networks. Descending CINs (dCINs) are suggested to synchronize the left-right motoneurons innervating antagonist muscles (Butt and Kiehn, 2003; Kiehn and Butt, 2003); ascending CINs (aCINs) are activated to alternate the left-right

motoneurons innervating synergist muscles (Kiehn, 2006; Lanuza et al., 2004). Based on these suggestions, the spinal interneurons examined in the present studies could be accommodated into the neuron circuits involved in locomotion (Figure 6.1).

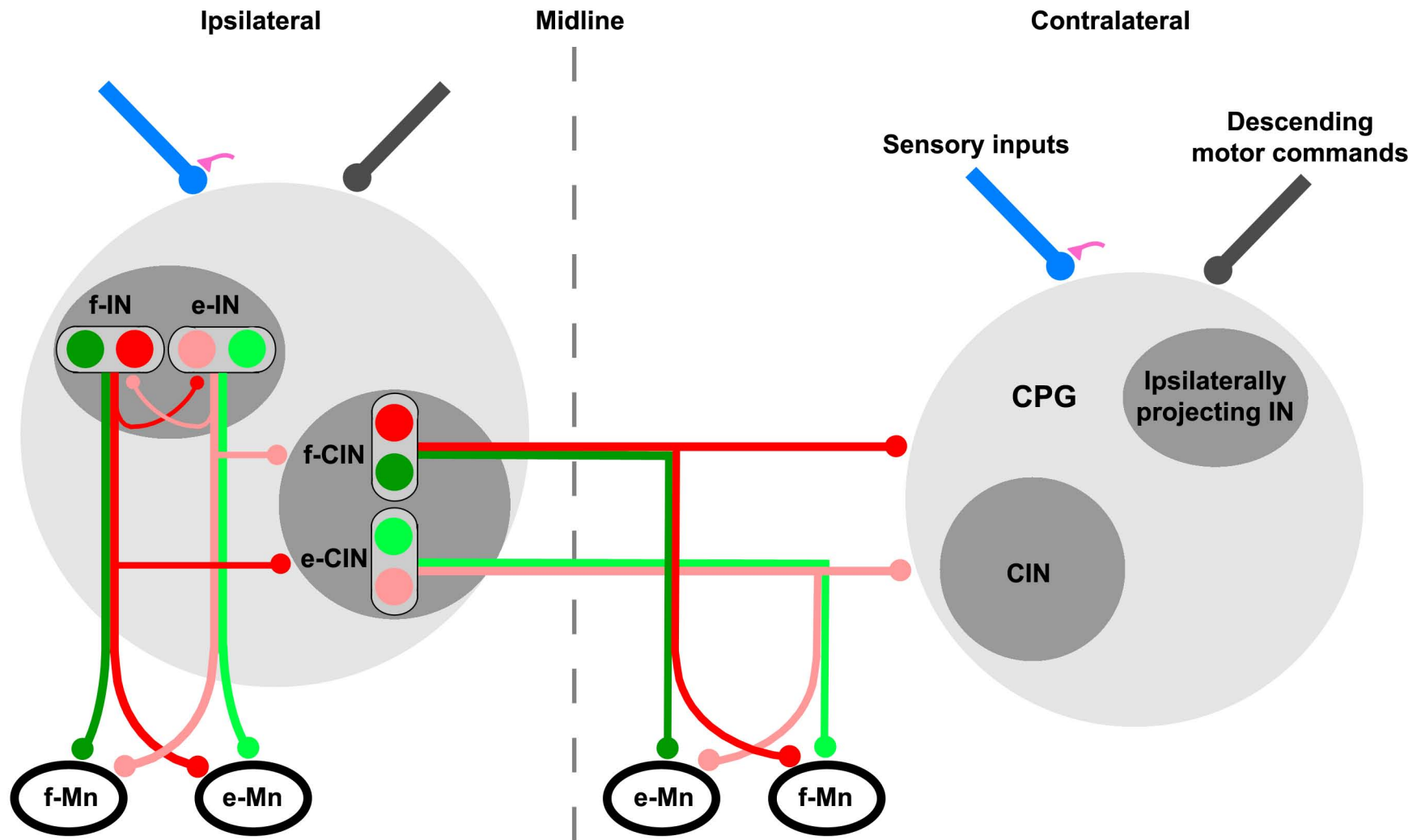
Since the concept of CPGs was first proposed by Graham Brown, and hypotheses about how they are organized have been developed from the first generation (i.e. a “single-layer” model: rhythm and pattern of extensor and flexor are generated by two excitatory interneuron populations with mutual inhibitory interconnections) to the third generation (i.e. a more advanced “three-layers” model: rhythm and pattern are generated by separate excitatory interneuron populations rather than by the same population; see McCrea and Rybak, 2008). The significant effect of sensory inputs on motor output is another major alteration presented in the advanced CPG models. Interneurons with monosynaptic primary afferent inputs included both excitatory and inhibitory cells, and both ipsilaterally and contralaterally projecting neurons. In other words, sensory information may act on at least two functional units of CPG (as shown in Figure 6.1). These populations of interneurons were found mainly to have inhibitory rather than excitatory actions on themselves; consequently, this arrangement may provide a mechanism of how sensory information adjusts the pattern and/or rhythm of motor outputs. For example, during swing phase of forward walking, if the dorsum of the paw contacts an obstacle, then the stumbling correction reaction is evoked (Quevedo et al., 2005a; b). The reaction includes a hyper-flexion of the limb and a brief activation of the ankle extensors to lift the paw over and move away from the obstacle. That is, sensory information excites the extensors which were originally inhibited in swing phase. The mutual inhibition between inhibitory flexor-interneurons and extensor-interneurons (see Figure 6.1) may be responsible for this short-duration mixed synergy. If the stumbling correction happens in the transition of swing-stance phase, then in order to keep the body in balance, those “stance-phase” limbs should not transit into swing phase before the correction is complete. Therefore, the CIN population, which is responsible for left-right alternation, should be inhibited to stop the transition. This inhibition may arise from ipsilaterally projecting interneuron population (see Figure 6.1).

In addition, a subgroup of CINs located in lamina VIII were found to receive monosynaptic input from MLF only, while some interneurons with monosynaptic primary afferent input were found to be activated by MLF also. Recent studies by Berkowitz (2002; 2007; 2008)

have shown that in turtles, swimming and scratching shared a spinal interneuron network but there was another group of interneurons that were selectively activated during scratching only. Therefore, it might be reasonable to hypothesize that those interneurons with only one type of identified input (such as primary afferents or MLF) are relatively specialized for a subset of hindlimb movement types which may or may not be locomotor activities. On the other hand, those interneurons which were co-activated by more than one type of input (such as both primary afferents and MLF) may be involved in the interneuron circuits shared by different movements.

To summarize, the present project revealed a number of interesting aspects of spinal interneurons responsible for the integration of descending motor commands and sensory information. However, in order to fully understand functional flexibility of neuron circuits, considerably more work will need to be done to determine the network organizations of these interneurons and their underlying events. The studies also provided clear evidence showing that glutamate is neither colocalized in central synapses of adult motoneurons nor acts via an APMA receptor, although glutamate was observed in a population of small cholinergic terminals and acts via AMPA receptor. Therefore, it would be interesting to investigate the origin of these terminals.

Figure 6.1. Schematic diagram illustrating putative organizations of interneurons in sensory-motor circuit assembly. The larger “light grey” circles on each side represent CPGs. The inside smaller “dark grey” ovals and circles represent ipsilaterally projecting interneuron population and CIN population, respectively. Green and red circles represent excitatory and inhibitory interneurons, respectively. Excitatory and inhibitory connections are shown by green and red lines ending with small green and red circles, respectively. f-IN indicates the population of interneurons activating flexor motoneurons and inhibiting extensor motoneurons. e-IN indicates the population of interneurons activating extensor motoneurons and inhibiting flexor and motoneurons. The excitatory interneuron populations are suggested to generate rhythmic activities and the inhibitory interneuron populations are involved in alteration between flexor-extensor motoneurons. These ipsilaterally projecting neuron populations also provide inhibitory control on CIN populations. f-CIN and e-CIN indicate the CIN populations that are activated during ipsilateral extensor and flexor motoneurons firing phase, respectively. They excite corresponding antagonist motoneurons and inhibit corresponding agonist motoneurons on the contralateral side; therefore, they contribute to left-right coordination. They also mutually inhibit contralateral CPG. Blue and grey input lines indicate sensory inputs and descending tract fibres, respectively. The small red triangles indicate presynaptic terminals associated with sensory afferent terminals. f-Mn, flexor motoneurons; e-Mn, extensor motoneurons. The same network connections are assumed contralaterally but not illustrated for the sake of simplicity.



References

- Aggelopoulos NC, Burton MJ, Clarke RW, Edgley SA 1996 Characterization of a descending system that enables crossed group II inhibitory reflex pathways in the cat spinal cord. *J Neurosci* 16: 723-729
- Airaksinen MS, Eilers J, Garaschuk O, Thoenen H, Konnerth A, Meyer M 1997 Ataxia and altered dendritic calcium signaling in mice carrying a targeted null mutation of the calbindin D28k gene. *Proc Natl Acad Sci U S A* 94: 1488-1493
- Alstermark B, Lundberg A, Pinter M, Sasaki S 1987 Long C3-C5 propriospinal neurones in the cat. *Brain Res* 404: 382-388
- Alstermark B, Kummel H 1990 Transneuronal transport of wheat germ agglutinin conjugated horseradish peroxidase into last order spinal interneurons projecting to acromio- and spinodeltoideus motoneurons in the cat. 1. Location of labelled interneurons and influence of synaptic activity on the transneuronal transport. *Exp Brain Res* 80: 83-95
- Alvarez FJ, Dewey DE, McMillin P, Fyffe RE 1999 Distribution of cholinergic contacts on Renshaw cells in the rat spinal cord: a light microscopic study. *J Physiol* 515: 787-797
- Anden NE, Jukes MGM, Lundberg A, Vyklicky L 1966 Effect of Dopa on Spinal Cord .I. Influence on Transmission from Primary Afferents. *Acta Physiologica Scandinavica* 67: 373-386
- Andersen P, Eccles JC, Sears TA 1962 Presynaptic inhibitory action of cerebral cortex on the spinal cord. *Nature* 194: 740-741
- Andressen C, Blumcke I, Celio MR 1993 Calcium-binding proteins: selective markers of nerve cells. *Cell Tissue Res* 271: 181-208
- Antal M, Freund TF, Polgar E 1990 Calcium-binding proteins, parvalbumin- and calbindin-D 28k-immunoreactive neurons in the rat spinal cord and dorsal root ganglia: a light and electron microscopic study. *J Comp Neurol* 295: 467-484
- Antal M, Polgar E, Chalmers J, Minson JB, Llewellyn-Smith I, Heizmann CW, Somogyi P 1991 Different populations of parvalbumin- and calbindin-D28k-immunoreactive neurons contain GABA and accumulate 3H-D-aspartate in the dorsal horn of the rat spinal cord. *J Comp Neurol* 314: 114-124
- Armstrong DM 1986 Supraspinal contributions to the initiation and control of locomotion in the cat. *Prog Neurobiol* 26: 273-361
- Armstrong DM 1988 The supraspinal control of mammalian locomotion. *J Physiol* 405: 1-37
- Arvidsson U, Riedl M, Elde R, Meister B 1997 Vesicular acetylcholine transporter (VACHT) protein: a novel and unique marker for cholinergic neurons in the central and peripheral nervous systems. *J Comp Neurol* 378: 454-467
- Arya T, Bajwa S, Edgley SA 1991 Crossed reflex actions from group II muscle afferents in the lumbar spinal cord of the anaesthetized cat. *J Physiol* 444: 117-131

- Aubrey KR, Rossi FM, Ruivo R, Alboni S, Bellenchi GC, Le Goff A, Gasnier B, Supplisson S 2007 The transporters GlyT2 and VIAAT cooperate to determine the vesicular glycinergic phenotype. *J Neurosci* 27: 6273-6281
- Bai L, Xu H, Collins JF, Ghishan FK 2001 Molecular and functional analysis of a novel neuronal vesicular glutamate transporter. *J Biol Chem* 276: 36764-36769
- Ballion B, Morin D, Viala D 2001 Forelimb locomotor generators and quadrupedal locomotion in the neonatal rat. *Eur J Neurosci* 14: 1727-1738
- Bannatyne BA, Edgley SA, Hammar I, Jankowska E, Maxwell DJ 2003 Networks of inhibitory and excitatory commissural interneurons mediating crossed reticulospinal actions. *Eur J Neurosci* 18: 2273-2284
- Bannatyne BA, Edgley SA, Hammar I, Jankowska E, Maxwell DJ 2006 Differential projections of excitatory and inhibitory dorsal horn interneurons relaying information from group II muscle afferents in the cat spinal cord. *J Neurosci* 26: 2871-2880
- Bannatyne BA, Liu TT, Hammar I, Stecina K, Jankowska E, Maxwell DJ 2009 Excitatory and inhibitory intermediate zone interneurons in pathways from feline group I and II afferents: differences in axonal projections and input. *J Physiol* 587: 379-399
- Barajon I, Vizzotto L, Pizzini G, Tredici G 1990 Different neuronal types in transneuronally WGA-HRP-labeled premotor interneurons of the rat spinal cord. *Behav Brain Res* 38: 77-81
- Barber RP, Phelps PE, Houser CR, Crawford GD, Salvaterra PM, Vaughn JE 1984 The morphology and distribution of neurons containing choline acetyltransferase in the adult rat spinal cord: an immunocytochemical study. *J Comp Neurol* 229: 329-346
- Bastianelli E 2003 Distribution of calcium-binding proteins in the cerebellum. *Cerebellum* 2: 242-262
- Beal JA, Knight DS, Nandi KN 1990 Nerve cell bodies in the dorsal funiculus of the rat spinal cord. *Exp Brain Res* 81: 372-376
- Beitz AJ, Ecklund LJ 1988 Colocalization of fixative-modified glutamate and glutaminase but not GAD in rubrospinal neurons. *J Comp Neurol* 274: 265-279
- Berkowitz A 2002 Both shared and specialized spinal circuitry for scratching and swimming in turtles. *J Comp Physiol A Neuroethol Sens Neural Behav Physiol* 188: 225-234
- Berkowitz A 2004 Propriospinal projections to the ventral horn of the rostral and caudal hindlimb enlargement in turtles. *Brain Res* 1014: 164-176
- Berkowitz A 2007 Spinal interneurons that are selectively activated during fictive flexion reflex. *J Neurosci* 27: 4634-4641
- Berkowitz A 2008 Physiology and morphology of shared and specialized spinal interneurons for locomotion and scratching. *J Neurophysiol* 99: 2887-2901

- Bing Z, Villanueva L, Le Bars D 1990 Ascending pathways in the spinal cord involved in the activation of subnucleus reticularis dorsalis neurons in the medulla of the rat. *J Neurophysiol* 63: 424-438
- Birinyi A, Parker D, Antal M, Shupliakov O 2001 Zinc co-localizes with GABA and glycine in synapses in the lamprey spinal cord. *J Comp Neurol* 433: 208-221
- Birinyi A, Viszokay K, Weber I, Kiehn O, Antal M 2003 Synaptic targets of commissural interneurons in the lumbar spinal cord of neonatal rats. *J Comp Neurol* 461: 429-440
- Blatow M, Caputi A, Burnashev N, Monyer H, Rozov A 2003 Ca²⁺ buffer saturation underlies paired pulse facilitation in calbindin-D28k-containing terminals. *Neuron* 38: 79-88
- Borges LF, Iversen SD 1986 Topography of choline acetyltransferase immunoreactive neurons and fibers in the rat spinal cord. *Brain Res* 362: 140-148
- Bowker RM, Steinbusch HW, Coulter JD 1981 Serotonergic and peptidergic projections to the spinal cord demonstrated by a combined retrograde HRP histochemical and immunocytochemical staining method. *Brain Res* 211: 412-417
- Bowker RM, Westlund KN, Sullivan MC, Coulter JD 1982 Organization of descending serotonergic projections to the spinal cord. *Prog Brain Res* 57: 239-265
- Bowker RM, Abbott LC 1990 Quantitative re-evaluation of descending serotonergic and non-serotonergic projections from the medulla of the rodent: evidence for extensive co-existence of serotonin and peptides in the same spinally projecting neurons, but not from the nucleus raphe magnus. *Brain Res* 512: 15-25
- Bradley K, Eccles JC 1953 Analysis of the fast afferent impulses from thigh muscles. *J Physiol* 122: 462-473
- Bras H, Cavallari P, Jankowska E 1988 An investigation of local actions of ionophoretically applied DOPA in the spinal cord. *Exp Brain Res* 71: 447-449
- Bras H, Cavallari P, Jankowska E, McCrea D 1989 Comparison of effects of monoamines on transmission in spinal pathways from group I and II muscle afferents in the cat. *Exp Brain Res* 76: 27-37
- Bras H, Jankowska E, Noga B, Skoog B 1990 Comparison of Effects of Various Types of NA and 5-HT Agonists on Transmission from Group II Muscle Afferents in the Cat. *Eur J Neurosci* 2: 1029-1039
- Brink E, Jankowska E, McCrea DA, Skoog B 1983 Inhibitory interactions between interneurons in reflex pathways from group Ia and group Ib afferents in the cat. *J Physiol* 343: 361-373
- Brosamle C, Schwab ME 1997 Cells of origin, course, and termination patterns of the ventral, uncrossed component of the mature rat corticospinal tract. *J Comp Neurol* 386: 293-303
- Brown A 1981 organization in the spinal cord. Berlin: springer-Verlag,

- Brown LT 1974 Rubrospinal projections in the rat. *J Comp Neurol* 154: 169-187
- Brown LT, Jr. 1971 Projections and termination of the corticospinal tract in rodents. *Exp Brain Res* 13: 432-450
- Burger PM, Hell J, Mehl E, Krasel C, Lottspeich F, Jahn R 1991 GABA and glycine in synaptic vesicles: storage and transport characteristics. *Neuron* 7: 287-293
- Butt SJ, Kiehn O 2003 Functional identification of interneurons responsible for left-right coordination of hindlimbs in mammals. *Neuron* 38: 953-963
- Cabaj A, Stecina K, Jankowska E 2006 Same spinal interneurons mediate reflex actions of group Ib and group II afferents and crossed reticulospinal actions. *J Neurophysiol* 95: 3911-3922
- Cai YL, Ma WL, Wang JQ, Li YQ, Li M 2008 Excitatory pathways from the vestibular nuclei to the NTS and the PBN and indirect vestibulo-cardiovascular pathway from the vestibular nuclei to the RVLM relayed by the NTS. *Brain Res* 1240: 96-104
- Cangiano A, Lutzemberger L 1972 The action of selectively activated group II muscle afferent fibers on extensor motoneurons. *Brain Res* 41: 475-478
- Carpenter D, Lundberg A, Norrsell U 1963 Primary afferent depolarization evoked from the sensorimotor cortex. *Acta Physiol Scand* 59: 126-142
- Carr PA, Alvarez FJ, Leman EA, Fyffe RE 1998 Calbindin D28k expression in immunohistochemically identified Renshaw cells. *Neuroreport* 9: 2657-2661
- Cavallari P, Edgley SA, Jankowska E 1987 Post-synaptic actions of midlumbar interneurons on motoneurons of hind-limb muscles in the cat. *J Physiol* 389: 675-689
- Cavallari P, Pettersson LG 1991 Synaptic effects in lumbar alpha-motoneurons evoked from group II muscle afferents via two different interneuronal pathways in the cat. *Neurosci Lett* 129: 225-228
- Cazalets JR, Borde M, Clarac F 1995 Localization and organization of the central pattern generator for hindlimb locomotion in newborn rat. *J Neurosci* 15: 4943-4951
- Cazalets JR, Borde M, Clarac F 1996 The synaptic drive from the spinal locomotor network to motoneurons in the newborn rat. *J Neurosci* 16: 298-306
- Celio MR 1990 Calbindin D-28k and parvalbumin in the rat nervous system. *Neuroscience* 35: 375-475
- Chaudhry FA, Reimer RJ, Bellocchio EE, Danbolt NC, Osen KK, Edwards RH, Storm-Mathisen J 1998 The vesicular GABA transporter, VGAT, localizes to synaptic vesicles in sets of glycinergic as well as GABAergic neurons. *J Neurosci* 18: 9733-9750
- Chen S, Aston-Jones G 1995 Evidence that cholera toxin B subunit (CTb) can be avidly taken up and transported by fibers of passage. *Brain Res* 674: 107-111

- Cheron G, Gall D, Servais L, Dan B, Maex R, Schiffmann SN 2004 Inactivation of calcium-binding protein genes induces 160 Hz oscillations in the cerebellar cortex of alert mice. *J Neurosci* 24: 434-441
- Conway BA, Hultborn H, Kiehn O 1987 Proprioceptive input resets central locomotor rhythm in the spinal cat. *Exp Brain Res* 68: 643-656
- Crone C, Hultborn H, Jespersen B, Nielsen J 1987 Reciprocal Ia inhibition between ankle flexors and extensors in man. *J Physiol* 389: 163-185
- Crone C, Nielsen J 1989 Spinal mechanisms in man contributing to reciprocal inhibition during voluntary dorsiflexion of the foot. *J Physiol* 416: 255-272
- Curtis DR, Ryall RW 1964 Nicotinic and muscarinic receptors of Renshaw cells. *Nature* 203: 652-653
- Davies HE, Edgley SA 1994 Inputs to group II-activated midlumbar interneurons from descending motor pathways in the cat. *J Physiol* 479: 463-473
- Deliagina TG, Orlovsky GN 1980 Activity of Ia inhibitory interneurons during fictitious scratch reflex in the cat. *Brain Res* 193: 439-447
- Deliagina TG, Zelenin PV, Orlovsky GN 2002 Encoding and decoding of reticulospinal commands. *Brain Res Brain Res Rev* 40: 166-177
- Dourado M, Sargent PB 2002 Properties of nicotinic receptors underlying Renshaw cell excitation by alpha-motor neurons in neonatal rat spinal cord. *J Neurophysiol* 87: 3117-3125
- Duenas SH, Rudomin P 1988 Excitability changes of ankle extensor group Ia and Ib fibers during fictive locomotion in the cat. *Exp Brain Res* 70: 15-25
- Dutton RC, Carstens MI, Antognini JF, Carstens E 2006 Long ascending propriospinal projections from lumbosacral to upper cervical spinal cord in the rat. *Brain Res* 1119: 76-85
- Duysens J, Loeb GE, Weston BJ 1980 Crossed flexor reflex responses and their reversal in freely walking cats. *Brain Res* 197: 538-542
- Eccles JC, Fatt P, Landgren S, Winsbury GJ 1954a Spinal Cord Potentials Generated by Volleys in the Large Muscle Afferents. *J Physiol* 125: 590-606
- Eccles JC, Fatt P, Koketsu K 1954b Cholinergic and inhibitory synapses in a pathway from motor-axon collaterals to motoneurons. *J Physiol* 126: 524-562
- Eccles JC, Fatt P, Landgren S 1956 Central pathway for direct inhibitory action of impulses in largest afferent nerve fibres to muscle. *J Neurophysiol* 19: 75-98
- Eccles JC, Eccles RM, Lundberg A 1957 Synaptic actions on motoneurons caused by impulses in Golgi tendon organ afferents. *J Physiol* 138: 227-252

- Eccles RM, Lundberg A 1959 Synaptic actions in motoneurons by afferents which may evoke the flexion reflex. *Arch Ital Biol* 97: 199-221
- Edgley SA, Jankowska E 1987a Field potentials generated by group II muscle afferents in the middle lumbar segments of the cat spinal cord. *J Physiol* 385: 393-413
- Edgley SA, Jankowska E 1987b An interneuronal relay for group I and II muscle afferents in the midlumbar segments of the cat spinal cord. *J Physiol* 389: 647-674
- Edgley SA, Jankowska E, Shefchyk S 1988 Evidence that mid-lumbar neurones in reflex pathways from group II afferents are involved in locomotion in the cat. *J Physiol* 403: 57-71
- Edgley SA, Jankowska E, Krutki P, Hammar I 2003 Both dorsal horn and lamina VIII interneurons contribute to crossed reflexes from feline group II muscle afferents. *J Physiol* 552: 961-974
- Edgley SA, Jankowska E, Hammar I 2004 Ipsilateral actions of feline corticospinal tract neurons on limb motoneurons. *J Neurosci* 24: 7804-7813
- Edmonds B, Reyes R, Schwaller B, Roberts WM 2000 Calretinin modifies presynaptic calcium signaling in frog saccular hair cells. *Nat Neurosci* 3: 786-790
- Eguibar JR, Quevedo J, Rudomin P 1997 Selective cortical and segmental control of primary afferent depolarization of single muscle afferents in the cat spinal cord. *Exp Brain Res* 113: 411-430
- Eide AL, Glover J, Kjaerulff O, Kiehn O 1999 Characterization of commissural interneurons in the lumbar region of the neonatal rat spinal cord. *J Comp Neurol* 403: 332-345
- Engberg I, Lundberg A 1969 An electromyographic analysis of muscular activity in the hindlimb of the cat during unrestrained locomotion. *Acta Physiol Scand* 75: 614-630
- Ericson H, Blomqvist A 1988 Tracing of neuronal connections with cholera toxin subunit B: light and electron microscopic immunohistochemistry using monoclonal antibodies. *J Neurosci Methods* 24: 225-235
- Fahandejsaadi A, Leung E, Rahaii R, Bu J, Geula C 2004 Calbindin-D28K, parvalbumin and calretinin in primate lower motor neurons. *Neuroreport* 15: 443-448
- Fedina L, Hultborn H 1972 Facilitation from ipsilateral primary afferents of interneuronal transmission in the Ia inhibitory pathway to motoneurons. *Acta Physiol Scand* 86: 59-81
- Feldman AG, Orlovsky GN 1975 Activity of interneurons mediating reciprocal Ia inhibition during locomotion. *Brain Res* 84: 181-194
- Frank K, Fuortes MGF 1957 Presynaptic and postsynaptic inhibition of monosynaptic reflexes. *Fed Proc* 19: 39-40

- Fremeau RT, Jr., Troyer MD, Pahner I, Nygaard GO, Tran CH, Reimer RJ, Bellocchio EE, Fortin D, Storm-Mathisen J, Edwards RH 2001 The expression of vesicular glutamate transporters defines two classes of excitatory synapse. *Neuron* 31: 247-260
- Fu TC, Jankowska E, Lundberg A 1975 Reciprocal Ia Inhibition During Late Reflexes Evoked from Flexor Reflex Afferents After Dopa. *Brain Research* 85: 99-102
- Fukushima K, Kato M 1975 Spinal interneurons responding to group II muscle afferent fibers in the cat. *Brain Res* 90: 307-312
- Garcia-Segura LM, Baetens D, Roth J, Norman AW, Orci L 1984 Immunohistochemical mapping of calcium-binding protein immunoreactivity in the rat central nervous system. *Brain Res* 296: 75-86
- Giesler GJ, Jr., Spiel HR, Willis WD 1981 Organization of spinothalamic tract axons within the rat spinal cord. *J Comp Neurol* 195: 243-252
- Giesler GJ, Jr., Nahin RL, Madsen AM 1984 Postsynaptic dorsal column pathway of the rat. I. Anatomical studies. *J Neurophysiol* 51: 260-275
- Giuffrida R, Rustioni A 1989 Glutamate and aspartate immunoreactivity in corticospinal neurons of rats. *J Comp Neurol* 288: 154-164
- Gossard JP, Brownstone RM, Barajon I, Hultborn H 1994 Transmission in a locomotor-related group Ib pathway from hindlimb extensor muscles in the cat. *Exp Brain Res* 98: 213-228
- Grillner S 1985 Neurobiological bases of rhythmic motor acts in vertebrates. *Science* 228: 143-149
- Grillner S, Dubuc R 1988 Control of locomotion in vertebrates: spinal and supraspinal mechanisms. *Adv Neurol* 47: 425-453
- Grillner S, Deliagina T, Ekeberg O, el Manira A, Hill RH, Lansner A, Orlovsky GN, Wallen P 1995 Neural networks that co-ordinate locomotion and body orientation in lamprey. *Trends Neurosci* 18: 270-279
- Grillner S 2006 Biological pattern generation: the cellular and computational logic of networks in motion. *Neuron* 52: 751-766
- Grkovic I, Anderson CR 1997 Calbindin D28K-immunoreactivity identifies distinct subpopulations of sympathetic pre- and postganglionic neurons in the rat. *J Comp Neurol* 386: 245-259
- Gutierrez R 2005 The dual glutamatergic-GABAergic phenotype of hippocampal granule cells. *Trends Neurosci* 28: 297-303
- Hammar I, Bannatyne BA, Maxwell DJ, Edgley SA, Jankowska E 2004 The actions of monoamines and distribution of noradrenergic and serotonergic contacts on different subpopulations of commissural interneurons in the cat spinal cord. *Eur J Neurosci* 19: 1305-1316

- Harrison PJ, Jankowska E, Johannisson T 1983 Shared reflex pathways of group I afferents of different cat hind-limb muscles. *J Physiol* 338: 113-128
- Harrison PJ, Hultborn H, Jankowska E, Katz R, Storai B, Zytnicki D 1984 Labelling of interneurons by retrograde transsynaptic transport of horseradish peroxidase from motoneurons in rats and cats. *Neurosci Lett* 45: 15-19
- Harrison PJ, Jankowska E 1985 Sources of input to interneurons mediating group I non-reciprocal inhibition of motoneurons in the cat. *J Physiol* 361: 379-401
- Harrison PJ, Jankowska E, Zytnicki D 1986 Lamina VIII interneurons interposed in crossed reflex pathways in the cat. *J Physiol* 371: 147-166
- Harrison PJ, Jankowska E 1989 Primary afferent depolarization of central terminals of group II muscle afferents in the cat spinal cord. *J Physiol* 411: 71-83
- Headley PM, Duggan AW, Griersmith BT 1978 Selective reduction by noradrenaline and 5-hydroxytryptamine of nociceptive responses of cat dorsal horn neurones. *Brain Res* 145: 185-189
- Hellstrom J, Arvidsson U, Elde R, Cullheim S, Meister B 1999 Differential expression of nerve terminal protein isoforms in VAcHT-containing varicosities of the spinal cord ventral horn. *J Comp Neurol* 411: 578-590
- Hellstrom J, Oliveira AL, Meister B, Cullheim S 2003 Large cholinergic nerve terminals on subsets of motoneurons and their relation to muscarinic receptor type 2. *J Comp Neurol* 460: 476-486
- Herzog E, Landry M, Buhler E, Bouali-Benazzouz R, Legay C, Henderson CE, Nagy F, Dreyfus P, Giros B, El Mestikawy S 2004 Expression of vesicular glutamate transporters, VGLUT1 and VGLUT2, in cholinergic spinal motoneurons. *Eur J Neurosci* 20: 1752-1760
- Holstege JC, Kuypers HG 1987a Brainstem projections to lumbar motoneurons in rat-I. An ultrastructural study using autoradiography and the combination of autoradiography and horseradish peroxidase histochemistry. *Neuroscience* 21: 345-367
- Holstege JC, Kuypers HG 1987b Brainstem projections to spinal motoneurons: an update. *Neuroscience* 23: 809-821
- Hongo T, Jankowska E, Lundberg A 1969 The rubrospinal tract. II. Facilitation of interneuronal transmission in reflex paths to motoneurons. *Exp Brain Res* 7: 365-391
- Hongo T, Jankowska E, Lundberg A 1972a The rubrospinal tract. III. Effects on primary afferent terminals. *Exp Brain Res* 15: 39-53
- Hongo T, Jankowska E, Lundberg A 1972b The rubrospinal tract. IV. Effects on interneurons. *Exp Brain Res* 15: 54-78
- Hongo T, Pettersson LG 1988 Comments on group II excitation in hindlimb motoneurons in high and low spinal cats. *Neurosci Res* 5: 563-566

- Hoover JE, Durkovic RG 1992 Retrograde labeling of lumbosacral interneurons following injections of red and green fluorescent microspheres into hindlimb motor nuclei of the cat. *Somatosens Mot Res* 9: 211-226
- Houser CR, Crawford GD, Barber RP, Salvaterra PM, Vaughn JE 1983 Organization and morphological characteristics of cholinergic neurons: an immunocytochemical study with a monoclonal antibody to choline acetyltransferase. *Brain Res* 266: 97-119
- Huang A, Noga BR, Carr PA, Fedirchuk B, Jordan LM 2000 Spinal cholinergic neurons activated during locomotion: localization and electrophysiological characterization. *J Neurophysiol* 83: 3537-3547
- Hultborn H, Jankowska E, Lindstrom S 1971a Recurrent inhibition from motor axon collaterals of transmission in the Ia inhibitory pathway to motoneurons. *J Physiol* 215: 591-612
- Hultborn H, Jankowska E, Lindstrom S 1971b Recurrent inhibition of interneurons monosynaptically activated from group Ia afferents. *J Physiol* 215: 613-636
- Hultborn H, Jankowska E, Lindstrom S 1971c Relative contribution from different nerves to recurrent depression of Ia IPSPs in motoneurons. *J Physiol* 215: 637-664
- Hultborn H, Udo M 1972 Convergence in the reciprocal Ia inhibitory pathway of excitation from descending pathways and inhibition from motor axon collaterals. *Acta Physiol Scand* 84: 95-108
- Hultborn H, Santini M 1972 Supraspinal control of monosynaptically activated group Ia interneurons in the ventral horn. *Acta Physiol Scand* 84: 142-144
- Hultborn H, Illert M, Santini M 1976a Convergence on interneurons mediating the reciprocal Ia inhibition of motoneurons. I. Disynaptic Ia inhibition of Ia inhibitory interneurons. *Acta Physiol Scand* 96: 193-201
- Hultborn H, Illert M, Santini M 1976b Convergence on interneurons mediating the reciprocal Ia inhibition of motoneurons. II. Effects from segmental flexor reflex pathways. *Acta Physiol Scand* 96: 351-367
- Hultborn H, Illert M, Santini M 1976c Convergence on interneurons mediating the reciprocal Ia inhibition of motoneurons. III. Effects from supraspinal pathways. *Acta Physiol Scand* 96: 368-391
- Hultborn H 2006 Spinal reflexes, mechanisms and concepts: from Eccles to Lundberg and beyond. *Prog Neurobiol* 78: 215-232
- Ichikawa H, Deguchi T, Nakago T, Jacobowitz DM, Sugimoto T 1994 Parvalbumin, calretinin and carbonic anhydrase in the trigeminal and spinal primary neurons of the rat. *Brain Res* 655: 241-245
- Iles JF 1986 Reciprocal inhibition during agonist and antagonist contraction. *Exp Brain Res* 62: 212-214

- Iles JF, Pisini JV 1992 Cortical modulation of transmission in spinal reflex pathways of man. *J Physiol* 455: 425-446
- Ito T, Iino S, Nojyo Y 2005 A part of cholinergic fibers in mouse superior cervical ganglia contain GABA or glutamate. *Brain Res* 1046: 234-238
- Jankowska E, Lindstrom S 1972 Morphology of interneurons mediating Ia reciprocal inhibition of motoneurons in the spinal cord of the cat. *J Physiol* 226: 805-823
- Jankowska E, Padel Y, Tanaka R 1976 Disynaptic inhibition of spinal motoneurons from the motor cortex in the monkey. *J Physiol* 258: 467-487
- Jankowska E, Johannisson T, Lipski J 1981 Common interneurons in reflex pathways from group Ia and Ib afferents of ankle extensors in the cat. *J Physiol* 310: 381-402
- Jankowska E, McCrea DA 1983 Shared reflex pathways from Ib tendon organ afferents and Ia muscle spindle afferents in the cat. *J Physiol* 338: 99-111
- Jankowska E, Skoog B 1986 Labelling of midlumbar neurones projecting to cat hindlimb motoneurons by transneuronal transport of a horseradish peroxidase conjugate. *Neurosci Lett* 71: 163-168
- Jankowska E, Noga BR 1990 Contralaterally projecting lamina VIII interneurons in middle lumbar segments in the cat. *Brain Res* 535: 327-330
- Jankowska E 1992 Interneuronal relay in spinal pathways from proprioceptors. *Prog Neurobiol* 38: 335-378
- Jankowska E, Edgley S 1993 Interactions between pathways controlling posture and gait at the level of spinal interneurons in the cat. *Prog Brain Res* 97: 161-171
- Jankowska E, Riddell JS 1994 Interneurons in pathways from group II muscle afferents in sacral segments of the feline spinal cord. *J Physiol* 475: 455-468
- Jankowska E, Maxwell DJ, Dolk S, Krutki P, Belichenko PV, Dahlstrom A 1995 Contacts between serotonergic fibres and dorsal horn spinocerebellar tract neurons in the cat and rat: a confocal microscopic study. *Neuroscience* 67: 477-487
- Jankowska E, Hammar I, Djouhri L, Heden C, Szabo LZ, Yin XK 1997a Modulation of responses of four types of feline ascending tract neurons by serotonin and noradrenaline. *Eur J Neurosci* 9: 1375-1387
- Jankowska E, Maxwell DJ, Dolk S, Dahlstrom A 1997b A confocal and electron microscopic study of contacts between 5-HT fibres and feline dorsal horn interneurons in pathways from muscle afferents. *J Comp Neurol* 387: 430-438
- Jankowska E, Bichler E, Hammar I 2000a Areas of operation of interneurons mediating presynaptic inhibition in sacral spinal segments. *Exp Brain Res* 133: 402-406
- Jankowska E, Hammar I, Chojnicka B, Heden CH 2000b Effects of monoamines on interneurons in four spinal reflex pathways from group I and/or group II muscle afferents. *Eur J Neurosci* 12: 701-714

- Jankowska E 2001 Spinal interneuronal systems: identification, multifunctional character and reconfigurations in mammals. *J Physiol* 533: 31-40
- Jankowska E, Slawinska U, Hammar I 2002 Differential presynaptic inhibition of actions of group II afferents in di- and polysynaptic pathways to feline motoneurons. *J Physiol* 542: 287-299
- Jankowska E, Hammar I, Slawinska U, Maleszak K, Edgley SA 2003 Neuronal basis of crossed actions from the reticular formation on feline hindlimb motoneurons. *J Neurosci* 23: 1867-1878
- Jankowska E, Edgley SA, Krutki P, Hammar I 2005 Functional differentiation and organization of feline midlumbar commissural interneurons. *J Physiol* 565: 645-658
- Jankowska E, Stecina K, Cabaj A, Pettersson LG, Edgley SA 2006 Neuronal relays in double crossed pathways between feline motor cortex and ipsilateral hindlimb motoneurons. *J Physiol* 575: 527-541
- Jankowska E 2008 Spinal interneuronal networks in the cat: elementary components. *Brain Res Rev* 57: 46-55
- Jankowska E, Bannatyne BA, Stecina K, Hammar I, Cabaj A, Maxwell DJ 2009 Commissural interneurons with input from group I and II muscle afferents in feline lumbar segments: neurotransmitters, projections and target cells. *J Physiol* 587: 401-418
- Ji ZQ, Aas JE, Laake J, Walberg F, Ottersen OP 1991 An electron microscopic, immunogold analysis of glutamate and glutamine in terminals of rat spinocerebellar fibers. *J Comp Neurol* 307: 296-310
- Jones SL, Light AR 1990 Termination patterns of serotonergic medullary raphespinal fibers in the rat lumbar spinal cord: an anterograde immunohistochemical study. *J Comp Neurol* 297: 267-282
- Jones SL, Light AR 1992 Serotonergic medullary raphespinal projection to the lumbar spinal cord in the rat: a retrograde immunohistochemical study. *J Comp Neurol* 322: 599-610
- Jordan LM, McCrea DA, Steeves JD, Menzies JE 1977 Noradrenergic synapses and effects of noradrenaline on interneurons in the ventral horn of the cat spinal cord. *Can J Physiol Pharmacol* 55: 399-412
- Kanda K, Rymer WZ 1977 An estimate of the secondary spindle receptor afferent contribution to the stretch reflex in extensor muscles of the decerebrate cat. *J Physiol* 264: 63-87
- Kemplay SK, Webster KE 1986 A qualitative and quantitative analysis of the distributions of cells in the spinal cord and spinomedullary junction projecting to the thalamus of the rat. *Neuroscience* 17: 769-789
- Kevetter GA, Willis WD 1983 Collaterals of spinothalamic cells in the rat. *J Comp Neurol* 215: 453-464

- Kiehn O, Butt SJ 2003 Physiological, anatomical and genetic identification of CPG neurons in the developing mammalian spinal cord. *Prog Neurobiol* 70: 347-361
- Kiehn O 2006 Locomotor circuits in the mammalian spinal cord. *Annu Rev Neurosci* 29: 279-306
- Kjaerulff O, Kiehn O 1996 Distribution of networks generating and co-ordinating locomotor activity in the neonatal rat spinal cord in vitro: a lesion study. *J Neurosci* 16: 5777-5794
- Kremer E, Lev-Tov A 1997 Localization of the spinal network associated with generation of hindlimb locomotion in the neonatal rat and organization of its transverse coupling system. *J Neurophysiol* 77: 1155-1170
- Krutki P, Jankowska E, Edgley SA 2003 Are crossed actions of reticulospinal and vestibulospinal neurons on feline motoneurons mediated by the same or separate commissural neurons? *J Neurosci* 23: 8041-8050
- Kudo N, Yamada T 1987 N-methyl-D,L-aspartate-induced locomotor activity in a spinal cord-hindlimb muscles preparation of the newborn rat studied in vitro. *Neurosci Lett* 75: 43-48
- Kullander K, Butt SJ, Le Bret JM, Lundfald L, Restrepo CE, Rydstrom A, Klein R, Kiehn O 2003 Role of EphA4 and EphrinB3 in local neuronal circuits that control walking. *Science* 299: 1889-1892
- Laing I, Todd AJ, Heizmann CW, Schmidt HH 1994 Subpopulations of GABAergic neurons in laminae I-III of rat spinal dorsal horn defined by coexistence with classical transmitters, peptides, nitric oxide synthase or parvalbumin. *Neuroscience* 61: 123-132
- Lamotte dB, Ascher P 2008 Four excitatory postsynaptic ionotropic receptors coactivated at the motoneuron-Renshaw cell synapse. *J Neurosci* 28: 14121-14131
- Lanuza GM, Gosgnach S, Pierani A, Jessell TM, Goulding M 2004 Genetic identification of spinal interneurons that coordinate left-right locomotor activity necessary for walking movements. *Neuron* 42: 375-386
- Leah J, Menetrey D 1989 Neuropeptides in propriospinal neurones in the rat. *Brain Res* 495: 173-177
- Leblond H, Menard A, Gossard JP 2001 Corticospinal control of locomotor pathways generating extensor activities in the cat. *Exp Brain Res* 138: 173-184
- Li W, Ochalski PA, Brimijoin S, Jordan LM, Nagy JI 1995 C-terminals on motoneurons: electron microscope localization of cholinergic markers in adult rats and antibody-induced depletion in neonates. *Neuroscience* 65: 879-891
- Liang FY, Moret V, Wiesendanger M, Rouiller EM 1991 Corticomotoneuronal connections in the rat: evidence from double-labeling of motoneurons and corticospinal axon arborizations. *J Comp Neurol* 311: 356-366

- Lindh B, Aldskogius H, Hokfelt T 1989 Simultaneous immunohistochemical demonstration of intra-axonally transported markers and neuropeptides in the peripheral nervous system of the guinea pig. *Histochemistry* 92: 367-376
- Lindstrom S, Schomburg ED 1974 Group I inhibition in Ib excited ventral spinocerebellar tract neurones. *Acta Physiol Scand* 90: 166-185
- Lloyd DPC 1941 A direct central inhibitory action of dromically conducted impulses. *Journal of Neurophysiology* 4: 184-190
- Lomeli J, Quevedo J, Linares P, Rudomin P 1998 Local control of information flow in segmental and ascending collaterals of single afferents. *Nature* 395: 600-604
- Lundberg A, Voorhoeve P 1962 Effects from the pyramidal tract on spinal reflex arcs. *Acta Physiol Scand* 56: 201-219
- Lundberg A, Weight F 1971 Functional organization of connexions to the ventral spinocerebellar tract. *Exp Brain Res* 12: 295-316
- Lundberg A, Malmgren K, Schomburg ED 1975 Convergence from Lb, cutaneous and joint afferents in reflex pathways to motoneurons. *Brain Res* 87: 81-84
- Lundberg A, Malmgren K, Schomburg ED 1978 Role of joint afferents in motor control exemplified by effects on reflex pathways from Ib afferents. *J Physiol* 284: 327-343
- Lundberg A 1982 Inhibitory control from the brain stem of transmission from primary afferents to motoneurons, primary afferent terminals and ascending pathways. In: SJÖLUND B, BJÖRKLUND A: *Brain Stem Control of Spinal Mechanisms*. Elsevier Biomedical Press, Amsterdam, 179-225
- Lundberg A, Malmgren K, Schomburg ED 1987 Reflex pathways from group II muscle afferents. 1. Distribution and linkage of reflex actions to alpha-motoneurons. *Exp Brain Res* 65: 271-281
- Lundberg A, Malmgren K 1988 The dynamic sensitivity of Ib inhibition. *Acta Physiol Scand* 133: 123-124
- Mackie M, Hughes DI, Maxwell DJ, Tillakaratne NJ, Todd AJ 2003 Distribution and colocalisation of glutamate decarboxylase isoforms in the rat spinal cord. *Neuroscience* 119: 461-472
- Magnuson DS, Lovett R, Coffee C, Gray R, Han Y, Zhang YP, Burke DA 2005 Functional consequences of lumbar spinal cord contusion injuries in the adult rat. *J Neurotrauma* 22: 529-543
- Masson RL, Jr., Sparkes ML, Ritz LA 1991 Descending projections to the rat sacrocaudal spinal cord. *J Comp Neurol* 307: 120-130
- Matsushita M, Ikeda M, Hosoya Y 1979 The location of spinal neurons with long descending axons (long descending propriospinal tract neurons) in the cat: a study with the horseradish peroxidase technique. *J Comp Neurol* 184: 63-80

- Matsushita M, Hosoya Y 1979 Cells of origin of the spinocerebellar tract in the rat, studied with the method of retrograde transport of horseradish peroxidase. *Brain Res* 173: 185-200
- Matsuyama K, Mori S 1998 Lumbar interneurons involved in the generation of fictive locomotion in cats. *Ann N Y Acad Sci* 860: 441-443
- Matsuyama K, Jankowska E 2004 Coupling between feline cerebellum (fastigial neurons) and motoneurons innervating hindlimb muscles. *J Neurophysiol* 91: 1183-1192
- Matsuyama K, Nakajima K, Mori F, Aoki M, Mori S 2004 Lumbar commissural interneurons with reticulospinal inputs in the cat: morphology and discharge patterns during fictive locomotion. *J Comp Neurol* 474: 546-561
- Matsuyama K, Kobayashi S, Aoki M 2006 Projection patterns of lamina VIII commissural neurons in the lumbar spinal cord of the adult cat: an anterograde neural tracing study. *Neuroscience* 140: 203-218
- Matthews PBC 1972 *Mammalian Muscle Receptors and their Central Actions*. Arnold, London
- Mattson MP, Rychlik B, Chu C, Christakos S 1991 Evidence for calcium-reducing and excitoprotective roles for the calcium-binding protein calbindin-D28k in cultured hippocampal neurons. *Neuron* 6: 41-51
- Maxwell DJ, Leranath C, Verhofstad AA 1983 Fine structure of serotonin-containing axons in the marginal zone of the rat spinal cord. *Brain Res* 266: 253-259
- Maxwell DJ, Christie WM, Short AD, Brown AG 1990 Direct observations of synapses between GABA-immunoreactive boutons and muscle afferent terminals in lamina VI of the cat's spinal cord. *Brain Res* 530: 215-222
- Maxwell DJ, Jankowska E 1996 Synaptic relationships between serotonin-immunoreactive axons and dorsal horn spinocerebellar tract cells in the cat spinal cord. *Neuroscience* 70: 247-253
- Maxwell DJ, Kerr R, Jankowska E, Riddell JS 1997 Synaptic connections of dorsal horn group II spinal interneurons: synapses formed with the interneurons and by their axon collaterals. *J Comp Neurol* 380: 51-69
- Maxwell DJ, Riddell JS 1999 Axoaxonic synapses on terminals of group II muscle spindle afferent axons in the spinal cord of the cat. *Eur J Neurosci* 11: 2151-2159
- Maxwell DJ, Riddell JS, Jankowska E 2000 Serotonergic and noradrenergic axonal contacts associated with premotor interneurons in spinal pathways from group II muscle afferents. *Eur J Neurosci* 12: 1271-1280
- McCrea DA 2001 Spinal circuitry of sensorimotor control of locomotion. *J Physiol* 533: 41-50
- McCrea DA, Rybak IA 2008 Organization of mammalian locomotor rhythm and pattern generation. *Brain Res Rev* 57: 134-146

- McIntire SL, Reimer RJ, Schuske K, Edwards RH, Jorgensen EM 1997 Identification and characterization of the vesicular GABA transporter. *Nature* 389: 870-876
- Mentis GZ, Alvarez FJ, Bonnot A, Richards DS, Gonzalez-Forero D, Zerda R, O'Donovan MJ 2005 Noncholinergic excitatory actions of motoneurons in the neonatal mammalian spinal cord. *Proc Natl Acad Sci U S A* 102: 7344-7349
- Mentis GZ, Siembab VC, Zerda R, O'Donovan MJ, Alvarez FJ 2006 Primary afferent synapses on developing and adult Renshaw cells. *J Neurosci* 26: 13297-13310
- Miles GB, Hartley R, Todd AJ, Brownstone RM 2007 Spinal cholinergic interneurons regulate the excitability of motoneurons during locomotion. *Proc Natl Acad Sci U S A* 104: 2448-2453
- Miller KE, Douglas VD, Richards AB, Chandler MJ, Foreman RD 1998 Propriospinal neurons in the C1-C2 spinal segments project to the L5-S1 segments of the rat spinal cord. *Brain Res Bull* 47: 43-47
- Mockel V, Fischer G 1994 Vulnerability to excitotoxic stimuli of cultured rat hippocampal neurons containing the calcium-binding proteins calretinin and calbindin D28K. *Brain Res* 648: 109-120
- Mori S, Matsuyama K, Mori F, Nakajima K 2001 Supraspinal sites that induce locomotion in the vertebrate central nervous system. *Adv Neurol* 87: 25-40
- Morona R, Lopez JM, Gonzalez A 2006 Calbindin-D28k and calretinin immunoreactivity in the spinal cord of the lizard *Gekko gekko*: Colocalization with choline acetyltransferase and nitric oxide synthase. *Brain Res Bull* 69: 519-534
- Nagy GG, Al Ayyan M, Andrew D, Fukaya M, Watanabe M, Todd AJ 2004 Widespread expression of the AMPA receptor GluR2 subunit at glutamatergic synapses in the rat spinal cord and phosphorylation of GluR1 in response to noxious stimulation revealed with an antigen-unmasking method. *J Neurosci* 24: 5766-5777
- Nagy JI, Yamamoto T, Jordan LM 1993 Evidence for the cholinergic nature of C-terminals associated with subsurface cisterns in alpha-motoneurons of rat. *Synapse* 15: 17-32
- Nahin RL, Micevych PE 1986 A long ascending pathway of enkephalin-like immunoreactive spinoreticular neurons in the rat. *Neurosci Lett* 65: 271-276
- Nahin RL, Madsen AM, Giesler GJ, Jr. 1986 Funicular location of the ascending axons of neurons adjacent to the spinal cord central canal in the rat. *Brain Res* 384: 367-372
- Nielsen J, Petersen N, Deuschl G, Ballegaard M 1993 Task-related changes in the effect of magnetic brain stimulation on spinal neurones in man. *J Physiol* 471: 223-243
- Nishimaru H, Restrepo CE, Ryge J, Yanagawa Y, Kiehn O 2005 Mammalian motor neurons corelease glutamate and acetylcholine at central synapses. *Proc Natl Acad Sci U S A* 102: 5245-5249

- Noga BR, Shefchyk SJ, Jamal J, Jordan LM 1987 The role of Renshaw cells in locomotion: antagonism of their excitation from motor axon collaterals with intravenous mecamylamine. *Exp Brain Res* 66: 99-105
- Noga BR, Kriellaars DJ, Brownstone RM, Jordan LM 2003 Mechanism for activation of locomotor centers in the spinal cord by stimulation of the mesencephalic locomotor region. *J Neurophysiol* 90: 1464-1478
- Oliveira AL, Hydling F, Olsson E, Shi T, Edwards RH, Fujiyama F, Kaneko T, Hokfelt T, Cullheim S, Meister B 2003 Cellular localization of three vesicular glutamate transporter mRNAs and proteins in rat spinal cord and dorsal root ganglia. *Synapse* 50: 117-129
- Ornung G, Shupliakov O, Ottersen OP, Storm-Mathisen J, Cullheim S 1994 Immunohistochemical evidence for coexistence of glycine and GABA in nerve terminals on cat spinal motoneurons: an ultrastructural study. *Neuroreport* 5: 889-892
- Ornung G, Shupliakov O, Linda H, Ottersen OP, Storm-Mathisen J, Ulfhake B, Cullheim S 1996 Qualitative and quantitative analysis of glycine- and GABA-immunoreactive nerve terminals on motoneuron cell bodies in the cat spinal cord: a postembedding electron microscopic study. *J Comp Neurol* 365: 413-426
- Ornung G, Ottersen OP, Cullheim S, Ulfhake B 1998 Distribution of glutamate-, glycine- and GABA-immunoreactive nerve terminals on dendrites in the cat spinal motor nucleus. *Exp Brain Res* 118: 517-532
- Ottersen OP, Storm-Mathisen J 1985 Different neuronal localization of aspartate-like and glutamate-like immunoreactivities in the hippocampus of rat, guinea-pig and Senegalese baboon (*Papio papio*), with a note on the distribution of gamma-aminobutyrate. *Neuroscience* 16: 589-606
- Pauvert V, Pierrot-Deseilligny E, Rothwell JC 1998 Role of spinal premotoneurons in mediating corticospinal input to forearm motoneurons in man. *J Physiol* 508: 301-312
- Peng YY, Frank E 1989 Activation of GABAB-b receptors causes presynaptic inhibition at synapses between muscle spindle afferents and motoneurons in the spinal cord of bullfrogs. *J Neurosci* 9: 1502-1515
- Phelps PE, Barber RP, Houser CR, Crawford GD, Salvaterra PM, Vaughn JE 1984 Postnatal development of neurons containing choline acetyltransferase in rat spinal cord: an immunocytochemical study. *J Comp Neurol* 229: 347-361
- Polgar E, Watanabe M, Hartmann B, Grant SG, Todd AJ 2008 Expression of AMPA receptor subunits at synapses in laminae I-III of the rodent spinal dorsal horn. *Mol Pain* 4: 5
- Pratt CA, Jordan LM 1987 Ia inhibitory interneurons and Renshaw cells as contributors to the spinal mechanisms of fictive locomotion. *J Neurophysiol* 57: 56-71
- Puskar Z, Antal M 1997 Localization of last-order premotor interneurons in the lumbar spinal cord of rats. *J Comp Neurol* 389: 377-389

- Quevedo J, Stecina K, Gosgnach S, McCrea DA 2005a Stumbling corrective reaction during fictive locomotion in the cat. *J Neurophysiol* 94: 2045-2052
- Quevedo J, Stecina K, McCrea DA 2005b Intracellular analysis of reflex pathways underlying the stumbling corrective reaction during fictive locomotion in the cat. *J Neurophysiol* 94: 2053-2062
- Reed WR, Shum-Siu A, Onifer SM, Magnuson DS 2006 Inter-enlargement pathways in the ventrolateral funiculus of the adult rat spinal cord. *Neuroscience* 142: 1195-1207
- Ren K, Ruda MA, Jacobowitz DM 1993 Immunohistochemical localization of calretinin in the dorsal root ganglion and spinal cord of the rat. *Brain Res Bull* 31: 13-22
- Ren K, Ruda MA 1994 A comparative study of the calcium-binding proteins calbindin-D28K, calretinin, calmodulin and parvalbumin in the rat spinal cord. *Brain Res Brain Res Rev* 19: 163-179
- Renshaw B 1946 Central Effects of Centripetal Impulses in Axons of Spinal Ventral Roots. *Journal of Neurophysiology* 9: 191-204
- Resibois A, Rogers JH 1992 Calretinin in rat brain: an immunohistochemical study. *Neuroscience* 46: 101-134
- Riddell JS, Jankowska E, Huber J 1995 Organization of neuronal systems mediating presynaptic inhibition of group II muscle afferents in the cat. *J Physiol* 483: 443-460
- Ridet JL, Rajaofetra N, Teilhac JR, Geffard M, Privat A 1993 Evidence for nonsynaptic serotonergic and noradrenergic innervation of the rat dorsal horn and possible involvement of neuron-glia interactions. *Neuroscience* 52: 143-157
- Rivero-Melian C, Rosario C, Grant G 1992 Demonstration of transganglionically transported cholera toxin in rat spinal cord by immunofluorescence cytochemistry. *Neurosci Lett* 145: 114-117
- Robbins A, Pfaff DW, Schwartz-Giblin S 1992 Reticulospinal and reticuloreticular pathways for activating the lumbar back muscles in the rat. *Exp Brain Res* 92: 46-58
- Rogers JH, Resibois A 1992 Calretinin and calbindin-D28k in rat brain: patterns of partial co-localization. *Neuroscience* 51: 843-865
- Rousseau F, Aubrey KR, Supplisson S 2008 The glycine transporter GlyT2 controls the dynamics of synaptic vesicle refilling in inhibitory spinal cord neurons. *J Neurosci* 28: 9755-9768
- Rudomin P, Schmidt RF 1999 Presynaptic inhibition in the vertebrate spinal cord revisited. *Exp Brain Res* 129: 1-37
- Rustioni A, Weinberg R 1989 The somatosensory system. In: Bjorklund A, Hokfelt T, Swanson L: *Handbook of chemical neuroanatomy*. Elsevier, Amsterdam, 219-320
- Sakata-Haga H, Kanemoto M, Maruyama D, Hoshi K, Mogi K, Narita M, Okado N, Ikeda Y, Nogami H, Fukui Y, Kojima I, Takeda J, Hisano S 2001 Differential localization and

- colocalization of two neuron-types of sodium-dependent inorganic phosphate cotransporters in rat forebrain. *Brain Res* 902: 143-155
- Sandler R, Smith AD 1991 Coexistence of GABA and glutamate in mossy fiber terminals of the primate hippocampus: an ultrastructural study. *J Comp Neurol* 303: 177-192
- Scheibel ME, Scheibel AB 1966 Terminal axonal patterns in cat spinal cord. I. The lateral corticospinal tract. *Brain Res* 2: 333-350
- Schneider SP, Fyffe RE 1992 Involvement of GABA and glycine in recurrent inhibition of spinal motoneurons. *J Neurophysiol* 68: 397-406
- Schomburg ED, Steffens H 1988 The effect of DOPA and clonidine on reflex pathways from group II muscle afferents to alpha-motoneurons in the cat. *Exp Brain Res* 71: 442-446
- Schwaller B, Meyer M, Schiffmann S 2002 'New' functions for 'old' proteins: the role of the calcium-binding proteins calbindin D-28k, calretinin and parvalbumin, in cerebellar physiology. Studies with knockout mice. *Cerebellum* 1: 241-258
- Segovia G, Porras A, Del Arco A, Mora F 2001 Glutamatergic neurotransmission in aging: a critical perspective. *Mech Ageing Dev* 122: 1-29
- Shefchyk S, McCrea D, Kriellaars D, Fortier P, Jordan L 1990 Activity of interneurons within the L4 spinal segment of the cat during brainstem-evoked fictive locomotion. *Exp Brain Res* 80: 290-295
- Shefchyk SJ, Jordan LM 1985 Excitatory and inhibitory postsynaptic potentials in alpha-motoneurons produced during fictive locomotion by stimulation of the mesencephalic locomotor region. *J Neurophysiol* 53: 1345-1355
- Sherriff FE, Henderson Z 1994 A cholinergic propriospinal innervation of the rat spinal cord. *Brain Res* 634: 150-154
- Shupliakov O, Ornung G, Brodin L, Ulfhake B, Ottersen OP, Storm-Mathisen J, Cullheim S 1993 Immunocytochemical localization of amino acid neurotransmitter candidates in the ventral horn of the cat spinal cord: a light microscopic study. *Exp Brain Res* 96: 404-418
- Skinner RD, Coulter JD, Adams RJ, Rempel RS 1979 Cells of origin of long descending propriospinal fibers connecting the spinal enlargements in cat and monkey determined by horseradish peroxidase and electrophysiological techniques. *J Comp Neurol* 188: 443-454
- Stokke MF, Nissen UV, Glover JC, Kiehn O 2002 Projection patterns of commissural interneurons in the lumbar spinal cord of the neonatal rat. *J Comp Neurol* 446: 349-359
- Stone LS, Broberger C, Vulchanova L, Wilcox GL, Hokfelt T, Riedl MS, Elde R 1998 Differential distribution of alpha2A and alpha2C adrenergic receptor immunoreactivity in the rat spinal cord. *J Neurosci* 18: 5928-5937
- Taal W, Holstege JC 1994 GABA and glycine frequently colocalize in terminals on cat spinal motoneurons. *Neuroreport* 5: 2225-2228

- Terro F, Yardin C, Esclaire F, Ayer-Lelievre C, Hugon J 1998 Mild kainate toxicity produces selective motoneuron death with marked activation of Ca²⁺-permeable AMPA/kainate receptors. *Brain Res* 809: 319-324
- Todd AJ, Sullivan AC 1990 Light microscope study of the coexistence of GABA-like and glycine-like immunoreactivities in the spinal cord of the rat. *J Comp Neurol* 296: 496-505
- Todd AJ 1991 Immunohistochemical evidence that acetylcholine and glycine exist in different populations of GABAergic neurons in lamina III of rat spinal dorsal horn. *Neuroscience* 44: 741-746
- Todd AJ, Spike RC, Price RF, Neilson M 1994 Immunocytochemical evidence that neurotensin is present in glutamatergic neurons in the superficial dorsal horn of the rat. *J Neurosci* 14: 774-784
- Todd AJ, Hughes DI, Polgar E, Nagy GG, Mackie M, Ottersen OP, Maxwell DJ 2003 The expression of vesicular glutamate transporters VGLUT1 and VGLUT2 in neurochemically defined axonal populations in the rat spinal cord with emphasis on the dorsal horn. *Eur J Neurosci* 17: 13-27
- Tracey DJ 1995 Ascending and descending pathways in the spinal cord. In: Paxinos G: *The rat nervous system*. London: Academic Press, San Diego, 67-80
- Valtschanoff JG, Weinberg RJ, Rustioni A 1993 Amino acid immunoreactivity in cortico-spinal terminals. *Exp Brain Res* 93: 95-103
- Varoqui H, Schafer MK, Zhu H, Weihe E, Erickson JD 2002 Identification of the differentiation-associated Na⁺/PI transporter as a novel vesicular glutamate transporter expressed in a distinct set of glutamatergic synapses. *J Neurosci* 22: 142-155
- Villanueva L, de Pommery J, Menetrey D, Le Bars D 1991 Spinal afferent projections to subnucleus reticularis dorsalis in the rat. *Neurosci Lett* 134: 98-102
- Watson AH, Bazzaz AA 2001 GABA and glycine-like immunoreactivity at axoaxonic synapses on 1a muscle afferent terminals in the spinal cord of the rat. *J Comp Neurol* 433: 335-348
- Weber I, Veress G, Szucs P, Antal M, Birinyi A 2007 Neurotransmitter systems of commissural interneurons in the lumbar spinal cord of neonatal rats. *Brain Res* 1178: 65-72
- Welton J, Stewart W, Kerr R, Maxwell DJ 1999 Differential expression of the muscarinic m2 acetylcholine receptor by small and large motoneurons of the rat spinal cord. *Brain Res* 817: 215-219
- Wheatley M, Jovanovic K, Stein RB, Lawson V 1994 The activity of interneurons during locomotion in the in vitro necturus spinal cord. *J Neurophysiol* 71: 2025-2032
- Wilson JM, Rempel J, Brownstone RM 2004 Postnatal development of cholinergic synapses on mouse spinal motoneurons. *J Comp Neurol* 474: 13-23

- Wilson VJ, Kato M 1965 Excitation of extensor motoneurons by group II afferent fibres in ipsilateral muscle nerves. *J Neurophysiol* 28: 545-554
- Windhorst U 1996 On the role of recurrent inhibitory feedback in motor control. *Prog Neurobiol* 49: 517-587
- Wojcik SM, Katsurabayashi S, Guillemin I, Friauf E, Rosenmund C, Brose N, Rhee JS 2006 A shared vesicular carrier allows synaptic corelease of GABA and glycine. *Neuron* 50: 575-587
- Yamada J, Shirao K, Kitamura T, Sato H 1991 Trajectory of spinocerebellar fibers passing through the inferior and superior cerebellar peduncles in the rat spinal cord: a study using horseradish peroxidase with pedunculotomy. *J Comp Neurol* 304: 147-160
- Yang JF, Stein RB 1990 Phase-dependent reflex reversal in human leg muscles during walking. *J Neurophysiol* 63: 1109-1117
- Yates BJ, Kasper J, WILSON VJ 1989 Effects of muscle and cutaneous hindlimb afferents on L4 neurons whose activity is modulated by neck rotation. *Exp Brain Res* 77: 48-56
- Yingcharoen K, Rinvik E, Storm-Mathisen J, Ottersen OP 1989 GABA, glycine, glutamate, aspartate and taurine in the perihypoglossal nuclei: an immunocytochemical investigation in the cat with particular reference to the issue of amino acid colocalization. *Exp Brain Res* 78: 345-357

Publications

CHOLINERGIC TERMINALS IN THE VENTRAL HORN OF ADULT RAT AND CAT: EVIDENCE THAT GLUTAMATE IS A COTRANSMITTER AT PUTATIVE INTERNEURON SYNAPSES BUT NOT AT CENTRAL SYNAPSES OF MOTONEURONS

T. T. LIU,^a B. A. BANNATYNE,^a E. JANKOWSKA^b AND D. J. MAXWELL^{a*}

^aSpinal Cord Group, Neuroscience and Molecular Pharmacology, Faculty of Biomedical and Life Sciences, University of Glasgow, Glasgow G12 8QQ, UK

^bDepartment of Physiology, Göteborg University, 405 30 Göteborg, Sweden

Abstract—Until recently it was generally accepted that the only neurotransmitter to be released at central synapses of somatic motoneurons was acetylcholine. However, studies on young mice (P0–10) have provided pharmacological evidence indicating that glutamate may act as a cotransmitter with acetylcholine at synapses between motoneurons and Renshaw cells. We performed a series of anatomical experiments on axon collaterals obtained from intracellularly labeled motoneurons from an adult cat and labeled by retrograde transport in adult rats to determine if glutamate is co-localized with acetylcholine by these terminals. We could find no evidence for the presence of vesicular glutamate transporters in motoneuron axon terminals of either species. In addition, we were unable to establish any obvious relationship between motoneuron terminals and the R2 subunit of the AMPA receptor (GluR2). However we did observe a population of cholinergic terminals in lamina VII which did not originate from motoneurons but were immunoreactive for the vesicular glutamate transporter 2 and formed appositions to GluR2 subunits. These were smaller than motoneuron terminals and, unlike them, formed no relationship with Renshaw cells. The evidence suggests that glutamate does not act as a cotransmitter with acetylcholine at central synapses of motoneurons in the adult cat and rat. However, glutamate is present in a population of cholinergic terminals which probably originate from interneurons where its action is via an AMPA receptor. © 2009 IBRO. Published by Elsevier Ltd. All rights reserved.

Key words: spinal cord, motor control, Renshaw cell, acetylcholine, immunocytochemistry.

The assertion that acetylcholine (ACh) is the only neurotransmitter released at both central and peripheral syn-

*Corresponding author. Tel: +44-0141-330-6455; fax: +44-141-330-2868.

E-mail address: d.maxwell@bio.gla.ac.uk (D. J. Maxwell).

Abbreviations: ACh, acetylcholine; CTb, B-subunit of cholera toxin; DAB, 3,3'-diaminobenzidine; GluR2, R2 subunit of the AMPA receptor; HRP, horseradish peroxidase; NOS, nitric oxide synthase; PB, phosphate buffer; PBS, phosphate-buffered saline; PBST, phosphate-buffered saline Triton; TSA, tyramide signal amplification; VAcHT, vesicular acetylcholine transporter; VGLUT, vesicular glutamate transporter.

0306-4522/09 \$ - see front matter © 2009 IBRO. Published by Elsevier Ltd. All rights reserved.
doi:10.1016/j.neuroscience.2009.03.034

apses of somatic motoneurons (e.g. Eccles et al., 1954; Curtis and Ryall, 1964; Windhorst, 1996) has been challenged recently (Herzog et al., 2004; Mentis et al., 2005; Nishimaru et al., 2005). It has been known for many years that the activation of Renshaw cells evoked by stimulation of motoneuron axon collaterals could not be totally blocked by cholinergic antagonists (Eccles et al., 1954; Noga et al., 1987; Schneider et al., 1992; Dourado et al., 2002) and pharmacological studies, using *in vitro* preparations of young (P0–4) mouse spinal cord, show that this activation can be abolished by application of both cholinergic and glutamatergic antagonists (Mentis et al., 2005; Nishimaru et al., 2005). Recently, Lamotte d'Incamps and Ascher (2008) confirmed that the glutamatergic component of this response is mediated by AMPA and NMDA receptors in P5–10 mice. However anatomical evidence supporting a role for glutamate as a cotransmitter with ACh is inconsistent in adult and young animals. Herzog et al. (2004) provided evidence that in adult rats, motoneurons express mRNA for both vesicular glutamate transporters 1 and 2 (VGLUT1; VGLUT2), a finding that is in conflict with previous reports of absence of mRNA for any of the three known VGLUTs in motoneurons (Kullander et al., 2003; Oliveira et al., 2003). Immunocytochemical studies have also produced conflicting evidence. Nishimaru et al. (2005), were unable to detect the presence of VGLUT1 or VGLUT3 in motoneuron axon collaterals but found some evidence for VGLUT2 co-localization, but curiously only three cholinergic terminals (labeled with the vesicular cholinergic transporter, VAcHT) in this region out of a sample of more than a thousand were positively labeled for VGLUT2. To some extent this is consistent with findings reported by Herzog et al. (2004) who proposed that VAcHT and VGLUT2 were not co-localized in the same terminals but that individual collateral branches of motoneurons contained either one or the other. Conversely, Mentis et al. (2005) reported the absence of immunoreactivity for any of the VGLUTs in motoneuron axon collaterals but nevertheless concluded that some terminals may be enriched with glutamate.

In summary, it seems that there is good pharmacological evidence to suggest that glutamate may be coreleased along with ACh at synapses formed between motoneurons and Renshaw cells in very young mice but anatomical evidence supporting this is inconsistent. We performed a series of anatomical studies in the adult cat and rat to determine if there was evidence to support the hypothesis

that glutamate is co-localized in axon collaterals of mature animals and operates via an AMPA receptor. There were two principal aims of the study: (1) to determine if axon collaterals of adult motoneurons contain VGLUTs; (2) to determine if axon collaterals of adult motoneurons are apposed to AMPA receptors. During the course of this study we identified a group of cholinergic axon terminals in the ventral horn that did not originate from motoneurons but contained VGLUT2 and apposed AMPA receptors.

EXPERIMENTAL PROCEDURES

Experiments were performed on three adult rats (250–350 g; 10–14 weeks old Harlan, Bicester, UK) and one adult cat (3.6 kg; 6 months old) which was bred at the University of Göteborg. Rat experiments were conducted according to British Home Office legislation and were approved by the University of Glasgow Ethics Committee. The cat experiment was conducted according to NIH guidelines and was approved by the Göteborg University Ethics Committee. All necessary steps were taken to minimize suffering and the number of animals used.

Cat experiment

The cat was deeply anaesthetized with sodium pentobarbital (40–44 mg/kg i.p.) and supplemented with intermittent doses of α -chloralose as required to maintain full anaesthesia (Rhône-Poulenc, Santé, France; doses of 5 mg/kg administered every 1–2 h, up to 55 mg/kg i.v.). A laminectomy was performed to expose lumbar (L4–L7) segments of the spinal cord. Motoneurons were searched for in L6–L7 segments and identified on the basis of antidromic activation following stimulation of gastrocnemius and soleus nerves. Following identification, motoneurons were labeled intracellularly with a mixture of equal parts of 2% tetramethylrhodamine-dextran (Molecular Probes, Inc., Eugene, OR, USA) and 2% neurobiotin (Vector, UK) in saline (pH 6.5). The marker was injected by passing depolarizing constant current 100–140 nA for 5–8 min. New injection sites were a minimum of 2 mm away from previous sites. At the conclusion of the experiment, the animal was given a lethal dose of pentobarbital and perfused, initially with physiological saline, and subsequently with paraformaldehyde (4%) in 0.1 M phosphate buffer (PB) (pH 7.4). Lumbar segments of the spinal cord containing labeled cells were removed and placed in the same fixative for 8 h at 4 °C. Axon collaterals from an intracellularly labeled excitatory interneuron (e.g. see Bannatyne et al., 2006) were obtained from the same animal for control material.

Rat experiments

Three Sprague–Dawley rats were deeply anaesthetized with halothane and the left sciatic nerve was exposed under strict aseptic conditions. A micropipette containing a 1% solution of the B-subunit of cholera toxin (CTb; Sigma-Aldrich, Co., Poole, UK) in sterile distilled water was inserted into the perineurium and 3–4 μ l of this solution were pressure injected into the nerve. Following 3–5 days of survival, the rats were anaesthetized with pentobarbitone (1 ml i.p.) and perfused through the left ventricle with saline followed by a fixative containing 4% formaldehyde in 0.1 M PB pH 7.4. L3 to L5 spinal cord segments were removed from each animal and post-fixed in the same fixative for 2–8 h at 4 °C. Segments were then cut into two blocks.

The L7 segment of the cat and L3–L5 segments of rats were rinsed several times in 0.1 M PB. All the segments were cut into 50 μ m thick transverse sections with a vibratome (Oxford Instruments, Technical Products International, Inc., USA) and sections of cat segments were collected in strict serial order to enable reconstruction of labeled cells. All sections were treated with an

aqueous solution of 50% ethanol for 30 min to enhance antibody penetration. Following this treatment, cat sections were mounted in serial order on glass slides with Vectashield (Vector Laboratories, Peterborough, UK) and examined with a fluorescence microscope. Sections containing labeled motoneurons were reacted firstly with avidin–rhodamine (1:1000; Jackson ImmunoResearch, Luton, UK) and photographed with a digital camera attached to a fluorescent microscope. Sections containing labeled motoneuron axon terminals were then selected for further analysis.

Aim 1: do adult motoneuron axon collateral terminals contain VGLUTs?

Sections were incubated in the combinations of primary antibodies listed in Table 1. All antibodies were diluted in phosphate-buffered saline containing 0.3% Triton X-100 (PBST) and incubated for 48 h. They were rinsed in phosphate-buffered saline (PBS) and incubated for 3 h in solutions of secondary antibodies coupled to fluorophores before mounting with anti-fade medium (see Table 1 for details).

Sections containing axon terminals from the three labeled cat motoneurons were reacted with guinea-pig anti-VGLUT1 and rabbit anti-VGLUT2. Motoneuron terminals obtained from rat experiments were identified by the presence of transported CTb from sciatic nerve injections (see above) which was co-localized with immunoreactivity for VACHT. Triple immunofluorescence was performed initially with VGLUT1, -2 and -3 antibodies (groups A, B and C in Table 1). Also, as some cholinergic interneurons contain nitric oxide synthase (NOS; Miles et al., 2007), we attempted to determine if any cholinergic axons that were positive for VGLUT2 (see below) originate from this source by reacting tissue with a combination of anti-NOS, anti-VACHT and anti-VGLUT2 antibodies (group D in Table 1).

As motoneuron axon collaterals are known to form synapses with Renshaw cells and calbindin is thought to be a reliable marker for Renshaw cells (Carr et al., 1998; Alvarez et al., 1999), rat sections containing labeled collaterals were reacted with CTb and calbindin antisera along with one of the following: antibodies: VGLUT1 (group E), VGLUT2 (group F), or VACHT (group G). We performed sequential immunocytochemistry on sections from groups F and G. When analysis of sections with these initial combinations was complete, sections were re-incubated with a fourth antibody: goat anti-VACHT antibody (for group F) or guinea-pig anti-VGLUT1 (for group G). The sections were remounted and the same field that had been scanned previously was identified and scanned again. By comparing labeling before and after the re-incubation in the VGLUT1 or VACHT antiserum, we could detect the additional staining, which represents immunoreactivity for VACHT and VGLUT1 in groups F and G, respectively.

Aim 2: are axon collaterals of adult motoneurons apposed to AMPA receptors?

An antigen unmasking method was used to reveal whether AMPA receptors subunits are associated with labeled motoneuron terminals. Sections containing axon collaterals from three motoneurons and one interneuron were processed. Pepsin treatment was performed by incubating sections at 37 °C for 30 min in PBST, followed by 10 min in 0.2 M HCl containing 1 mg/ml pepsin (Dako, Glostrup, Denmark) with continuous agitation. After rinsing, sections were incubated in a mouse anti-R2 subunit of the AMPA receptor (GluR2) antibody (1:300; Chemicon, Harlow, UK) for 72 h at 4 °C. Sections were then incubated in a species-specific donkey secondary antibody conjugated to Alexa488 (1:500; Molecular Probes) for 24 h.

Cholinergic terminals in rat tissue were examined to determine if they form associations with the GluR2 subunit of AMPA receptors. As GluR2 subunits are present in 98% AMPA-containing synapses in the rat spinal cord (Nagy et al., 2004), this subunit

Table 1. Summary of primary and secondary antibody combinations and concentrations used in the current study

	Primary antibody combination	Primary antibody concentration	Supplier	Secondary antibodies	Sequential immuno-reaction	Secondary antibodies
Cat	gp VGLUT1	1:5000	Chemicon	Cy-5		
	rbt VGLUT2	1:5000	Chemicon	Alexa488		
Rat	mo. CTb	1:250	A. Wikström, University of Gothenburg	Rh. Red		
	gt. VACHT	1:5000	Millipore, USA	Alexa488		
A	gp VGLUT1	1:5000		Cy-5		
	mo. CTb	1:250		Rh. Red		
B	gt. VACHT	1:5000		Alexa488		
	gp VGLUT2	1:5000	Chemicon	Cy-5		
C	mo. CTb	1:250		Rh. Red		
	gt. VACHT	1:5000		Alexa488		
D	gp VGLUT3	1:5000	Chemicon	Cy-5		
	shp NOS	1:2000	P. Emson, University of Cambridge	Rh. Red		
E	gp VACHT	1:5000	Millipore	Alexa488		
	rbt VGLUT2	1:5000	Chemicon	Cy-5		
F	mo. CTb	1:250		Rh. Red		
	gp VGLUT1	1:5000		Alexa488	gt. VACHT	Cy-5
G	rbt CB	1:2000	Swant, Bellizona, Switzerland	Cy-5		
	mo. CTb	1:250		Rh. Red		
G	gp VGLUT2	1:5000		Alexa488		
	rbt CB	1:2000		Cy-5	gp VGLUT1	Cy-5

All secondary antibodies were raised in donkey and conjugated to Rhodamine Red (Rh. Red; 1:100), Cyanine 5.18 (Cy-5; 1:100; both supplied by Jackson ImmunoResearch) and Alexa-fluor 488 (Alexa488; 1:500; Molecular Probes). CB; calbindin, gp, guinea pig; gt., goat; mo, mouse; rbt, rabbit; shp, sheep.

can be used as a general marker for this class of receptor. Before applying the antigen unmasking method to expose GluR2 subunits as described above, sections from three rats were incubated in goat anti-VACHT antibody (1:50,000) for 72 h and then subjected to a tyramide signal amplification (TSA) reaction in order to preserve labeling for VACHT following pepsin treatment. Sections were initially incubated for 4 h in anti-goat horseradish peroxidase (HRP; 1:500; Jackson ImmunoResearch, West Grove, PA, USA). The sections were then rinsed and processed with a tetramethylrhodamine fluorophore (diluted 1:50 in amplification diluent; PerkinElmer Life Sciences, Boston, MA, USA) for 7 min (see Nagy et al., 2004 for details). Sections were rinsed, treated with pepsin, and incubated for 72 h in mouse anti-GluR2 (1:300), followed by 24 h in a species-specific donkey secondary antibody conjugated to Alexa 488 (1:500). We also performed a control experiment to determine the association between glutamatergic boutons and GluR2 subunits. Sections from three rats were incubated for 72 h in a combination of guinea pig anti-VGLUT1 (1:50,000) and guinea pig anti-VGLUT2 (1:50,000) antibodies. The sections were rinsed and placed in anti-guinea pig HRP (1:500; Jackson ImmunoResearch, West Grove, PA, USA) for 4 h. They were processed according to the TSA and pepsin treatment described above and incubated in mouse anti-GluR2 (1:300).

Confocal microscopy and analysis

All sections were mounted in a glycerol-based antifade medium (Vectashield, Vector Laboratories) and examined with a Bio-Rad MRC 1024 confocal laser scanning microscope (Bio-Rad, Hemel Hempstead, UK).

Cat sections with VGLUT markers were scanned by using a $\times 60$ oil-immersion lens at a zoom factor of 3.5 and at 0.5 μm steps in the z-axis, while sections with GluR2 staining were examined with a $\times 60$ oil-immersion lens at a zoom factor of 2 and at 0.2 μm steps in the z-axis. Image stacks were analyzed with

NeuroLucida for Confocal software (MBF Bioscience, Colchester, VT, USA). To avoid bias, all labeled motoneuron axon terminals and VGLUT markers (or GluR2 immunoreactivity) were viewed in individual channels for every single optical section initially and then examined in merged image stacks showing all three (or two) channels by switching between different channels. When scanning of immunoreactive boutons was complete, the sections were retrieved from the slides and rinsed in PBS. These sections together with the other sections containing soma and axons of labeled motoneurons were reacted with avidin–biotin–peroxidase complex technique (ABC technique). This involved an overnight incubation in a fresh solution of avidin–biotin–complex (Vector Laboratories, Ltd.) followed by a further rinse with PBS then PB. The sections were then placed in a solution containing hydrogen peroxide plus 3,3'-diaminobenzidine (DAB; Sigma, Dorset, UK) diluted in PB for a period of approximately 4 min. During this time, the reaction was monitored constantly. Following the DAB reaction, sections were dehydrated in a series of ethanol solutions and mounted in serial order on gelatinized slides for cell reconstruction. This method provides a permanent record of the cells from which detailed reconstructions were made using a drawing tube.

Rat sections from the lumbar segments (L3–L5) were examined within the ventral region of lamina VII, between medial and lateral motoneuron pools, which contains most Renshaw cells (Carr et al., 1998). Sections reacted with antibodies against CTb, VACHT and VGLUT (i.e. groups A, B and C) were scanned by using a $\times 60$ oil-immersion lens with a zoom factor of 2 at 0.5 μm intervals. The stacks of images were analyzed with NeuroLucida for Confocal software. Two hundred CTb labeled terminals that were also immunoreactive for VACHT were randomly selected from each rat. To avoid bias, a $100 \times 100 \mu\text{m}$ grid was placed on the image and the terminal closest to bottom right corner of each grid square was selected. Selected terminals were then examined in the blue channel (representing the VGLUTs) to determine

whether they were positive for VGLUT immunoreactivity. Sections reacted with antibodies for CTb, calbindin and VGLUT (i.e. group E and F) or CTb, calbindin and VACHT (i.e. group G) were scanned with a $\times 40$ oil-immersion lens and zoom factor of 2 at 0.5 μm intervals. Image stacks were analyzed with NeuroLucida to investigate the proportion of CTb-labeled terminals that made contact with Renshaw cells and were also immunolabeled for VGLUT1, VGLUT2 or VACHT in each group.

Sections reacted for VACHT and GluR2 were mounted in Vectashield anti-fade medium and scanned with the confocal microscope. Lamina VII of sections from each of the three rats was scanned by using a $\times 60$ oil-immersion lens with a zoom factor of 2 at 0.2 μm steps in the z-axis. In each section, two scanning fields were obtained from both sides with a $100 \times 100 \mu\text{m}$ scanning area. By using NeuroLucida software, image stacks were initially viewed so that only VACHT immunoreactivity was visible. All VACHT immunoreactive boutons within the scanning box from each animal were selected for analysis. GluR2 staining was then examined, and it was determined whether VACHT terminals were apposed to GluR2 puncta. Control material reacted with a combination of VGLUT1 and -2 and GluR2 was analyzed in exactly the same way.

In order to determine if axon terminals with different immunohistochemical characteristics belonged to different populations, we made a comparison between five groups of axon terminals. The equivalent diameter of axonal swellings that were double labeled for: (1) VACHT and GluR2; (2) VACHT and VGLUT2; (3) VACHT and no GluR2; (4) CTb and VACHT and (5) CTb and VGLUT1 was measured from projected confocal images obtained from all three rats by using Image J software (National Institutes of Health, USA, <http://rsb.info.nih.gov/ij/>). A one-way ANOVA was used to determine if there were statistically significant differences in the diameters of these groups ($P < 0.05$). This was followed by a Tukey's post hoc pairwise comparison to determine which groups were significantly different from each other.

Confocal microscope images for publication were prepared by using Adobe Photoshop to adjust brightness and contrast.

RESULTS

Do adult motoneuron axon collateral terminals contain VGLUTs?

In total, 63 axon terminals obtained from three intracellularly labeled motoneurons from the cat experiment were analyzed. Terminals that could not be traced back to the parent axon were excluded from the sample. Sections, which contained 11 motoneuron axon terminals, were reacted with antibodies against VGLUT1 and VGLUT2. Confocal microscope analysis showed that none of the 11 terminals were positive for either VGLUT1 or VGLUT2 immunoreactivity (Fig. 1). The remaining 55 axon terminals were reacted for the presence of GluR2 (see below).

In rat experiments, both motoneuron axon terminals and primary afferent axons were labeled by injection of the tracer CTb. Retrogradely labeled motoneurons were found in lamina IX ipsilateral to the injection site of the L3 to L5 segments of the spinal cord. Initially, we performed a series of three triple labeling experiments on each animal to determine if VACHT and glutamate vesicular transporters were co-localized in motoneuron collateral terminals. Three groups of sections were reacted: (A) CTb+VACHT+VGLUT1; (B) CTb+VACHT+VGLUT2; and (C) CTb+VACHT+VGLUT3. In each group, a total of 600 terminals,

doubled-labeled for CTb and VACHT, were randomly selected from the three rats (200 from each rat). Confocal microscope images revealed that none of the selected terminals was positive for VGLUT1, VGLUT2 and VGLUT3 immunoreactivity (Fig. 2). In addition, we also measured the equivalent diameter of 150 axon terminals which were labeled by both CTb and VACHT but not VGLUT1 (50 from each rat), and the equivalent diameter of 150 presumed primary afferent terminals which were labeled by both CTb and VGLUT1 but not VACHT (50 from each rat). As predicted, there was a significant difference between these two types of terminal; the average (\pm SD) equivalent diameters of the motoneuron terminals and the primary afferent terminals were $1.99 \pm 0.51 \mu\text{m}$ and $3.58 \pm 0.78 \mu\text{m}$, respectively (see below). In CTb+VACHT+VGLUT2 (group B) experiments, we not only found that there was no overlap of immunoreactivity for CTb and VGLUT2, but we also identified a small population of VGLUT2-labeled axons with VACHT staining (Fig. 2B). The equivalent diameter of VACHT/VGLUT2 terminals was $0.89 \pm 0.23 \mu\text{m}$ (50 terminals from each rat). These were significantly smaller than the CTb/VACHT and the CTb/VGLUT1 terminals (see below). We further investigated the relationship between VACHT/VGLUT2 terminals and NOS (group D) to determine if they originated from the NOS-containing subgroup of cholinergic interneurons (see Miles et al., 2007). A total of 50 VACHT/VGLUT2 terminals was randomly selected but none of them displayed NOS immunoreactivity (Fig. 2D).

Terminals which formed contacts with Renshaw cells identified by calbindin labeling (Carr et al., 1998; Alvarez et al., 1999) were investigated by performing immunoreactions with two antibody combinations: group E CTb+VGLUT1+calbindin; and group F CTb+VGLUT2+calbindin. For each combination, a sample of 15 calbindin-labeled Renshaw cells (five from each of the three animals) located within ventral lamina VII between motor nuclei was analyzed. Each of the scanning areas was $151 \mu\text{m} \times 151 \mu\text{m}$ and contained at least one cell body of a Renshaw cell and its proximal dendrites. In group E, a total of 285 CTb-labeled terminals which contacted Renshaw cells were recorded (mean \pm SD, 19 ± 5.6 contacts per cell). Of these terminals, $99\% \pm 3\%$ (281 out of 285) was found to be negative for VGLUT1 immunoreactivity (Fig. 3A). We then measured the size of the remaining 1% (four out of 285) terminals which were immunoreactive for VGLUT1. Their equivalent diameters ranged from 3.65 to 6.15 μm (mean \pm SD, $4.85 \pm 1.25 \mu\text{m}$). In group F, a total of 339 CTb-labeled terminals (mean \pm SD, $23 \pm 3.5/\text{cell}$) which were apposed Renshaw cells were analyzed. None of the terminals that contacted Renshaw cells were labeled with VGLUT2 immunoreactivity (Fig. 3B). Sequential immunocytochemistry with a fourth antibody against VACHT enabled us to confirm that the CTb-positive VGLUT2-negative terminals originated from motoneurons as all VGLUT2-negative terminals were positively labeled for VACHT immunoreactivity (Fig. 3C). In sequential experiments, we also noted that some VGLUT2 positive/CTb negative ter-

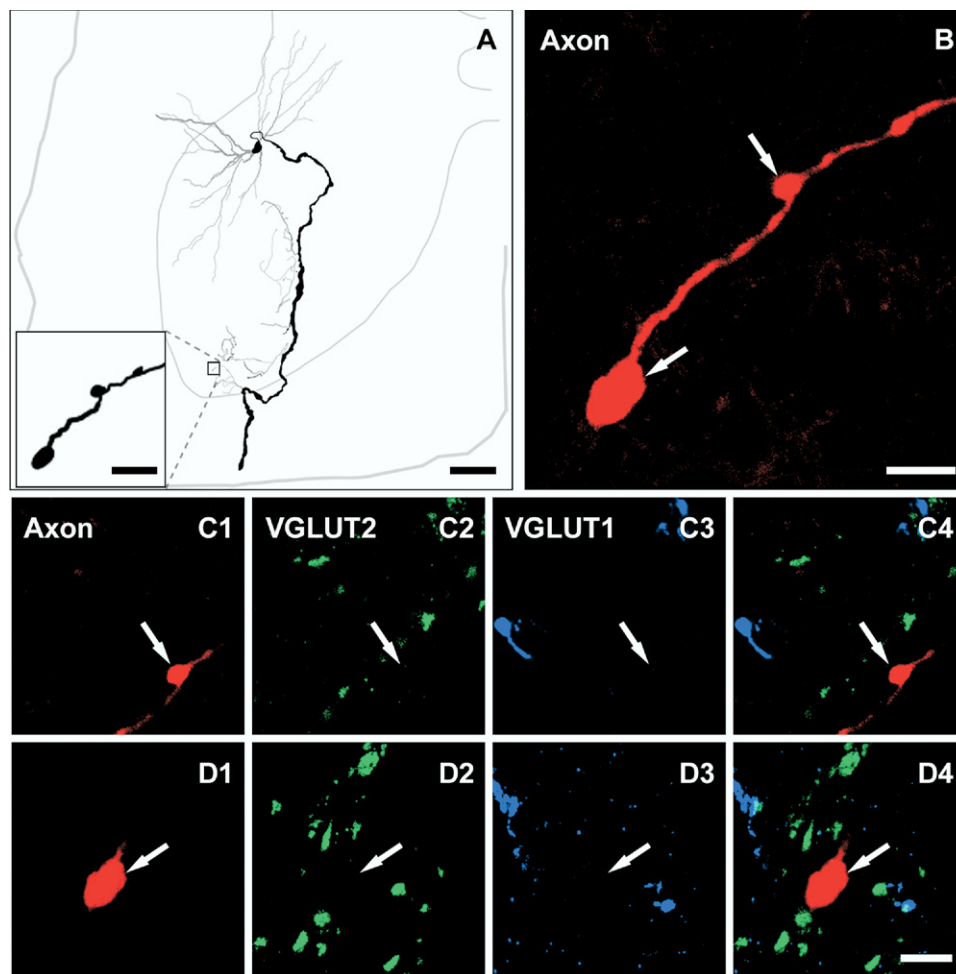


Fig. 1. A reconstruction of a cat motoneuron and its axon collaterals that was intracellularly labeled with neurobiotin (A) and a series of confocal microscope images illustrating the absence of VGLUT1 and -2 immunoreactivity within the motoneuron axon terminals (B–D). (A) The soma and axonal arborization are shown in black and dendrites in grey. The thinner grey line represents the outline of the grey matter and the central canal; the thicker grey line represents the border of the spinal cord. The axon terminals illustrated in B–D are taken from the area outlined by the box in A. (B) A projected image through a series of terminals. (C1–C4) Single optical sections and (D1–D4) projected images of two individual terminals (arrows). (C4, D4) Merged images confirming the absence of overlap of immunoreactivity for VGLUT1 and VGLUT2 and labeled motoneuron terminals. Scale bars=200 μm (large panel in A); 10 μm (small panel in A and B); 5 μm (C1–C4 and D1–D4).

minals were positive for VACHT immunoreactivity but that they did not form contacts with Renshaw cells (not shown). These results suggest that some cholinergic terminals located in the deep ventral horn which do not originate from motoneurons contain glutamate.

To confirm the above findings, we used a further combination of CTb, VACHT and calbindin (group G). Another sample of 15 calbindin-labeled Renshaw cells was examined (five from each of the three animals). In $151\mu\text{m} \times 151\mu\text{m}$ scanning fields, a total of 364 CTb-labeled terminals which contacted Renshaw cells were analyzed (mean \pm SD, $24 \pm 5.6/\text{cell}$). Of these terminals, $97\% \pm 4\%$ (352 out of 364) was found to be positive for VACHT (Fig. 4A, C). Sequential immunocytochemistry with a fourth antibody against VGLUT1 enabled us to show that the 12 VACHT-negative terminals were immunoreactive for VGLUT1. None of the 352 (out of 364) CTb/VACHT terminals was labeled for VGLUT1 (Fig. 4B, D).

Are axon collaterals of adult motoneurons apposed to AMPA receptors?

The remaining 52 collateral terminals from the three cat motoneurons were used to investigate the relationship between labeled axon collateral swellings and GluR2 subunits in postsynaptic membrane receptors. Fig. 5 shows an example of a reconstructed motoneuron and the organization of its axon. Collateral axons from this cell were used in the analysis (Fig. 6A–C). We could find no evidence of any obvious relationship between GluR2-immunoreactive puncta and motoneuron axon collaterals. However, all axon terminals from an interneuron which was labeled in the same animal as the motoneurons were apposed to GLUR2-immunoreactive puncta (Fig. 6D–G).

Associations between VACHT-labeled terminals and GluR2 immunoreactive puncta were also investigated in rat tissue. Confocal microscope images showed that al-

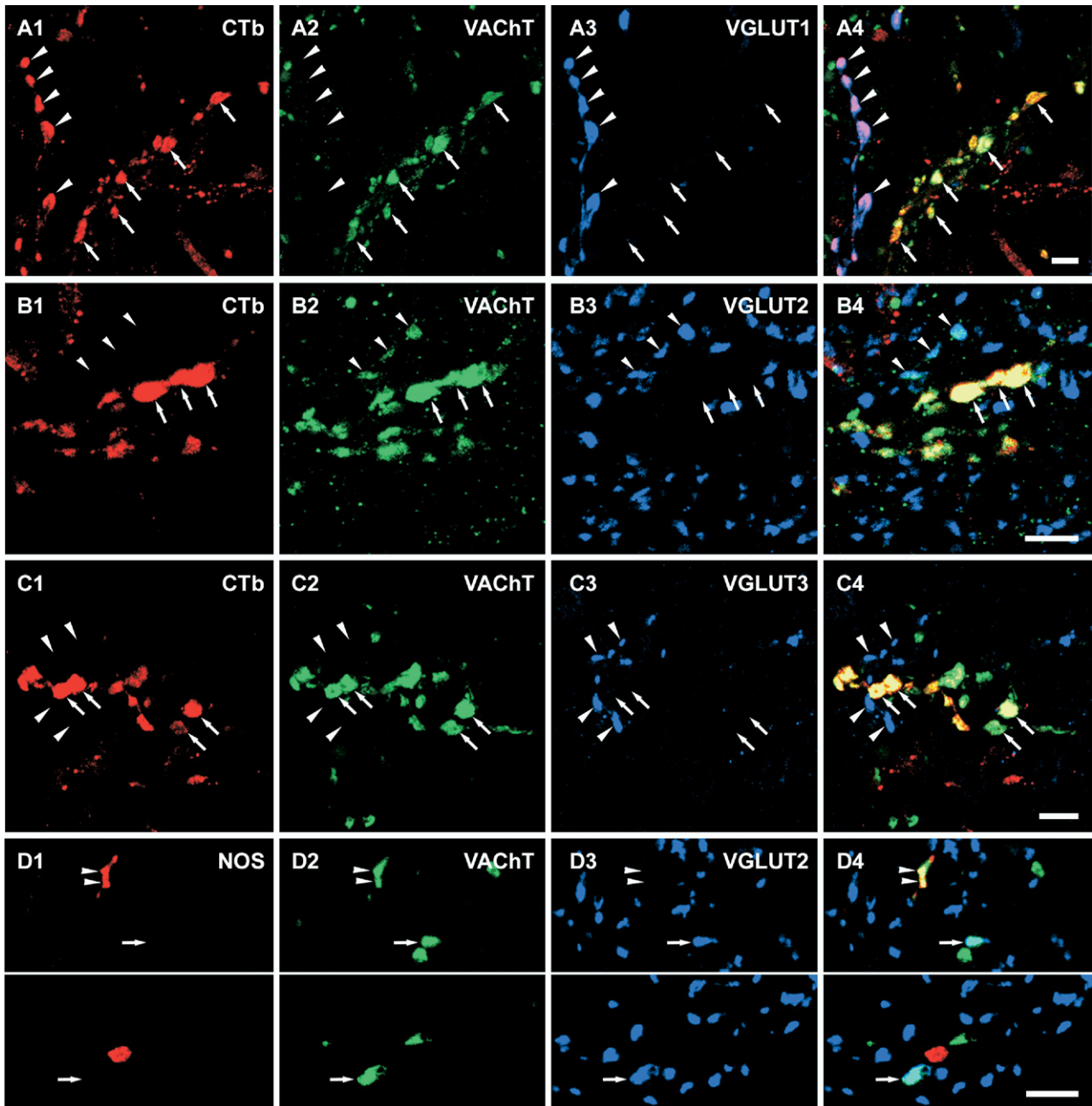


Fig. 2. Three color confocal images showing CTb-labeled motoneuron terminals that are positive for VAcHt-immunoreactivity but are negatively labeled for all three VGLUTs (A–C) and the relationship of VAcHt/VGLUT2 double-labeled terminals with NOS immunoreactivity (D). (A1–A4, B1–B4) Projected images of three single optical sections. C1–C4 and D1–D4 are single optical sections. Arrows in A–C indicate CTb-labeled motoneuron terminals that were VAcHt immunoreactive. Arrows in D indicate terminals that were immunopositive for both VAcHt and VGLUT2. Arrowheads in A indicate VGLUT1 immunoreactive terminals also labeled by CTb that are likely to originate from proprioceptive primary afferent fibers. Arrowheads in B indicate VGLUT2 immunoreactive terminals that also contain VAcHt staining but are not labeled with CTb. Arrowheads in C indicate VGLUT3 terminals. Arrowheads in D indicate NOS immunopositive terminals that were also labeled by VAcHt. (A4, B4, C4, D4) Merged images. Scale bar = 5 μm .

though most VAcHt immunoreactive boutons were not apposed to GluR2 puncta (Fig. 7A–C), a small number of VAcHt boutons were associated with GluR2 staining (Fig. 7D–F). The average (\pm SD) equivalent diameters of the former group and the latter group were $1.95 \pm 0.53 \mu\text{m}$ and $0.87 \pm 0.23 \mu\text{m}$, respectively. For comparison, we exam-

ined the relationship between glutamatergic terminals (labeled with a combination of VGLUT1 and -2 antibodies) and GluR2 immunoreactive puncta in deep lamina VII. Despite an intensive search, we only detected an occasional VGLUT immunoreactive axon terminal which was not apposed to GluR2-immunoreactive puncta (Fig. 7G–I).

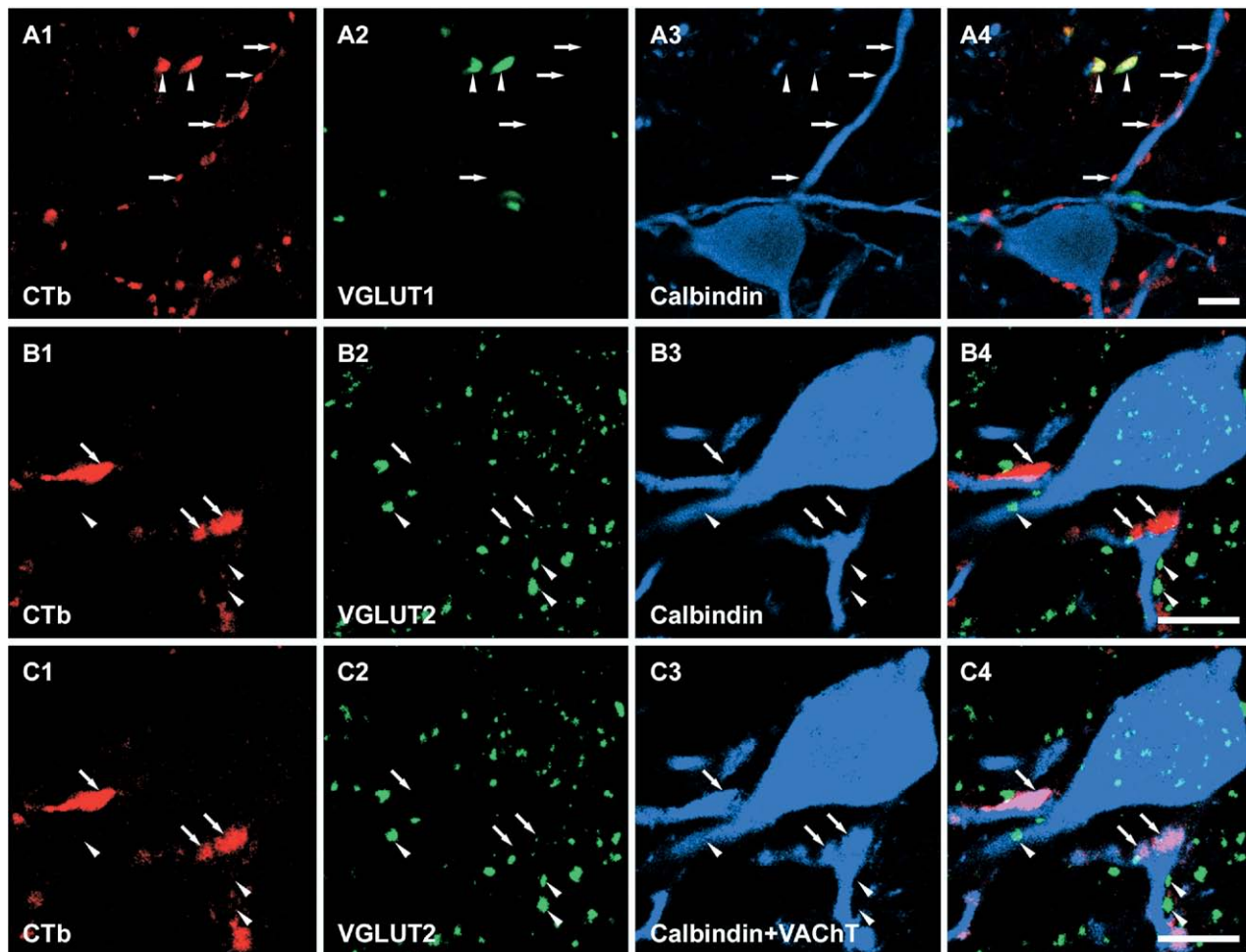


Fig. 3. Single optical sections illustrating CTb-labeled motoneuron terminals in contact with Renshaw cells. (A1–A4, B1–B4) All of the CTb-labeled motoneuron terminals making contact with two calbindin-labeled cells were negative for VGLUT1- and VGLUT2-immunoreactivity, respectively. Arrows indicate selected motoneuron terminals which contact the calbindin-labeled cells. Arrowheads indicate VGLUT1 and VGLUT2 terminals in A and B, respectively. (C1–C4) Single optical sections of the same area shown in B1–B4 that have been rescanned after sequential incubation with a fourth antibody for VACHT. The extra labeling present in C3 (indicated by arrows), which was absent in B3, corresponds to the additional VACHT-immunostaining. Note that all CTb terminals that form contacts with the Renshaw cell are immunoreactive for VACHT (profiles indicated by arrows in C4, merged image on the right) and hence can be confirmed to be motoneuron axon terminals. (A4, B4, C4) Merged images. Scale bar=10 μm .

Comparison of equivalent diameters of populations of cholinergic and glutamatergic terminals in the rat

We made a comparison of the equivalent diameters of five groups of terminals investigated in this study: (A) those that were labeled with VACHT and were associated with GluR2; (B) those that were labeled with VACHT and VGLUT2; (C) those that were labeled with VACHT but were not associated with GluR2; (D) those that were labeled with VACHT and CTb; and (E) those that were labeled with CTb and VGLUT1 (see Fig. 8). Each group consisted of 50 randomly selected terminals obtained from each of the three rats. By using ANOVA analysis, we found that there was a highly significant difference between these groups ($P < 0.0005$). A post hoc Tukey's pairwise comparison showed that there was no statistical difference between groups A and B or between groups C and D but that all other comparisons were significantly different.

DISCUSSION

In the series of experiments reported here we have shown: (1) that axon collateral swellings of adult cat motoneurons do not contain the VGLUTs VGLUT1 or VGLUT2 and have no obvious association with the GluR2 subunit of the AMPA receptor; (2) that axon collateral swellings of adult rat motoneurons also do not contain VGLUTs VGLUT1, VGLUT2 or VGLUT3 and have no obvious association with the GluR2 subunit of the AMPA receptor; (3) that a group of cholinergic axon terminals within lamina VII of the rat spinal cord, contains VGLUT2 and forms associations with the GluR2 subunit of the AMPA receptor.

In the cat experiment, our analysis was confined to terminals which could be traced back to the parent axon and hence could be identified unequivocally as motoneuron collaterals. In rat experiments, terminals were classi-

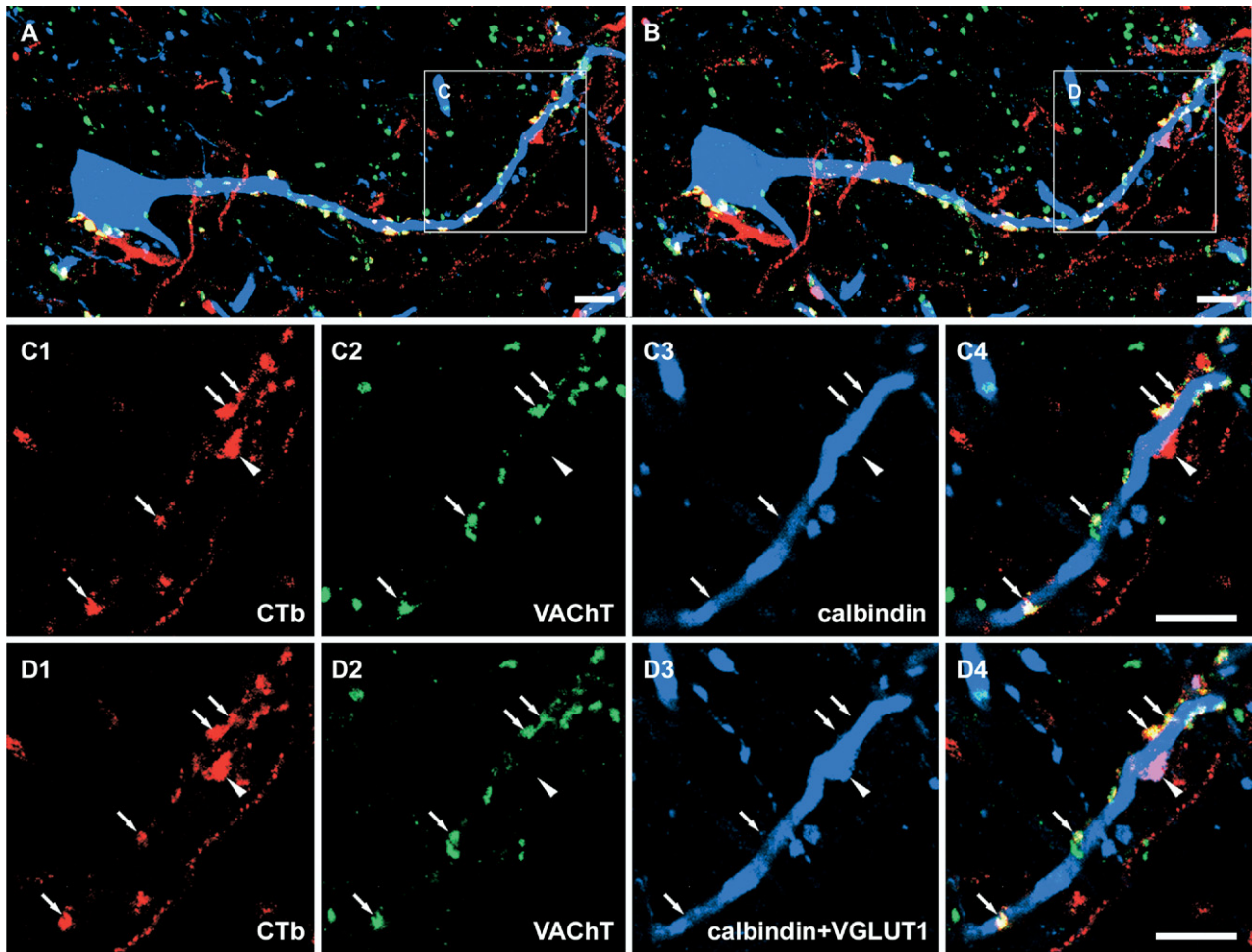


Fig. 4. Sequential immunocytochemistry for CTb-labeled terminals in contact with a Renshaw cell. (A, B) A general overview of CTb-labeled terminals in contact with a calbindin-labeled cell before and after a reaction with a fourth antibody against VGLUT1. Details of the areas demarcated by the boxes are shown in C1–C4 and D1–D4. (C1–C4) Single optical sections illustrating that most of the CTb-labeled terminals in contact with the calbindin cell were positive for VACHT. Arrows indicate double-labeled CTb axon terminals with VACHT staining. The arrowhead indicates a single CTb-labeled terminal on the Renshaw cell that was negative for VACHT. (D1–D4) Single optical sections of the same terminals that were rescanned after sequential incubation with a fourth antibody against VGLUT1. The extra labeling present in D3 (indicated by arrowhead), which was absent in C3, corresponds to additional VGLUT1-immunostaining (see D4). Note that this VGLUT1 positive terminal, which forms an apposition with the Renshaw cell, is bigger than CTb-labeled motoneuron terminals, and is likely to be a primary afferent terminal. A, B, C4 and D4 are merged images. Scale bar = 10 μm .

fied into three distinct populations according to their immunocytochemical characteristics and equivalent diameters: (1) CTb-labeled cholinergic terminals were identified as motoneuron axon collateral terminals. This group of axons had intermediate-sized terminals (approximately 2 μm in diameter) and made numerous contacts with Renshaw cells which were labeled with calbindin (Carr et al., 1998; Alvarez et al., 1999). Alvarez et al. (1999) also measured size of VACHT terminals contacting Renshaw cells and the mean diameter ($2.26 \pm 0.94 \mu\text{m}$) was similar to that described here. (2) CTb labeled noncholinergic terminals that were immunopositive for VGLUT1 which were classified as primary afferent terminals because VGLUT1 is generally present in terminals of myelinated primary afferent axons but not in spinal interneurons (Varoqui et al., 2002; Todd et al., 2003). These terminals were the largest of the three

groups and had an average diameter of 3.52 μm . This is consistent with previous reports of the sizes of Group Ia afferent terminals (Watson and Bazzaz, 2001) which are likely to constitute the majority of primary afferents terminating in lamina VII (Brown, 1981). These terminals made occasional contacts with Renshaw cells. (3) The third group of terminals was the most intriguing of all. This group was composed of small cholinergic terminals (approximately 0.92 μm in diameter), that were never labeled with CTb but were immunoreactive for VGLUT2 immunoreactivity. These axons apparently made no contacts with Renshaw cells.

Our observation that adult cat and rat motoneuron axon collaterals do not contain VGLUT 2 is at variance with findings from previous studies where this vesicular transporter was reported to be present in axon collaterals of

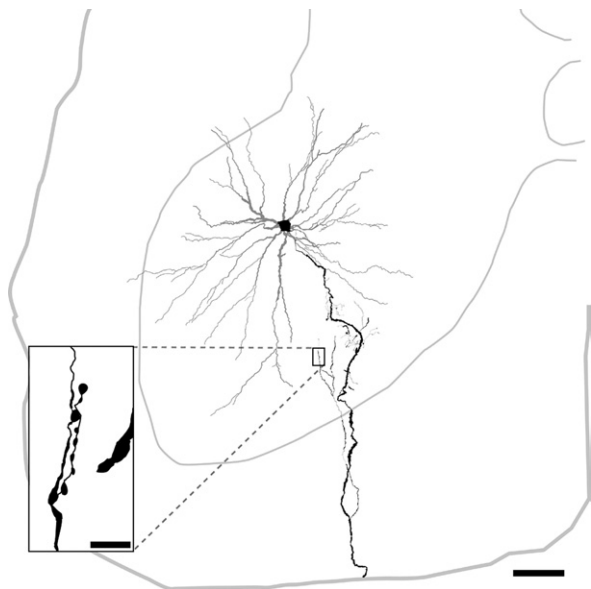


Fig. 5. Reconstruction of a motoneuron and its axon collaterals that was intracellularly labeled with neurobiotin. The soma and axonal arborization are shown in black and dendrites in grey. The thinner grey line represents the outline of the grey matter and the central canal; the thicker grey line represents the border of the spinal cord. The axon terminals illustrated in Fig. 6 are taken from the area outlined by the box. Scale bar=200 μm (in big panel), 10 μm (in small panel).

adult rat (Herzog et al., 2004) and neonatal mouse (Nishimaru et al., 2005). However they are consistent with the findings of Mentis et al. (2005) who also noted absence of immunoreactivity for all three VGLUTs in collaterals of young mice. In addition, it is also consistent with reports of absence of mRNAs for all three VGLUTs in motoneurons (Kullander et al., 2003; Oliveira et al., 2003; but cf Herzog et al., 2004). Herzog et al. (2004) suggested that motoneuron collaterals gave rise to axon branches which contained ACh but not glutamate and vice versa. We could find no evidence for this arrangement and, in fact, any CTb-labeled terminals that were not immunoreactive for VACHT were invariably immunoreactive for VGLUT1 and were most probably terminals of primary afferent proprioceptors (see above). We also could detect no obvious relationship between cat or rat motoneuron terminals and immunoreactivity for the GluR2 subunit of the AMPA receptor. According to Nagy et al. (2004), 98% of AMPA receptors in the rat spinal grey matter contain this subunit and therefore it can be considered to be a marker for almost all AMPA receptors. In theory, there is a small probability that synapses formed by motoneuron collaterals appose AMPA receptors that do not possess this subunit. However, this seems an improbable explanation for our negative findings. Firstly, our control experiments showed that GluR2 subunits were abundant in deep lamina VII in rat and cat tissue and that, in the rat, VGLUT immunoreactive terminals were invariably associated with them. Secondly, Lamotte d'Incamps and Ascher (2008) provided evidence that the AMPA receptor-mediated current recorded between motoneurons and Renshaw cells in young mice has a low permeability to calcium ions and therefore it would be pre-

dicted that the receptors present at this synapse possess GluR2 subunits. In the cat experiment, all axon terminals could be traced to the parent motoneuron axon but in the rat we had to confirm by statistical analysis that the population of VACHT terminals which did not appose GluR2 puncta belonged to the same population that was labeled for VACHT and CTb (group 1 discussed above) because the antigen retrieval method combined with TSA only enables two antibodies to be used on the same tissue and, for this reason, we were unable to label these terminals for CTb also. Taken together, the two sets of observations presented above suggest that glutamate is not co-localized with ACh at central synapses of adult motoneurons and does not act through an AMPA receptor.

Mentis et al. (2005); Nishimaru et al. (2005) and Lamotte d'Incamps and Ascher (2008) produced pharmacological evidence that glutamate is coreleased along with ACh at motoneuron/Renshaw cell synapses in young mice (P0–10) and therefore a possible reason for differences in the findings of these studies and our anatomical observations may be related to the maturity of the experimental animals they used. The original observations of Eccles et al. (1954) on adult cats indicated that cholinergic antagonists do not completely block transmission at motoneuron/Renshaw cell synapses and therefore it remains possible that another transmitter is coreleased along with ACh. Our data suggest that if glutamate is this transmitter, then it is not stored conventionally in vesicles and it does not act via AMPA receptors. Mentis et al. (2005) reported that motoneuron central terminals did not contain VGLUTs but that glutamate was enriched in them and argued that this was tentative evidence for a transmitter pool of glutamate. However, glutamate may be enriched in structures for a variety of reasons which are unrelated to transmitter function. It is also possible that glutamate acts via kainate or activated NMDA receptors in the adult. However, the antagonist, CNQX, used by Mentis et al. (2005) and Nishimaru et al. (2005) and the NBQX, used by Lamotte d'Incamps and Ascher (2008) demonstrated a specific AMPA component of the current. The most likely explanation of this discrepancy with our findings is that the expression of AMPA receptors decreases during development to adulthood but further studies on young animals will be required to establish this.

Two further observations arose from this study. Firstly, we found evidence that a small number of primary afferent axons form contacts with Renshaw cells in adult rats. The classic view of Renshaw cells is that they are not monosynaptically activated by primary afferent axons (Renshaw, 1946; Eccles et al., 1954). However according to a recent report by Mentis et al. (2006), the density of primary afferent contacts on Renshaw cells decreases during development but the overall numbers of contacts remains approximately the same as a consequence of the enlargement of the cell. They suggest that there is a “functional deselection” of such contacts during development and although such synapses are still present, they become less effective and have a limited influence on Renshaw cells in adulthood. Although, we did not attempt to quantify the

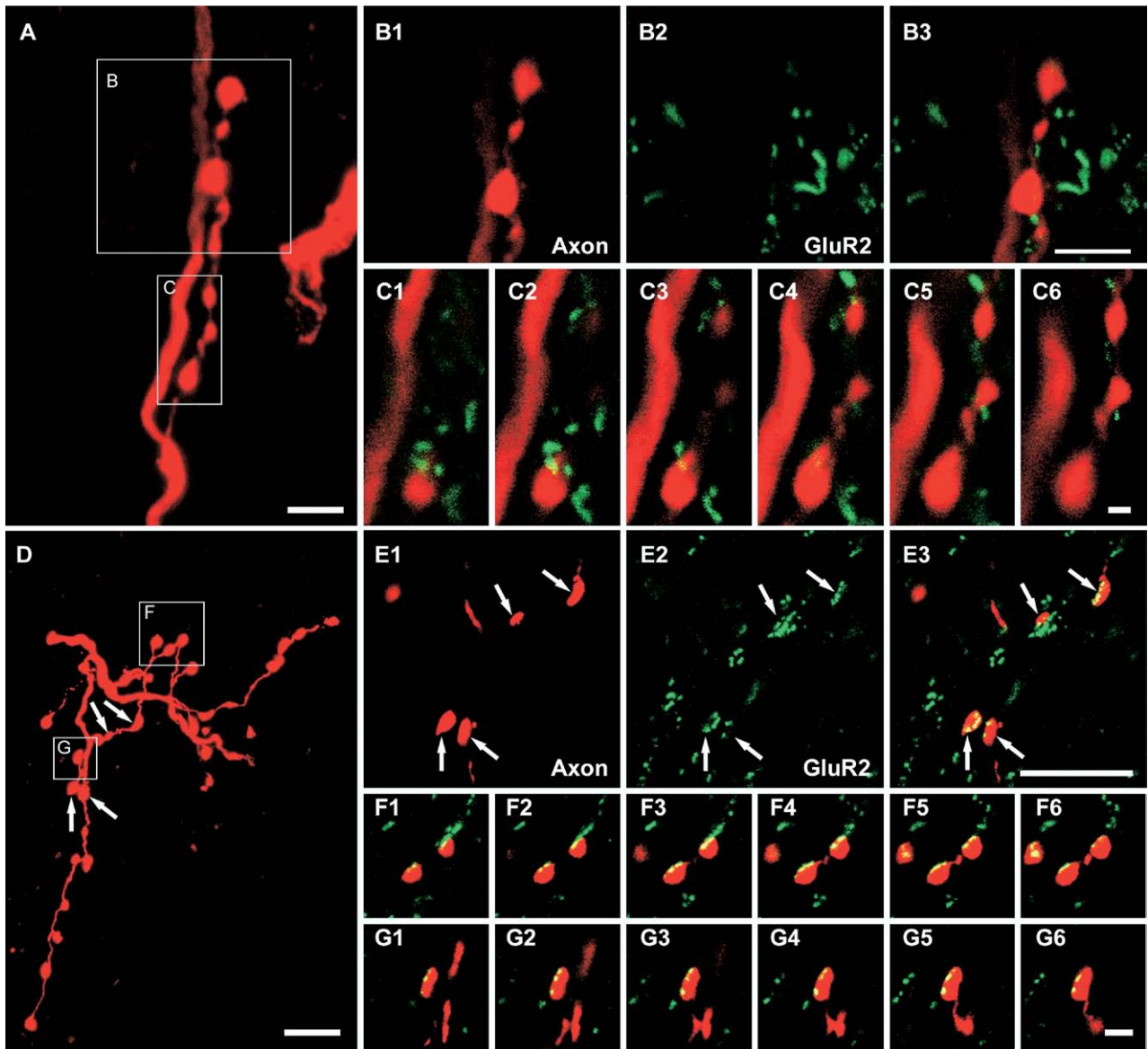


Fig. 6. Relationships between intracellularly labeled axon terminals and immunoreactivity for the GluR2 subunit of the AMPA receptor following antigen unmasking with pepsin. (A–C) There is no obvious association between motoneuron axon terminals and GluR2 immunoreactivity. (D–F) Associations between interneuronal axon terminals and immunoreactivity for GluR2. The large panels on the top left (A) and on the bottom left (D) show projected images of a series of terminals originating from a motoneuron and an excitatory interneuron, respectively. Details of the areas demarcated by the boxes are shown in B1–B3, C1–C6, E1–E3, F1–F6, and G1–G6. (B1–B3) Motoneuron axon terminals (B1), GluR2 (B2), and a merged image (B3) of the same single optical sections. (C1–C6) A series of merged single optical sections through the motoneuron terminals taken at intervals of $0.3 \mu\text{m}$. (E1–E3) Interneuron axon terminals (E1), GluR2 (E2), and a merged image (E3) of the same single optical section. (F1–F6, G1–G6) Series of merged single optical sections through the interneuron terminals taken at intervals of $0.2 \mu\text{m}$. Scale bar = $5 \mu\text{m}$ (A, B1–B3, D, E1–E3); $1 \mu\text{m}$ (C1–C6); $2 \mu\text{m}$ (F1–F6, and G1–G6).

numbers of CTb/VGLUT1 contacts on Renshaw cells, our impression was that that they were sparse in comparison to cholinergic contacts which would be consistent with their limited influence in adulthood.

The second observation was perhaps the most novel of all. We found a population of cholinergic axons in lamina VII which were immunoreactive for VGLUT2 and also formed associations with GluR2 subunit immunoreactivity. These axon terminals were considerably smaller than

those originating from motoneurons and were not seen to make contacts onto Renshaw cells. At present we are unable to determine the origin of these axons but it is very unlikely that they originate from descending systems or primary afferents as neither of these groups of neuron uses ACh as a neurotransmitter (e.g. Rustioni and Weinberg, 1989). However, it is highly likely that they originate from local interneurons (Barber et al., 1984) or propriospinal neurons (Sherriff and Henderson, 1994)

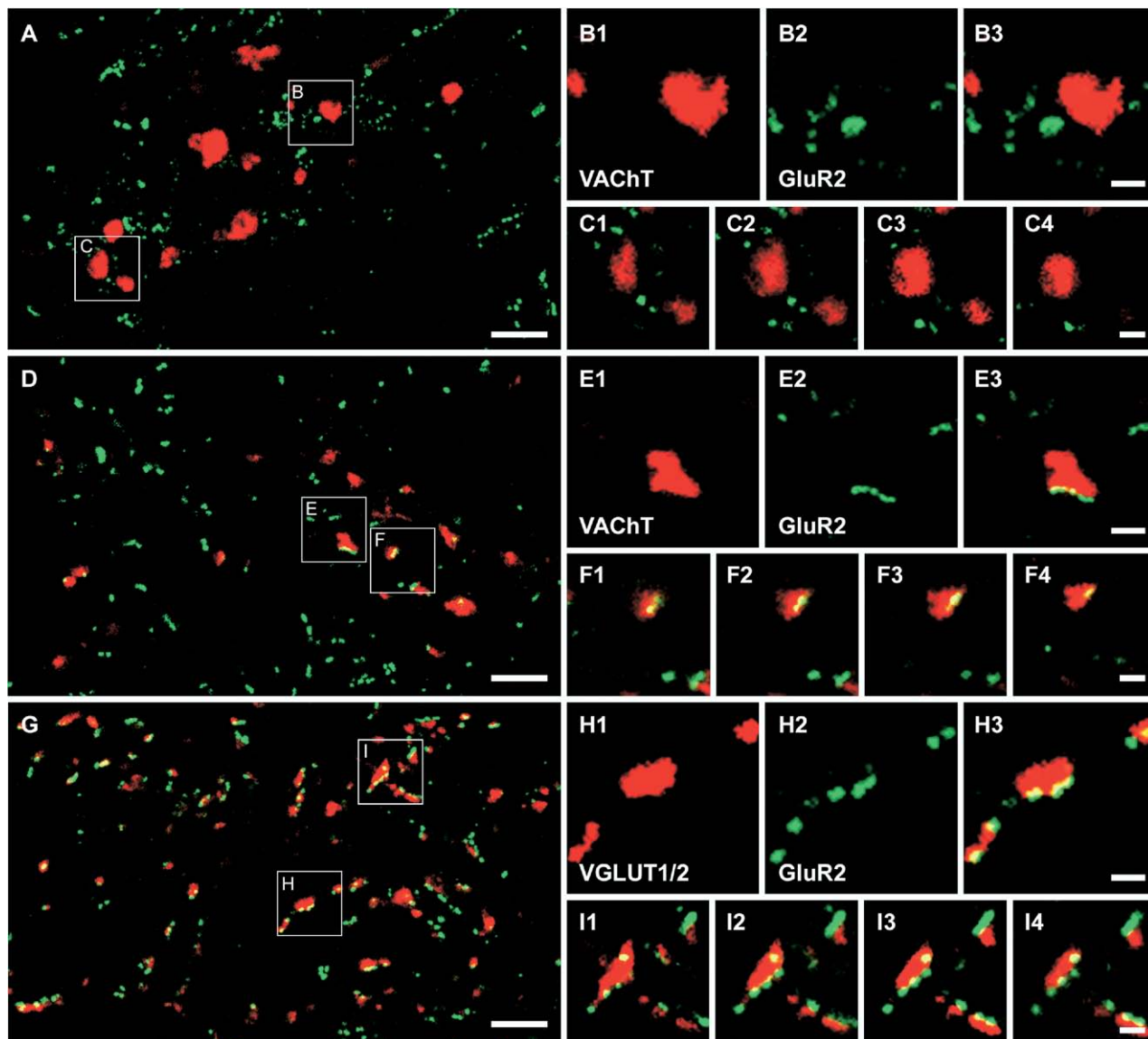


Fig. 7. Relationships between VAcHT-labeled terminals and VGLUT-labeled terminals and immunoreactivity for the GluR2 subunit of the AMPA receptor following antigen unmasking with pepsin. (A, D) General overviews of groups of VAcHT-immunostained terminals (red) and their relationships with GluR2-immunoreactive puncta (green). (G) A general overview of a group of VGLUT1 and VGLUT2 immunoreactive terminals in lamina VII and their relationship with GluR2-immunoreactive puncta. Details of the areas demarcated by the boxes are shown in B1–B3, C1–C4, E1–E3, F1–F4, H1–H3, and I1–I4. (B1–B3, E1–E3, H1–H3) VAcHT terminals (B1, E1), VGLUT1 and VGLUT2 terminals (H1), GluR2 puncta (B2, E2, H2), and merged images (B3, E3, H3) of the same single optical sections. C1–C4, F1–F4 and I1–I4. Series of merged single optical sections through the selected terminals taken at intervals of $0.2 \mu\text{m}$. Note that the VAcHT terminals which lack any association with GluR2 puncta (B, C), are bigger than the terminals which form appositions with GluR2 puncta (E, F). Scale bar = $5 \mu\text{m}$ A, D and G; $1 \mu\text{m}$ (B, C, E, F, H, I).

which are known to be cholinergic. In the intermediate grey matter of the lumbar spinal cord there is a concentration of cholinergic neurons in lamina X and lateral to the central canal in lamina VII (Barber et al., 1984). There are two principal types of cholinergic cell in this region which are characterized by the presence or absence of NOS in their cell bodies (Miles et al., 2007). Our findings indicate that VAcHT/VGLUT2 terminals do not originate from the NOS-containing group and so, at present, their precise origin remains uncertain. Some cholinergic interneurons which lack NOS are located

principally in lamina VII lateral to the central canal and are likely to be the origin of the large “C-terminals” on motoneurons. These cells therefore are also unlikely to be the source of the small terminals we observed.

CONCLUSION

We have not found any evidence to support the proposition that glutamate is co-localized in central synapses of adult motoneurons and acts via an AMPA receptor. However, some cholinergic terminals which probably originate from

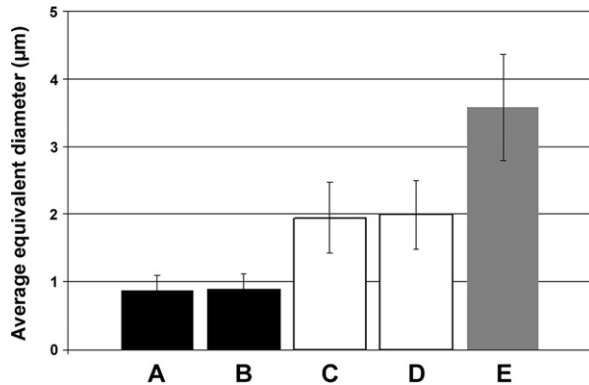


Fig. 8. Comparison of the average equivalent diameters of five groups of terminals. (A, B) The average equivalent diameters of VACHT terminals with GluR2 association and with VGLUT2 labeling, respectively. (C, D) The average equivalent diameters of VACHT terminals without association with GluR2 and with CTb labeling, respectively. (E) The average equivalent diameters of CTb terminals with VGLUT1 immunoreactivity. One way ANOVA showed that there was a significant difference between these groups and a post hoc comparison showed no difference between groups A and B and between groups C and D. All other comparisons were significantly different. Bars show standard deviations.

interneurons are likely to use glutamate as a cotransmitter and act via AMPA receptors.

Acknowledgments—The study was supported by a grant from NINDS/NIH (R01 NS040863). Ting Ting Liu is a University of Glasgow FBLs Scholar.

REFERENCES

- Alvarez FJ, Dewey DE, McMillin P, Fyffe REW (1999) Distribution of cholinergic contacts on Renshaw cells in the rat spinal cord: a light microscopic study. *J Physiol (Lond)* 515:787–797.
- Bannatyne BA, Edgley SA, Hammar I, Jankowska E, Maxwell DJ (2006) Differential projections of excitatory and inhibitory dorsal horn interneurons relaying information from group II muscle afferents in the cat spinal cord. *J Neurosci* 26:2871–2880.
- Barber RP, Phelps PE, Houser CR, Crawford GD, Salvaterra PM, Vaughn JE (1984) The morphology and distribution of neurons containing choline acetyltransferase in the adult rat spinal cord: an immunocytochemical study. *J Comp Neurol* 229:329–346.
- Brown AG (1981) *Organization in the spinal cord*. Berlin: Springer-Verlag.
- Carr PA, Alvarez FJ, Leman EA, Fyffe REW (1998) Calbindin D28k expression in immunohistochemically identified Renshaw cells. *Neuroreport* 9:2657–2661.
- Curtis DR, Ryall RW (1964) Nicotinic and muscarinic receptors of Renshaw cells. *Nature* 203:652–653.
- Dourado M, Sargent PB (2002) Properties of nicotinic receptors underlying Renshaw cell excitation by a-motor neurons in neonatal rat spinal cord. *J Neurophysiol* 87:3117–3125.
- Eccles JC, Fatt P, Koketsu K (1954) Cholinergic and inhibitory synapses in a pathway from motor axon collaterals to motoneurons. *J Physiol Lond* 126:524–562.
- Herzog E, Landry M, Buhler E, Bouali-Benazzouz R, Legay C, Henderson CE, Nagy F, Dreyfus P, Giros B, El Mestikawy S (2004) Expression of vesicular glutamate transporters, VGLUT1 and VGLUT2, in cholinergic spinal motoneurons. *Eur J Neurosci* 20:1752–1760.
- Kullander K, Butt SJ, Lebrecht JM, Lundfald L, Restrepo CE, Rydström A, Klein R, Kiehn O (2003) Role of EphA4 and EphrinB3 in local neuronal circuits that control walking. *Science* 299:1889–1892.
- Lamotte d'Incamps B, Ascher P (2008) Four excitatory postsynaptic ionotropic receptors coactivated at the motoneuron-Renshaw cell synapse. *J Neurosci* 28:14121–14131.
- Mentis GZ, Alvarez FJ, Bonnot A, Richards DS, Gonzalez-Forero D, Zerda R, O'Donovan MJ (2005) Noncholinergic excitatory actions of motoneurons in the neonatal mammalian spinal cord. *Proc Natl Acad Sci U S A* 102:7344–7349.
- Mentis GZ, Siembab VC, Zerda R, O'Donovan MJ, Alvarez FJ (2006) Primary afferent synapses on developing and adult Renshaw cells. *J Neurosci* 26:13297–13310.
- Miles GB, Hartley R, Todd AJ, Brownstone RM (2007) Spinal cholinergic interneurons regulate the excitability of motoneurons during locomotion. *Proc Natl Acad Sci U S A* 104:2448–2453.
- Nagy GG, Al Ayyan M, Andrew D, Fukaya M, Watanabe M, Todd AJ (2004) Widespread expression of the AMPA receptor GluR2 subunit at glutamatergic synapses in the rat spinal cord and phosphorylation of GluR1 in response to noxious stimulation revealed with an antigen-unmasking method. *J Neurosci* 24:5766–5777.
- Nishimaru H, Restrepo CE, Ryge J, Yanagawa Y, Kiehn O (2005) Mammalian motor neurons corelease glutamate and acetylcholine at central synapses. *Proc Natl Acad Sci U S A* 102:5245–5249.
- Noga BR, Shefchyk SJ, Jamal J, Jordan LM (1987) The role of Renshaw cells in locomotion: antagonism of their excitation from motor axon collaterals with intravenous mecamylamine. *Exp Brain Res* 66:99–105.
- Oliveira AL, Hydling F, Olsson E, Shi T, Edwards RH, Fujiyama F, Kaneko T, Hokfelt T, Cullheim S, Meister B (2003) Cellular localization of three vesicular glutamate transporter mRNAs and proteins in rat spinal cord and dorsal root ganglia. *Synapse* 50:117–129.
- Renshaw B (1946) Central effects of centripetal impulses in axons of spinal central roots. *J Neurophysiol* 9:191–204.
- Rustioni A, Weinberg RJ (1989) The somatosensory system. In: *Handbook of chemical neuroanatomy* (Björklund A, Hökfelt T, Swanson LW, eds), pp 219–320. Amsterdam: Elsevier.
- Schneider SP, Fyffe REW (1992) Involvement of GABA and glycine in recurrent inhibition of spinal motoneurons. *J Neurophysiol* 68:397–406.
- Sherriff FE, Henderson Z (1994) A cholinergic propriospinal innervation of the rat spinal cord. *Brain Res* 634:150–154.
- Todd AJ, Hughes DI, Polgár E, Nagy GG, Mackie M, Ottersen OP, Maxwell DJ (2003) The expression of vesicular glutamate transporters VGLUT1 and VGLUT2 in neurochemically defined axonal populations in the rat spinal cord with emphasis on the dorsal horn. *Eur J Neurosci* 17:13–27.
- Varoqui H, Schafer MK, Zhu H, Weihe E, Erickson JD (2002) Identification of the differentiation-associated Na⁺/PI transporter as a novel vesicular glutamate transporter expressed in a distinct set of glutamatergic synapses. *J Neurosci* 22:142–155.
- Watson AHD, Bazzaz AA (2001) GABA and glycine-like immunoreactivity at axoaxonic synapses on 1a muscle afferent terminals in the spinal cord of the rat. *J Comp Neurol* 433:335–348.
- Windhorst U (1996) On the role of recurrent inhibitory feedback in motor control. *Prog Neurobiol* 49:517–587.

Excitatory and inhibitory intermediate zone interneurons in pathways from feline group I and II afferents: differences in axonal projections and input

B. A. Bannatyne¹, T. T. Liu¹, I. Hammar², K. Stecina², E. Jankowska² and D. J. Maxwell¹

¹Spinal Cord Group, Institute of Biomedical and Life Sciences, University of Glasgow, Glasgow G12 8QQ, UK

²Department of Physiology, Göteborg University, 405 30 Göteborg, Sweden

The aim of the present study was to compare properties of excitatory and inhibitory spinal intermediate zone interneurons in pathways from group I and II muscle afferents in the cat. Interneurons were labelled intracellularly and their transmitter phenotypes were defined by using immunocytochemistry. In total 14 glutamatergic, 22 glycinergic and 2 GABAergic/glycinergic interneurons were retrieved. All interneurons were located in laminae V–VII of the L3–L7 segments. No consistent differences were found in the location, the soma sizes or the extent of the dendritic trees of excitatory and inhibitory interneurons. However, major differences were found in their axonal projections; excitatory interneurons projected either ipsilaterally, bilaterally or contralaterally, while inhibitory interneurons projected exclusively ipsilaterally. Terminal projections of glycinergic and glutamatergic cells were found within motor nuclei as well as other regions of the grey matter which include the intermediate region, laminae VII and VIII. Cells containing GABA/glycine had more restricted projections, principally within the intermediate zone where they formed appositions with glutamatergic axon terminals and unidentified cells and therefore are likely to be involved in presynaptic as well as postsynaptic inhibition. The majority of excitatory and inhibitory interneurons were found to be coexcited by group I and II afferents (monosynaptically) and by reticulospinal neurons (mono- or disynaptically) and to integrate information from several muscles. Taken together the morphological and electrophysiological data show that individual excitatory and inhibitory intermediate zone interneurons may operate in a highly differentiated way and thereby contribute to a variety of motor synergies.

(Received 4 July 2008; accepted after revision 25 November 2008; first published online 1 December 2008)

Corresponding author B. A. Bannatyne: Spinal Cord Group, Institute of Biomedical and Life Sciences, University of Glasgow, Glasgow G12 8QQ, UK. Email: bab1c@udcf.gla.ac.uk

It has long been established that interneurons in excitatory and inhibitory reflex pathways from muscle afferents are under the control of different supraspinal systems (Holmqvist & Lundberg, 1959; Holmqvist & Lundberg, 1961; Lundberg, 1982; Aggelopoulos *et al.* 1996) and recent studies show that activation of excitatory and inhibitory interneurons is regulated differentially in some behavioural contexts. For instance, inhibition of motoneurons dominates under resting conditions but is depressed during locomotion (Gossard *et al.* 1994; McCrea *et al.* 1995; Perreault *et al.* 1995, 1999; Quevedo *et al.* 2000) or following spinal cord injury, when excitation is released (Arya *et al.* 1991; Aggelopoulos & Edgley, 1995; Aggelopoulos *et al.* 1996). However, the extent to which this differential regulation might depend on properties of premotor interneurons mediating excitation or inhibition

of motoneurons, or on neurons that provide input to premotor interneurons, has not been established.

Excitatory and inhibitory interneurons that are activated by primary afferents clearly play different roles in motor behaviour and it is of fundamental importance that we know what differences exist between them in terms of input properties, morphology and, especially, axonal projections and target cells. However, until recently, possibilities to compare properties of excitatory and inhibitory premotor interneurons have been limited. In the cat, a number of extracellularly recorded interneurons inducing EPSPs or IPSPs in motoneurons were identified by using spike-triggered averaging (Brink *et al.* 1981, 1983; Cavallari *et al.* 1987), but as these interneurons could only be penetrated in exceptional circumstances (see Fig. 1 in Cavallari *et al.* 1987), this precluded a

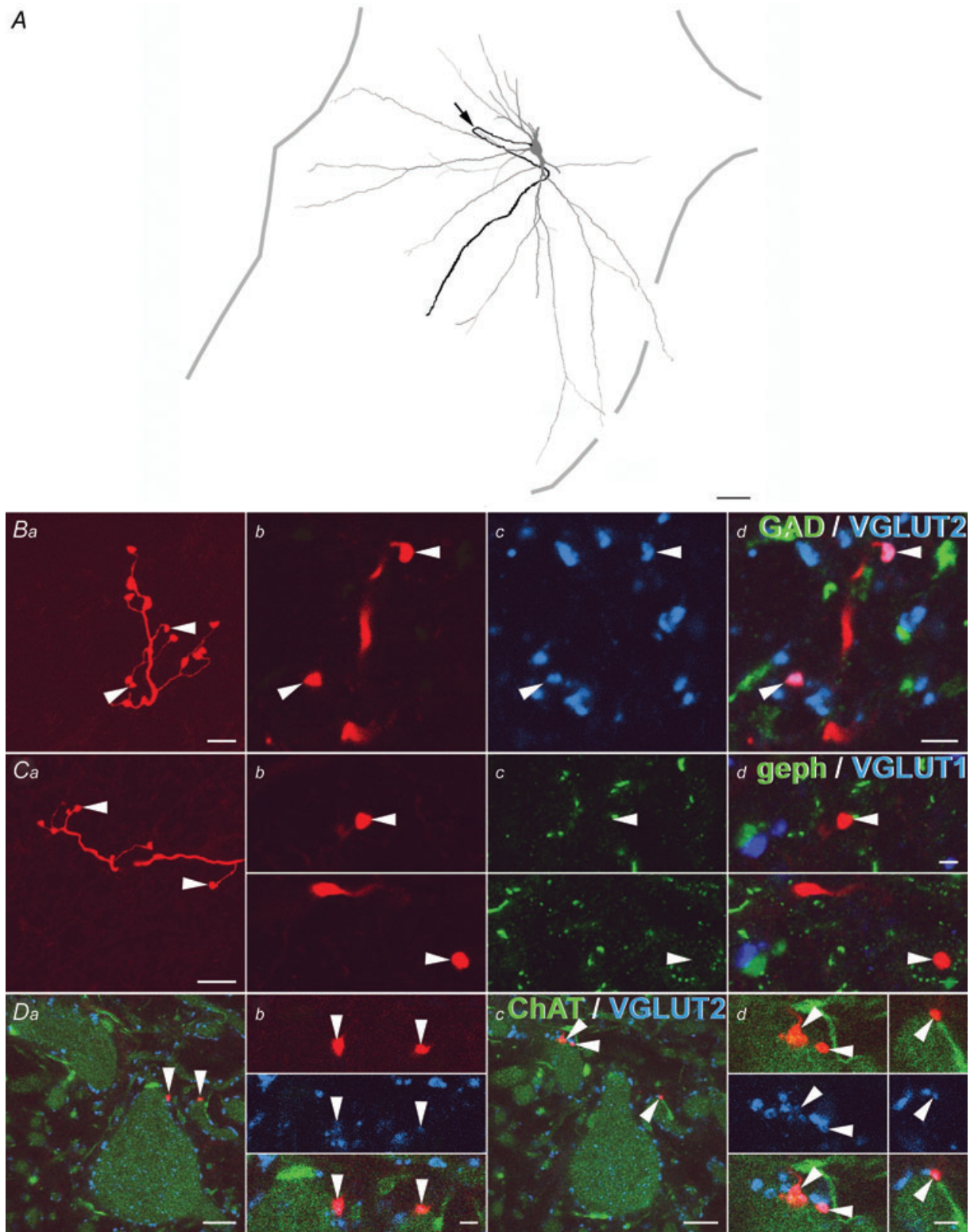


Figure 1. An ipsilaterally projecting glutamatergic interneuron

A, a reconstruction of the soma, dendrites and initial course of the axon of interneuron C in Fig. 6. B and C, series of confocal microscope images showing terminals of this interneuron and their relationships with immunoreactivity for neurotransmitter markers. B_a and C_a show projected images of the axon (red) through a number of optical sections; panels b–d show single optical sections illustrating axon terminals (red, arrowheads) and neurotransmitter

Table 1. Association of terminals of GABAergic/glycinergic interneurons with VGLUT1-immunoreactive axons

Cell Ref. in Fig. 8	No. of terminals analysed	No. associated with VGLUT1 terminals
A	110	60
B	105	10

systematic comparison of excitatory and inhibitory interneurons according to input, morphology and immunohistochemistry. Recently, spike-triggered averaging has been used to analyse actions of premotor interneurons on motoneurons in lamprey (see, e.g. Biro *et al.* 2008), frog tadpole (see, e.g. Li *et al.* 2007), zebra fish (see, e.g. Ritter *et al.* 2001) and neonatal rats and mice *in vitro* (Butt *et al.* 2002; Butt & Kiehn, 2003; Kiehn & Butt, 2003; Kiehn, 2006; Quinlan & Kiehn, 2007). Records from these interneurons were obtained by using whole-cell-tight-seal recording that also permitted the use of intracellular markers and subsequent visualization of recorded cells. Comparison of morphology of excitatory and inhibitory subpopulations of these neurons involved mapping cell locations and projections of stem axons. The pharmacology of their actions on motoneurons was analysed by using antagonists to putative neurotransmitters and examining firing patterns during fictive locomotion or other forms of rhythmic activity. However *in vitro* preparations provide limited opportunities to analyse input to neurons and to differentiate between input-output related functional subpopulations. In the present study we used immunohistochemistry to identify excitatory and inhibitory intermediate zone interneurons in reflex pathways from group I and II muscle afferents which were labelled intracellularly (Bannatyne *et al.* 2003, 2006; Stecina *et al.* 2008).

Methods

Preparation

The experiments were performed on a total of 13 young adult cats under deep anaesthesia. All procedures were approved by the Göteborg University Ethics Committee and complied with US National Institutes of Health and European Union guidelines. General anaesthesia was induced with sodium pentobarbital

(40–44 mg kg⁻¹, I.P.) and maintained with intermittent doses of α -chloralose as required to maintain full anaesthesia (Rhône-Poulenc Santé, France; doses of 5 mg kg⁻¹ administered every 1–2 h, up to 55 mg kg⁻¹, I.V.) after cannulation of the trachea, one carotid artery and both cephalic veins. Blood pressure and heart rate were monitored continuously. Additional doses of α -chloralose were given when increases in blood pressure or heart rate were evoked by noxious stimulation, or if the pupils dilated. During recordings, neuromuscular transmission was blocked by pancuronium bromide (Pavulon, Organon, Sweden; about 0.2 mg kg⁻¹ h⁻¹ I.V.) and the animals were artificially ventilated. Mean blood pressure was kept at 100–130 mmHg and the end-tidal concentration of CO₂ at about 4% by adjusting the parameters of artificial ventilation and the rate of continuous infusion of a bicarbonate buffer solution with 5% glucose (1–2 ml h⁻¹ kg⁻¹). Core body temperature was kept at about 37.5°C by servo-controlled infrared lamps. Experiments were terminated by a lethal dose of pentobarbital followed by perfusion with a solution of paraformaldehyde.

The third to seventh lumbar (L3–L7), and low thoracic (Th11–Th13) segments were exposed by laminectomy. Neurons in the lumbar segments were approached through small holes (about 1–2 mm²) made in the dura mater. Two pairs of stimulating electrodes were placed in contact with the left and right lateral funiculi at low thoracic levels to allow detection of neurons with axons ascending beyond this level by antidromic activation using stimulus intensities of 1 mA. Two contralateral hindlimb nerves (the quadriceps, Q and sartorius, Sart) and a number of ipsilateral nerves were transected and mounted on stimulating electrodes. The latter included Q, Sart, the posterior biceps and semitendinosus (PBST), anterior biceps and semi-membranosus (ABSM), gastrocnemius and soleus (GS), plantaris (Pl) and deep peroneal (DP) nerves. The nerves were stimulated by constant voltage 0.2 ms long current pulses, with the intensity expressed in multiples of threshold (*T*) for the most excitable fibres in a given nerve. In most experiments a tungsten electrode (impedance 40–250 k Ω) was placed in the ipsilateral medial longitudinal fascicle (MLF) after having exposed the caudal part of the cerebellum. The electrode was inserted at an angle of 30 deg (with the tip directed rostrally). The initial target was at Horsley–Clarke

markers: the sequence in *Bb–d* shows that the terminals are immunoreactive for VGLUT2 (blue) but not GAD (green). *Cb–d*, no association was found with either VGLUT1 (shown in blue) or gephyrin (shown in green). *Da–d*, a series of single optical sections showing contacts between the terminals of this axon (red, arrows) and the soma (*a* and *b*) and dendrites (*c* and *d*) of motoneurons labelled with antibodies raised against ChAT (green) in the lateral motor nucleus of the L6 segment. VGLUT2 immunoreactivity is shown in blue. Scale bars: *A* 100 μ m; *Ba–d* 5 μ m; *Ca* 5 μ m; *Cb–d* 2 μ m; *Da, Dc* 5 μ m; *Db, Dd* 2 μ m.

co-ordinates P9, L0.6, H-5 but its final position was adjusted on the basis of records of descending volleys from the surface of the lateral funiculus at the Th11 level. The site of the tip of the electrode was marked by an electrolytic lesion (0.4 mA constant current passed for 10 s) and subsequently verified on 100 μm thick frontal sections of the brainstem, cut in the plane of insertion of the electrodes using a freezing microtome.

Cells to be labelled were selected on the basis of input from group II or both group I and II afferents and axonal projections restricted to the lumbosacral enlargement (cells antidromically activated from the last thoracic segment were not included in the sample). A search was made in the L3–L7 segments, within regions 1–2 mm apart, where distinct field potentials were evoked from both group I and II afferents (Edgley & Jankowska, 1987*a,b*). The sample was intentionally non-homogeneous and included interneurons projecting ipsilaterally as well as contralaterally (i.e. intermediate zone commissural interneurons). Short distance projections (ipsilateral and/or contralateral) were defined by reconstructing the trajectories of the axons. Longer distance projections were established by antidromic activation of some of the interneurons from the area between the gastrocnemius–soleus and posterior semitendinosus motor nuclei where stimuli (0.2 ms, 5–100 μA) were applied via a thin tungsten electrode (100–300 k Ω).

Electrophysiological analysis of the labelled interneurons and their classification

Micropipettes with tips broken to about 2 μm , filled with a mixture of tetramethylrhodamine-dextran and Neurobiotin in saline (see next section) with impedances of 12–20 M Ω were used. Recording from neurons commenced prior to penetration, provided that extracellular spike potentials were sufficiently distinct. At this stage it was verified that the neurons were (1) activated by stimulation of the Q nerve and/or other muscle nerves at 5T and at latencies compatible with oligosynaptic input, (2) that they were activated antidromically from the contralateral G-S motor nuclei (when tested), and (3) that they were not activated antidromically by stimuli applied to the lateral funiculi at the low thoracic level. A collision test with synaptically evoked spikes was used in order to evaluate whether the neurons were activated antidromically. After penetration, effects of the same stimuli were rapidly scanned to ensure that we had penetrated the same neuron; thereafter the ejection of the marker was started by passing a depolarizing current. More detailed analysis of the peripheral and descending input to the labelled neurons was made while the depolarizing current was passed. To this end, PSPs evoked by stimulation of all

of the dissected nerves were first recorded while using 5T stimuli and graded stimuli were subsequently applied only to the effective nerves. If the condition of a neuron allowed, recording was repeated after labelling had been completed but the best quality records were usually obtained just after the penetration (when the injury discharges stopped) and at the beginning of the injection. Unless stated otherwise, all of the records illustrated were obtained at the beginning of depolarization. In cases where the electrode penetrated an interneuron which had not been analysed extracellularly, characterization of the neuron was made intracellularly and the beginning of the ejection of the marker was delayed. Both original records and averages of 10–20 records made on-line were stored using a sampling and analysis system of E. Eide, T. Holmström and N. Pihlgren, Göteborg University.

The aim of the study was to compare excitatory and inhibitory intermediate zone interneurons. However, in order to achieve this, it was necessary to differentiate these cells from two other populations of interneurons that have been previously described: (1) dorsal horn interneurons located more dorsally and (2) lamina VIII interneurons located more ventrally (Edgley & Jankowska, 1987*b*; Jankowska *et al.* 2005) both of which have input from group II but not from group I afferent fibres. When somata of labelled interneurons were located within laminae VI–VII, IV–V or VIII, classification was straightforward. However, additional criteria were required to establish the identity of neurons located within the border zones between laminae V and VI and between laminae VII and VIII where different cell categories may be intermixed. In such cases additional criteria based on established properties of larger samples of interneurons at various locations were used. ‘Typical’ dorsal horn or lamina VIII interneurons were not found to be coexcited by group I afferents and those which were coexcited were classified as intermediate zone interneurons even if their somata were located in the most ventral part of lamina V or the most dorsal part of lamina VIII. Conversely, interneurons located within the same border zones but not coexcited by group I afferents or showing typical properties of lamina VIII interneurons were classified as belonging to that class. Such properties included selective input from either MLF or group II afferents to lamina VIII interneurons (Jankowska *et al.* 2003, 2005). After applying these principles, only one inhibitory interneuron located within the lamina VII–VIII border zone was classified as not belonging to the group of intermediate zone interneurons (see interneuron no. 14 in the companion paper: Jankowska *et al.* 2009) and three excitatory interneurons were classified as belonging to the group of intermediate zone interneurons because they were coexcited by group I and II afferents (interneurons B and D in Fig. 6 and G in Fig. 7) or by group II afferents and from the MLF (interneuron P in Fig. 7).

Labelling and morphological and immunocytochemical analysis of the interneurons

Commissural interneurons were labelled intracellularly with a mixture of equal parts of 5% tetramethyl-

rhodamine-dextran (Molecular Probes, Eugene, OR, USA) and 5% Neurobiotin (Vector Laboratories, Peterborough, UK) in saline (pH 6.5). The marker was applied by passing 5 nA positive constant current for 5–8 min. At the end of the experiment the

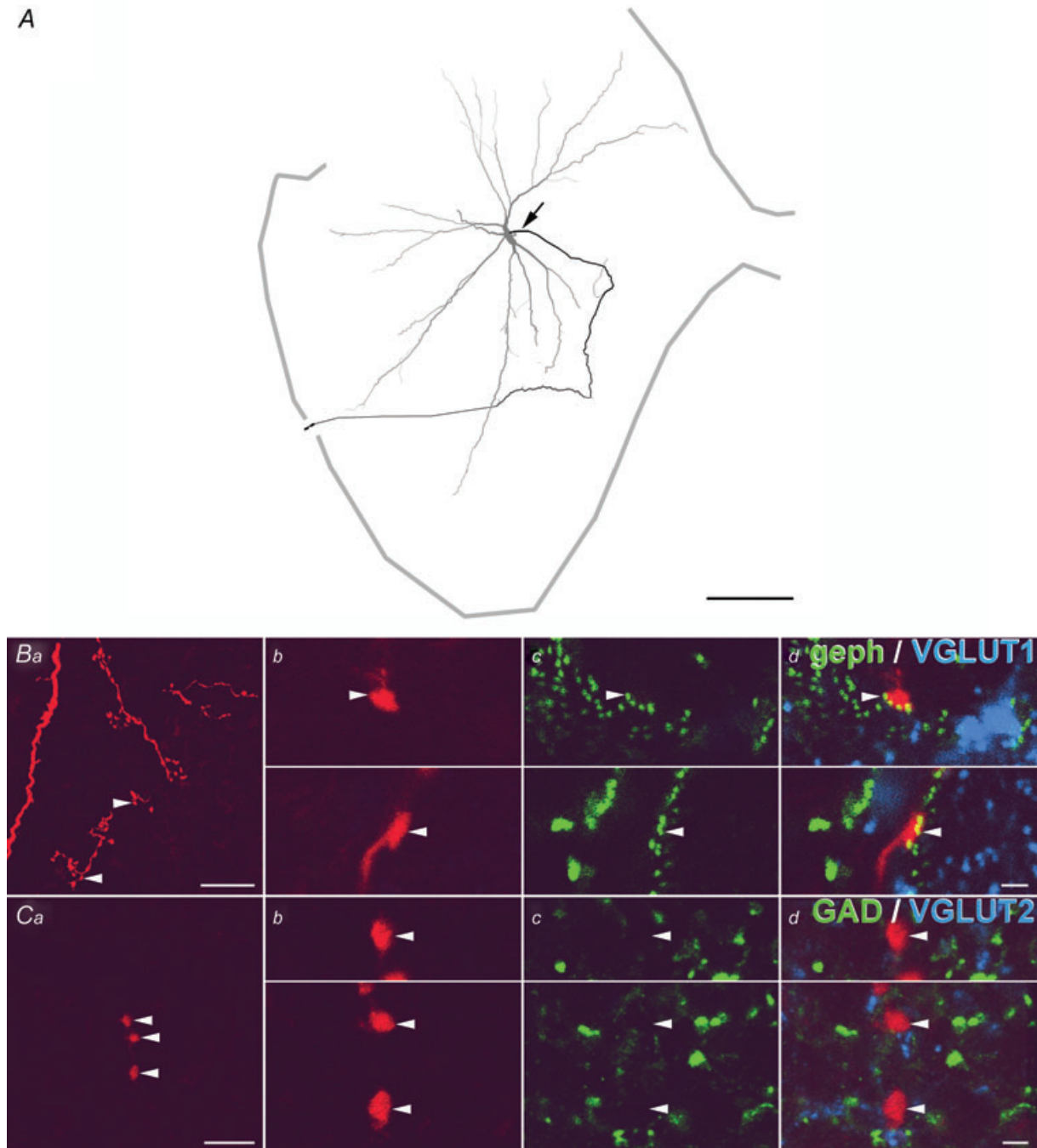


Figure 2. An ipsilaterally projecting glycinergic interneuron

A, reconstruction of the soma, dendrites and initial course of the axon of interneuron M in Fig. 7. B–C, series of confocal microscope images showing terminals of this interneuron and their relationship with immunoreactivity for neurotransmitter markers. Panel a in each case shows a projected image of the axon (red) through a number of optical sections; panels b–d show single optical sections illustrating axon terminals (red, arrowheads) and neurotransmitter markers. The sequence in Bb–d shows that the terminals are apposed to gephyrin puncta (green) but do not contain VGLUT1 (blue) and the images in Cb–d confirm that there is no association with either VGLUT2 (shown in blue) or GAD (shown in green). Scale bars: A 100 μm ; Ba, Ca 10 μm ; Bb–d 5 μm ; Cb–d 2 μm .

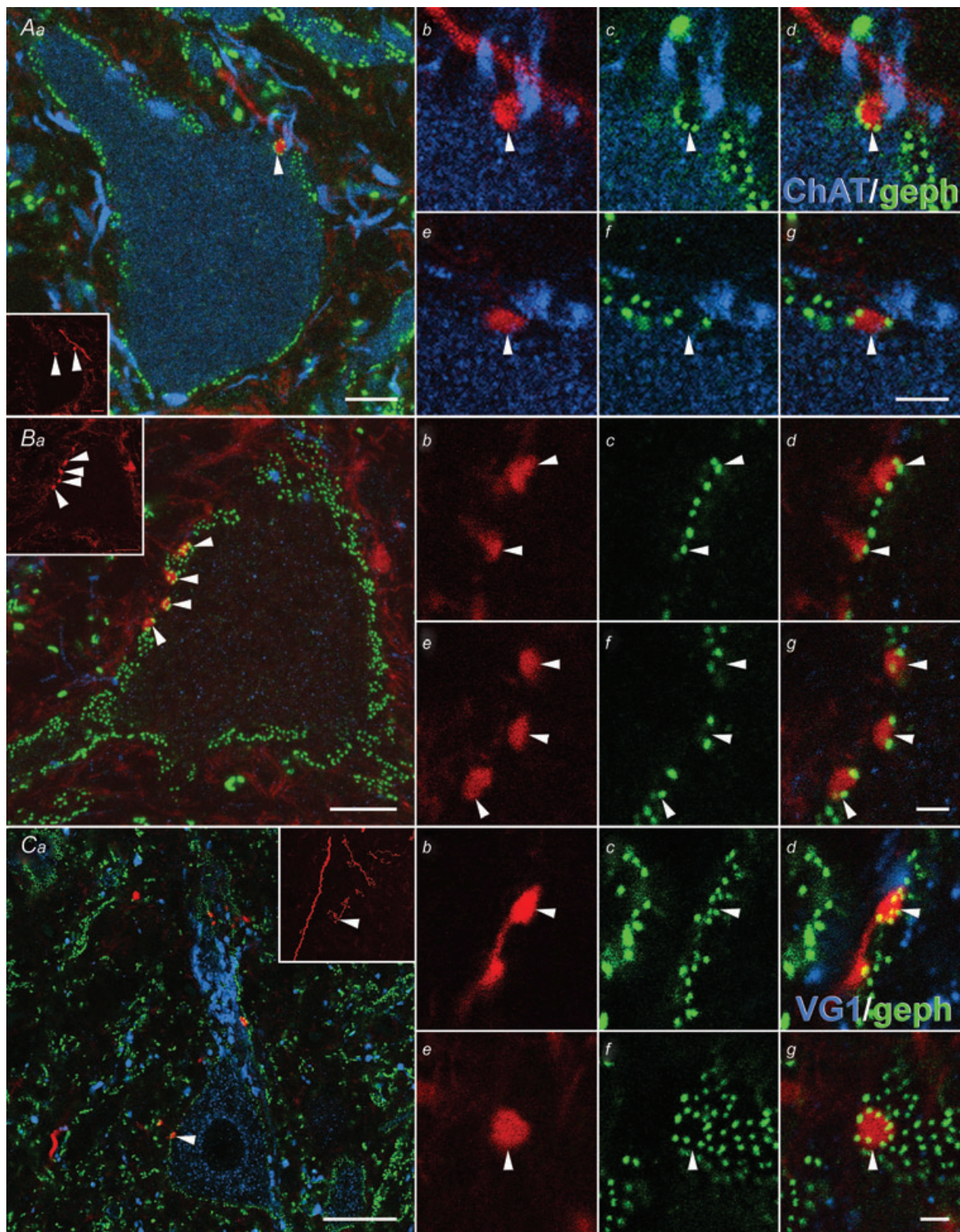


Figure 3. Postsynaptic targets of inhibitory interneurons

Series of images showing contacts formed by terminals of inhibitory interneurons J, D and M in Fig. 7 with ventral horn neurons. Note that all of the putative contacts are associated with gephyrin immunoreactivity, thus confirming that they are synaptic in nature. *A*, a motoneuron which is labelled positively for ChAT (blue). *B*, a gephyrin rich cell at the border between lamina VII and IX. *C*, a lamina VII cell with a high density of VGLUT1 terminals on proximal

animals were perfused through the descending aorta with a solution containing 4% paraformaldehyde in phosphate buffer. Sections containing labelled interneurons were reacted firstly with avidin–rhodamine (1:1000, Jackson ImmunoResearch, Luton, UK) and the transmitter content of terminals was identified by incubating sections containing axonal processes in a combination of antibodies for either vesicular glutamate transporter 1 (VGLUT1, 1:5000; Chemicon, Harlow, UK) and gephyrin (1:100, Synaptic Systems, Gottingen, Germany), or a second combination containing antibodies for glutamic acid decarboxylase (GAD; recognizing both 65 and 67 isoforms, 1:2000; Sigma, Poole, UK) and vesicular glutamate transporter 2 (VGLUT2, 1:5000; Chemicon) as previously described (Bannatyne *et al.* 2006). Axonal contacts formed with motoneurons were revealed by using antibodies for choline acetyltransferase (ChAT 1:100, Chemicon). The sections were scanned with a confocal laser scanning microscope (Biorad 1024, Zeiss, Hemel Hempstead, UK) and reconstructions of somata and dendritic trees were drawn using NeuroLucida for Confocal (MBF Bioscience, Williston, Vermont, USA). Axonal projections, including terminal branches and/or terminals, were mapped for the total sample of 38 labelled neurons (see Table 1).

Results

Identification of excitatory and inhibitory interneurons

Transmitter content could be defined for terminals of 38 labelled interneurons analysed in this study. VGLUT2 was found in terminals of 14 interneurons and therefore these cells were glutamatergic and excitatory. Twenty-two interneurons had terminals that apposed gephyrin puncta but were not immunoreactive for GAD and hence were glycinergic. Terminals from the remaining two interneurons were immunolabelled for GAD and apposed gephyrin puncta and thus were likely to contain a mixture of GABA and glycine.

Glutamatergic interneurons

The sample of glutamatergic interneurons included five ipsilaterally projecting, six bilaterally projecting and three contralaterally projecting interneurons. Interneurons with contra- or bilateral projections are described in more detail in the accompanying publication (Jankowska *et al.* 2009).

Figure 1 shows details of a typical ipsilaterally projecting glutamatergic interneuron.

Glycinergic interneurons

All 22 glycinergic cells had ipsilateral projections (see below). Axon terminals of these cells apposed gephyrin puncta but were not immunoreactive for VGLUT1, VGLUT2 or GAD. Properties of a typical glycinergic interneuron are shown in Fig. 2.

Target cells of glutamatergic and glycinergic interneurons

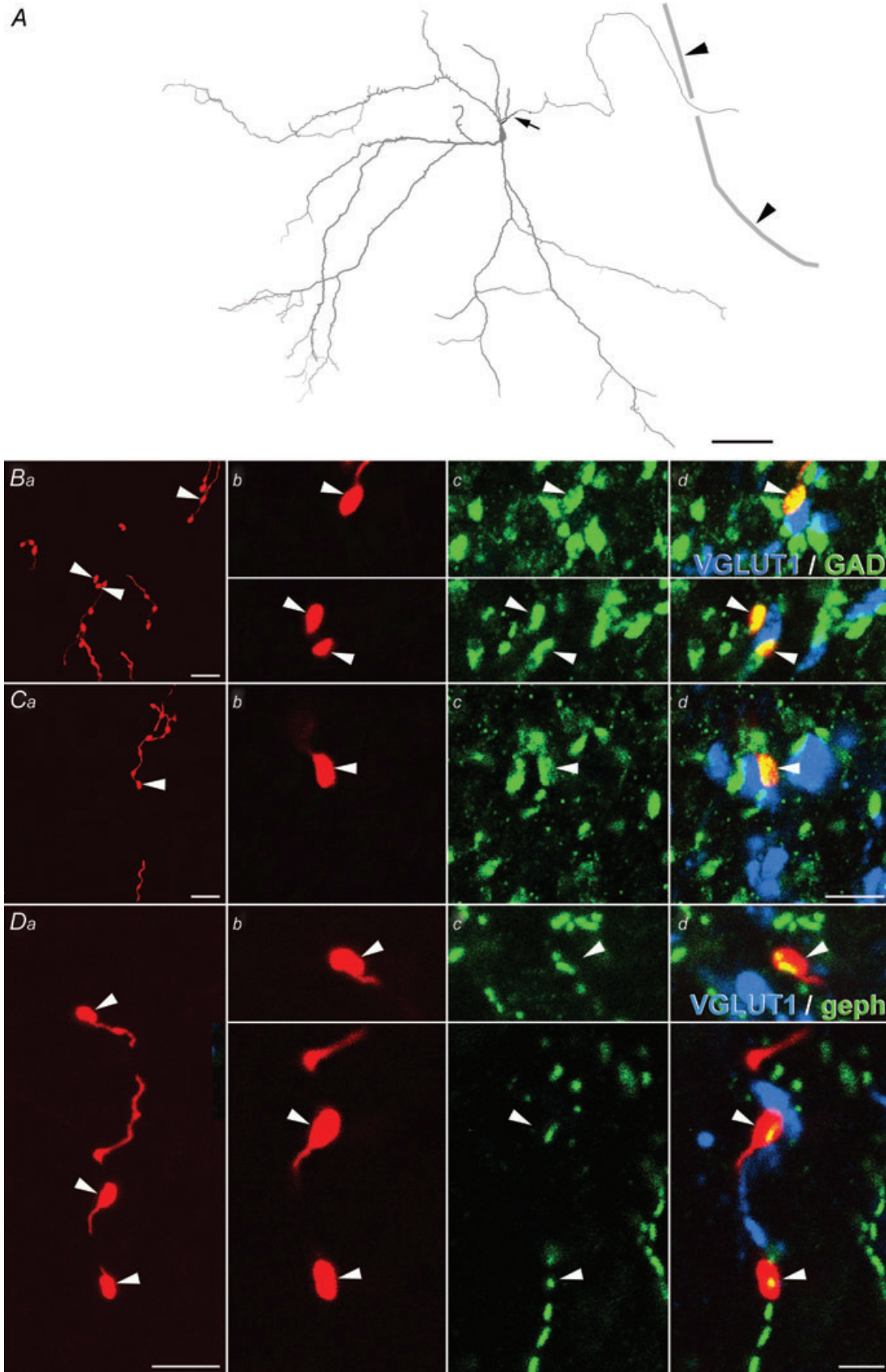
The majority (4/5) of glutamatergic cells with ipsilateral terminations within motor nuclei formed contacts with cell bodies and dendrites of motoneurons which were identified by using ChAT immunoreactivity (Fig. 1D). In addition, many terminals were located in regions outside motor nuclei where they formed contacts with unidentified neurons. However, none of the contralaterally projecting interneurons could be shown to form contacts with motoneurons, although one out of the three cells labelled had terminations within motor nuclei. Finally, only one of the six bilaterally projecting interneurons made contacts with ipsilateral motoneurons. Findings from electrophysiological studies to investigate target cells of group I and II activated commissural interneurons are discussed in the accompanying paper (Jankowska *et al.* 2009).

Glycinergic interneurons (9/22) also made contacts with cell bodies and dendrites of motoneurons within ipsilateral motor nuclei and with cells in areas surrounding them (Fig. 3A). Motoneurons could readily be identified by the presence of ChAT immunoreactivity and, as gephyrin is found at postsynaptic densities (e.g. see Todd *et al.* 1995), this confirms that such contacts are synaptic. On a limited number of occasions we were able to discern characteristics of other target cells of the labelled interneurons in addition to motoneurons. Firstly, they formed contacts with gephyrin-rich cells located at the border of laminae VII and IX (Fig. 3B). They also contacted cells with concentrations of VGLUT1 terminals on proximal dendrites (Fig. 3C).

GABAergic/glycinergic interneurons

Two of the cells in the sample had axon terminals that apposed gephyrin puncta but were also immunoreactive

areas of the dendritic tree. Left hand panels (a) show images projected from several sections; small panels (b–d, e–g) show details of the axon (red), apposed gephyrin puncta (green) and either ChAT (A, blue) or VGLUT1 (C, blue). Insets Ba and Ca show projected images of the axon collaterals present in each section. Scale bars: Aa, Ba, Ca 5 μ m; panels b–d and e–g 2 μ m.



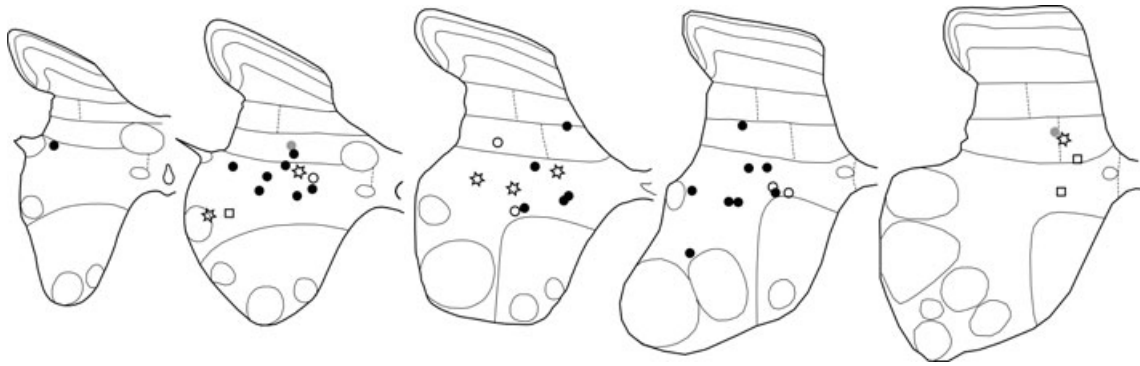


Figure 5. Location of excitatory and inhibitory interneurons

Location of cell bodies of labelled interneurons. Circles, squares and stars represent cells with ipsilateral, contralateral and bilateral projections, respectively; open symbols denote glutamatergic, filled black symbols glycinergic and filled grey symbols GABAergic cells.

for GAD. Properties of one of these cells are shown in Fig. 4. Neither cell had terminals that were immunoreactive for VGLUT1 or VGLUT2. However, their terminals formed associations with other axon terminals that were immunoreactive for VGLUT1, which is localized principally within large myelinated primary afferent fibres (Varoqui *et al.* 2002; Todd *et al.* 2003). Approximately 50% of the terminals of the first cell and 10% of the second formed close appositions with VGLUT1 immunoreactive terminals (Table 1) but no appositions were formed with VGLUT2-containing axons. Gephyrin immunoreactivity was not present at the site of contact between interneuron and VGLUT1 terminals but was present at other locations (Fig. 4D), on the same interneuron terminals which were probably sites of contact with dendrites or cell bodies of other cells.

Comparison of location, somata and dendritic trees of excitatory and inhibitory interneurons

A search was made for interneurons to be labelled primarily in the L4–L6 segments but some were penetrated in the L3 and L7 segments. In all of these segments, cell bodies of the current sample of interneurons were located within laminae VI–VII. No obvious differences were observed between the locations of inhibitory *versus* excitatory interneurons, which were intermixed in all laminae (Fig. 5), or in the organization of their dendritic

trees, which ramified within laminae IV to IX but rarely extended into the white matter; cf. e.g. dendritic trees of interneurons illustrated in Fig. 1A and Fig. 2A and of interneurons illustrated in Figs 1A and 2A in the companion paper. Cell bodies of glycinergic interneurons tended to be smaller than those of glutamatergic interneurons, with diameters $39.4 \pm 11.9 \mu\text{m}$ and $48.1 \pm 14.3 \mu\text{m}$, respectively (mean \pm standard deviation; glycinergic $n = 13$, glutamatergic $n = 8$) but this difference was not statistically significant (Student's *t* test; $P < 0.05$). The diameters were measured as diameters of equivalent circles from projected images using ImageJ software (available from NIH, USA).

Comparison of axonal projections and terminal projection areas of glutamatergic and glycinergic interneurons

In contrast to the similarities in location of cell bodies and morphology of dendritic trees, major differences were found in axonal projections of glutamatergic and glycinergic intermediate zone interneurons. As stated above, excitatory interneurons were found to project ipsilaterally, bilaterally or contralaterally while axonal projections of inhibitory interneurons were exclusively ipsilateral. Projections of individual excitatory and inhibitory interneurons are shown in Figs 6 and 7. For further details of projections of commissural interneurons

Figure 4. Immunocytochemistry of a GABAergic/glycinergic interneuron

A, reconstruction of the soma, dendrites and initial course of the stem axon (arrow) of one of the interneurons (A in Fig. 8). The axon of this cell entered the dorsal column (border indicated by grey line and arrowheads on right). B–D, series of confocal microscope images showing terminals of the interneuron and their relationships with immunoreactivity for neurotransmitter markers. Panel a in each case shows a projected image of the axon (red) through a number of optical sections; panels b–d show single optical sections illustrating axon terminals (red, arrowheads). Terminals of this interneuron were immunoreactive for GAD (B and C; green) and associated with gephyrin puncta (D; green). Terminals were frequently observed apposed to profiles that were immunoreactive for VGLUT1 (Bd, Cd; blue). Scale bars: A 100 μm ; Ba, Ca 10 μm ; Bb–d 5 μm ; Cb–d 2 μm .

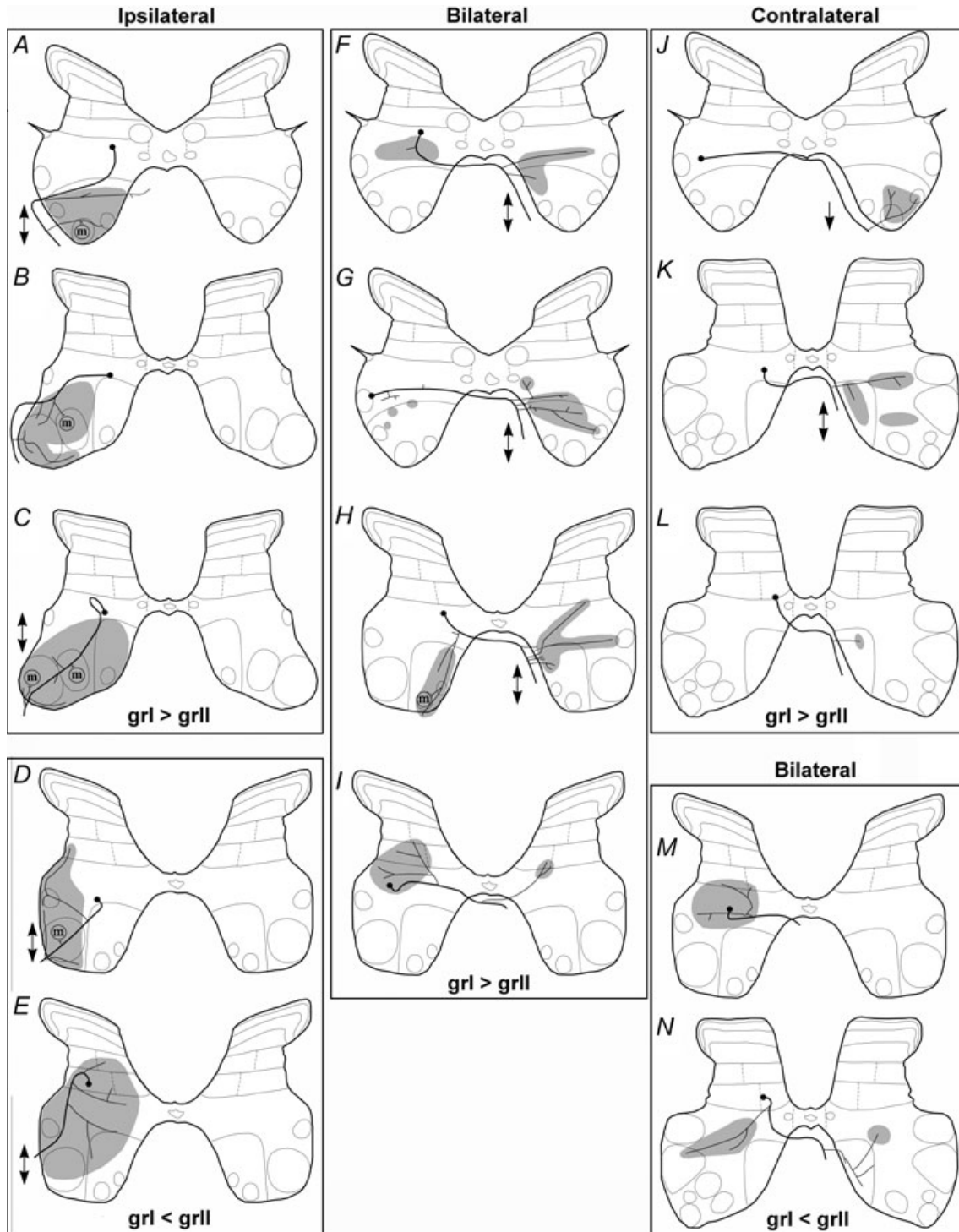


Figure 6. Projection areas of excitatory interneurons

A–N Circles represent somata and thick lines stem axons, and shading summarizes locations of terminals for all rostrocaudal levels where terminals were observed. Arrows indicate rostral and/or caudal projections where the axon could be followed more than 250 μm in either direction from the soma. 'm' indicates presence of synaptic contacts with interneurons. Cells are grouped depending on whether the axonal projections were ipsilateral (A–E), bilateral (F–I, M, N) or contralateral (J–L) and also on the basis of their dominant excitatory input from group I or from group II afferents. gr I < gr II and gr I > gr II at the bottom of each frame indicate that in neurons depicted in this frame monosynaptic EPSPs evoked from group I afferents were smaller or larger than EPSPs from group II afferents.

of our sample as well as of more ventrally located interneurons, see the accompanying paper (Jankowska *et al.* 2009).

Figure 6 shows that stem axons of ipsilaterally projecting interneurons run towards the white matter within a short distance from the soma and enter either the middle or the ventral part of the lateral funiculus, or the ventral funiculus, after giving off a number of initial axon collaterals. A similar pattern of projection was found for ipsilaterally projecting glycinergic interneurons (Fig. 7). Both figures show also that on entering the white matter the stem axons commonly bifurcated and projected both rostrally and caudally. Axonal projections of all contralaterally projecting glutamatergic interneurons were similar; their stem axons were directed towards the ventral commissure where they crossed the midline within about 0.5 mm distance from the soma and entered the contralateral ventral funiculus. The most strongly labelled axons could be followed both caudally and rostrally (see arrows in Fig. 6) for up to 1–2 mm total distances and gave rise to axon collaterals that ramified within the contralateral ventral horn. Stem axons of bilaterally projecting glutamatergic interneurons behaved in the same way as the contralaterally projecting ones. Their ipsilateral projections were found exclusively within the grey matter and none entered the ipsilateral lateral or ventral funiculi, which indicates that they might have affected contralaterally located neurons over a length of spinal cord but act fairly locally ipsilaterally.

Although stem axons of ipsilateral glycinergic and glutamatergic cells had different trajectories, their terminal projection areas were similar. These included motor nuclei as well as other regions of the grey matter, principally the intermediate region and lamina VII and VIII. The distribution of terminal projection areas appeared in part to be related to the location of interneurons as there was a tendency for interneurons located in the L3 and 4 segments to terminate primarily in laminae VI–VIII and for interneurons located in the L5 and L6 segments to extend their projection areas to lamina IX. However, only the terminal branches of the earliest axon collaterals could be reconstructed and therefore we cannot exclude the possibility that more caudally located motoneurons are the main targets of these interneurons.

Axonal projections of GABAergic/glycinergic interneurons

Projection areas of the two cells that had GAD-immunoreactive axons and apposed gephyrin puncta are shown in Fig. 8. The cell body of the first interneuron was located in the central part of lamina VI with the major dendritic fields confined laterally and ventrally in the grey matter of laminae V–VII (Fig. 4A).

The axon gave rise to several collaterals before entering the ipsilateral dorsal column. The axon collaterals terminated within the envelope of the dendritic tree and deeper within lamina VII and IX. The soma and dendrites of the second cell were also located within lamina VI and its axon could be followed to the dorsal part of the lateral funiculus where it bifurcated to run both rostrally and caudally. Collateral axons were observed in the intermediate grey matter and also more ventrally. Records show that neuron A was excited by group I afferents of gastrocnemius soleus but not by group II afferents because the amplitude of the EPSPs evoked by near maximal stimulation of group I afferents did not increase when the intensity of the stimuli was increased from 2*T* to 5*T* to include group II afferents. In contrast EPSPs evoked in neuron B appeared only when the intensity of the stimuli was increased from 2*T* to 5*T*. However, in both neurons IPSPs were apparently evoked from both group I and II afferents as indicated both by threshold and latency. Axonal projections of these neurons were located in regions that would be predicted for interneurons mediating presynaptic inhibition of group Ia, Ib and II afferents (for references see Jankowska, 1992 and Rudomin & Schmidt, 1999).

Comparison of input to excitatory and inhibitory interneurons

Figure 9 and Table 2 show that group I and group II afferents provided input to all three subgroups of excitatory interneurons as well as to inhibitory interneurons. Peripheral nerves were stimulated with different stimulus intensities to allow differentiation of synaptic actions from group Ia muscle afferents and group Ib tendon organ afferents (pooled as group I afferents) and from group II muscle spindle afferents. PSPs evoked by stimuli not exceeding 2*T* (at latencies not exceeding 1.1 ms for monosynaptic EPSPs and 1.8 ms for disynaptic EPSPs or IPSPs) were classified as evoked by group I afferents whereas PSPs evoked at thresholds between 2*T* and 4*T* (at latencies ranging between 2 and 4.5 ms) were classified as evoked from group II afferents.

For the majority of neurons, quantitative estimates of the relationships between excitatory input from group I and II afferents to individual neurons were approximate because comparisons of amplitudes of EPSPs evoked from these afferents were hampered by several factors. There was overlap between EPSPs and IPSPs that either followed monosynaptic EPSPs from group I afferents or both preceded and followed EPSPs from group II afferents. Another factor was rapidly progressive deterioration of the majority of the neurons caused by penetration and the resulting depolarization (with frequent injury discharges) which was exacerbated by the passage of current needed to inject the marker and an increase in the volume of the neurones. However, the passage of 5 nA depolarizing

current would not have interfered with detection of EPSPs by itself. This was indicated by records from neurones that were only moderately affected by the penetration (as judged by their membrane potential and amplitudes of action potentials) where amplitudes of monosynaptic EPSPs decreased by only some 20–30% during 5–10 min of passage of 5 nA. This interpretation is supported by previous studies where considerably stronger depolarizing current was needed to bring the neurones to the reversal potential of EPSPs (see, e.g. Flatman *et al.* 1982) or where amplitudes of EPSPs remained substantially unchanged during passage of 20–40 nA under similar experimental

conditions (see, e.g. Fetz *et al.* 1979). For these reasons we were only able to estimate whether input from group I afferents appeared stronger or weaker than input from group II afferents. In addition, we could not exclude the possibility that small EPSPs evoked from group I and II afferents were undetectable with the recording methods described or that there was input from group I and II afferents in untested peripheral nerves. Therefore, the numbers of neurones with inputs from these groups of afferents may be underestimated in Table 2.

Notwithstanding these limitations, excitatory input from group I afferents was generally stronger to excitatory

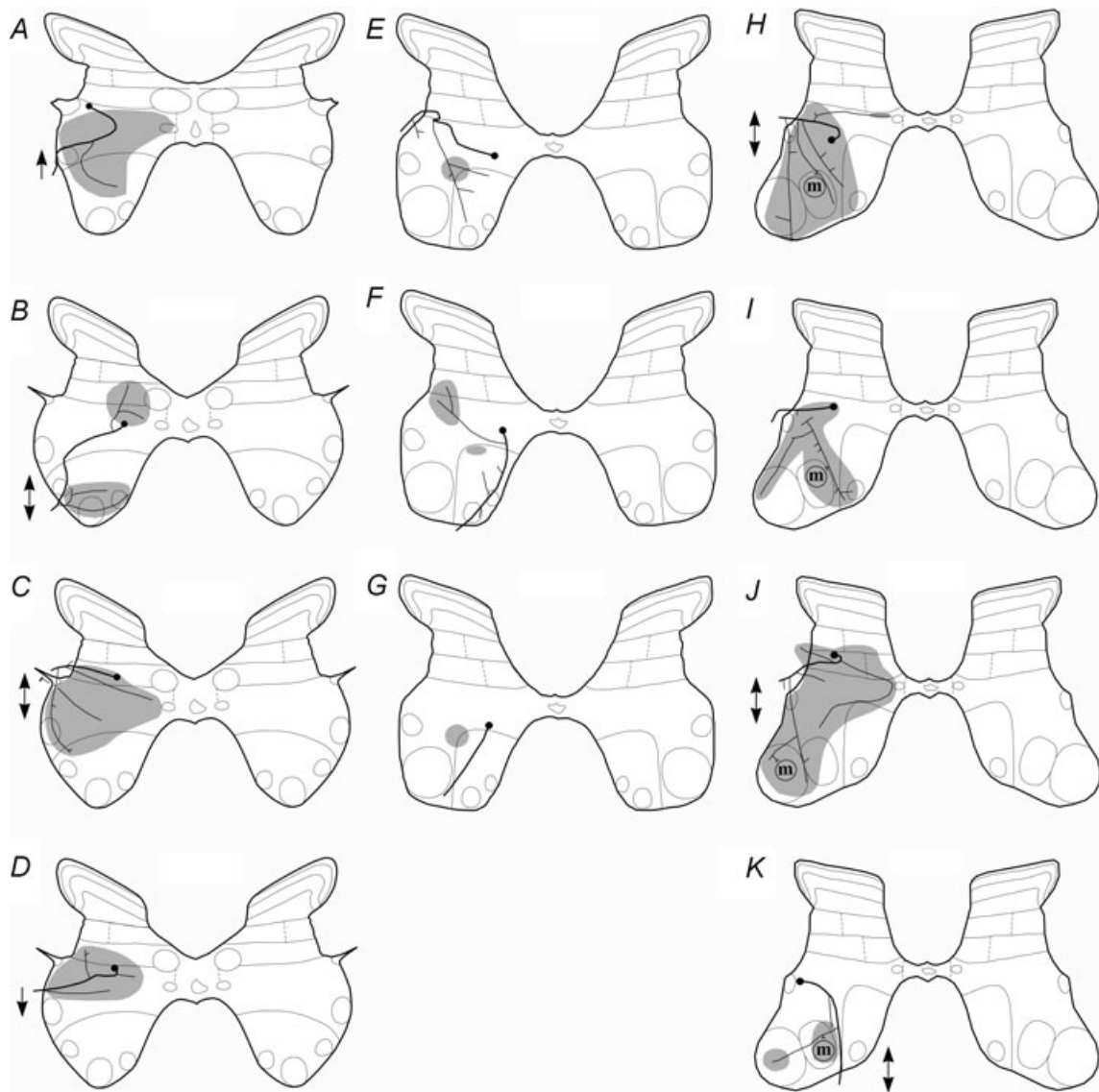


Figure 7. Projection areas of inhibitory interneurons

A–V, projection areas of 22 interneurons grouped depending on their dominant excitatory input from group I (A–K) or II afferents (L–V). Circles represent somata and thick lines stem axons, and shading summarizes locations of terminals for all rostrocaudal levels where terminals were observed as in Fig. 6. Arrows indicate rostral and/or caudal projections where the axon could be followed more than 250 μm in either direction from the soma.

interneurons, especially those projecting contralaterally, since monosynaptic EPSPs evoked from group I afferents were larger in amplitude than those from group II afferents in a greater proportion of excitatory interneurons (Table 2).

The presence of IPSPs following EPSPs was estimated from the extent of the declining slope of the EPSPs. As illustrated in the first and third columns in Fig. 9, IPSPs might have been minimal in the top records but the larger IPSPs could not only increase the declining slope of the EPSPs but also start during the rising slope of these EPSPs and prevent the full development of the EPSP (Fig. 10C). EPSPs evoked from group II afferents not only could be cut short by IPSPs that followed them, but were also often preceded by IPSPs; examples of this are shown in the

middle column in Fig. 9, where the approximate onset of the IPSPs is indicated by the second dotted line and of the EPSPs by the third dotted line.

In previous studies, evidence for IPSPs associated with faster decays was provided by reversal following Cl⁻ injection or hyperpolarization of the neurons. Such tests could not be made during labelling associated with passage of the depolarizing current, but reversal was occasionally seen when the cells remained in a relatively good state after the injection of Neurobiotin had been terminated.

Table 3 shows that no obvious differences occurred between sources of peripheral input to inhibitory and to ipsilaterally and contralaterally projecting excitatory neurons, as in all these subpopulations EPSPs and IPSPs were evoked from the same muscle nerves. In individual

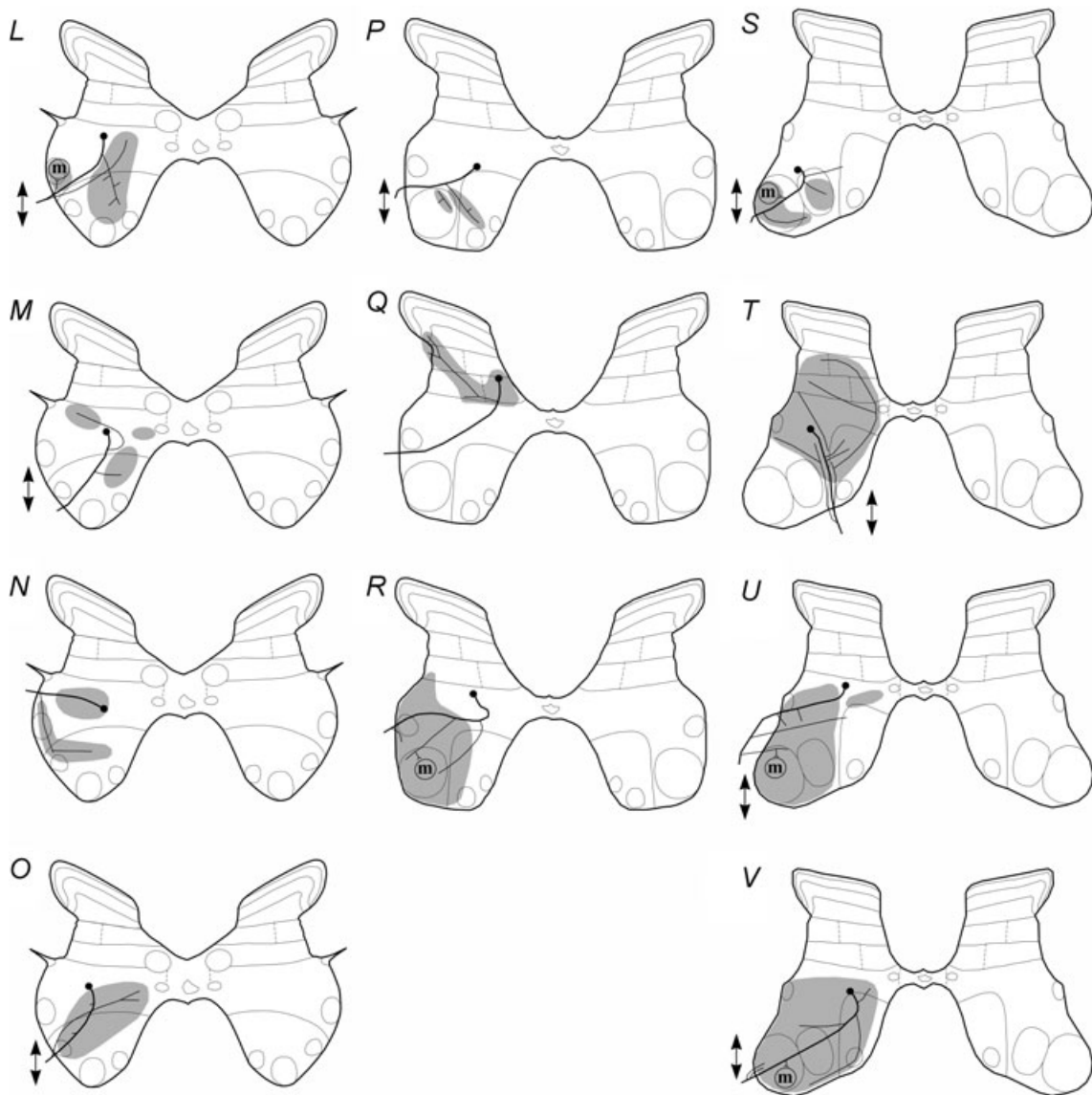


Figure 7. continued

interneurons both EPSPs and IPSPs were most often evoked from several nerves (1–3 nerves and 1–5 nerves, respectively). In some cases both excitation and inhibition could be evoked from the same nerve while only IPSPs were evoked from other nerves.

Reticulospinal fibres likewise were found to provide input to all three subgroups of excitatory interneurons as well as to inhibitory interneurons. The proportions of interneurons in which monosynaptic and disynaptic EPSPs and disynaptic IPSPs were evoked are given in Table 2 and an example of this is shown in Fig. 9D. These observations suggest that monosynaptic input from the MLF was strongest to ipsilaterally projecting excitatory interneurons but MLF fibres did not appear either to

favour or to counteract any particular subpopulations of intermediate zone interneurons which might assist the selection of excitatory interneurons during locomotion or after spinal cord lesions.

Discussion

Properties of intermediate zone interneurons

The most striking observations made in the present study were the major differences in axonal projections of the three classes of interneuron (defined according to their transmitter content), with direct input from group I and II muscle afferents. They show that excitatory

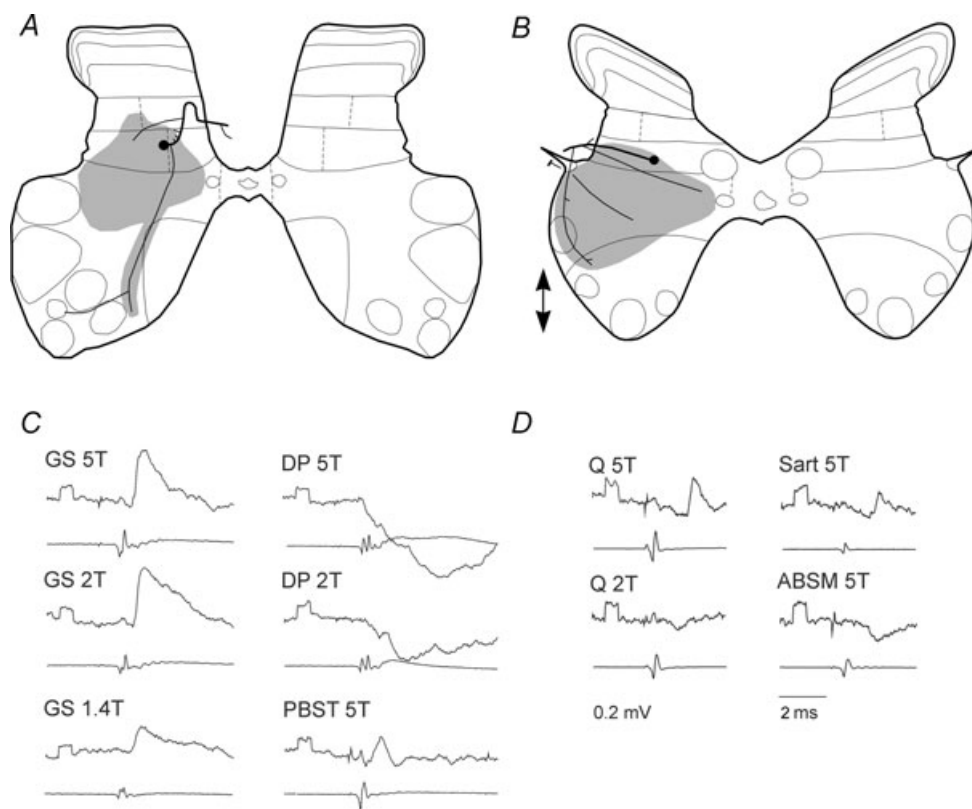


Figure 8. Axonal projection areas of GABAergic/glycinergic interneurons

A and B, location and reconstruction of axonal projections of two interneurons. Circles represent somata and thick lines stem axons, and shading summarizes locations of terminals for all rostrocaudal levels where terminals were observed. Arrows indicate rostral and/or caudal projections where the axon could be followed more than 250 μm in either direction from the soma of interneuron B. C and D, intracellular records from these interneurons obtained at the beginning of the injection of the marker by passing 5 nA depolarizing current (upper traces) and records from the cord dorsum of the afferent volleys (lower traces). They show that the first interneuron was excited by group I afferents of gastrocnemius–soleus (GS) and posterior biceps–semitendinosus (PBST) and the second by group II afferents of quadriceps (Q) and sartorius (Sart) and that they were inhibited by group I and II afferents of DP and by group II afferents of anterior biceps–semimembranosus (ABSM), respectively. The latencies of the EPSPs were 0.9 ms in C and 2.7 and 2.9 ms in D, in both cases from group I afferent volleys, and compatible with monosynaptically evoked actions of group I and group II afferents, respectively. 5T, 2T and 1.4T, stimulus intensity expressed in multiples of threshold intensities. In this and in the following figures all the records are averages of 10 or 20 consecutive single sweeps. Negativity is downwards in intracellular records and upwards in records of afferent volleys. Rectangular pulses at the beginning of the records are calibration pulses (0.2 mV). Time calibration (2 ms) in D is for all of the records.

intermediate zone interneurons not only target cells ipsilaterally or contralaterally but also bilaterally in the spinal grey matter. In contrast, inhibitory intermediate zone interneurons were found to project exclusively to ipsilateral target cells. This statement is valid for all cells classified as intermediate zone interneurons according to the criteria outlined in Methods. It should nevertheless be noted that we encountered one inhibitory interneuron with crossed projections that was located within the border zone between laminae VII and VIII (see interneuron no. 14 in the companion paper) which therefore could be considered as either an intermediate zone or a borderline lamina VIII interneuron. However, as its properties conformed with those of lamina VIII interneurons (Jankowska *et al.* 2003, 2005; see Methods), it was classified as lamina VIII rather than an aberrant intermediate zone interneuron.

The majority of *glutamatergic interneurons* that had projections which were exclusively ipsilateral formed direct contacts with motoneurons. It is therefore likely that most ipsilaterally projecting excitatory interneurons

activated monosynaptically by group I and II primary afferent axons have direct actions on motoneurons, thus corroborating conclusions from previous electrophysiological experiments (Edgley & Jankowska, 1987b; Cavallari *et al.* 1987). However, it is likely that the numbers of cells making such contacts and the numbers of contacts themselves were underestimated because labelling of the finest and most distal axon branches and terminals was incomplete even though stem axons were well labelled and could often be traced over several hundred micrometres.

The extent of terminal projection areas of glutamatergic interneurons of our sample shows that these interneurons formed terminations not only within motor nuclei but also within surrounding regions of the ventral horn and in the intermediate zone. Therefore, in addition to their actions on motoneurons, individual interneurons should provide excitatory input to other interneuronal or projection systems.

Axonal projections and target cells of bilaterally and contralaterally projecting glutamatergic interneurons are discussed in detail in the accompanying paper (Jankowska

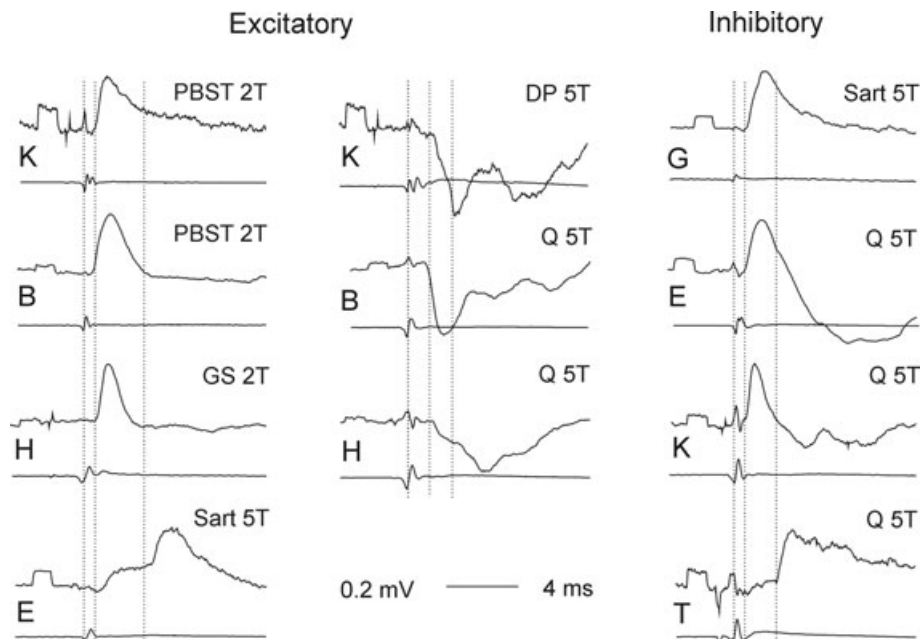


Figure 9. Examples of PSPs evoked in four excitatory interneurons and four inhibitory interneurons

Upper and lower traces in each panel are averaged intracellular records (negativity downwards; obtained during passage of 5 nA of depolarizing current) and records from the cord dorsum (negativity upwards), respectively. Intracellular records from the top to bottom are from excitatory interneurons labelled K, B, H and E in Fig. 6 and from inhibitory interneurons labelled G, E, K and T in Fig. 7, as indicated in each panel. Amplitudes of these records have been normalized to make it easier to compare the declining phases of EPSPs in the left and right columns. In the three top rows, amplitudes of EPSPs evoked from group I afferents exceeded those from group II afferents; they were evoked in excitatory interneurons projecting contralaterally, ipsilaterally and bilaterally, respectively, and in three ipsilaterally projecting inhibitory interneurons. In contrast, in the bottom row EPSPs evoked from group I afferents were smaller than those from group II afferents; they were evoked in ipsilaterally projecting excitatory and inhibitory interneurons. First dotted lines indicate the arrival of afferent volleys from group I afferents. Second and third dotted lines indicate the approximate onset of EPSPs from group I and from group II afferents in the left and right columns and of IPSPs of group I origin and EPSPs of group II origin in the middle row. Rectangular pulses at the beginning of records are voltage calibration pulses (0.2 mV). Time calibration (4 ms) is for all records.

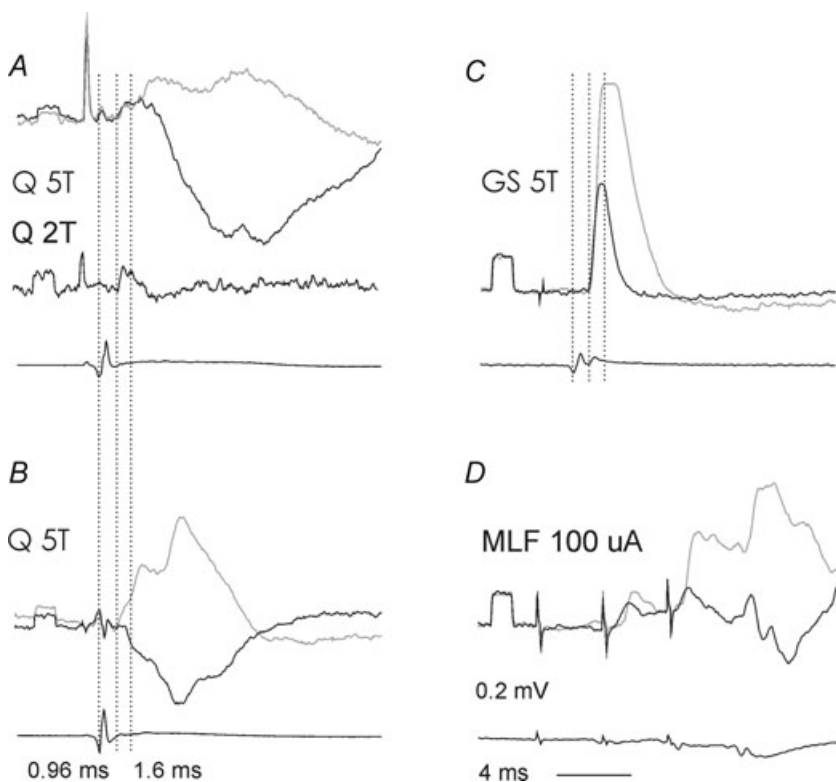
Table 2. Distribution of monosynaptic excitatory and inhibitory input from group I and II afferents and from the ipsilateral MLF to excitatory and inhibitory interneurons

	Glutamatergic			Glycinergic Ipsilateral	GABA/glycine Ipsilateral
	Ipsilateral	Bilateral	Contralateral		
<i>n</i>	5	6	3	22	2
Excitatory input					
Group I > II	3	4	3	11	1
Group I < II	2	2	0	11	1
MLF mono	4 of 4	1 of 4	1 of 3	8 of 18	
MLF disyn		3 of 4		5 of 18	
No MLF	0	0	2 of 3	5 of 18	2
Inhibitory input					
Group I and II	5	6	2	18	2
No IPSPs	0	0	1	4	
MLF disyn	2 of 4	3 of 4	2 of 3	7 of 18	
No MLF	0	0	1 of 3	11 of 18	2

The subgroups of interneurons are those illustrated in Figs 6–8. Excitatory input is classified as stronger either from group I ($I > II$) or from group II ($I < II$) afferents on the basis of comparison of amplitudes of monosynaptic EPSPs evoked by these afferents. Interneurons with input apparently from only group I afferents were included in the first group and interneurons with input apparently from only group II afferents were included in the second group. Input from the MLF was classified as monosynaptic when EPSPs were evoked at latencies not exceeding 0.9 ms from the first component of descending volleys evoked by stimulation of the MLF and did not show temporal facilitation when 2 or 3 as opposed to single stimuli were used (see Jankowska *et al.* 2003). EPSPs and IPSPs were classified as evoked disynaptically if they appeared at latencies 1–2 ms from descending volleys.

et al. 2009). Briefly, one out of the sample of six bilaterally projecting interneurons was found to form contacts with ipsilateral but not contralateral motoneurons and none of the three glutamatergic interneurons that had

projections that were exclusively contralateral formed direct contacts with motoneurons. However, all these cells had terminations within the ipsilateral intermediate zone, and contralaterally in a region that ‘mirrored’ ipsilateral

**Figure 10. Examples of reversal of IPSPs at the end of labelling**

A and *B–D*, upper traces: averaged intracellular records from two interneurons (*A* in Fig. 7 and *H* in Fig. 6); lowest traces in each panel are from the cord dorsum. Black records were taken during ejection of the marker by passage of 5 nA depolarizing current and grey records after the current was reduced to 0.5 or 0 nA and the cells repolarized. Dotted lines in *A*, *B* and *C* indicate afferent volleys and the onset of monosynaptic EPSPs and disynaptic IPSPs from group I afferents. Note large IPSPs following EPSPs during the depolarization and their subsequent reversal. Note also that IPSPs were evoked not only from group I afferents (*B* and *C*) and group II afferents (*A* and *B*) but also from the MLF (*D*).

Table 3. Proportions of glutamatergic and glycinergic interneurons in which monosynaptic EPSPs and oligosynaptic IPSPs were evoked by stimulation of group I and II afferents of various nerves

	Group I				Group II			
	Excitatory			Inhibitory	Excitatory			Inhibitory
	Ipsilateral	Bilateral	Contralateral	Ipsilateral	Ipsilateral	Bilateral	Contralateral	Ipsilateral
<i>n</i>	5	6	3	22	5	6	3	22
EPSPs from nerves:								
Q	2	5	1	7	4	2	0	13
Sart	1	1	1	1	2	1	1	7
PBST	2	1	1	3	0	0	0	0
ABSM	2	1	0	3	0	0	0	0
GS	2	4	1	1	0	0	0	0
DP	0	1	1	2	3	1	2	10
IPSPs from nerves:								
Q	4	4	2	14	1	5	0	9
Sart	5	2	0	2	1	4	0	4
PBST	2	0	0	3	0	0	0	1
ABSM	1	0	0	2	0	1	0	0
GS	2	1	0	1	1	1	0	0
DP	1	3	2	2	4	5	2	6
From same nerve as EPSP	4	4	2	10	3	5	1	10
From other nerves	11	6	2	14	4	11	1	10

PSPs evoked by stimuli not exceeding 2T were classified as being evoked from group I afferents, and as monosynaptic or disynaptic if the latencies were less than 1.1 ms (EPSPs) or 1.8 ms (EPSPs and IPSPs), respectively. PSPs evoked at thresholds 2–4T and latencies ranging from 2 to 4.5 ms were classified as being evoked from group II afferents.

terminations suggesting that these interneurons target similar types of neuron on both sides of the spinal cord and hence are well suited to be involved in left–right co-ordination of activity at a premotor level.

If contralaterally and bilaterally projecting intermediate zone interneurons form only sparse synaptic contacts with contralateral motoneurons, this would explain why interneurons located in laminae VI–VII were not labelled, or were labelled only occasionally, in experiments where retrograde transport (of either WGA-HRP or latex microspheres) from within contralateral motor nuclei led to labelling of interneurons located in lamina VIII (Alstermark & Kummel, 1986; Harrison *et al.* 1986; Jankowska & Skoog, 1986; Hoover & Durkovic, 1992).

All of the *glycinergic interneurons* in our sample gave rise to axonal projections that were exclusively ipsilateral but the termination regions of individual neurons varied. Some projected to motor nuclei and regions of lamina VII surrounding them whereas others were found to project only to regions outside motor nuclei, in particular within the intermediate zone itself. This observation is in good agreement with previous descriptions of terminal projection areas of intermediate zone interneurons of unknown transmitter phenotype that were labelled with HRP (Czarkowska *et al.* 1976; Bras *et al.* 1989) and of IPSPs recorded from the ventral roots by using spike-triggered averaging of population PSPs evoked by

single interneurons (Brink *et al.* 1981, 1983; Cavallari *et al.* 1987).

Although we did not specifically search for other target cells of glycinergic interneurons, we noted that some of them made contact with cells that were rich in gephyrin and were located at the border of laminae VII and IX. These cells are in a similar location to Renshaw cells which are also rich in gephyrin (Alvarez *et al.* 1997). However, the pattern of gephyrin labelling associated with cells described here appears to differ from that described by Alvarez *et al.* who showed that Renshaw cells are associated with intense rings of immunoreactivity (see their Fig. 1B). Furthermore, according to Gonzalez-Forero *et al.* (2005) most of the inhibitory cells that form synaptic contacts with Renshaw cells release a mixture of GABA and glycine. None of the terminals that formed contacts with gephyrin-rich cells contained GAD and therefore these cells are unlikely to be Renshaw cells. We also saw inhibitory contacts on a type of cell that has large numbers of VGLUT1-immunoreactive axons on proximal dendrites, and this will form the basis of a future report. We know that this type of cell receives powerful monosynaptic input from group I and II muscle afferents but that some of them are inhibitory whereas others are excitatory. The fact that they also have input from glycinergic cells that are activated by the same classes of afferent, provides an anatomical basis for the primary afferent-evoked disynaptic IPSPs that

are frequently observed to follow monosynaptic EPSPs recorded from intermediate zone interneurons in the present and other studies (see, e.g. Brink *et al.* 1983; Edgley & Jankowska, 1987b).

Consistent differences were not found between termination patterns of excitatory and inhibitory interneurons, or between termination patterns of interneurons with dominating input from group I or from group II afferents, but considerable variability was found in each of these interneuronal subpopulations. The variability of both input and output in these subpopulations appears to be an intrinsic property of intermediate zone interneurons and is essential for them to fulfil their integrative roles in sensorimotor networks. This would be in keeping with previous electrophysiological evidence that subsets of excitatory and inhibitory interneurons in reflex pathways from group I and/or II afferents contribute to different motor synergies and may be either coexcited or counteract each other's actions depending on the behavioural context (see, e.g. Lundberg *et al.* 1987; Jankowska, 1992).

The final group of interneurons provided perhaps the most novel information. These two cells had axons which were immunoreactive for GAD and apposed gephyrin puncta. They are therefore likely to contain a mixture of GABA and glycine (e.g. see Todd & Spike, 1993). These are the first two examples of GABAergic interneurons that we have seen in the studies we have performed to date (Bannatyne *et al.* 2003, 2006; Stecina *et al.* 2008; Jankowska *et al.* 2009). The cells had discrete axonal projections that ramified ipsilaterally in the deep laminae of the dorsal horn and intermediate zone, although one cell had an axon collateral that projected towards the ipsilateral motor nucleus. Terminals of these cells apposed other axons containing VGLUT1 that are likely to originate from large myelinated primary afferent fibres (Varoqui *et al.* 2002; Todd *et al.* 2003). It was also observed that gephyrin was not present at the point of contact between interneuron axon terminals and those labelled for VGLUT1; this is consistent with observations made by Todd *et al.* (1995) who showed that gephyrin was not present at axo-axonic synapses formed by axons that contained a mixture of GABA and glycine. Gephyrin was present, however, at other sites of contact, which were presumably dendrites of other neurons. It is very likely that the contacts between interneuron axon terminals and VGLUT1-labelled axons are axo-axonic synapses (see Hughes *et al.* 2005) and that these cells are involved in presynaptic inhibition associated with primary afferent depolarization (PAD), i.e. they are PAD interneurons. As far as we are aware, these are the first two examples of PAD interneurons in higher vertebrates to be characterized electrophysiologically and labelled intracellularly. However as they also contact dendrites it seems that they not only mediate presynaptic inhibition but also exert postsynaptic inhibitory control over other neurons

in the deep parts of the dorsal horn and intermediate zone as proposed by Rudomin (see, e.g. Rudomin & Schmidt, 1999). Furthermore ultrastructural studies of identified group I (Watson & Bazzaz, 2001) and group II afferents (Maxwell & Riddell, 1999) show that presynaptic boutons which contain a mixture of GABA and glycine not only form axo-axonic synapses with primary afferent terminals but frequently also form synapses with the same dendrite that is postsynaptic to the primary afferent, i.e. they form synaptic triads.

Limited information is available about input to interneurons mediating primary afferent depolarization. The two cells identified in the present study were monosynaptically activated by group I and group II primary afferents, respectively. However according to the classical studies of Eccles *et al.* (1962), measurements of the latency of PAD in large muscle afferents suggest that they are not driven monosynaptically by primary afferents but are last order neurons in trisynaptic or short polysynaptic pathways. Disynaptic coupling was proposed for PAD interneurons with input from group I afferents (see, e.g. Rudomin & Schmidt, 1999), but this might not apply to those excited by slower conducting group II afferents (cf. latencies of EPSPs in Fig. 8C and D), which may be excited monosynaptically although at longer latencies. In addition, in the dorsal horn, candidate PAD neurons which contain a mixture of GABA and acetylcholine are known to receive direct input from primary afferent axons (Olave *et al.* 2002). It should be borne in mind that the classical studies of PAD were focused on the ventral horn, and the circuitry proposed by Eccles and colleagues may only be valid for PAD interneurons which form axo-axonic synapses with group Ia terminals in lamina IX, which probably constitute a particular subset of PAD interneuron as they do not contain glycine (see Hughes *et al.* 2005). The PAD interneurons we have identified belong to a group of cells that contain a mixture of GABA and glycine. Presynaptic axo-axonic terminals on Ia and group II afferents outside motor nuclei contain a mixture of GABA and glycine (Maxwell & Riddell, 1999; Watson & Bazzaz, 2001) and therefore the interneurons described here may be the origin of such terminals.

Comparison of axonal projections of intermediate zone interneurons with input from group I and/or group II afferents and of interneurons with similar inputs at other locations

Diagrams in Fig. 11 summarize differences in axonal projections between subpopulations of intermediate zone interneurons and dorsal horn interneurons and lamina VIII interneurons analysed previously (Bannatyne *et al.* 2003, 2006). The three groups of interneurons are represented in left, middle and right hand diagrams,

respectively, and their ipsilateral and/or contralateral axonal projections to the left and right.

The results of the present study show that projections and target cells of intermediate zone excitatory and inhibitory interneurons differ from projections of other interneurons in several respects. Firstly, bilateral projections are characteristic of a subtype of excitatory intermediate zone interneuron but are a distinguishing feature of inhibitory dorsal horn interneurons. Secondly, bilaterally projecting excitatory intermediate interneurons and contralaterally projecting lamina VIII interneurons terminate within laminae VII–IX, whereas bilateral projections of dorsal horn interneurons also extend to laminae IV–VI. Thirdly, excitatory and inhibitory intermediate zone interneurons but only inhibitory dorsal horn interneurons were found to project to ipsilateral motor nuclei. These differences are likely to reflect the various roles played by intermediate zone, dorsal horn and lamina VIII interneurons in coordination of movement.

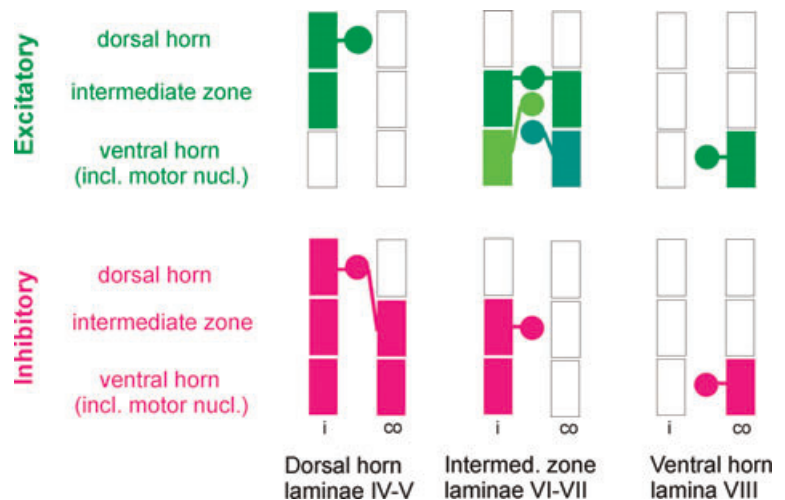
On factors favouring activation of excitatory or inhibitory intermediate zone interneurons

As pointed out above, one of the main findings of this study has been that a considerable proportion of excitatory but not inhibitory intermediate zone interneurons with group I and/or II input project bilaterally or contralaterally, which makes these interneurons particularly well suited to co-ordinate activity on both sides of the spinal cord. Excitatory intermediate zone interneurons might thus play a key role in movements for which such coordination is of particular importance, e.g. locomotion. The higher probability of activation of inhibitory interneurons with group I input under resting conditions and of excitatory interneurons during locomotion induced

by supraspinal stimulation (see Introduction and, e.g. Angel *et al.* 2005 for a review) and differential recruitment during the stance and swing phases of the locomotor cycle (Gossard *et al.* 1994; McCrea *et al.* 1995; Angel *et al.* 1996, 2005) might depend on the balance between peripheral and descending inhibitory and excitatory input to intermediate zone interneurons under different circumstances. As centrally initiated locomotion depends to a great extent on reticulospinal neurons (Jordan *et al.* 2008), it was of particular interest to compare input from reticulospinal neurons with that from peripheral nerves to the excitatory and inhibitory interneurons. However, no consistent differences were found in effects of reticulospinal neurons with axons descending in the medial longitudinal fascicle (MLF) on excitatory and inhibitory interneurons of our sample, indicating that other descending neurones might be more essential in this respect. Monoamines were found to facilitate responses of some intermediate zone interneurons with input from group I and II muscle afferents but depress responses of other interneurons (Jankowska *et al.* 2000). Although it was not possible to link these effects to either excitatory or inhibitory interneurons, monoaminergic neurons thus could play a decisive role in their selection. Models of neuronal circuitry draw particular attention to connections between neurons initiating locomotion and excitatory interneurons (see Rybak *et al.* 2006*a,b*). When more is known about connections between neurons initiating locomotion and excitatory and inhibitory intermediate zone interneurons in pathways from group I and II afferents, models of neuronal circuitry of locomotion (see McCrea & Rybak, 2007, 2008) might use the knowledge of these connections to explain the release of actions of excitatory interneurons on motoneurons during locomotion and thereby to deepen our understanding of its mechanisms.

Figure 11. Main projection areas of excitatory and inhibitory intermediate zone interneurons compared with projection areas of dorsal horn and lamina VIII interneurons

Circles represent excitatory and inhibitory interneurons located in the dorsal horn (left), the intermediate zone (middle) and lamina VIII (right). Different shades are used for the three subpopulations of intermediate zone interneurons (projecting bilaterally, ipsilaterally or contralaterally). Rectangular spaces to the left and right of these circles represent ipsilateral (i) and contralateral (co) projection areas within the dorsal horn, intermediate zone and the ventral horn, including motor nuclei. Data for dorsal horn interneurons are from Bannatyne *et al.* (2006) and those for ventral horn lamina VIII interneurons were reported previously (Bannatyne *et al.* 2003) and in the companion paper (Jankowska *et al.* 2009).



References

- Aggelopoulos NC, Burton MJ, Clarke RW & Edgley SA (1996). Characterization of a descending system that enables crossed group II inhibitory reflex pathways in the cat spinal cord. *J Neurosci* **16**, 723–729.
- Aggelopoulos NC & Edgley SA (1995). Segmental localisation of the relays mediating crossed inhibition of hindlimb motoneurons from group II afferents in the anaesthetized cat spinal cord. *Neurosci Lett* **185**, 60–64.
- Alstermark B & Kummel H (1986). Transneuronal labelling of neurones projecting to forelimb motoneurons in cats performing different movements. *Brain Res* **376**, 387–391.
- Alvarez FJ, Dewey DE, Harrington DA & Fyffe REW (1997). Cell-type specific organization of glycine receptor clusters in the mammalian spinal cord. *J Comp Neurol* **379**, 150–170.
- Angel MJ, Guertin P, Jimenez T & McCrea DA (1996). Group I extensor afferents evoke disynaptic EPSPs in cat hindlimb extensor motoneurons during fictive locomotion. *J Physiol* **494**, 851–861.
- Angel MJ, Jankowska E & McCrea DA (2005). Candidate interneurons mediating group I disynaptic EPSPs in extensor motoneurons during fictive locomotion in the cat. *J Physiol* **563**, 597–610.
- Arya T, Bajwa S & Edgley SA (1991). Crossed reflex actions from group II muscle afferents in the lumbar spinal cord of the anaesthetized cat. *J Physiol* **444**, 117–131.
- Bannatyne BA, Edgley SA, Hammar I, Jankowska E & Maxwell DJ (2003). Networks of inhibitory and excitatory commissural interneurons mediating crossed reticulospinal actions. *Eur J Neurosci* **18**, 2273–2284.
- Bannatyne BA, Edgley SA, Hammar I, Jankowska E & Maxwell DJ (2006). Differential projections of excitatory and inhibitory dorsal horn interneurons relaying information from group II muscle afferents in the cat spinal cord. *J Neurosci* **26**, 2871–2880.
- Biro Z, Hill RH & Grillner S (2008). The activity of spinal commissural interneurons during fictive locomotion in the lamprey. *J Neurophysiol* **100**, 716–722.
- Bras H, Cavallari P, Janowska E & Kubin L (1989). Morphology of midlumbar interneurons relaying information from group II muscle afferents in the cat spinal cord. *J Comp Neurol* **290**, 1–15.
- Brink E, Harrison PJ, Jankowska E, McCrea DA & Skoog B (1983). Post-synaptic potentials in a population of motoneurons following activity of single interneurons in the cat. *J Physiol* **343**, 341–359.
- Brink E, Jankowska E, McCrea D & Skoog B (1981). Use of sucrose gap for recording postsynaptic population potentials evoked by single interneurons in spinal motoneurons. *Brain Res* **223**, 165–169.
- Butt SJ, Harris-Warrick RM & Kiehn O (2002). Firing properties of identified interneuron populations in the mammalian hindlimb central pattern generator. *J Neurosci* **22**, 9961–9971.
- Butt SJ & Kiehn O (2003). Functional identification of interneurons responsible for left–right coordination of hindlimbs in mammals. *Neuron* **38**, 953–963.
- Cavallari P, Edgley SA & Jankowska E (1987). Post-synaptic actions of midlumbar interneurons on motoneurons of hind-limb muscles in the cat. *J Physiol* **389**, 675–689.
- Czarkowska J, Jankowska E & Sybiraska E (1976). Axonal projections of spinal interneurons excited by group I afferents in the cat, revealed by intracellular staining with horseradish peroxidase. *Brain Res* **118**, 115–118.
- Eccles JC, Magni F & Willis WD (1962). Depolarization of central terminals of Group I afferent fibres from muscle. *J Physiol* **160**, 62–93.
- Edgley SA & Jankowska E (1987a). Field potentials generated by group II muscle afferents in the middle lumbar segments of the cat spinal cord. *J Physiol* **385**, 393–413.
- Edgley SA & Jankowska E (1987b). An interneuronal relay for group I and II muscle afferents in the midlumbar segments of the cat spinal cord. *J Physiol* **389**, 647–674.
- Fetz EE, Jankowska E, Johannisson T & Lipski J (1979). Autogenetic inhibition of motoneurons by impulses in group Ia muscle spindle afferents. *J Physiol* **293**, 173–195.
- Flatman JA, Engberg I & Lambert JD (1982). Reversibility of Ia EPSP investigated with intracellularly iontophoresed QX-222. *J Neurophysiol* **48**, 419–430.
- Gonzalez-Forero D, Pastor AM, Geiman EJ, Benítez-Temiño B & Alvarez FJ (2005). Regulation of gephyrin cluster size and inhibitory synaptic currents on Renshaw cells by motor axon excitatory inputs. *J Neurosci* **25**, 417–429.
- Gossard JP, Brownstone RM, Barajon I & Hultborn H (1994). Transmission in a locomotor-related group Ib pathway from hindlimb extensor muscles in the cat. *Exp Brain Res* **98**, 213–228.
- Harrison PJ, Jankowska E & Zytnicki D (1986). Lamina VIII interneurons interposed in crossed reflex pathways in the cat. *J Physiol* **371**, 147–166.
- Holmqvist B & Lundberg A (1959). On the organization of the supraspinal inhibitory control of interneurons of various spinal reflex arcs. *Arch Ital Biol* **97**, 340–356.
- Holmqvist B & Lundberg A (1961). Differential supraspinal control of synaptic actions evoked by volleys in the flexion reflex afferents in alpha motoneurons. *Acta Physiol Scand Suppl* **186**, 1–15.
- Hoover JE & Durkovic RG (1992). Retrograde labeling of lumbosacral interneurons following injections of red and green fluorescent microspheres into hindlimb motor nuclei of the cat. *Somatosens Mot Res* **9**, 211–226.
- Hughes DI, Mackie M, Nagy GG, Riddell JS, Maxwell DJ, Szabo G, Erdelyi F, Veress G, Szucs P, Antal M & Todd AJ (2005). P boutons in lamina IX of the rodent spinal cord express high levels of glutamic acid decarboxylase-65 and originate from cells in deep medial dorsal horn. *Proc Natl Acad Sci U S A* **102**, 9038–9043.
- Jankowska E (1992). Interneuronal relay in spinal pathways from proprioceptors. *Prog Neurobiol* **38**, 335–378.
- Jankowska E, Bannatyne BA, Liu TT, Cabaj A, Stecina K, Hammar I & Maxwell DJ (2009). Commissural interneurons with input from muscle afferents in midlumbar segments in the cat; axonal projections, transmitter content and target cells. *J Physiol* **587**, 401–418.

- Jankowska E, Edgley SA, Krutki P & Hammar I (2005). Functional differentiation and organization of feline midlumbar commissural interneurons. *J Physiol* **565**, 645–658.
- Jankowska E, Hammar I, Chojnicka B & Heden CH (2000). Effects of monoamines on interneurons in four spinal reflex pathways from group I and/or group II muscle afferents. *Eur J Neurosci* **12**, 701–714.
- Jankowska E, Hammar I, Slawinska U, Maleszak K & Edgley SA (2003). Neuronal basis of crossed actions from the reticular formation upon feline hindlimb motoneurons. *J Neurosci* **23**, 1867–1878.
- Jankowska E & Skoog B (1986). Labelling of midlumbar neurones projecting to cat hindlimb motoneurons by transneuronal transport of a horseradish peroxidase conjugate. *Neurosci Lett* **71**, 163–168.
- Jordan L, Liu J, Hedlund P, Akay T & Pearson K (2008). Descending command systems for the initiation of locomotion in mammals. *Brain Res Rev* **57**, 183–191.
- Kiehn O (2006). Locomotor circuits in the mammalian spinal cord. *Ann Rev Neurosci* **29**, 279–306.
- Kiehn O & Butt SJ (2003). Physiological, anatomical and genetic identification of CPG neurons in the developing mammalian spinal cord. *Prog Neurobiol* **70**, 347–361.
- Li WC, Cooke T, Sautois B, Soffe SR, Borisyuk R & Roberts A (2007). Axon and dendrite geography predict the specificity of synaptic connections in a functioning spinal cord network. *Neural Develop* **2**, 17.
- Lundberg A (1982). Inhibitory control from the brain stem of transmission from primary afferents to motoneurons, primary afferent terminals and ascending pathways. In *Brain Stem Control of Spinal Mechanisms*, ed. Sjölund B & Björklund A, pp. 179–225. Elsevier Biomedical Press, Amsterdam.
- Lundberg A, Malmgren K & Schomburg ED (1987). Reflex pathways from group II muscle afferent. 3. Secondary spindle afferents and the FRA: a new hypothesis. *Exp Brain Res* **65**, 294–306.
- Maxwell DJ & Riddell JS (1999). Axoaxonic synapses on terminals of group II muscle spindle afferent axons in the spinal cord of the cat. *Eur J Neurosci* **11**, 2151–2159.
- McCrea DA & Rybak IA (2007). Modeling the mammalian locomotor CPG: insights from mistakes and perturbations. *Prog Brain Res* **165**, 235–253.
- McCrea DA & Rybak IA (2008). Organization of mammalian locomotor rhythm and pattern generation. *Brain Res Rev* **57**, 134–146.
- McCrea DA, Shefchyk SJ, Stephens MJ & Pearson KG (1995). Disynaptic group I excitation of synergist ankle extensor motoneurons during fictive locomotion in the cat. *J Physiol* **487**, 527–539.
- Olave MJ, Puri N, Kerr R & Maxwell DJ (2002). Myelinated and unmyelinated primary afferent axons form contacts with cholinergic interneurons in the spinal dorsal horn. *Exp Brain Res* **145**, 448–456.
- Perreault MC, Angel MJ, Guertin P & McCrea DA (1995). Effects of stimulation of hindlimb flexor group II afferents during fictive locomotion in the cat. *J Physiol* **487**, 211–220.
- Perreault MC, Shefchyk SJ, Jimenez I & McCrea DA (1999). Depression of muscle and cutaneous afferent-evoked monosynaptic field potentials during fictive locomotion in the cat. *J Physiol* **521**, 691–703.
- Quevedo J, Fedirchuk B, Gosgnach S & McCrea DA (2000). Group I disynaptic excitation of cat hindlimb flexor and bifunctional motoneurons during fictive locomotion. *J Physiol* **525**, 549–564.
- Quinlan KA & Kiehn O (2007). Segmental, synaptic actions of commissural interneurons in the mouse spinal cord. *J Neurosci* **27**, 6521–6530.
- Ritter DA, Bhatt DH & Fetcho JR (2001). In vivo imaging of zebrafish reveals differences in the spinal networks for escape and swimming movements. *J Neurosci* **21**, 8956–8965.
- Rudomin P & Schmidt RF (1999). Presynaptic inhibition in the vertebrate spinal cord revisited. *Exp Brain Res* **129**, 1–37.
- Rybak IA, Shevtsova NA, Lafreniere-Roula M & McCrea DA (2006a). Modelling spinal circuitry involved in locomotor pattern generation: insights from deletions during fictive locomotion. *J Physiol* **577**, 617–639.
- Rybak IA, Stecina K, Shevtsova NA & McCrea DA (2006b). Modelling spinal circuitry involved in locomotor pattern generation: insights from the effects of afferent stimulation. *J Physiol* **577**, 641–658.
- Stecina K, Jankowska E, Cabaj A, Pettersson L-G, Bannatyne BA & Maxwell DJ (2008). Premotor interneurons contributing to actions of feline pyramidal tract neurones on ipsilateral hindlimb motoneurons. *J Physiol* **586**, 557–574.
- Todd AJ, Hughes DI, Polgár E, Nagy GG, Mackie M, Ottersen OP & Maxwell DJ (2003). The expression of vesicular glutamate transporters VGLUT1 and VGLUT2 in neurochemically defined axonal populations in the rat spinal cord with emphasis on the dorsal horn. *Eur J Neurosci* **17**, 13–27.
- Todd AJ & Spike RC (1993). The localization of classical transmitters and neuropeptides within neurons in laminae I–III of the mammalian spinal dorsal horn. *Prog Neurobiol* **41**, 609–638.
- Todd AJ, Spike RC, Chong D & Neilson M (1995). The relationship between glycine and gephyrin in synapses of the rat spinal cord. *Eur J Neurosci* **7**, 1–11.
- Varoqui H, Schafer MK, Zhu H, Weihe E & Erickson JD (2002). Identification of the differentiation-associated Na⁺/P_i transporter as a novel vesicular glutamate transporter expressed in a distinct set of glutamatergic synapses. *J Neurosci* **22**, 142–155.
- Watson AHD & Bazzaz AA (2001). GABA and glycine-like immunoreactivity at axoaxonic synapses on Ia muscle afferent terminals in the spinal cord of the rat. *J Comp Neurol* **433**, 335–348.

Acknowledgements

The study was supported by a grant from NINDS/NIH (R01 NS040863) and from the Swedish Research Council (to I.H.). We wish to thank Mrs Rauni Larsson for her invaluable assistance.

Author's present address

K. Stecina: Department of Neuroscience and Pharmacology, Copenhagen University, Panum Institute, Copenhagen DK-2200.